COLD-MOLD ARC MELTING AND CASTING

By R. A. Beall and others

This publication has been cataloged as follows:

PREFACE

The author claims a unique position in the development of the cold-mold furnace as an observer during the opportune time and circumstance. As a member of a large research group I was able to see, from inside, the developments that led to the present melting scheme for zirconium, and to participate in the challenge and excitement of the demands for reactor-grade zirconium for the first Nautilus engine, and slightly later, in the push for high-quality titanium alloy for aircraft.

Now that the arc-melting technique has largely gone beyond laboratory development it seems appropriate to collect the research reports, to annotate them to remove the glaring errors time has revealed, and to make available to the next generation of engineers and scientists a view of what has occurred and the present state of the technique.

Acknowledgment must be made to many people in addition to the authors whose chapters are included. To W. J. Kroll, whose faith in the man at the bench seemed unlimited; to Admiral H. G. Rickover, who knew the job could be done speedily and economically; to S. M. Shelton and W. W. Stephens, who had the drive to get it done; to S. V. Arnold, now of the Army Materials Research Agency and whose encouragement led to skull casting; to the late Henry L. Gilbert, who introduced me to cold-mold melting; and to A. H. Roberson, recently retired Research Director of the Albany Metallurgy Research Center, who stood up to our most outrageous demands for space and money; to these and to a host of others who took active part in the development this book is dedicated.

CONTENTS

ILLUSTRATIONS

TABLES

Frontispiece.—Robert Hare's deflagrator. The first controlled atmosphere arc furnace. (*Reproduced from article published in 1839.*)

COLD-MOLD ARC MELTING AND CASTING

by

R. A. Beall[1] and others[2]

ABSTRACT

This bulletin reviews the historical background of the cold-mold arc-melting technology, with specific references to the development that led to homogeneous zirconium ingots. Descriptions are given of modern production arc-furnaces for vacuum melting of both exotic and conventional metals. Besides zirconium, specific data are given for production of chromium, thorium, and copper. The development of the skull-casting technique for titanium is detailed, and the application of the technique to such refractory metals as molybdenum and tungsten is described. Factors of operation of the apparatus and furnace design are considered.

INTRODUCTION

The objectives of this book are twofold: To accumulate and update Bureau of Mines contributions to cold-mold arc melting and casting, and, by addition of pertinent chapters, to provide production melters and researchers with the best possible view of the overall technique.

The cold-mold arc furnace is a significant addition to the spectrum of tools available to the metals industry. Its primary virtue, minimum crucible contamination, is gained with a water-cooled copper vessel.

Crucible contamination has never been a severe problem with the so-called conventional metals, but other less conventional metals are so reactive in the liquid state that even the most stable refractories are attacked. Titanium and zirconium are typical examples. In the liquid state they react readily with Al_2O_3, Y_2O_3, ZrO_2, and MgO. Since both dissolve carbon, titanium dissolving it up to 0.7 percent, this has a marked effect on physical properties, hence the need for an "inert" crucible. Other metals conventionally melted in the cold-mold furnace include tantalum, columbium, molybdenum, and tungsten, as well as many others.

The second advantage is the potential purification through application of high temperature and vacuum or controlled atmosphere. Actually, this advantage is not limited to cold-mold melting; it can be achieved through vacuum induction melting or to some degree by any degassing operation. However, because of furnace construction, cold-mold melting is particularly adaptable to controlled atmosphere or vacuum operation.

As originally conceived, the cold-mold furnace was applied only to high-priced metals. The author recalls a remark of Kroll's that some day we would see common metals melted in this fashion. As a matter of fact, steel producers have picked up the cold-mold furnace and have literally run away with the technique. Whereas the largest titanium ingot regularly produced is around 30-in diam, steel ingots twice this diameter and weighing up to 40 tons are being cold-mold arc melted today.

The beginnings of the cold-mold arc furnace can be traced to Davy's electric "arch." This discovery awaited Volta's concept in 1800 of placing single voltaic cells in series to gain a sufficiently high potential to support an arc. Shortly after Volta presented this idea of a battery to the Royal Society of London, Davy demonstrated his arc between charcoal tips. A

recent article in "Scientific American" (2) [3] shows a contemporary illustration of the event.

The second noteworthy step, reported by Robert Hare in Philadelphia in 1839 (6), was the enclosure of the arc in a controlled atmosphere. Hare's work was so outstanding as to deserve a closer look. His furnace is shown in the frontispiece. Note that most of the essentials of the modern furnace are included: A movable upper electrode, a lower hearth capable of retraction, provision for evacuation and backfilling with a selected gas, and good visibility. Actually, Hare complained of eye trouble from the brilliance of his arc. Doremus (3) gave a careful evaluation of Hare's work in 1908 and proposed his furnace as a symbol of the beginning of electrochemistry.

The final step in development of the cold-mold furnace was the introduction of the water-cooled crucible which is generally attributed to Werner Von Bolton. Kroll (10) remarks that in 1932 he saw Vol Bolton's furnace, which was equipped with a water-cooled "plug," and Balke (1) recalls that Von Bolton melted tantalum on a water-cooled plate. There is no mention of this feature in Von Bolton's articles or patents (15–17). Pirani's recollection (12) of this early furnace shows it equipped with a nickel plug on which melting took place. Weiss (18), also of Germany, showed illustrations in 1910 of furnaces that included water-cooled shafts and shell. To our knowledge, the first published description of a water-cooled hearth is in the patent of Siemens and Halske granted in 1931 (13). Kroll (9) contributed the thoriated-tungsten electrode, indispensable for nonconsumable-electrode arc melting.

The first major scaleup of the cold-mold arc furnace is reported by Parke and Ham (11) in 1946. Other early contributors to the technique include Herres (7–8), Simmons (14), and Gilbert (4).

It is interesting to note the metals involved: Von Bolton was working with tantalum to gain light-bulb filaments, Kroll with titanium, then later with zirconium. Herres' and Simmons' interests were in titanium; Gilbert's was in zirconium. Parke and Ham's development yielded molybdenum ingots.

The Bureau of Mines' interest in cold-mold melting stemmed from the research on zirconium. In the mid-1940's research was initiated at the Bureau's Albany Metallurgy Research Center on a means to achieve ductile zirconium.

W. J. Kroll's assistance as a consultant was enlisted. By 1949, the project had attracted the attention of the Naval Reactors Division of the Bureau of Ships and the Atomic Energy Commission (AEC) as a possible source of zirconium for reactor use. Shortly thereafter a program of construction leading to zirconium production was instituted at the Albany station under the joint sponsorship of the two groups.

Initially, the sponge zirconium produced at the Albany Center was to have been used for the De Boer Process solely as a feed material leading to "crystal-bar." As development proceeded considerable economy was achieved through direct production of sponge-to-ingot, without the additional purification of the crystal-bar process. The melting-process refinements that contributed to this saving included the consumable-electrode double arc-melting technique (the essentials of the process are covered in a patent (5)) and, slightly later, the application of vacuum to the melting step. The cold-mold crucible was basic to the work.

By 1954 the Bureau of Mines had made its contribution to the zirconium process, and the attention of the research group was directed to other problems. Among the projects of particular interest and appropriate to the subject of cold-mold arc melting was the development of the skull-casting process for titanium sponsored by the Army through Watertown Arsenal, and later the development of a thorium-melting technology under the sponsorship of the Atomic Energy Commission. Other projects and problems of interest were tantalum melting sponsored by Fansteel Metallurgical Corp., melting and casting problems sponsored by AEC through the Lawrence Radiation Laboratory, a study of composition and mechanical properties of cold-mold and skull-cast titanium alloys sponsored by the Army through Watertown Arsenal, and numerous other small projects in cooperation with Government and industrial groups.

In 1966 the Albany Center research program included research and development in the following areas:

Bureau Sponsorship:
  Melting and casting of tungsten and molybdenum
  Melting and casting of beryllium
  Melting of tungsten in high-pressure atmosphere
  Electron-beam melting of vanadium
  Vapor pressure of molten reactive metals
  Electric discharge and plasma processes

---

[3] Italic numbers in parentheses refer to items in the list of references at the end of each chapter.

Residual gas analyses of high-temperature
processes
Atomic Energy Commission Sponsorship:
Tungsten-rhenium alloy melting
Cold-mold induction melting
Hafnium carbide melting and casting
Melting services for University of
California Lawrence Radiation
Laboratory
Army Materials Research Agency Sponsorship:
Slab-shaped titanium ingots

REFERENCES [4]

1. Balke, Clarence W. The Study of Tantalum. Chem. and Ind., No. 6, Feb. 7, 1948, pp. 83–86.
2. deSantillana, Giorgio. Allesandro Volta. Sci. Am., v. 212, No. 1, January 1965,, pp. 82–91.
3. Doremus, Charles A. Robert Hare's Electric Furnace. Trans. Am. Electrochem. Soc., v. 13, 1908, pp. 347–358.
4. Gilbert, H. L., W. A. Aschoff, and W. E. Brennan. Arc Melting of Zirconium Metal. J. Electrochem. Soc., v. 99, No. 5, May 1952, pp. 191–193.
5. Gordon, R. B., and W. J. Hurford (assigned to Westinghouse Electric Corp.). Method of Producing Sound and Homogenous Ingots. U.S. Pat. 3,072,982, Jan. 15, 1963.
6. Hare, Robert. Description of an Apparatus for Deflagrating Carburets, Phosphurets, or Cyanides, in Vacuo or in an Atmosphere of Hydrogen, With an Account of Some Results Obtained by These and by Other Means; Especially the Isolation of Calcium. Trans. Am. Philosophic Soc., v. 7, article 5, New Series, 1841, pp. 53–67.

7. Herres, S. A., and J. A. Davis. Arc Melting Refractory Metals. Steel, v. 124, May 2, 1949, pp. 82–86, 135.
8. ———. Electric Apparatus For Melting Refractory Metals. U.S. Patent 2,541,764, Apr. 15, 1948.
9. Kroll, W. J. Production of Ductile Titanium. Trans. Electrochem. Soc., v. 78, 1940, pp. 35–47.
10. ———. Titanium. Metal Ind., v. 87, No. 7, Aug. 12, 1965, pp. 130–134.
11. Parke, R. M., and J. L. Ham. The Melting of Molybdenum in the Vacuum Arc. Trans. AIME, v. 171, 1947, pp. 416–427.
12. Pirani, M. von. An Early Method of Vacuum-Melting Tantalum. Vacuum, v. 11, No. 2, Apr. 1952, pp. 159–160.
13. Siemens und Halske A.G. Verfahren zum Schmelzen schwerschmelzbarer Metalle, insbesondere von Tantal, Wolfram, Thorium oder Legierungen dieser Metalle in einem wassergekuhlten Behalter (Process for the Melting of High-Melting Metals Particularly Tantalum, Tungsten, Thorium, and Their Alloys in a Water-Cooled Vessel). German pat. 518,499, Jan. 29, 1931; Univ. California, Lawrence Radiation Lab., Livermore, Calif., transl. by Z. F. St-Gallay, UCRL–Trans–10034, March 1966.
14. Simmons, O. W., C. T. Greenridge, and L. W. Eastwood. Arc Melting of Titanium. Metal Progr., v. 55, 1949, pp. 197–200.
15. Von Bolton, Werner. Apparatus For Producing Homogeneous Ductile Bodies From Metals of a Highly Refractory Nature. U.S. Pat. 925,798, June 22, 1909.
16. ———. Homogeneous Body of Highly Refractory Metals. U.S. Pat. 817,733, Apr. 10, 1906.
17. ———. Tantalum. Ztschr. fur Elektrochem., v. 11, No. 3, Jan. 20, 1905, pp. 45–51.
18. Weiss, L., and E. Neumann. Preparation and Investigation of Reguline Zirconium. Ztschr. anorg. Chem., v. 65, No. 3, Jan. 8, 1910, pp. 248–278.

---

[4] Titles enclosed in parentheses are translations from the language in which the item was originally published.

CHAPTER 1.—LABORATORY TECHNIQUE FOR ARC MELTING

By R. A. Beall

THE FURNACE

Small-scale arc melting in controlled atmosphere or vacuum has now reached an advanced state of development. A great number of laboratories have come up with many variations of design. It would be difficult to list the contributors to this field. One of the neatest fixed-electrode furnaces for compactness of design and ease of operation is reported by Geach and Summers-Smith (2). This equipment permits excellent visibility and allows tipping of the buttons without breaking the vacuum seal. The small arc-melting furnace used at the Albany Metallurgy Research Center is a variation of previous designs, particularly of the furnace used at the Westinghouse Atomic Power Division (1) for melting DeBoer-process zirconium. The Albany furnace (fig. 1) was designed to afford flexibility in type (that is, consumable or nonconsumable electrode) and in size of melt. Figure 2 is a schematic representation of the furnace.

This particular furnace is equipped with a sufficiently large water jacket to permit use of mold cups up to 5-in ID by 12-in long. Without change of water jacket, other size cups can be used, down to simple saucer types of 15 g capacity. This permissible cup variation is the chief virtue of this equipment.

The crucibles are constructed of seamless copper tubing, the wall thickness ranging from three-sixteenths to one-fourth inch. This is brazed to a round 1/4-in-thick copper plate, which serves both as power conductor and flange separating the water cooling and the furnace atmosphere. The crucible base is likewise a 1/4-in disk brazed in place.

The electrode shaft is made from 1-in hard-drawn copper tubing. Provision is made for insertion of an inside coaxial copper tubing to allow end-to-end water cooling. A solid copper plug is brazed in the lower end of the shaft. A 1/2-in N.C. tapped hole accommodates either a thoriated tungsten or a consumable electrode. Electrode motion is provided by a brake motor connected by means of a rack and pinion. An O-ring, lightly greased, serves as a vacuum seal to the moving electrode shaft.
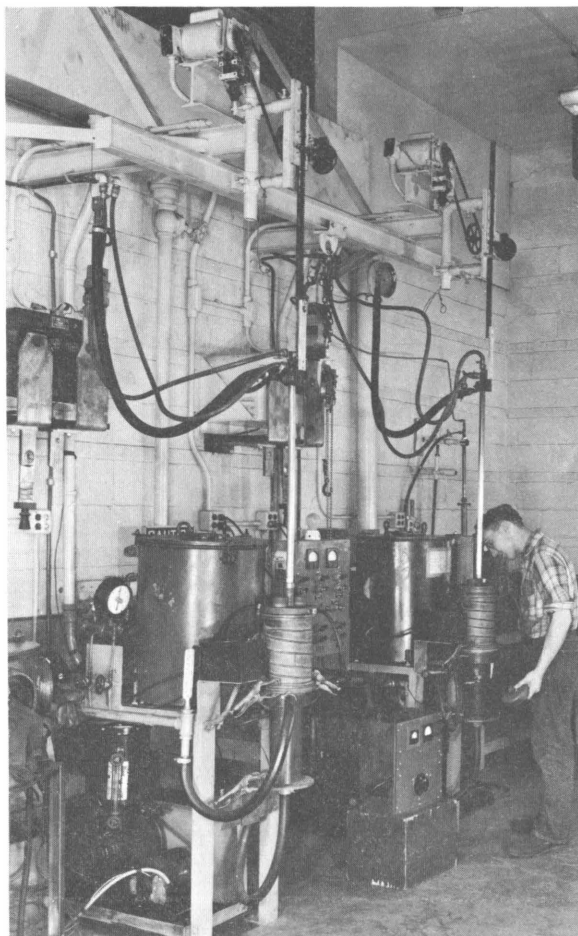
Figure 1.—Two laboratory arc furnaces.

Whereas this furnace was designed particularly for melting with a threaded tungsten electrode, it also serves perfectly for consumable-electrode operation with either pressed compacts or metallic electrodes. Length of course is a limitation. A typical consumable-electrode operation would involve melting a pair of 1-in-square by 10-in-long electrodes welded end to end, into a 2½-in-diam cup. Round metallic electrodes, usually a product of a previous melt, can be melted safely in cups 1 in larger in diameter than the electrode. Naturally, the larger the electrode in

5

A Power connection
B Vacuum-tight gland
C Sight glass
D Tungsten electrode
E Crucible
F Vacuum port
G Feed hopper
H Vacuum-tight hopper shell
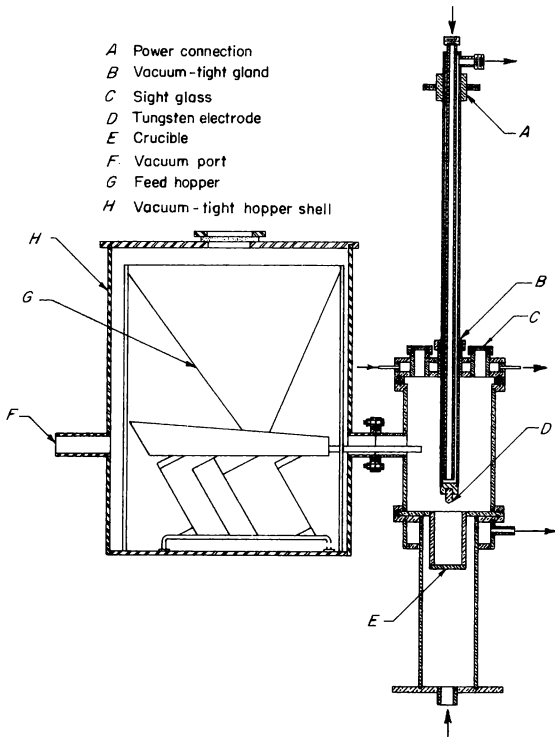
Figure 2.—Diagram of laboratory arc furnace.

relation to the cup diameter, the greater the heat economy because of reduced radiation loss upward.

Double melting is recommended for alloy preparation. Most alloying materials can be safely added to the electrode compact for consumable-electrode melting. For fixed-electrode melting, rotary feeders with up to 100 cups that can be dumped one at a time into the vibrating feeder are available. (See fig. 16, chapter 4.)

The power supply for the several arc-melting furnaces at the Albany Center consists of 18 selenium rectifier dc welding machines connected to a bus-bar network in parallel. The rectifiers are air cooled. The current output of eight rectifiers is controlled by saturable reactors which in turn are controlled at any of the several "remote" furnace-operating stands. Fresh air for the entire block of 18 machines is supplied by a 30,000-cfm blower; each rectifier, in addition, is equipped with an individual fan.

As was mentioned, the flange supporting the melting crucible serves also as the power contact (positive). In general, the current is led from the main bus-bar network to the crucible by solid copper bars. On the other hand, the negative

connection to the electrode shaft must permit movement.

Two systems are in use in the laboratory to give this flexibility. The simplest is to use water-cooled cables. Practice is to strip the insulation from a 0000 welding cable and insert this into an oversized water hose with appropriate lugs at each end for power contact and water fittings. (See fig. 1.) Such an arrangement can handle a current of 4,000 amp. If more capacity is desired, extra cables can be used.

A second method to connect the power supply to the moving electrode shaft is by means of a water-cooled sliding contact. Graphite, or better, copper-impregnated graphite, is used against the copper shaft with good results.

A mechanical vacuum pump (25 to 50 cfm free air capacity) is used to evacuate the furnace. Where extraordinary care is required, a diffusion pump or rotary blower may be used in addition. Experience in this laboratory indicates that leak rate and occluded gas are greater factors in atmospheric contamination than ultimate vacuum, once a nominal 50μ pressure is obtained.

There are at least three possible modes of operation of the laboratory furnace: Button melting, side feeding, and consumable-electrode melting. For button melting, a sample of 5 to 200 g of metal is placed in a water-cooled mold, the arc is drawn, and a fused sample is produced in a very few minutes. Generally, it is worthwhile to tip the button over and remelt to obtain maximum homogeneity. The electrode may be pure tungsten or thoriated tungsten, the latter being less likely to melt and contaminate the sample. By this technique practically every metal on the periodic table, except for the very low melting-point materials, can be prepared as a fused button. Alloys, likewise, can be handled (1) if provision is made to encourage mixing and (2) if the vapor pressures of the components are sufficiently similar to prevent elimination of one or more components.[1]

"Side-feeding" is sometimes resorted to in instances in which (1) the required size of the specimen is greater than the biggest possible button, yet too small for convenient consumable-electrode melting, or (2) no possible means is available to compact or otherwise prepare a consumable electrode. Various systems can be used to feed the metal to the molten pool, including vibrating hoppers, screw feeders, and multiple cup tilters. Despite the inconveniences

---

[1] A recently developed Bureau arc furnace may be operated at 3,000 psi to repress volatilization during melting. For instance, samples of tungsten-nickel alloy may thus be prepared.

of attempting to drop small pellets or increments into the pool from a mechanical device, this is not a serious problem. A minor disadvantage of side feeding is the lack of vertical homogeneity in the ingot occasioned by the relatively shallow molten pool.

A serious problem, however, does exist in maintaining a nonconsumable electrode. Because of electrical attraction, plus mechanical splashing, and spatter from boiling of volatile impurities, the tungsten electrode ultimately receives some molten metal. Since nearly every alloy of tungsten has a lower melting point than tungsten, the electrode consumes and contaminates the melt. In practice, it is very difficult to produce 10-lbs ingots (3-in diam) of zirconium from sponge with less than 200 ppm tungsten contamination.

Consumable-electrode melting is much to be desired over the other modes mentioned (1) because of elimination of the possiblity of contamination of the melt by the electrode, (2) because of the vertical homogeneity of the deep molten pool, and (3) because of the possibility of purification through use of reduced pressure. The lower limiting size of consumable-electrode ingots at Albany is 1-in diam. To the writer's knowledge, the upper limit of size in consumable-electrode melting has not been discovered.

GENERAL OPERATION

The operation begins with the selection of the furnace atmosphere. Whenever possible, consumable-electrode arc melting is conducted in vacuum. However, operation in partial pressure is often less difficult. Nearly always, tungsten electrodes are used in partial pressure, the exception being when the ingot (or button) is tungsten also, and electrode loss is not a problem. It is the practice in this laboratory to maintain the furnace pressure of helium below atmospheric to gain the added effect of atmospheric pressure for securing the flanges tightly shut.

Argon gives a slightly more stable arc than helium. and a lower melting rate. Likewise, the arc-gap, arc-potential relationship is different (3). These minor effects seldom justify the use of one noble gas over the other. Convenience and economy generally specify the choice.

The water flow through all cooled parts is important, and, through the crucible system, essential. A general rule for water flow specifies 10 gpm of water per 1,000 amp of arc current.

It is convenient in small-scale melting (particularly with a tungsten electrode) to initiate the arc with a high-frequency discharge. This prevents contact and possible sticking of the electrode. The starting material in the crucible may be sponge, powder, chips, or solid metal. The quantity of metal in the starter pad depends upon the density of the material, as well as on the rate of increase of power application. Table 1 shows typical starting charges of zirconium.

The arc may be moved about the charge (in small-scale melting) by use of a hand magnet. Some skill is required for the production of smooth buttons and small ingots. The water jacket can be wound with a solenoid to give centering stability to the arc as well as a gentle stiring motion to the pool. (Details are given in chapter 2.)

As the melt proceeds, the shaft position must be adjusted to maintain proper arc length as the electrode consumes, or the pool rises. Arc potential as read on a voltmeter is usually a sufficient guide for manual operation. Normally, automatic arc-length control is unnecessary for laboratory-scale operation. Other instrumentation need only include an ammeter. Unless data are required, water temperatures need only be monitored with an occasional dipping of the finger.

Upon termination of the heat, the cooling cycle begins. If vacuum has been used during melting, the furnace should be back-filled with gas; otherwise the ingot will remain hot for hours. Helium is much more effective than argon during this phase of the operation.

Table 1.—Starting charges of zirconium

Cup diameter, in	Minimum, g	Suggested, g
1½	50	75
2	50	75
2½	50	75
3	150	250
3½	200	300
4	300	350
5	500	800
6	800	1,000
7	1,000	1,500
8	1,500	2,000
10	2,000	3,000

Safety in arc melting is a matter of considerable importance, particularly as the size of the heat increases. Arbitrarily, it is considered in this laboratory that ingots in excess of 5-in diam must be melted in a furnace remote from

the operator. Steel partitions serve as a protective shield for the larger scale laboratory-melting units. The optical system used to permit viewing of the heat is described in chapter 11.

REFERENCES

1. Beall, R. A., and W. J. Hurford. Arc Melting. Melting and Shaping of Zirconium and Its Alloys. I. Melting of Zirconium. Ch. 2 in Metallurgy of Zirconium, ed. by Benjamin Lustman and Frank Kerze, Jr., McGraw-Hill Book Co., Inc., New York, 1955, p. 221.

2. Geach, G. A., and D. Summers-Smith. A Laboratory Arc-Furnace for Melting Alloys Containing the Refractory Transition Metals. Metallurgia, v. 42, August 1950, pp. 153–156.

3. Wood, F. W., and R. A. Beall. Studies of High-Current Metallic Arcs. BuMines Bull. 625, 1965, 84 pp.

CHAPTER 2.—BEGINNING OF CONSUMABLE-ELECTRODE PRODUCTION OF ZIRCONIUM

By R. A. Beall, F. Caputo,[1] and E. T. Hayes [2]

Homogeneous zirconium-alloy ingots were cast in 1952, 1953, and 1954 on a production basis by the consumable-electrode arc-melting process at the Albany Metallurgy Research Center. This chapter describes the various methods used to introduce alloying materials into the ingot and evaluates each method by the degree of homogeneity of resulting ingots, as determined in tests on sections cut from the ingots. As many as 30 or more ingots, each 6 to 10 in diam and weighing 300 to 500 lbs, were melted, using each method; and, as most of them subsequently were fabricated to strip 0.1-in thick, the test results were considered to be representative of production practice at that time.[3]

Ingot homogeneity has been considered more difficult to achieve in arc-melting practice than by methods where the molten metal is poured into molds and the addition can be stirred into the total mass of metal before casting. Owing to the unique requirements of consumable-electrode arc melting, the addition can be made only to that part of the total mass of the ingot that is molten at one time. Observation of the flowlines in 500-lb ingots produced at Albany indicated that the molten pool had a maximum depth about equal to the ingot diameter. The weight of metal molten at one time was, therefore, not over 100 lbs. Characteristically, the arc-melting process is conducive to segregation, which was overcome, at least partly, by adding the alloy constituents almost continuously during casting.

Zircaloy 1 and Zircaloy 2 were produced; the former contained 2.5 percent tin, and the latter, a quaternary alloy, contained 1.5 percent tin, 0.12 percent iron, 0.10 percent chromium, and 0.05 percent nickel. Three addition meth-ods tried were: (1) the pressed-in method, (2) tin-chopper method, and (3) the pill method. Other means of improving ingot homogeneity were magnetic stirring and double melting.

ARC-MELTING PROCEDURE

The details of construction of the first melting unit were described by Stephens and others [4] in an earlier paper. For that unit, pressed sponge 2- by 2- by 20-in bars were end-welded within the arc-melting furnace into a continuous 2-in-square electrode. Water-cooled copper contact rolls provided a power connection to the electrode; steel rolls provided a means of raising or lowering the electrode. Both sets of rolls were driven by a motor drive or hand crank. A water-cooled copper cup of 6-, 7-, 8-, or 10-in diam was used as a mold. Because rubber gloves were incorporated in the top of the furnace wall to allow the operator to line up and weld the bars, the furnace was maintained at approximately atmospheric pressure. Direct current was provided either by rotary converters or selenium rectifiers. Figure 3 shows the lower or melting section of the furnace and the pressed electrodes and ingots.

In operation, the furnace was loaded with bars, a starter pad of machine turnings was placed in the copper cup, the furnace was sealed, a vacuum was drawn to 150μ, and the furnace was backfilled with inert gas, 20 percent and 80 percent helium. The arc was initiated by advancing the electrode until contract was made with the turnings, at which time the melting began. A second operator welded the bars with a tungsten electrode arc as the melting progressed. A typical melt required a current of 3,700 amp at 45 v to give a melting rate of 4 lb/min. When the cup was filled to a reasonable height, the power was first lowered to

---

[1] Formerly physical chemist, Albany Metallurgy Research Center, Bureau of Mines, Albany, Oreg.; now associated with Oregon Metallurgical Corp., Albany, Oreg.
[2] Deputy Director, Bureau of Mines, Washington, D.C.
[3] Some of these results were presented at the 1953 Metallurgical Information Meeting (Classified) at Brookhaven National Laboratory in April 1953.

[4] Stephens, W. W., H. L. Gilbert, and R. A. Beall. Consumable-Electrode Arc Melting of Zirconium Metal. Trans. ASM, v. 45, 1953, p. 862.
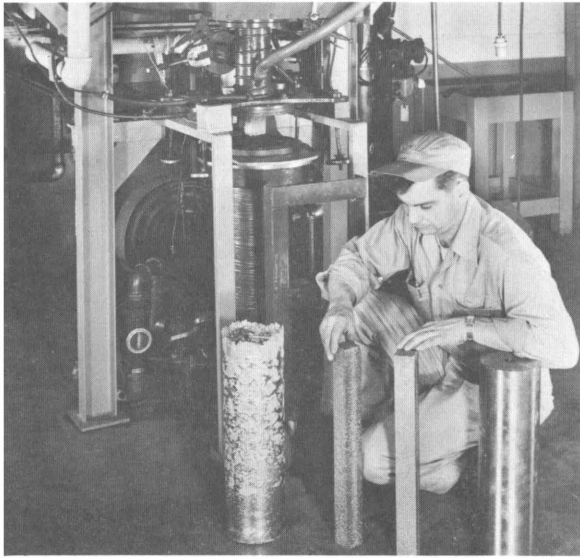
Figure 3.—Melting section of furnace with consumable pressed electrodes and ingots in foreground.

reduce depth of the molten pool and consequent depth of the shrink hole and was then turned off. After a 30-min cooling period the ingot had shrunk from the cup wall and could be removed by inverting the cup. In continuous operation a three-man crew produced 4 to 5 ingots per 8-hr shift.

ALLOY ADDITION METHODS
Pressed-In Method

The following method was first used to produce Zircaloy 1. Tin which had been extruded to $\frac{1}{16}$-in-diam wire was cut to fit the length of the die and was incorporated with the zirconium sponge before pressing into an electrode. Although this technique probably would be suitable for adding alloying materials of higher melting points, it was unsatisfactory for tin. Tin melts at a much lower temperature than zirconium, and, because of the temperature gradient along the zirconium electrode, the tin melted and ran out of the rod some distance away from the molten end.

Even though the tin did not melt at the appropriate moment, it did get into the ingot, and its flow rate from the electrode during the latter and greater part of the casting period apparently was proportional to the melting rate of the electrode. Chemical analyses and macroetched interior surfaces showed the ingots to be fairly uniform, though low in tin,

throughout their upper and greater part. Owing to the phenomenon described, the amount of tin in the lower part of the ingot exceeded the intended proportional amount. The distribution of the alloying constituent was determined by analysis of 1-g samples taken at $\frac{1}{2}$-in intervals along the side of the ingot.

Preferential etching, indicative of high tin content, was not observed when central surfaces of the ingot were macroetched. Results of a set of chemical analyses of 25 samples of Zircaloy 1 ingots produced by melting zirconium electrodes containing tin indicated an average tin content of 2.34 percent. Samples ranged from 2.12 to 2.89 percent, with all high values from the lower third of the ingot, 96 percent of the samples were within the 2.2–2.8 percent tin Zircaloy 1 specifications.

Tin-Chopper Method

In an effort to improve the overall ingot homogeneity a wire chopper was built to add tin at a controlled rate to the molten pool. This machine operated in a vacuum-tight box and cut $\frac{1}{4}$-in diam tin wire into short lengths. The chopper, shown in figure 4, consisted of

Figure 4.—Automatic tin-chopper mechanism.

four rubber-covered drive rolls geared to a rotary cutter, which in turn was driven through a vacuum seal by the variable-speed electric motor, which also drove the electrode feed rolls. Therefore, the feed rate of tin was proportional to the feed rate of the electrode. By appropriate gear reduction, the ratio of rates was adjusted for an alloy of 2.5 percent tin. In operation the pieces of wire dropped though a transparent plastic hose and into the furnace at a point directly over the melting cup.

Although the outward appearance of ingots by this method was excellent and chemical analyses of samples taken along the sidewall indicated a homogeneous alloy, macroetching of vertical sections revealed areas of extremely high tin. These areas, shown in figure 5, were due to pieces of tin or zirconium-tin compounds that sank to the bottom of the molten pool and solidified before completely mixing with the zirconium. These areas were usually near the center of the pool and at indeterminate levels within the ingot, although dispersion of tin throughout the cross section outside the center area was quite uniform, as shown by the fact that tin content in 98 percent of all analyses was within the specified 2.2 to 2.8 percent.

Figure 6.—Single melt ingot using 1.4 amp for solenoid stirring causing centrifuging of tin to sidewalls.

Magnetic Stirring

It had been observed that the metal in the molten pool could be rotated by the field of a direct current flowing through a solenoid surrounding the melting cup, and it was suggested that the rotation, if properly adjusted, would assist in mixing the melt. Accordingly, a coil of 4,000 turns of magnet wire was wound around a nonmagnetic water jacket, and several trials were made with various currents. First attempts resulted in an extremely high rotational velocity. In one attempt, using a current of 1.4 amp, an ingot was produced that was extensively porous and contained high tin concentrations along the walls of the ingot. These are shown in figure 6. Through trial it was found that a current of 0.2 amp mixed the molten pool enough to produce sound ingots. Macroetched internal sections from such ingots revealed the absence of unalloyed tin. A typical ingot section is shown in figure 7.

Figure 5.—Single melt ingot showing segregation of unmelted tin beads.
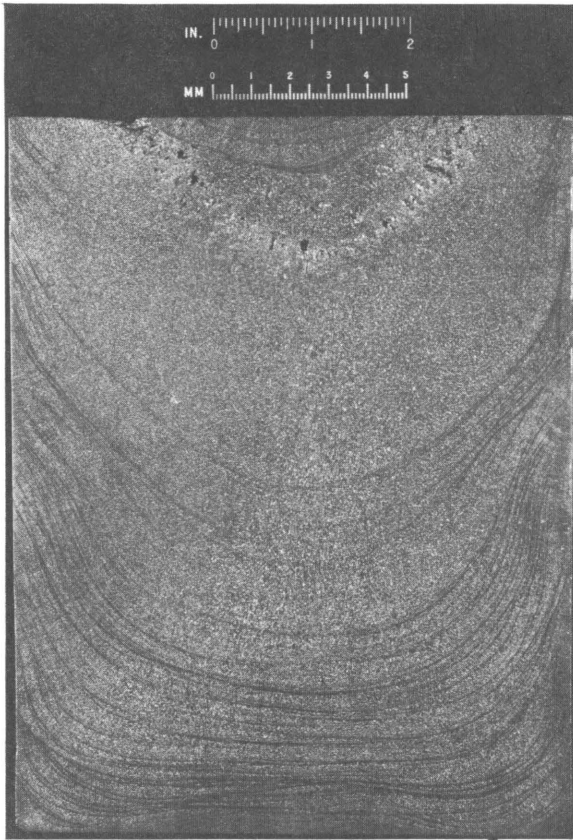
Figure 7.—Single melt solenoid stirred ingot of 0.2-amp type.

Double Melting

Double melting was undertaken to eliminate porosity. The furnace described earlier was the only one available at the time for melting large ingots, and it was necessary to reduce the first-melt 8-in-diam ingots to 2- by 2-in bars for remelting. These ingots were first press-forged to 4-in-square billets, and these were rolled to 2- by 2-in bars in a mill with grooved rolls in six passes. The bars were then shot-blasted, pickled in hydrochloric acid to remove iron contamination, washed, dried, and remelted. The principal defect in the first-melt ingots—the undissolved tin beads—gave a center flaw or weakness that often resulted in failure during rolling. Also, the oxide pickup during forging contributed to the hardness of the ingots, and nitrogen pickup was above the specification limit of 50 ppm.

A larger furnace, shown in figures 8 and 9, was constructed to remelt electrodes composed of several 6-in-diam ingots connected end to end. This eliminated forging and rolling and gave double-melted ingots of better quality. The furnace, simple in consruction, consisted of a melting cup and water jacket, a long tube to contain the prefabricated electrode, and a water-cooled copper rod which functioned as
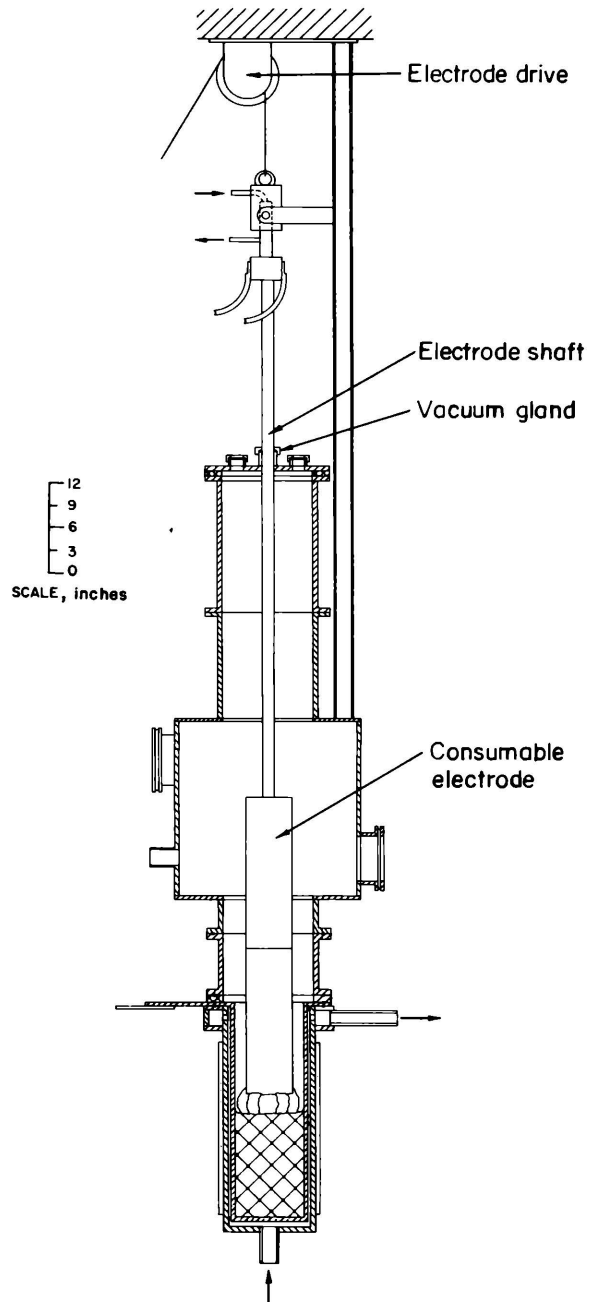
Figure 8.—Large furnace capable of remelting 6-in-diam ingots.

an electrode support and as a conductor to transfer current to the electrode. It entered the furnace through an O-ring gland. The rod and electrode were raised and lowered with a chain hoist.

Ingots produced by double melting in either furnace were found to be free of porosity and segregation. Numerous chemical analyses made on samples taken from internal portions of the ingots showed that the alloying constituents were uniformly distributed and within specified limits. For example, tin content ranged from 2.44 to 2.63 percent, averaging 2.53 percent, for 23 samples of a typical 2.5 percent tin alloy produced by melting a 6-in electrode in a 10-in cup. It is interesting to note that all tin values are well within the 2-2-2.8 percent tin Zircaloy 1 specification.

Pill Method

The production of Zircaloy 2, 1.5 percent tin, 0.12 percent iron, 0.10 percent chromium, and 0.05 percent nickel, posed a new problem in that it was difficult to form a wire to provide the addition.

The techniques for adding elements to make Zircaloy 2 included (1) adding iron and chromium in the briquetting operation to sponge prealloyed with nickel, (2) alloying the nickel with the tin wire, and (3) using tin-iron-chromium in the briquetting operation to sponge powders. Although these methods produced fair quality ingots, they were replaced by a superior method of feeding compressed pills made from powdered metal into the melt during casting. Pills, $\frac{3}{8}$-in-diam by $\frac{1}{4}$-in thick, were compacted in a high-speed commercial
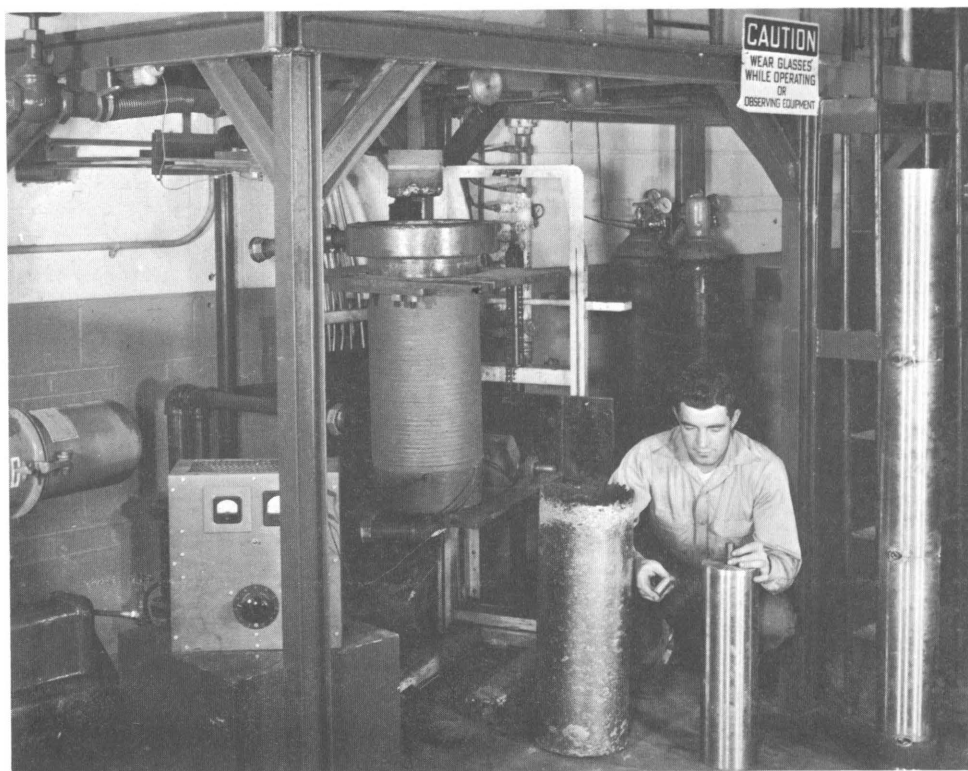
Figure 9.—Large furnace with ingot and electrode made of first-melt ingots.

tablet machine from blended tin, iron, chromium, and nickel powders. A pill counter geared to the electrode feed motor served as a means of adding the alloy at a rate proportional to the melting rate of the electrode.

The use of pills has resulted in ingots more homogeneous than any made by the other methods described. This method. in conjuction with magnetic stirring and double melting, yielded alloy ingots meeting rigid specifications. Reproducibility within the tolerances set for each alloy constituent was maintained without difficulty. Table 2 gives a typical Zircaloy 2 analysis. A typical ingot section is shown in figure 10.

At the time, the pill method for adding alloy during arc melting appeared to be the most adaptable developed. Pill feed rate could be controlled accurately and could be changed to compensate for variations in chemical compositions of the electrode or to produce an entirely different alloy; hence the method permitted pressing of electrodes long before melting.

Figure 10.—Macroetch of typical Zircaloy 2 ingot section.

Table 2.—Analysis of Zircaloy 2 ingot, percent

Element	Number of samples	Average	Range
Chromium	30	0.097	0.08–0.10
Iron	30	.13	.11– .15
Nickel	30	.051	.05– .06
Nitrogen	30	.001	<.001–.002
Tin	30	1.52	1.47–1.64
Brinell hardness number	11	179	178–181

CHAPTER 3.—COLD-MOLD ARC MELTING IN PRODUCTION

By R. A. Beall

One of the most significant aspects of cold-mold arc melting in U.S. industry is the degree of secrecy imposed. This probably is in part a holdover from early days in titanium production when a highly competitive situation existed and when each industrial group had developed, through much effort, unique equipment, and techniques.

As a result of the proprietory nature of much of operations, there has been no general survey of capacity nor comparing of methods. The writer, who has been admitted into some installations, has therefore prepared the descriptions below with some delicacy or reserve.

At least 21 steel-melting facilities which utilize cold-mold arc melting exist in the United States; at least five titanium and possibly three zirconium melting installations are known. Beyond these are units for the production of vanadium, hafnium, columbium, tantalum, molybdenum, and tungsten. These are exclusive of laboratory furnaces. The steel-melting capacity is probably in excess of 100,000 tons per yr.

EQUIPMENT

As was mentioned in the early development of cold-mold melting, each firm designed and constructed its own equipment. By the mid-1950's, several concerns developed furnaces for sale (or in at least one instance, sold "know-how"). At this writing, furnaces are known by the writer to be listed for sale by Consarc Corp., an affiliate of Inductotherm Corp., by Lectromelt, a division of McGraw Edison Corp., and by Zak Inc., in the United States, and by W. C. Heraeus G.m.b.H. in West Germany.

The Consarc model 30–12 is shown in figure 11. Figure 12 pictures the furnace constructed by Heraeus for Midvale-Heppenstall Co. in 1961. Figures 13 and 14 show the operating consoles and one of a bank of four arc furnaces (during unloading) of the Imperial Metals Industries Ltd., Birmingham, England. Figure 15 shows the electrode-drive mechanism of a pro-
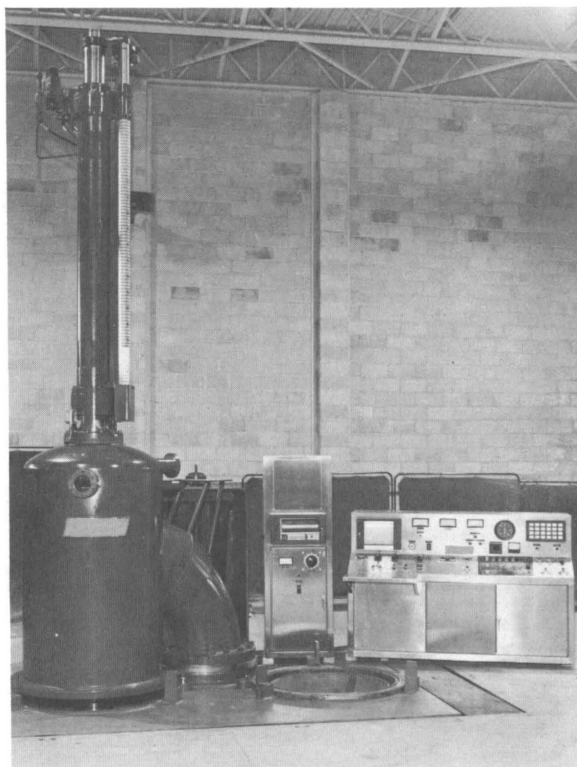
Figure 11.—Consarc 30–12 production vacuum arc furnace in test bay before shipment.

duction furnace at the Titanium Metals Corp. of America plant at Henderson, Nev. These are not shown to recommend the product or producer, but rather to give the reader a concept of the general designs.

In general the production models follow the early plan of an exterior-supported electrode shaft passing through a seal into the chamber where the electrode is fastened. Needless to mention, the early Bureau expedient of lowering the shaft with a simple chain-fall has been much improved by engineering. Likewise the arc-length sensing equipment has been developed beyond observing the arc potential and manually adjusting therefrom.

Crucibles follow two general patterns: Either

15

Figure 12.—The Midvale-Heppenstall furnace capable of producing 60-in-diam ingots.

Figure 13.—Operating consoles for vacuum arc furnaces in the Kynoch works of Imperial Metals Industries, Ltd., Birmingham, England.

Figure 14.—An Imperial Metals Industries Ltd. arc furnace during unloading operation.

the crucible is removed and inverted to allow the ingot to slide out, or the bottom is removed to allow the crucible to be lifted off the ingot. The latter requires a water seal at the bottom. Heavy ingots require heavily constructed crucibles. As sizes increased, it was found particularly expedient to reinforce or otherwise strengthen the crucible bottom to prevent bulging inward during the evacuation step. This bulging has led to formation of a steam pocket during startup, with attendant burn-through.

As far as can be ascertained, copper is the only material used for crucible walls, except for one organization which melts steel in steel crucibles. Direct current is used in nearly every instance, the exceptions being two organizations working with refractory metals that melt with alternating current.

Vacuum pumps range from steam ejectors to rotary blowers to elegant diffusion pumps. The degree of pressure, once a point of argument, is now conceded to be not less than the vapor pressure of the material melted at its melting point over the pool. The pressure gradient from the pool upward is a function of geometry, pumping rate, persistence of condensables, etc.

Power requirements vary widely from shop to shop. In general, the steel melters seem to be happier with lower melting rates and poorer wall conditions than those melting more expensive metals. Evidently lower power leads to fewer slag inclusions and better homogeneity.

Electrode fabrication depends upon the metal produced. For steel, the electrode may be air-melted and cast or prepared in vacuum-induction equipment. For titanium and zirconium, compacts are prepared by briquetting presses, the compacts being subsequently welded either with a shielded arc or by some other of the controlled-atmosphere devices. The refractory metal electrodes are commonly a powder-metallurgy product.

Length of time to prepare an ingot is a function of size and power. A rate of 20 lb/min at 35,000 amp for steel has been mentioned to the writer. At this rate, a 20-ton ingot would take

Figure 15.—An example of an electrode-drive assembly—Titanium Metals Corp. of America.

1½ days to melt. Provision is usually made to cool the ingot away from the furnace to permit the furnace to be kept busy.

In 1954 a titanium production operation suffered a disaster when the melting furnace exploded. On request of the firm, the Bureau appointed the author, R. W. Van Dolah, and R. W. Huber to investigate the accident. The details of the study are available (1). A second and similar explosion was studied in 1957 (3). Other explosions have been noted, but the details have not been made available.

To generalize on the cause of the explosions, in most instances some mechanism has prevailed which not only permitted but forced the molten titanium into intimate contact with the cooling water—for instance, a crucible rupture allowing water to flow over the molten metal, and coincidentally, the electrode becoming detached and falling, driving the water into contact with the metal.

As a result of these and other incidents all involving titanium, a committee was formed of technical personnel representing the five firms active at that time in titanium melting to consider safety procedures. The recommendations resulting from this effort were published in 1961 (1).

Owing to the hazard now apparent in titanium melting, protective shields are universally provided for titanium melting on production scale, along with other devices. (The protective cell is apparent around the industrial furnace pictured in figure 14.)

Since the furnace operator is therefore kept remote from the furnace during melting, viewing systems are often provided. Closed-circuit television can meet this need. The optical system used by the Bureau is described in chapter 11.

Three approaches have been taken to improve the safety of the cold-mold furnace through elimination of water and, hence, the water-metal reaction. Bureau researchers studied the possibility of cooling the cold-crucible with forced air (6). John Ham and others at the National Research Corp. developed a helium-cooled crucible for titanium casting (5). Cooper and Dilling (4) have reported on the use of liquid metal as a coolant. All of these schemes have worked, but to date none have been fully accepted by industry as a production technique. A further variation, useful only for small-scale furnaces, is the massive copper or massive titanium crucible. In this instance, the heat capacity of the crucible is sufficient to handle the heat generated by the arc for the short time involved. A good example of this technique is described by Torti and Ham (7).

In a discussion of safety hazards in cold-mold melting, the question rises—is only titanium hazardous? This is difficult to answer. To date, only titanium melting has led to disastrous explosions of the type mentioned. The author is aware of numerous small "incidents" resulting from water ingress and contact with molten metal. In none of these was anything but steam pressure and a minor hydrogen explosion involved. The metals have included all of the reactive and refractory metals plus copper. As to the potential hazard in steel melting, no opinion can be offered. To date, no furnace incident has been reported, and consequently, most steel furnaces are without operator protection.

A final point of discussion of the industrial cold-mold furnace is the degree of versatility. In general, a furnace designed for steel, titanium, zirconium, or columbium melting, is equally satisfactory for any of the other metals mentioned. For tantalum, molybdenum, or tungsten, more care must be taken to provide against crucible rupture. Typical examples are (1) limitation of water gap and increase of water velocity in the jacket, (2) use of heavier copper wall in the crucible, (3) use of a protective metal liner (that is, tungsten sheet liner in a tungsten melt), or (4) reduction in the electrode-to-crucible-diameter ratio.

To conclude, no attempt is made here to justify cold-mold melting over vacuum-induction melting, vacuum degassing, or other developments for steel. It is significant that the production by cold-mold is increasing. Time, however, will finally permit the intricate adjustments between supply, demand, price, and quality to show the comparative need for the various techniques. The same will hold for the more exotic metals.

REFERENCES

1. Battelle Memorial Institute (Columbus, Ohio). General Recommendations on Design Features for Titanium and Zirconium Production-Melting Furnaces. DMIC Memo. 116, July 19, 1961, 7 pp.
2. Beall, R. A., Van Dolah, R. W., and R. W. Huber. Report of Explosion Disaster, Titanium Melting Furnace, Mallory-Sharon Titanium Corp., Niles, Ohio, June 11, 1954; available on request from the Bureau of Mines Albany Metallurgy Research Center, Albany, Oreg.
3. Bureau of Mines. Investigation of January 28, 1957, Molten Titanium-Water Explosion at Mallory-Sharon Titanium Corporation Plant, Niles, Ohio. Report 3612, July 1, 1957, 5 pp.
4. Cooper, D. E., and E. D. Dilling. Liquid Metal Cooling for Consutrode Melting. J. Metals, v. 12, No. 2, February 1960, pp. 149–152.
5. Ham, John L. Operation of Helium Cooled Skull Arc Melting Furnace. National Res. Corp., Contractor's Rept. GS–OOP (D)–18155.
6. Kirk, M. M., P. C. Magnusson, and G. L. Schmidt. Air-Cooled Crucibles for Cold-Mold Arc Melting. BuMines Rept. of Inv. 5443, 1959, 23 pp.
7. Torti, M. L., and John L. Ham. Reactive Metal Melting Furnace Eliminates Water Cooling Hazard. Steel, v. 144, No. 10, Mar. 9, 1959, pp. 64–66.

CHAPTER 4.—COLD-MOLD ARC MELTING OF CHROMIUM AND CHROMIUM ALLOYS

By R. A. Beall, G. Asai,[1] and A. H. Roberson [2]

The melting of pure chromium and high-chromium alloys without contaminating the metal with oxygen, nitrogen, or crucible materials is a most difficult task. The extreme avidity of the element for oxygen and nitrogen makes melting in a vacuum or under a protective atmosphere of argon or helium a necessity.

Suitable crucible materials pose another serious problem. Only the pure sintered oxides are satisfactory. Most of the more common refractories soften below the melting point of chromium, and some of those which have higher softening points are attacked by the molten metal. This is true of alumina. Sully, Brandes, and Provan (7) report that the alumina crucibles used in their research were attacked slightly, the resulting metal containing 0.2 to 0.3 percent aluminum. These investigators, along with Carlisle, Christian, and Hume-Rothery (1) found that thoria was not attacked by molten chromium, and was a satisfactory refractory. Parke and Bens (1) report the use of zirconia, and Greenaway (3) used beryllia.

A much more satisfactory method for melting chromium is the inert-atmosphere, cold-mold, arc-melting practice that eliminates crucible contamination completely, and, when the consumable-electrode method is used, eliminated the possibility of minor contamination from the electrode.

Arc melting of chromium was reported by Gilbert, Johansen, and Nelson (2) of the Bureau of Mines, who used the nonconsumable-electrode (tungsten) process to produce hot forgeable chromium. More recent publications on this subject include those of Johansen, Gilbert, Nelson, and Carpenter (5) and Johansen and Asai (4).

THE ARC-MELTING PROCESS
Nonconsumable-Electrode Melting

Two general methods may be used for inert nonconsumable-electrode method, or the consumable-electrode method. The furnace equipment and technique used for melting chromium ingots up to 15 lbs by nonconsumable-electrode was covered in chapter 1.

Strictly, there is no completely satisfactory nonconsumable-electrode arc-melting method for chromium or any other metal, that is, due to the very high temperature of the electric arc, estimated to be in excess of 4,000° C, and due to the spatter during melting caused by mechanical splashing or by release of entrapped gases, there is invariably a consumption of the most refractory electrode. The erosion caused by splashing, subsequent alloying, and dripping from a tungsten electrode may be held to a reasonable tolerance (400 ppm) with care. The tungsten-chromium alloy does not dissolve readily, but remains as inhomogeneities which make it difficult to fabricate into rod, sheet, or wire. Nevertheless, for small-scale work, fixed-electrode melting is a useful tool. Thoriated tungsten (1 percent thoria) is considered the best material available for this application.

The most suitable feed material for tungsten-electrode melting is in the form of $\frac{1}{8}$ to $\frac{1}{4}$-in lumps. Powder is less satisfactory, since the severe convection currents in the furnace atmosphere tend to blow the material out of the mold. Side feeding of a fine powder is nearly impossible.

Because of the high vapor pressure of chromium at its melting point, it is conventional to melt it in an inert atmosphere rather than in a vacuum. The backfill gas may be argon, which promotes a steady arc, or helium, or a mixture of the two. The practice at the Bureau of Mines laboratory in Albany, Oreg. is to use a mixture of 20 percent argon and 80 percent

[1] Research chemist, Albany Metallurgy Research Center, Bureau of Mines, Albany, Oreg.

[2] Formerly research director, Albany Metallurgy Research Center, Bureau of Mines, Albany, Oreg.; now retired.

helium as a satisfactory compromise. The furnace is backfilled to a pressure of about 0.8 atmosphere. The partial vacuum insures that the flanges are tightly pressed together to prevent leakage and will prevent objectional vaporization of the chromium.

Currents up to 1,500 amp may be used with a ½-in-diam tungsten tip, although the chance of tungsten contamination is increased at this level. Normally, a 4-in-diam pool may be kept molten with 1,200 amp, while 900 amp is sufficient for a 3-in pool. The pool depth in either case probably will be less than 0.5 in. An arc potential of 30 v is common for the mixture of inert gases specified.

Tungsten-electrode arc-melting is a slow process, normally proceeding at a rate of about 100g/min. This slow rate, however, allows the operator to guide the arc as desired about the pool surface with a magnet, and for this reason the sidewall condition is often better than that of the alternative method, consumable-electrode melting.

During a long melt, the eyepieces will be fogged because of condensed chromium vapor. This may be minimized by use of an extension tube of about 4-in length on the eye piece.

Within 30 min after completion of the melting, a 4-in ingot is cold enough to be removed without danger of oxygen or nitrogen contamination. Shrinkage is sufficient to free the metal from the copper tube unless the cup has been damaged or is bent. A removable bottom is a benefit for assisting in removal, particularly for the small sizes (1½ to 2½-in-diam), where shrinkage is slight.

When alloy ingots are required, it is necessary to provide precisely proportional alloy additions since the portion of the ingot that is molten at any given instant is so small that it practically eliminates vertical mixing. A rotary feeder such as shown in figure 16 may be used. This equipment provides 116 cups which may be dumped one at a time at the will of the operator. Rotary motion is achieved by a shaft projecting through the top of the tank through an O-ring seal.

Consumable-Electrode Melting

Consumable-electrode melting of chromium has several advantages over the other method, particularly if high purity is a consideration. The chief problem, however, is in the preparation of the consumable electrode, which may be formed by pressing, sintering, or welding.
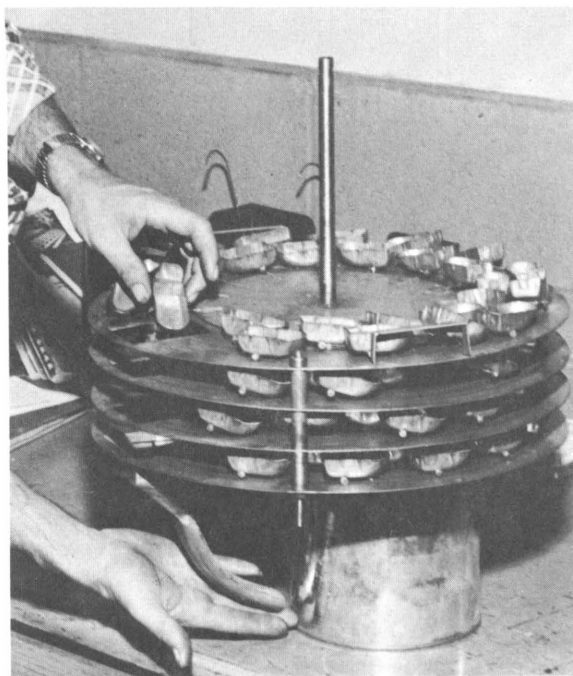
Figure 16.—Rotary feeder for nonconsumable-electrode melting.

Regardless of the method of preparation, the material to be melted must have sufficient electrical conductance to carry the arc current; it must be strong enough to carry its own weight; and be sufficiently straight not to strike the walls of the copper tube. At Albany the practice is to press the granular chromium into 1 by 1 by 10-in bars at 22 tons/in², or 220 tons total pressure. In general, crushed electrolytic chromium will not press into coherent bars unless the particles are about minus 100 mesh. However, if the surfaces of the particles have been purified by treatment in hydrogen, particles slightly larger than minus 60 mesh will press successfully. The cleanlines and/or purity of the particle surfaces has a definite effect on its pressing characteristics. For the preparation of chromium alloys the alloying material is mixed into the base material prior to electrode preparation. The particle sizes of the alloying materials will vary, depending on the plasticity and bonding characteristics of the individual material. For good homogeneity, however, the use of particles smaller than the chromium usually results in more uniform alloy distribution.

Pressed electrodes are sintered in a flowing dry-hydrogen atmosphere at 1,150° C to in-

crease their strength and to remove most of the occluded gases and surface contamination. These sintered bars are joined together by fusion welding in an inert atmosphere. Connection with the electrode holder usually is made by welding the sintered electrode to a chromium adapter which screws onto the electrode.

The operation of the consumable-electrode furnace is identical to that already described. The melting rate is considerably higher than for the other method, being on the order of 300 g/min.

In consumable-electrode melting the pool depth may equal the diameter of the crucible, and severe piping may result if proper care is not exercised to insure progressive solidification from the bottom of the pool when melting is stopped. Generally this is done by reducing the current until solidification starts and then reapplying power to form a new pool. Two blasts at full power and two with reduced current should prevent the formation of deep shrink holes.

The greater pool depth provided by this method is a distinct advantage over side-feed tungsten-electrode melting when alloys are prepared. The larger liquid volume encourages better homogeneity both from the standpoint of a longer solution time and from the possibility of stirring the melt to provide for better mixing.

Stirring is done most easily by the use of a solenoid coil consisting of 1,000 to 2,000 turns of magnet wire wound directly on the nonmagnetic cooling jacket. The passage of a small current through the coil will produce a gentle stirring of the molten pool beneath the arc. This device must be used judiciously, however. Too much current will spin the pool and produce a centrifugal effect.

Atmospheric contamination during melting by either process is negligible, and ingots have been made which consistently have the following analyses:

	Ppm
Oxygen	100 to 500
Hydrogen	8
Nitrogen	>20

Porosity in ingots is due principally to volatile impurities. As an example, ingots cast from as-deposited electrolytic chromium plate which usually contains much hydrogen, often contain
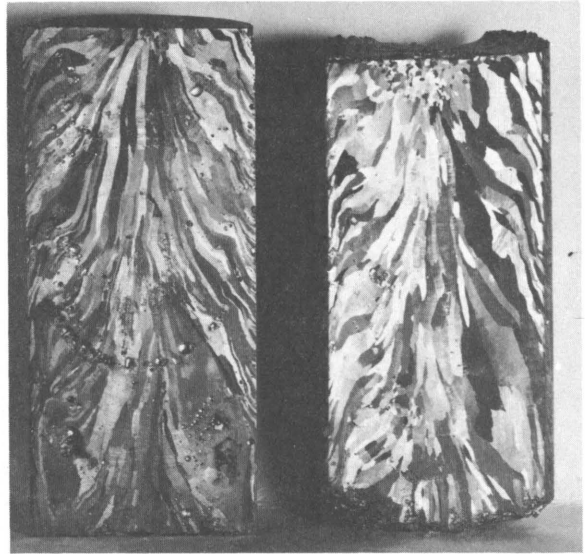
Figure 17.—Chromium ingots illustrating effect of premelting degassing treatment.

many huge gas holes. However, if the electrolytic plate is heated in vacuum to 500° C or to 1,000° C in an inert gas, the number of gas holes is greatly reduced, and only a few remain along the perimeter of the ingot. The effect of premelting treatment is shown clearly in figure 17. Any other volatile material probably will produce similar results. In addition to freedom from porosity, sidewall uniformity and smoothness are desirable. Rough sidewalls are an indication of insufficient heating during melting and can be remedied by using a higher melting current. The use of too much current, of course, will endanger the mold walls, and perhaps introduce some copper contamination. Several typical ingots are shown in figure 18.

THE FUTURE

The limitations to arc melting of chromium depend upon the product rather than the process. The similarity of this technique to that used for titanium suggests that chromium ingots up to 1 ton in weight could be achieved easily. The commercial application of high-purity massive chromium will be the controlling factor in the development of future melting techniques.

Figure 18.—Typical as-cast chromium ingots.

REFERENCES

1. Carlisle, J. S., J. W. Christian, and W. J. Hume-Rothery. J. Inst. Metals, v. 76, 1949, p. 169.

2. Gilbert, H. L., H. A. Johansen, and R. G. Nelson. Malleable Chromium And Its Alloys. BuMines Rept. Inv. 4905, 1952, 22 pp.

3. Greenaway, H. T. Pure Chromium, Its Production and Freezing Point. Commonwealth of Australia, Department of Supply, Aeronautical Res. Lab. Rept. SM 163, January 1951, 8 pp.

4. Johansen, H. A., and G. Asai. Room Temperature Ductile Chromium. Electrochem. Soc., v. 101, No. 12, December 1954, pp. 604–612.

5. Johansen, H. A., H. L. Gilbert, R. G. Nelson, and R. L. Carpenter. Tensile Properties of Pure Chromium At Elevated Temperature. BuMines Rept. of Inv. 5058, 1954, 8 pp.

6. Parke, R. M., and F. P. Bens. Chromium-Base Alloys. Paper in Proc. ASTM Symposium on Materials for Gas Turbines (49th ann. meeting of ASTM), Buffalo, N.Y., June 24–28, 1946; American Society for Testing Materials, Philadelphia, 1946, p. 80.

7. Sully, A. H., E. A. Brandes, and A. G. Provan. J. Inst. Metals, v. 81, 1953, p. 569.

CHAPTER 5.—CONSUMABLE-ELECTRODE ARC MELTING OF THORIUM

By A. H. Roberson and R. A. Beall

With the advent of the "breeding" of uranium 233 from thorium, it became necessary to re-examine the classical methods of melting thorium metal. Because of the stringent physical property and purity requirements for large sections of the metals, techniques once acceptable became intolerable. Metal once considered highly satisfactory for an alloying ingredient was not at all suitable for forging and rolling to strict dimensional and soundness specifications. Further, with the high cost of production, yields came under close screening.

Thorium, like titanium and zirconium, is one of a group of metals which is notorious for its attack on crucibles and its avidity for oxygen and nitrogen at high temperatures. No satisfactory refractory has been developed which will not be dissolved or attacked by the molten metal. At temperatures above 200° C the metal reacts with air to form stable oxides and nitrides. The immediate problem for melters becomes one of crucible material and atmosphere control.

The current industrial melting practice includes two methods: (1) Induction melting in a crucible under a protective atmosphere of argon or in a vacuum, and (2) consumable-electrode arc melting in a reduced-pressure argon-helium atmosphere. The first method has several potential advantages, the principal one being the ability to charge the crucibles with large random-shaped pieces of metal and after the charge is melted, to pour directly into molds. Because of severe limitations imposed by operating in a vacuum-type furnace, the advantages are not as great as they might appear at first glance. Adding materials to the crucibles is not accomplished without problems, and it is difficult to remove the slag or dross from the melted charge prior to pouring. In regard to crucibles, beryllia is said to be a satisfactory material, although its utility is limited by its high cost and health hazards. Stabilized zirconia has been used extensively, and probably is the most common crucible material. The at-tack by molten thorium must be recognized, however, for metal melted in zirconia often contains as much as 1 percent zirconium. Dense graphite is another possibility, its chief disadvantage being the fact that thorium forms carbides readily; hence, material melted in a graphite crucible may be expected to contain an appreciable amount of thorium carbide.

Experience has shown that the consumable-electrode arc furnace is well suited for thorium melting. It obviates crucible contamination, eliminates many impurities by volatilization in the arc, and produces a dense ingot, free of slag or nonmetallic inclusions. It is interesting to note that this is not a novel application, having been suggested by Moore[1] in 1923.

This chapter details some of the experience of the Melting Group of the Bureau of Mines laboratory at Albany, Oreg., which was active in the development of consumable-electrode melting of thorium metal for atomic-energy purposes. Two types of material were presented for melting; Regulus produced by the calcium reduction of thorium fluoride, usually referred to as derbies or biscuit, and electrolytic powder made by fused-salt electrolysis.

Most of the difficulties encountered in arc melting thorium were related to the purity of the raw material rather than to any specific properties of the metal. Unfortunately, some thorium melting stock now available on a commercial scale contains significant amounts of low-boiling point metals such as calcium, magnesium, volatile salts, oxides, or other chemical or metallic compounds that vaporize and dissociate during their passage through the arc. This vaporization or dissociation may absorb appreciable amounts of heat that otherwise would be available for melting and sustaining the arc discharge. The result is arc instability and incomplete metal fusion. Special precautions are necessary to trap condensable vapors and eliminate fumes in order to protect per-

---

[1] Moore, R. W. Preparation of Metallic Uranium. Trans. Electrochem. Soc., v. 43, 1923, pp. 317–328.

sonnel and equipment from radiation hazards. Conversely, this situation has its advantages, since the distillation and volatilization represent an additional purification step for the metal, and when the melting is repeated several times, acceptable ingots can be prepared from low-grade stock.

The basic modification in arc-furnace construction for thorium melting is required for a safety measure. Since the daughter products of thorium are in general volatile, the melting process tends to eliminate them. However, in process of elimination from the metal, they are condensed and concentrated inside the arc furnace and on the sidewall of the ingot. To protect the operating personnel from possible airborne radioactive dust, it is considered good practice to connect the arc furnace, through a large-diameter vacuum valve, to the room ventilation (evacuation) system. Upon opening the furnace to unload, the valve is opened and a heavy draft of air is drawn through the furnace with a large portion of the radioactive dust and fume.

To provide a suitable consumable electrode, the spongy biscuit-shaped metal regulus, which henceforth will be referred to as sponge, may be sawed to appropriate dimensions and then joined by welding in an inert atmosphere box. An alternative method for handling this sponge is to cut or crush the massive material into suitable sizes and then press the pieces into electrodes that again may be welded together. In properly designed equipment it may be possible to press large pieces into suitable shapes without much prior cutting or crushing. Since sponge is rather soft and smears readily, die plates and punches require regular cleaning to prevent galling. Costwise, this latter method has many attractive features. Excellent electrodes 2 by 2 by 10 in have been made by pressing odd-shaped sawed pieces at about 30 tons/in. The compacts were joined later to provide ingots of suitable size. Figure 19 shows the relationship of resistance, density, tensile strength, and pressure.

Both methods were used at the Bureau of Mines. The large biscuit-shaped pieces of sponge
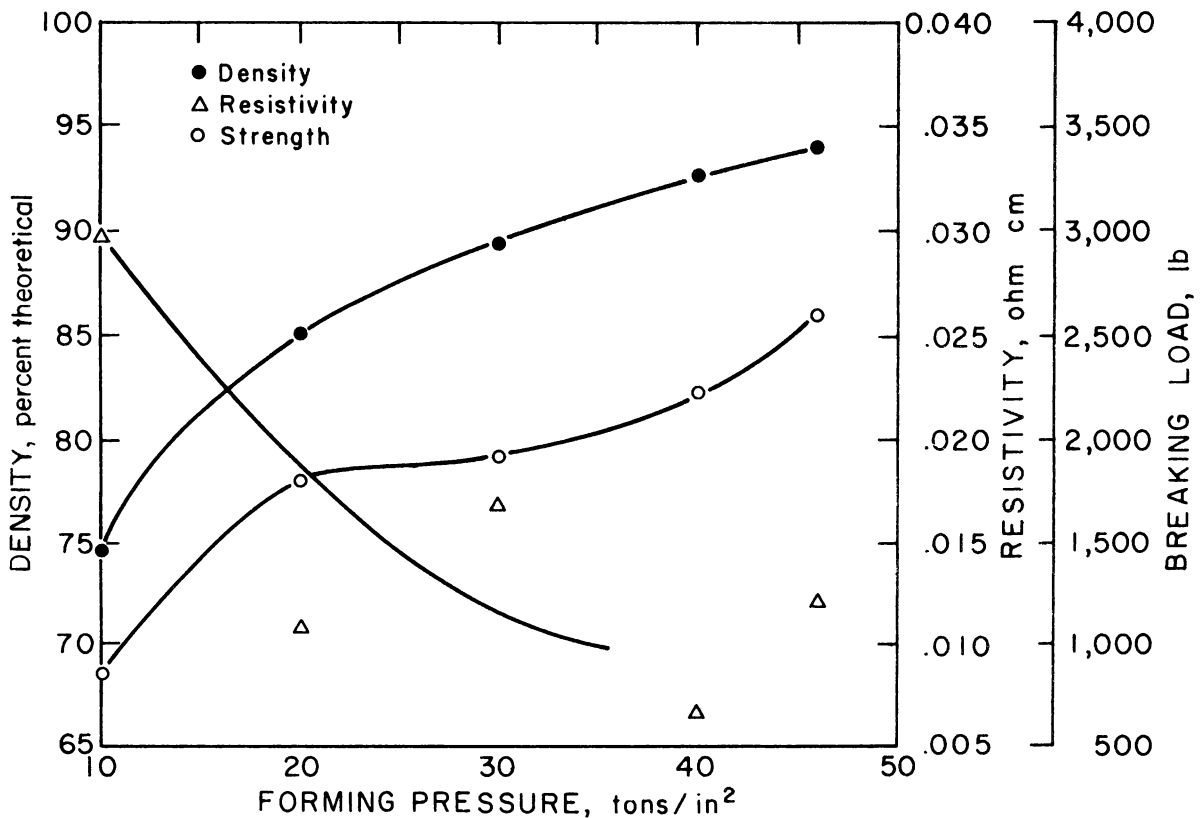
Figure 19.—Physical properties of 2- by 2- by 10-in thorium compacts pressed from ¾-in chopped sponge.

were sawed into suitable sizes and welded end-to-end to make primary electrodes. Scraps from this sawing were pressed into 2- by 2- by 10-inch compacts and welded into electrodes. Both methods worked well; however, sawing and welding involves considerable handling, and, therefore, may become too expensive for an extensive operation.

The extrusion of sponge metal into bars or rods should be considered. With proper equipment and techniques it seems likely that this would provide a cheap method of producing large-size primary electrodes.

Electrolytic powder compresses readily under a pressure of about 45 tons/in² to compacts of approximately 80 percent of the theoretical density. The compacts were joined by welding, although in some cases the powder contained so much adsorbed gas that welding was extremely difficult. Some of the powder from electrolytic cells appears to have a thin coat of oxide surrounding each grain of metal. Even though the powder was compacted into an electrode of acceptable strength and density, the presence of this surface film lowered the conductivity so much that the required amount of current could not be passed through the bar for satisfactory melting, and it was necessary to melt a continuous area long each face of the compact with an electric welding arc in order to obtain the necessary conductivity. This was not always easy to do, however, because the presence of a large amount of adsorbed gas caused boiling and sputtering.

Pretreatment involving heating the pressed bar to 1,000° C in vacuum for 8 hr eliminated the low conductivity and also removed some of the volatiles. The partial sintering of the bar decreased its resistivity from 36,000 ohm-cm to 85 x 10⁻⁶ ohm- cm, which generally permitted a satisfactory melting.

It should be emphasized that these observations on electrolytic powder concern only one lot. Other lots of different quality or perhaps of a different origin might have entirely different characteristics. The information is included simply as a guide for possible future work.

MELTING

The production of large ingots involved a two-step program. Generally, primary electrodes were melted into 4- or 5-in-diam ingots. These in turn became the secondary electrodes and were melted into a larger diameter ingot, the final size depending upon fabrication demands. In either step the melting operation was conducted under a partial pressure of helium and argon. It is generally recognized that argon alone will produce a more stable arc, while the helium assists in attaining a higher melting rate. The mixture afforded a satisfactory compromise. No attempt was made to purify either gas, since experience with zirconium melting showed that the amount of oxygen or nitrogen directly attributed to the inert gases generally was below the analytical thresholds.

This duplex melting was especially advantageous since it allowed two possible chances for the elimination of adsorbed gases and the contaminating volatiles. When electrodes of welded sponge were melted, it was not unusual for large quantities of dense fumes to be produced. The general remedy for this condition was to open the vacuum pump valve, pump out the chamber, and back fill with the argon-helium mixture. The presence of certain volatiles encouraged glow discharge at lower pressure and made melting under partial pressures mandatory [2]. This is not an isolated phenomenon; similar conditions have been reported when other metals of high vapor pressure are melted in an arc.

Remelting the primary ingots usually may be accomplished without difficulty. Most of the volatiles are removed in the first melting, and the ingots have sidewalls that usually require only light scalping prior to rolling or extrusion. Frequently, after an operator has gained experience, even this is not necessary, and the only machine work necessary is to surface the ends in order to produce satisfactory billets. Ingots are removed from the crucibles without difficulty, since a 7-in ingot shrink ⅛ in on solidification.

The melting of the electrolytic powder compacts, unless they have been vacuum sintered, is accompanied by a copious evolution of fumes. These must be removed by continuous pumping and melting at the lowest pressure which will permit the maintenance of an arc. In this instance low-pressure melting is possible, since the absence of metallic vapors result in stable arc conditions. Frequently it is necessary to remelt electrolytic thorium three times in order to eliminate completely gas holes in the ingot.

---

[2] More recent experience with higher quality metal shows that thorium can be handled in vacuum.

INGOT QUALITY

Double- or triple-melted ingots from good quality calcium-reduced sponge normally exhibit very little porosity or shrinkage if the melting is terminated gradually. Such a procedure permits a controlled freezing rate of the molten pool and confines the porosity or pipe to a narrow band at the top of the ingot. This is accomplished by extinguishing and restriking the arc for several cycles after the desired ingot length has been achieved. As a result, the molten pool is allowed to freeze gradually from the bottom up, and the shrink pipe accordingly becomes shorter as the pool depth is decreased. Most 7-in-diam ingots, about 18-in long, need to be cropped to eliminate shrink pipes, gas pockets, or porosity at the upper surface. Ingots may be inspected by ultrasonic methods to locate and to determine the size of internal imperfections. Figure 20 shows an etched longitudinal ingot section and reveals the amount of imperfections and their location in an average ingot. The sidewalls of remelted ingots generally are clean and smooth, free from salt inclusions or other condensed volatiles. Hardness is dependent on the quality of the starting material.

An additional remelt will show only a small increase in nitrogen, acid insoluble (ThO_2), and hardness, depending on the amount of machining, welding, etc., which is required to place the metal in the proper electrode shape. Table 3 shows a summary of the quality levels of 300 virgin ingots and 65 recycle ingots produced from derby thorium at the Albany Laboratory.

The electrolytic powder that was melted did not produce the high-quality ingots discussed previously. Impurities, perhaps adsorbed gases or entrained salts from incomplete leaching, caused the as-pressed electrodes to boil badly on melting, and the large volume of released volatiles made the operation difficult. First-melt ingots required heavy scalping, and the remaining metal was porous. Remelting in reduced pressure further eliminated volatiles, but at least one additional melt, and sometimes two, were required to produce acceptable quality ingots.

Leaching the powder in 5 to 10 percent sulfuric acid resulted in the lowering of the acid-insoluble residue in the final ingot, although the melting characteristics were not improved.

Leaching, followed by vacuum sintering at

Figure 20.—Longitudinal ingot section.

$1,000°$ C for 8 hr was an aid in producing acceptable ingots after three meltings.

SCRAP RECOVERY

The quality of ingots melted from scrap material is always lower, as evidenced by an increase in hardness. Ingot soundness is lowered also; longitudinal cracks along the outside of the ingot and severe cracking in the residual

Table 3.—Summary of levels of quality obtained in thorium ingots

	Virgin [1]		Recycle [2]	
	Average	95-percent confidence level	Average	95-percent confidence level
Density, g/cc	11.68	11.57–11.79	11.64	11.578–11.702
Percent:				
Thoria	.99	2.58	2.42	3.72
Zirconium	([3])	—	([3])	—
Parts per million:				
Aluminum	44.7	72.4	13.0	15.4
Beryllium	—	—	—	—
Boron	.61	1.11	.5	.8
Cadmium	<.2	<.2	<.2	<.2
Calcium	20	50	<50	100
Carbon	100	160	193	285
Chromium	60	95	<60	100
Copper	75	140	<60	125
Dysprosium	10	2.0	.93	2.0
Europium	<.1	<.1	<.1	<.1
Gadolinium	1.5	3.5	1.3	3.2
Hydrogen	—	—	—	—
Iron	373	600	441	641
Magnesium	8	15	6.9	10
Manganese	10	15	9.1	20
Nickel	557	750	486	686
Nitrogen	130	210	211	317
Samarium	.15	.35	.14	.35
Silica	24.5	48.5	30.0	52
Uranium	6.4	12.8	6.0	11.2
Zinc	98	250	43.0	100
Brinell hardness number	54.3	60.3	56.0	60.4

[1] Data from 300 ingots.
[2] Data from 65 ingots.
[3] Not detected.

pool area are not uncommon. Some of these imperfections may be removed by remelting the ingot once more.

Melting is accompanied by the evolution of a large volume of volatiles which condense on the cold crucible walls in layers as much as ½-in thick. The removal of these salts, therefore, requires rather severe scalping losses and the consequent generation of a more highly contaminated scrap which cannot be reclaimed by melting.

Massive scrap such as trim, ends, and collars are cut to a convenient size and tack-welded into usable shapes. When this material is melted, the resulting ingots are exceptionally clean and free from surface porosity. If contamination during cutting, welding, and melting remains low, metal that has been melted three or four times will show only a six to nine-point increase in Brinell hardness.

FURNACE RESIDUES

Furnace residues, fine powder, and salts deposited in the upper part of the furnace, pro-vide an ever-present hazard for the melter of thorium.[3] In the first place, this material is highly radioactive and often finely divided, and thus is a serious health hazard. Secondly, the residues are highly pyrophoric, often igniting as the furnace is opened. Adequate ventilation is essential. Small quantities of the dust should be isolated and stored in individual containers in a good fume hood. Final disposition may be accomplished by controlled burning in a well-filtered burner to prevent atmospheric dispersal of fine radioactive particles. Another alternative is to store the material underwater. In this event, one may expect a continued hydrogen evolution for 60 to 90 days. If for any reason the water is drained off, spontaneous combustion may occur, especially if the containers are stored under summer sun. Normally, residues that remain under water for 6 months are thoroughly passivated, although in one instance a barrel of these residues, after the water had been drained away, ignited spontaneously in cold weather. The material at best is

[3] Lowery, R. R. Radiation Hazards Encountered in Arc Melting Thorium. BuMines Rept. of Inv. 5969, 1962, 22 pp.

unstable and unpredictable, and burning seems to provide the only safe method for disposal.

First-melt furnace residues are quite variable in composition, but total beta plus gamma activities as high as 0.01 μc/g of residue can be expected. Residual accumulations as small as a pound can emit up to 20 milliroentgens per hr, or almost twice the safe level for chronic external exposure to radiation. With good ventilation and other reasonable precautions, the dispersion of furnace residues in the air generally can be limited to 10^{-8} μc/cc or less (beta plus gamma). Nevertheless, even in moderate-scale operations constant attention to safe storage and handling practices is necessary to avoid excessive external exposure or ingestion.

CONCLUSIONS

Consumable-electrode cold-mold arc melting is an efficient method for preparing sound, homogeneous ingots for extrusion or forging from thorium sponge or electrolytic powder.

Electrodes may be formed by cutting sponge into suitable shapes and welding them into suitable sizes, or by pressing the sponge into briquets which later are joined by welding. Electrolytic powder compresses into electrodes which usually require vacuum sintering to remove adsorbed gases.

At least two meltings at reduced pressures are required to remove volatiles and to produce sound gas-free ingots.

CHAPTER 6.—VACUUM ARC MELTING AND CASTING OF COPPER

By P. G. Clites [1]

The Bureau of Mines first investigated the use of the consumable-electrode arc furnace for copper casting when a complicated casting, needed for another research problem, could not be obtained from commercial sources. Since the consummable-electrode arc furnaces were readily available, the castings were attempted in this equipment. These early attempts were successful and indicated the suitability of the process, particularly for the production of centrifugal castings intended for use as vacuum-furnace components. A number of castings were produced that performed satisfactorily in high-vacuum applications.

The objective of the program was to determine whether consumable-electrode vacuum arc melting could be utilized to improve the quality of unalloyed copper ingots and castings. Other research has indicated the desirability of melting and casting copper in vacuum, but no similar work has been reported in which the consumable-electrode arc melting process was utilized. The results of this study indicate that satisfactory ingots and castings can be produced by vacuum arc melting; however, other melting techniques provide better temperature control and make it possible to hold the copper molten longer, thereby effecting greater purification.

The melting and casting techniques employed were similar to those used for reactive and refractory metals. Studies were conducted in which electrolytic tough-pitch copper, electrolytic-cathode copper, and oxygen-free copper were consumable-arc-melted in a vacuum. Samples of these materials were also melted in a vacuum-resistor furnace. Castings were produced in both static and dynamic molds.

EQUIPMENT

Electrical power requirements vary with the diameter of the ingot formed and with the material melted. The power supply for the equipment described furnishes dc power at an open circuit potential of approximately 70 v. Three-inch copper ingots melt satisfactorily at arc currents of 2,000 to 3,000 amp and an arc potential of 25 to 30 v. A general "rule of thumb" places the power requirements at approximately 1,000 amp of arc current per inch of ingot diameter.

Both large- and small-scale casting furnaces were available for this work. (See descriptions in chapter 11 and 13.) Power requirements are somewhat higher for casting heats than for ingot melting. Additional power is required to maintain the necessary volume of molten metal. In the case of copper casting, it was found necessary to line the copper crucible with a graphite cup to reduce the heat loss from the molten metal to the water-cooled ladle [2]. This cup was machined from graphite and pressed into the ladle.

In addition to the arc furnaces used for this study, a vacuum-resistor furnace was also available.[3] In this furnace, the metal to be melted is placed in a 3-in-diam graphite crucible which is located within a split, cylindrical, graphite heating element. This element is heated with a low-voltage, two-phase power supply and is capable of producing temperatures to 2,000° C. The furnace can be evacuated to pressures of less than 1μ, but during the melting of copper, the pressure was observed to increase to as much as 600μ.

The advantages offered by this furnace are that the metal can be held molten for as long as desired and that the furnace provides a convenient method of consolidating copper into electrode stock for the arc furnaces. The ability of the furnace to hold the copper for long periods in the graphite crucible also makes possible the carbon reduction of any copper oxide present.

PROCEDURE AND RESULTS

Ingots and castings were produced from electrolytic tough-pitch copper (ETP), electrolytic-cathode copper (CATH), and oxygen-free copper (OF). The electrolytic tough-pitch copper was in the form of wire bar or electrolytic tough-pitch copper scrap. The electrolytic cathode was a 3/4-in-thick plate as received from the electrolytic cell, and the oxygen-free copper was 2-in-diam rod. These materials were utilized as the electrodes for arc melting.

Electrolytic Tough Pitch Copper

Ingot Melting.—Ingots of electrolytic tough-pitch copper were produced by arc melting in sizes up to and including 8-in diam. Starting material for these ingots consisted of electrolytic tough-pitch copper. These electrodes were first melted into 6-in-diam ingots and then remelted into 8-in-diam ingots. These 8-in ingots were then used as electrodes for subsequent casting heats.

The first melting was accomplished at a furnace pressure of approximately 75μ and 6,000 to 6,500 amp of arc current at an arc potential of 28 to 30 v. The outer surface of each first-melt ingot was machined to remove impurities which tend to collect against the cold surface of the copper crucible. The cleaned first-melt ingots were then remelted into 8-in-diam ingots at 6.500 amp and 28 to 30 v.

Electrolytic tough-pitch copper, when vacuum melted for the first time, evolved a gaseous product that was indicated by the violent agitation of the molten pool. With subsequent vacuum melting, this agitation of the pool diminished. Analyses indicate that some purification of the copper was achieved during each melt. For example, when a wire bar was double-arc-melted in vacuum, the oxygen content was reduced from 537 to 429 ppm. The reduction in oxygen content undoubtedly resulted from the elimination of dissolved gases; dissociation of the copper oxide would not be expected at the furnace pressures observed.[4]

The resistor furnace described previously was used to melt electrolytic tough-pitch copper. Chopped copper was charged into the 3-in-diam graphite crucible of this furnace and melted under vacuum. The metal was allowed to chill in the melting crucible, and the re-

sulting 3-in-diam ingots were machined and joined by welding into electrodes. These electrodes were then double-arc-melted as has been described.

Casting.—The arc-melted ingots prepared from electrolytic tough-pitch copper were used as electrodes for the production of castings. All electrodes for casting heats of this material were fabricated from copper that had been vacuum-arc-melted at least twice. This practice was similar to the procedure followed when melting reactive metals. Attempts to utilize copper that had not been vacuum-melted prior to the casting heat resulted in lower casting efficiencies and made control of the melt more difficult.

Two types of centrifugal castings were produced. One type was a finned tube which was to be used as an air-cooled crucible for consumable-electrode arc furnaces. Castings of this type were prepared from electrolytic tough-pitch copper poured into centrifugal molds of two types: (1) An expendable mold of plaster and graphite and (2) a semiexpendable mold of steel and graphite.

One of the castings and a portion of the steel and graphite mold are shown in figure 21. This casting, which was 18-in long, had 7-in OD and about 3½-in ID. The fins were 3/4-in long and 1/8-in apart. Figure 22 shows this casting after the mold had been stripped and the outer surface had been lightly machined.

Five centrifugal castings similar to the one shown in figure 23 were produced for use as parts of an electron-beam furnace. Molds for these castings were of machined graphite. Four of the five castings were satisfactory, but the fifth was rejected because of porosity. The parts machined from the four satisfactory castings were successfully used in furnaces that operate at an absolute pressure of 10^{-4} to 10^{-6} mm Hg.

It is believed that the porosity noted in the one unsatisfactory casting resulted from gross impurities introduced in reclaimed electrolytic tough pitch copper. The electrode for this heat was prepared from material of questionable origin.

Table 4 summarizes the melting and casting data for these five castings.

One of the difficulties noted when attempting to produce large copper castings was the relatively low percentage of metal that could be poured from the ladle. The heavy skull of

---

4 Darling, A. S. Low Pressure Metallurgy, Vacuum As An Inert Atmosphere. Metallurgia, v. 62, No. 373, November 1960, pp. 187–191.
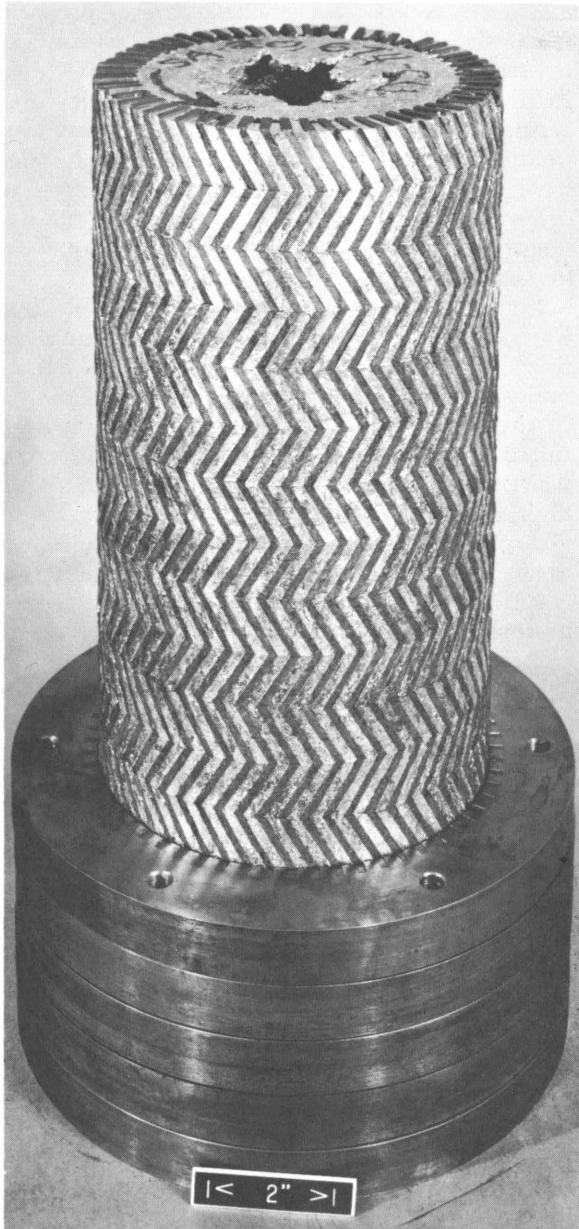
Figure 21.—Finned copper tube cast in steel and graphite mold.

Figure 22.—Finned copper casting after machining.

Figure 23.—Electron-beam furnace component of cast copper.

metal that remained in the ladle following the pour resulted from the high heat conductivity of the copper in contact with the water-cooled copper ladle. To help overcome this difficulty, a thin cup of machined graphite was pressed into the ladle for all the copper casting heats described.

This graphite liner was very effective when used with both 30-in³ ladle of the small-scale furn-

ace and the 300-in³ ladle of the large casting furnace. In these small ladles, all of the metal was poured from the ladle, leaving no skull. The graphite liner also effectively reduced the size of the skulls formed when larger ladles were used; however, the skulls were still heavier than desired. For the casting heats in-

cluded in table 4, 40 to 60 percent of the metal remained in the graphite-lined ladle as skull. When copper was cast from an unlined ladle of the same size, 70 percent remained as skull.

Table 4.—Operating data for melting and spin casting electrolytic tough-pitch copper tubes

Casting number	Nominal arc current, amp	Nominal arc potential, v	Casting weight, lb	Skull weight, lb
1	8,100	30	49.3	44.5
2	9,000	29	68.0	45.3
3	8,300	30	63.6	72.2
4	9,300	29	52.8	76.4
5	9,000	28	59.8	51.7

Data available were insufficient to indicate why the skull could not be completely eliminated from the large ladles as well as from the smaller ones. It was suspected that either the geometry of the larger ladles was at fault or that the time involved in melting was excessive. The larger ladles had a relatively large length-to-diameter ratio which was accentuated when the ladle was lined with graphite. It is believed that the geometry of the ladle was the most significant factor and that with a properly designed ladle and controlled melting variables, the skull could be eliminated from these ladles as well.

Electrolytic Cathode Copper and Oxygen-Free Copper

Ingot Melting.—Arc-melting equipment and procedures used for melting electrolytic-cathode and oxygen-free copper were the same as those discussed for melting electrolytic tough pitch copper.

Electrodes for arc melting were prepared from electrolytic-cathode copper by sawing 1¼-in strips from a ¾-in-thick cathode. These strips were cleaned with hydrochloric acid, washed, and dried, and a copper stub was welded to one end for attachment to the electrode shaft. The oxygen-free copper was received as 2-in-diam rod, cut to the desired length for electrodes, and threaded on one end for attachment to the electrode shaft.

Ingots were prepared by arc melting into water-cooled copper molds and also into graphite-lined molds. The ingots melted in graphite-lined molds had smoother sidewalls than those melted in the unlined molds. The rough sidewalls resulted when beads of spatter from the arc collected along the cold walls, and because of the high thermal conductivity of the copper, were not completely consolidated by the molten pool as melting progressed. The ingots melted in graphite were coated with a thin layer of graphite, however, and analyses indicated an increase in carbon content.

Table 5 summarizes data obtained from analyses of samples of these ingots. Values given are the average of analyses from duplicate samples from each of at least two ingots. Oxygen analyses were obtained by the Leco process, hydrogen by vacuum fusion, and nitrogen, carbon, and sulfur by wet-chemical methods. The arc-melted ingots included in these analyses were all double melted.

Results of the analyses of these ingots indicate that arc melting of electrolytic-cathode copper will remove oxygen, hydrogen, and sulfur to levels similar to the levels in the oxygen-free copper. Arc melting oxygen-free copper in vacuum raised the levels of oxygen and nitrogen slightly. The carbon content of the copper was generally increased whenever graphite crucibles were used.

Table 5.—Analyses of vacuum-melted copper

Sample	Analysis, ppm				
	O	N	H	S	C
Cathode:					
As-received	110	20	0.6	21	70
Arc-melted in copper	30	20	.2	10	60
Arc-melted in graphite	35	10	.1	8	190
Resistance-melted in graphite	20	10	(1)	<10	140
Oxygen-free:					
As-received	20–25	3	.5	8	70
Arc-melted in copper	35–40	15	.1	13	60
Arc-melted in graphite	35	20	.2	9	70

1 Analysis not obtained.

Also included in table 5 are analyses of electrolytic-cathode copper that was vacuum-melted in a graphite-resistor furnace equipped to melt 3-in-diam ingots in a graphite crucible. During melting, pressures in this furnace ranged from less than 1μ Hg, which was the lower limit of the vacuum gage used, to as much as 600μ. The pressure noted during any run was a function of power input, for such input determined the rate at which the impurities in the copper and the copper itself were vaporized.

During melting in this furnace, the copper was held molten for periods of up to 1 hr. This long melting cycle apparently allowed time for the graphite crucible to reduce part of the oxide present. In arc melting, even in graphite-lined crucibles, the copper remained molten for a much shorter time. Other research on vacuum melting of copper has been reported in which the molten copper was degassed for several hours.[5] Higher density was reported for increased degassing time and decreased pressure. While the work conducted at this laboratory did not verify the degree of purification claimed by Stauffer and coworkers, the same trends were noted; that is, the degree of purification increased with increased degassing time and with decreased furnace pressure.

Photomicrographs of the vacuum-melted copper revealed varying degrees of microporosity. Figures 24–28 include representative photomicrographs of samples of electrolytic cathode copper and oxygen-free copper melted by the techniques described. Figures 24–27 compare samples of these two materials after vacuum arc melting with and without a graphite liner in the crucible. Of these samples, oxygen-free copper exhibits less porosity than electrolytic-cathode copper by either arc melting technique, and the least porosity was noted when oxygen-free copper was melted in water-cooled copper. However, the porosity noted for electrolytic-cathode copper in figures 24 and 25 was greatly reduced, as shown in figure 28, when this material was melted in the graphite-resistor furnace.

Static Casting.—Several static castings of the type shown in figure 29 were produced from oxygen-free copper. These castings were produced by consumable-electrode arc melting the copper into a graphite-lined ladle and pouring it into simple, top-pour molds of machined

graphite. As mentioned, it was necessary to pour the molten metal from the ladle quickly to prevent it from solidifying in the ladle. Consequently, there was no opportunity to control either the temperature of the molten metal or the rate at which the mold was filled. Considerable improvement in the castings resulted when provisions were made to pour the molten metal into a reservoir of machined graphite from which the casting was slowly fed. The casting in figure 29 resulted when the metal was poured directly into the mold; the casting in figure 30 resulted when the reservoir was used. The $\frac{5}{16}$-in gate through which the metal poured from the reservoir into the mold can be seen in figure 30, as can the general shape of the reservoir.

The laboratory casting furnace in which these castings were produced did not provide adequate metal or room in the mold chamber for molds with other gating configurations. For this reason, no further efforts were spent in mold design; however, much work could be done in this area to improve the quality of static castings.

Centrifugal Casting.—Electrodes, composed of ingots produced in the arc-melting phase of this work, were used to produce three centrifugal casting. One electrode was of arc-melted electrolytic-cathode copper, one was of arc-melted oxygen-free copper, and one was of graphite-resistor-melted electrolytic-cathode copper. These castings were 8-in long, 7-in-diam cylindrical tubes with $1\frac{1}{4}$-in-thick walls. Each weighed approximately 50 lbs. All three castings were similar in appearance and quality.

Four standard $\frac{1}{2}$-in tensile specimens were machined from each casting. Tensile data obtained from these specimens are included in table 6. Each value represents the average of results obtained from four specimens.

Also included in table 6 are density determinations and electrical resistivity. Values for the resistivity were determined from samples of fully annealed, 0.080-in-diam wires which were drawn from each casting. These wires were annealed for 30 min at 500° C in a helium atmosphere. Resistivity measurements were made on 12-in lengths by means of a Kelvin double bridge.

The data presented in table 6 indicate the similarity of properties of these three castings. The lower density of the resistor-melted cathode copper would not be expected, since the photomicrographs indicate that this material has the least porosity.

---

[5] Stauffer, R. W., K. Fox, and W. O. DiPietro. Vacuum Melting and Casting of Copper. Ind. and Eng. Chem., v. 40, No. 5, May 1948, pp. 820–825.
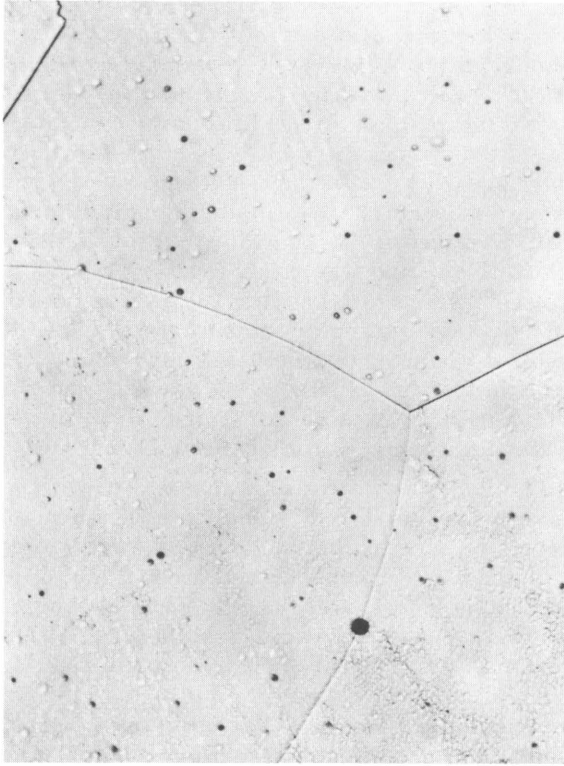
Figure 24.—Photomicrograph of electrolytic cathode copper vacuum-arc-melted in graphite-lined crucible (× 250).
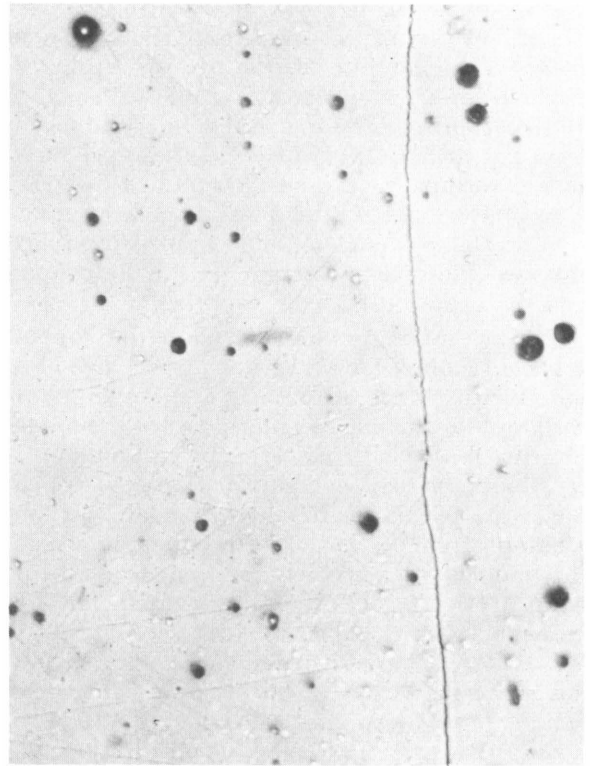
Figure 25.—Photomicrograph of electrolytic cathode copper vacuum-arc-melted in water-cooled copper crucible (× 250).

CONCLUSIONS

The consumable-electrode arc-melting process can be applied to the production of copper ingots by melting into water-cooled copper crucibles or into water-cooled copper crucibles lined with graphite. Copper ingots melted in graphite-lined crucibles will have better sidewalls but will also have a higher carbon content.

Copper ingots with 30 to 35 ppm oxygen can be prepared directly from electrolytic-cathode copper by this method. In general, the impurity levels will be slightly higher than in commercially available oxygen-free copper.

Cast shapes of copper can be produced by this method in both static and dynamic molds. Molds for static castings must be carefully designed to allow the metal to be poured from the ladle quickly and then feed the casting slowly. Casting copper from an unlined, water-cooled ladle is not practical because of the heavy skull formed. The size of the skull can be reduced by using a graphite liner in the ladle.

Although satisfactory ingots and castings can be produced by arc melting, it is advantageous to vacuum-melt copper by other methods that allow the copper to remain molten longer. Arc melting and casting do not permit the control of temperature of the molten metal possible with other methods.

Table 6.—Properties of centrifugally cast copper

Property	Electrode material		
	Arc-melted cathode	Arc-melted oxygen-free	Resistor-melted cathode
Rockwell H hardness	78	79	78
Density ...g/cc	8.9333	8.9348	8.9218
Tensile strength ..psi	22,375	22,175	22,225
Yield strength (0.2 percent offset)....psi	4,900	4,480	4,450
Elongation .... percent	55	55	52
Reduction in area..percent	85.1	84.4	82.6
Elctrical resistivity _____ ohm cm	1.70 x 10⁻⁶	1.70 x 10⁻⁶	1.69 x 10⁻⁶
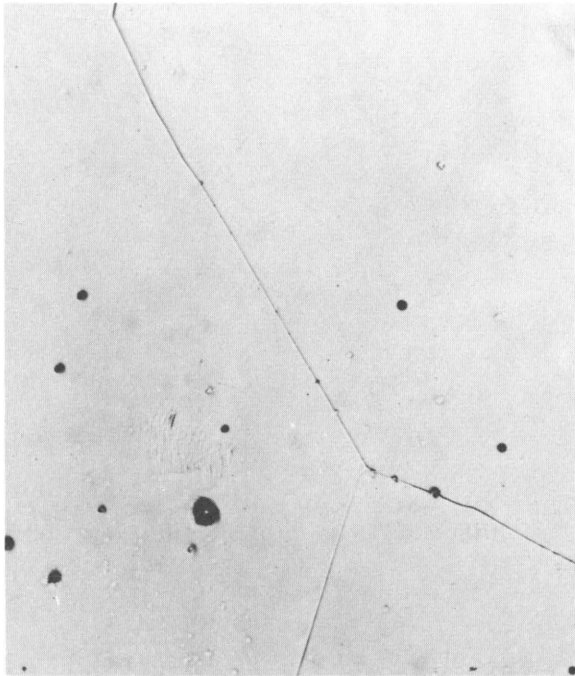
Figure 26.—Photomicrograph of oxygen-free copper vacuum-arc-melted in graphite-lined crucible ($\times$ 250).
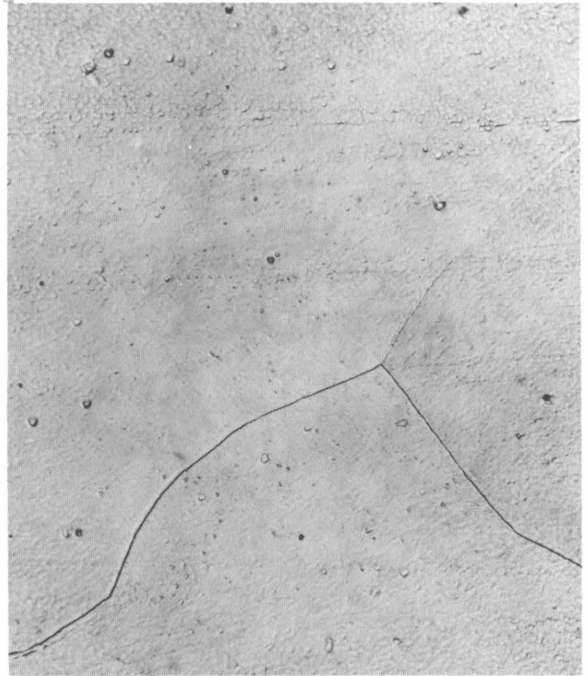
Figure 27.—Photomicrograph of oxygen-free copper vacuum-arc-melted in water-cooled copper crucible ($\times$ 250).
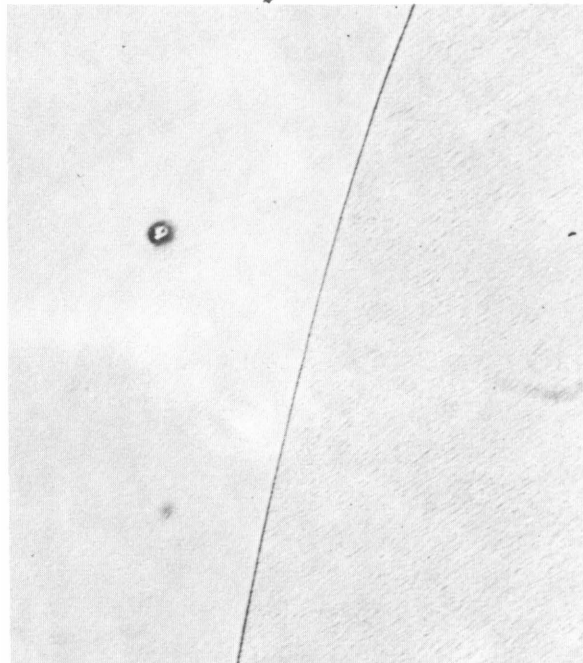
Figure 28.—Photomicrograph of electrolytic cathode copper vacuum-resistor-melted in graphite-lined crucible ($\times$ 250).
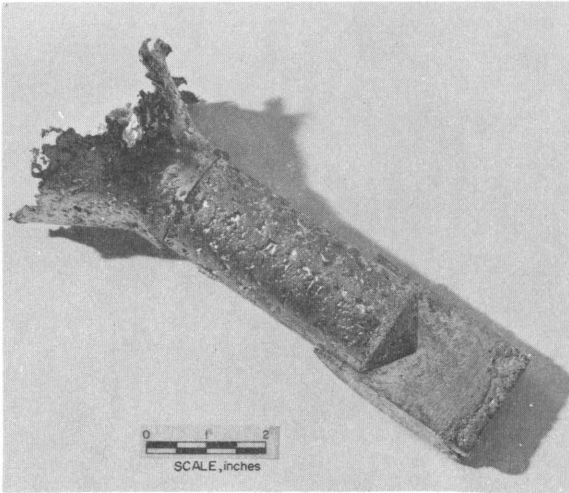
Figure 29.—Static-cast oxygen-free copper, graphite mold.
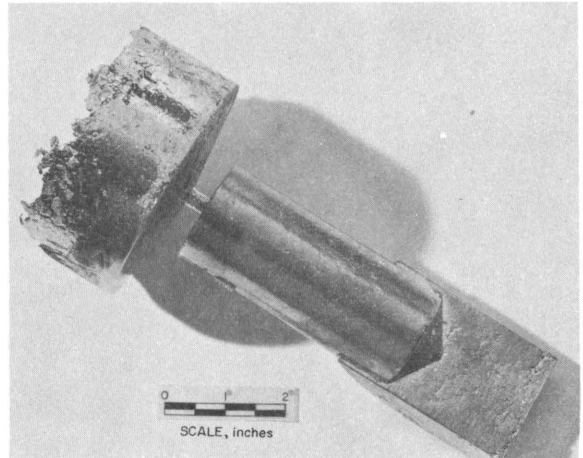
Figure 30.—Static-cast oxygen-free copper, graphite mold with provision for slow feed to casting.

CHAPTER 7.—VARIABLES IN CONSUMABLE-ELECTRODE ARC MELTING

By R. A. Beall, J. O. Borg,[1] and F. W. Wood [2]

As the development of the cold-mold melting technique proceeded, it was characterized by heavy demands for metal production at the expense of orderly study of the variables. This chapter details one of the early studies that helped to give arc-melting a better foundation of basic data upon which to build. The primary subject covered was the geometry of the molten pool. Other pertinent subjects included melting rate, mode of consumption of the electrode, use of alternating current, and ingot-sidewall condition.

EXPERIMENTAL WORK

Pool Studies Technique

For the purpose of this project, the use of a blend of zirconium sponge (BF–12) weighing 2,250 lbs was authorized. This metal was melted first from 2- by 2- by 20-in compacts to 5-in-diam ingots (series 1, see below), remelted into 8-in-diam ingots, quartered, fastened end to end, and remelted many times.

The first item considered in this study was the shape and size of the molten pool. The boundaries of the molten pools during operation are determined by dropping a small piece of alloying metal into the pool and instantly extinguishing the arc. The added metal mixes throughout the molten metal to form an alloy. The resulting ingot is sectioned lengthwise, etched, and photographed, the pool being revealed by the differential etch of the alloy. Figure 31 shows a typical pool.

The study of characteristics was confined to the remelted metal. As the available metal became less through machining loss after several remelts, it was not possible to conclude any of the later series without remelting some of the metal more than once; some of the metal
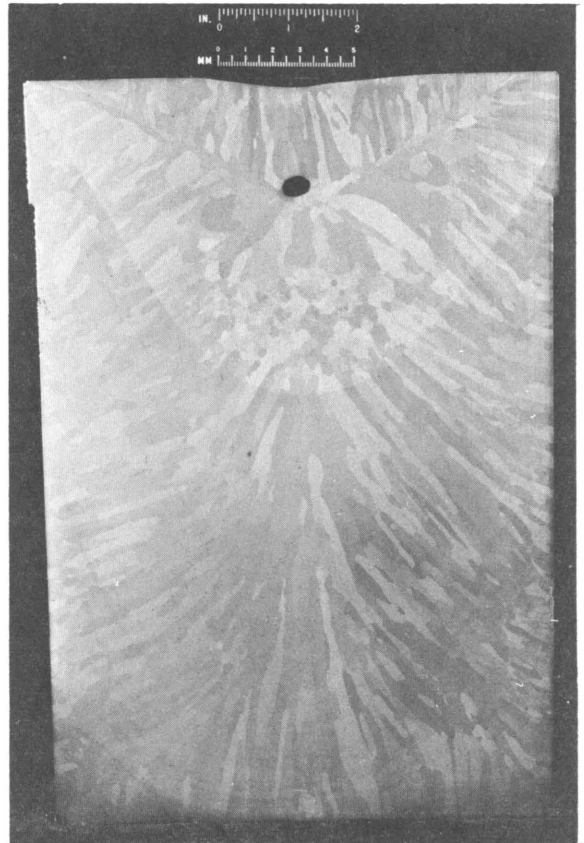
Figure 31.—Typical pool.

was remelted more than 10 times. The series are designated as follows:

Series 1. First melt of sponge to 5-in-diam ingots by regular production practice.

Series 2. Remelt in 8-in cups at 2,000, 3,000, and 4,000 amp at 2-, 20-, and 30-in vacuum, nine ingots; straight polarity direct current (electrode negative).

Series 3. Remelt in 8-in cups at 2,000, 3,000, and 4,000 amp at 2-, 20-, and 30-in vacuum, nine ingots; straight polarity direct current.

---

[1] Formerly chemical engineer with Bureau of Mines, Albany, Oreg., now associated with Boeing Aircraft, Seattle, Wash.

[2] Research physicist, Albany Metallurgy Research Center, Bureau of Mines, Albany, Oreg.

Series 4. Remelt in 8-in cups at 4,000, 5,000, and 6,000 amp at 2-, 20-, and 30-in vacuum, nine ingots; straight polarity direct current.

Series 5. Remelt in 8-in cups at 3,000, 4,000, 5,000, and 6,000 amp at 2-, 20-, and 30-in vacuum, 12 ingots; reverse polarity direct current.

Series 6. Remelt in 8-in cups at 2,000, 3,000, and 3,500 amp at 2-, and 20-in vacuum, six ingots; alternating current, 60 cycles.

The term "30-in vacuum" as applied here indicates not an exact degree of vacuum but rather that the valve between the furnace and the vacuum pump was open wide. The degree of vacuum or pressure in the melting zone in this circumstance depends upon two factors; the leak rate of the furnace and the rate of evolution of permanent gases and condensable vapors from the melting metal. The configuration represented by the hot arc closely confined at the end of a long cold wall tube promotes the possibility of the existence of a pressure gradient. As a matter of fact, during melting at 30-in vacuum, the vacuum gage in the line near the pump often reads less than 1 mm of pressure.

The data in series 2 suffered because of inaccurate voltage and amperage readings. The instruments were changed, and, for the subsequent series, arc potential and time were shown on a recording voltmeter and current on a corrected dial-type meter:

It was not possible to obtain the same spread of current and power in the alternating current series (series 6) because of the limitations of the transformers. Likewise, with this power limitation, it was found difficult to maintain an arc at the low-pressure range (30-in vacuum). The alloying materials used in series 2–6, in order, were chromium, nickel, iron, tin, and chromium.

The size and shape of the molten pool of an arc-melted ingot are important because to produce arc-melted alloys, it is desirable to maintain the largest possible pool and to promote the greatest possible mixing of metal to achieve homogeneity of the alloy. Now the size and shape of the molten pool must be the consequence of the rate of flow of heat into the ingot, the rate or flow of heat out of the ingot, and the distribution of the flow about the boundaries of the ingot. The rate of flow of heat into the ingot is the sum of heat contained in the metal deposited on the ingot from the consumption of the electrode in a given time plus the heat directed by the arc to the ingot, divided by the time involved. The rate of flow of heat from the ingot is primarily the sum of the rate of loss by radiation and convection upwards, plus the rate of loss by conduction to the water-cooled cup. In regard to heat flow by conduction, it must be recalled that a temperature gradient is necessary for flow.

To apply these general principles to specific details of furnace operation, it might be claimed that rate of flow of heat to the ingot is strictly a function of applied power, with the melting rate assumed to be a direct function of power. It will be shown later that this is an erroneous assumption as melting rate is influenced by other considerations. It might also be assumed that as an ingot becomes progressively larger, the rate of heat flow would become correspondingly greater as more surface of the ingot is exposed to water cooling. On the contrary, it is interesting to note that experiments have shown that the temperature at any point on the outside of a water-cooled copper cup during melting operatings is nominal except for a narrow boundary corresponding to the level of the top of the ingot. Since low cup temperature indicates low heat transfer, one is led to conclude that the ingot must be shrinking away from the cup sidewall just below the ingot top; further, a tall ingot should not necessarily have greater conduction loss owing to the larger surface exposed to the cup.

To conclude the discussion, if there is low heat flow about the ingot boundary except at the top, there must be low temperature gradient throughout the cross section of the ingot. If there is low temperature gradient in the ingot body, there is a distinct possibility of obtaining a deep pool by increasing the rate of flow of heat to the top of the ingot.

Pool Studies—Results

Figures 32–34 show the shape of the pools in series 3–6, as revealed by sawing the ingot in half and etching. Figure 32 shows that the pool volume is affected by the power input to the furnace; that is, at each of the three degrees of vacuum, pool sizes increase from left to right, as the power input increases. This is not unexpected. Secondly, the pool both broadens and increases in depth as furnace pressure is reduced. The reverse polarity (electrode positive, pool negative) heats shown in figure 33 have pools equal in depth to the straight polar-
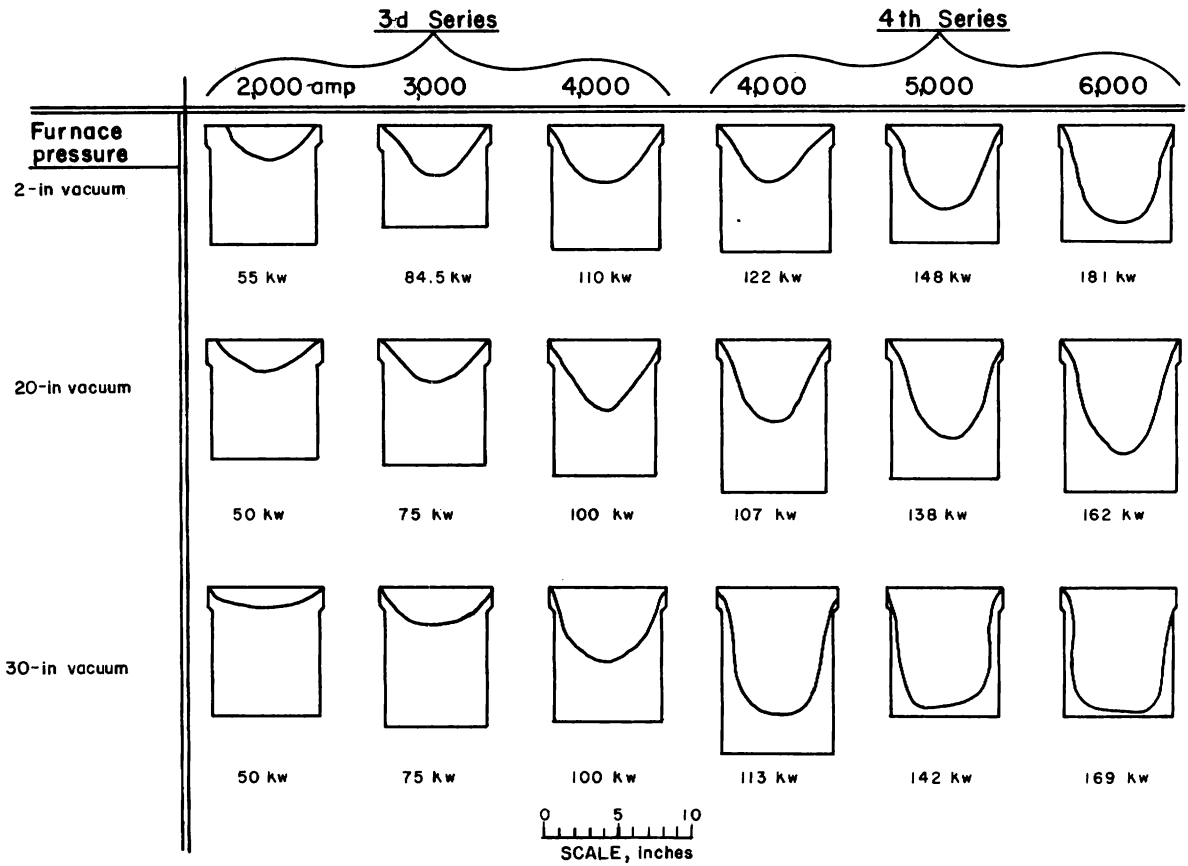
Figure 32.—Pool shapes for series 3 and 4 (straight polarity).
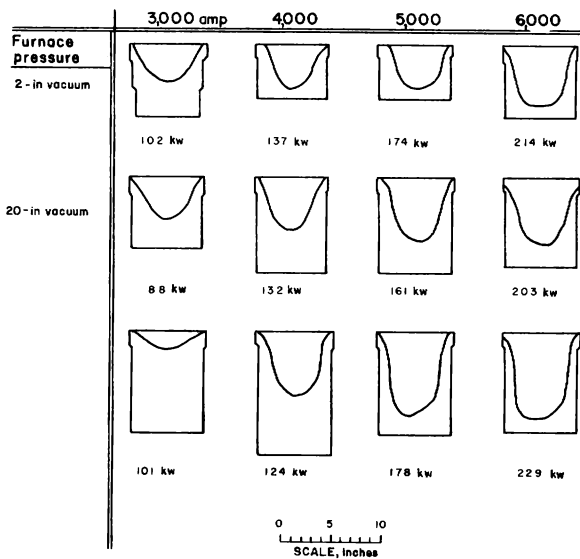
Figure 33.—Pool shapes for series 5
(reverse polarity).
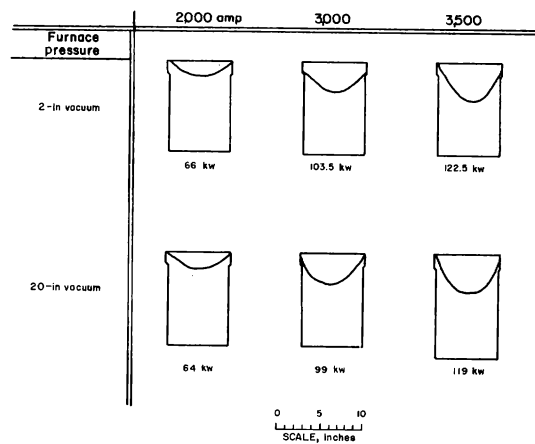
Figure 34.—Pool shapes for series 6
(alternating current).

ity runs, but they tend to be narrower and contain less metal. As might be expected, the ac pools seem to be a compromise between straight and reverse polarity runs.

Figures 35–37 show graphically the relationship between estimated pool volume and power input in kilowatts for series 3–6. It is again shown that ac pools are midway in volume between straight and reverse polarity pools of equal power inputs. Further, low pressure results in greater pool volume in every instance except the low power run at 30-in vacuum, series 5, when glow discharge, caused by too low furnace pressure, interrupted the arc.

Figure 39 shows that electrode consumption rate follows the same general trend observed in the pool-volume versus power-input graphs. This leads one to suspect that pool volume must be closely related to consumption rate. This is graphically confirmed in figure 38. Within the experimental error of the tests performed, it might be stated that molten-pool volume is a direct function of melting rate.

Melting Efficiency

The study of efficiency of consumable-electrode arc melting is not likely to be of interest as an electrical power conservation measure. However, indications are that with greater melting efficiency or rates of electrode consumption deeper molten pools may be achieved. This should lead to greater alloy homogeneity and, as will be shown later, to improved metal-yield efficiency.

Figure 40 shows the heat content of zirconium at various temperatures from experimental results and estimates of K. K. Kelley.[3] With at least 75° C superheat in the molten pool, the heat content of the melted metal is in the order of 20 cal/mole or 219 cal/g. Converting this to electrical units results in a heat content of 0.254 watt hr/g or 15.24 watt min/g. Inverting, this becomes 0.0656 g/watt min or 65.6 g/kw min. This we consider to be the 100 percent melting efficiency of zirconium. Figure 38 shows the maximum rate of electrode consumption as 5,500 g/min at a power input rate of 168 kw. This resolves to 32.7 g/kw min. The efficiency then would be 32.7/65.6 or 50 percent. Figures 41–43 show efficiency as a function of power input for the various series. It must be stated that these values apply only to the size of cup and electrode in use here.

Sidewall Studies

To date, all ingots produced by the consumable-electrode process have a layer of unfused material on the sidewall. It is not known at present if this is a necessary evil of the process or whether, with improvements in the technique, perfect sidewalls may be produced. However, since the sidewalls are unsound, it is important to consider the degree or depth of unsoundness, for this material must be removed before hot working. (Studies of technique for fusing this material to the sound ingot core by welding were published in RI 5149[4].)

Determination of sidewall quality by visual inspection is unreliable, for often what appears to be sound metal is actually full of holes just below the surface. In the final analysis, the interest is in producing a cylindrical ingot of the largest possible finished diameter. Therefore, sidewall quality in this study was dtermined by measuring, on the etched longitudinal cross section of the ingot, the maximum sound diameter, or the distance perpendicular to the axis of the ingot between the innermost flaws on each side. The ratio of the square of the maximum sound diameter to the square of the inside diameter of the melting cup (the ratio of rough volume to finished volume) is considered to be the yield or the metal efficiency. A certain error is inherent here because the as-cast diameter of an ingot is always less than the inside diameter of the melting cup because of shrinkage. Since the shrinkage, for some reason, is not uniform from top to bottom, the cup diameter has been used for consistency. A perfect ingot, if ever achieved, would, by this system of measurement, have a metal efficiency of about 97 percent.

Table 7 shows metal efficiencies for the 45 ingots cast for this program. Various unsuccessful schemes have been tried to correlate the metal efficiency directly with some other characteristics of operation. There appears to be some relationship between metal efficiency and melting efficiency in series 3 and 4 and possibly 6. In series 5 (reverse polarity), however, the relationship is very vague, possibly even inverted. A plot of metal efficiency against power input is shown in figure 44 at three pressures for series 3 and 4. Series 5 (reverse polarity) would show a generally lower metal

---

[3] Letter of Feb. 4, 1954.

[4] Wood, F. W., J. O. Borg, and R. A. Beall. Arc Ingot Conditioning by Sidewall Fusion. BuMines Rept. of Inv. 5149, 1955, 11 pp.

Table 7.—Sidewall studies data

Index	Vacuum, in	Power input, kw	Pool depth, in	Pool volume, in³	Rate of consumption, kg/min	G/min/kw	Melting efficiency, percent	Maximum sound diam, in	Metal efficiency, percent
				SERIES 2					
1a	2	55	1¾	38.2	1.30	23.7	36.1	6⅝	68.3
2a	20	50	2⅛	46.2	1.14	22.8	34.7	7¼	82.2
3a	30	50	1½	28.8	1.17	23.4	36.7	7⅛	79.5
1b	2	84.5	3¼	59.7	1.63	19.3	29.4	7⅛	79.5
2b	20	75	2¹³⁄₁₆	73.6	1.94	25.8	39.3	7⁷⁄₁₆	86.6
3b	30	75	3⁷⁄₁₆	89.7	1.96	26.2	40.0	7⅝	90.8
1c	2	110	4¹¹⁄₁₆	119.2	2.20	20.0	30.5	7⅜	85.0
2c	20	100	4¹³⁄₁₆	134.9	2.54	28.4	43.3	7⅝	90.8
3c	30	100	5¼	143.4	3.00	30.0	45.7	7¾	93.7
				SERIES 3					
1a	2	55	2³⁄₁₆	26.9	0.94	17.1	26.1	6¼	61
2a	20	50	2	34.7	1.05	21.0	32.0	6	56.3
3a	30	50	1¼	37.9	1.49	29.8	45.5	7¼	82.2
1b	2	84.5	3½	59.9	1.76	20.8	31.7	6⅜	63.2
2b	20	75	2⅞	71.5	1.68	22.4	32.2	7	76.5
3b	30	75	2⅞	84.6	2.15	28.7	43.7	7½	88.0
1c	2	110	4	91.7	2.34	21.3	32.5	6⅞	73.7
2c	20	100	4½	108.7	2.44	24.4	37.2	7¼	82.2
3c	30	100	4⅛	115.2	3.05	30.5	46.5	7⁹⁄₁₆	89.4
				SERIES 4					
1a	2	121.6	3½	91.0	2.63	21.6	32.9	7⅛	79.5
2a	20	106.8	5⅜	124.0	2.48	23.2	35.4	7⅜	85.0
3a	30	113.2	8¹¹⁄₁₆	269.9	3.39	29.8	45.5	7⅝	90.8
1b	2	147.5	5⅞	142.5	2.99	20.3	30.9	7½	88.0
2b	20	137.5	6⁵⁄₁₆	156.4	3.31	24.1	36.8	7¼	82.2
3b	30	141.5	8⅝	246.7	4.07	28.8	43.9	7½	88
1c	2	181.2	6¼	179.4	3.77	20.8	31.7	7¼	82.2
2c	20	162.0	7⅛	172.8	4.09	25.2	38.4	7⅜	85.0
3c	30	168.6	8¾	289.1	5.56	33.0	50.4	7½	88.0
				SERIES 5					
1a	2	102	3¾	65.0	2.1	20.6	31.4	6⅛	58.5
2a	20	87.6	4⁷⁄₁₆	83.6	2.1	23.9	36.5	6¼	61.0
3a	30	100.5	2⁵⁄₁₆	35.2	2.4	23.9	36.5	7⅛	79.5
1b	2	137.2	4⁷⁄₁₆	70.8	2.7	19.6	29.9	6¼	61.0
2b	20	132.0	5½	95.7	2.7	20.4	31.1	6⅜	63.2
3b	30	124.0	6⅝	118.9	3.3	26.6	40.6	6⅞	73.7
1c	2	174.0	4⅞	94.7	3.1	17.8	27.2	6⅜	63.2
2c	20	160.5	6⁷⁄₁₆	126.7	3.4	21.2	32.3	7¾	85.0
3c	30	178.5	8⁹⁄₁₆	186.3	4.1	23.0	35.1	6⅞	73.7
1d	2	214.2	6⅝	163.7	4.0	18.6	28.4	6⅞	73.7
2d	20	203.4	6¹⁵⁄₁₆	175.4	3.8	18.7	28.5	7¼	82.2
3d	30	229.2	9¹⁄₁₆	270.9	4.7	20.5	31.2	7	76.5
				SERIES 6					
1a	2	66	1⅞	36.2	1.1	16.6	25.3	6½	65.5
2a	20	64	2	35.6	1.3	20.3	30.9	6⅝	68.3
1b	2	103.5	3¾	89.9	2.5	24.2	36.9	7¾	93.7
2b	20	99.0	3¾	93.5	2.3	23.3	35.5	7	76.5
1c	2	122.5	4¾	119.5	3.2	26.1	39.8	7½	88.0
2c	20	119.0	4¹³⁄₁₆	115.1	3.0	25.2	38.4	7¼	82.2
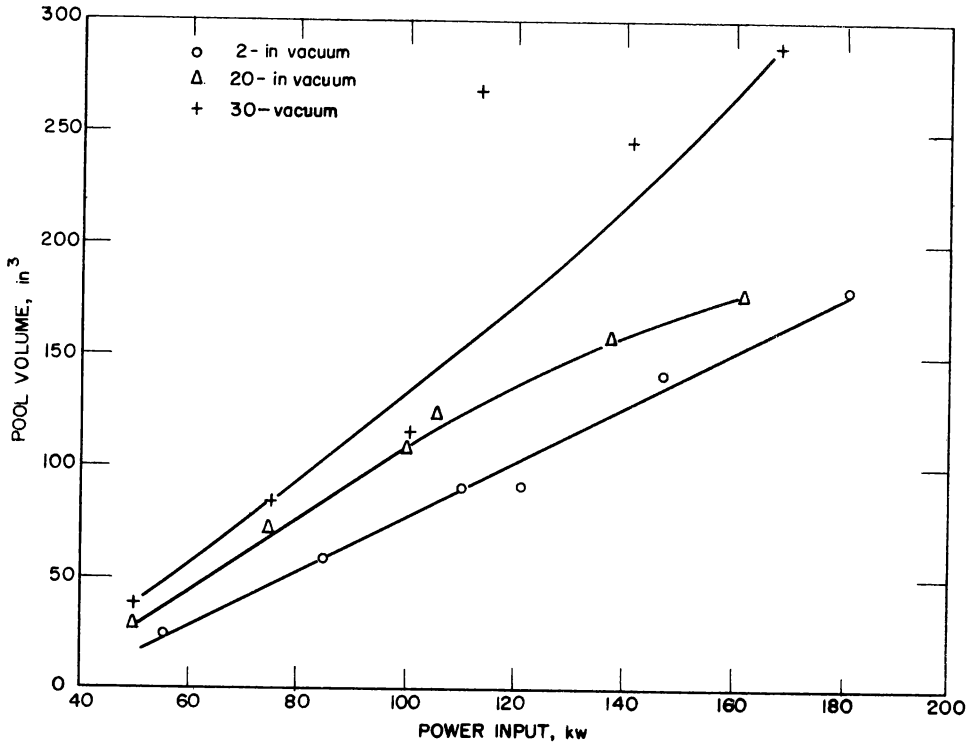
Figure 35.—Pool volume vs. power input, series 3 and 4 (straight polarity).
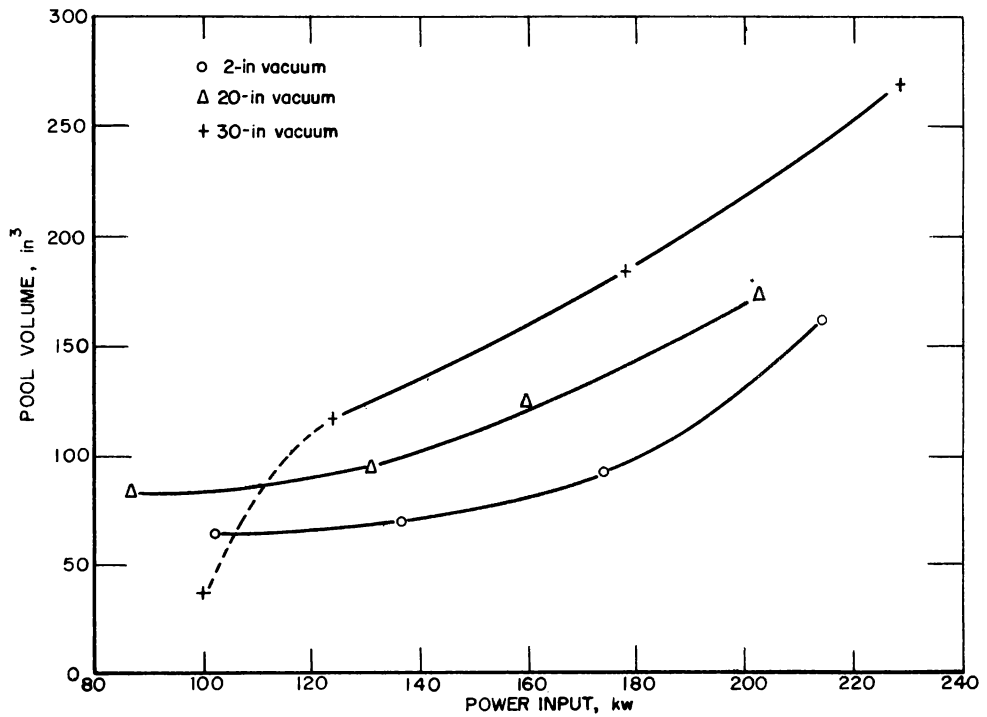
Figure 36.—Pool volume vs. power input, series 5 (reverse polarity).
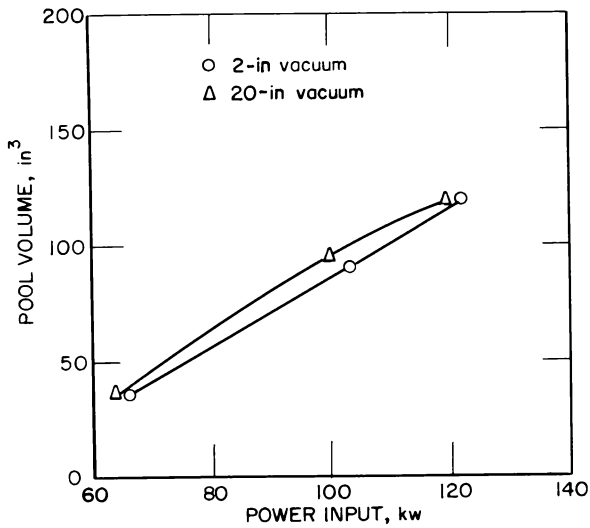
Figure 37.—Pool volume vs. power input, series 6 (alternating current).
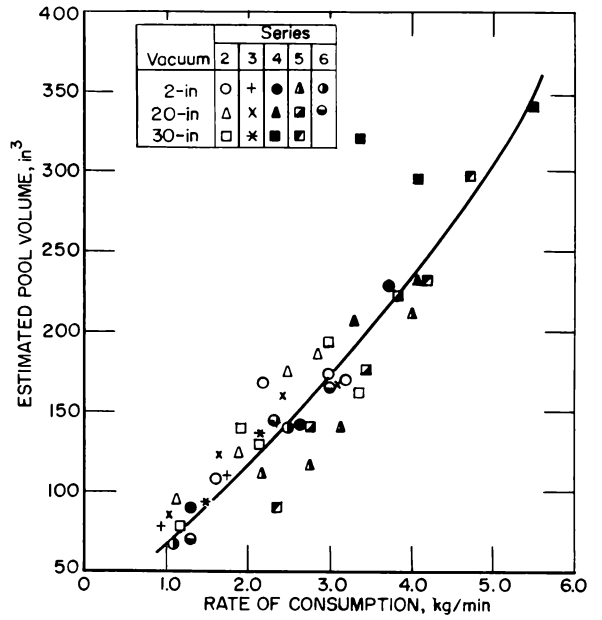
Figure 38.—Estimated pool volume vs. rate of consumption.
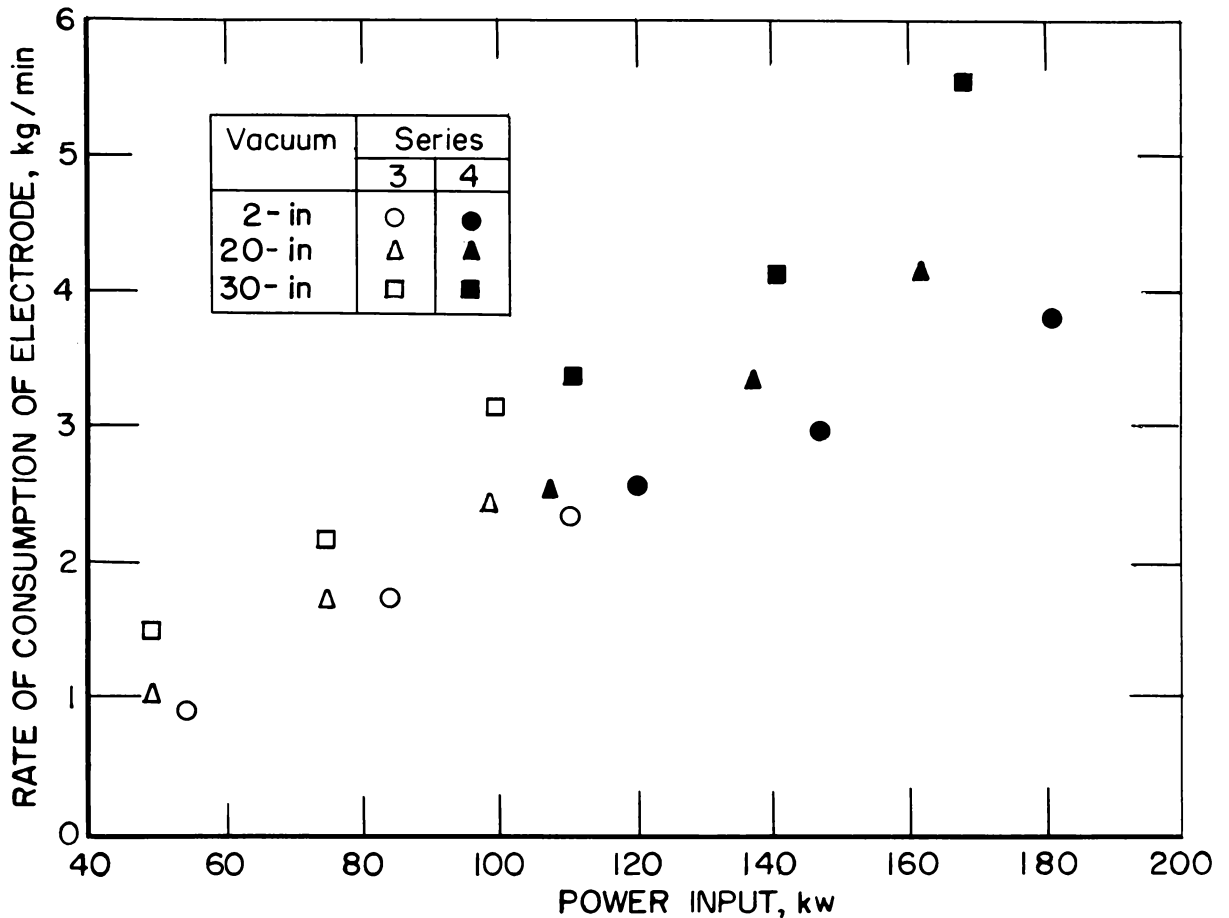
Figure 39.—Rate of consumption vs. power input.
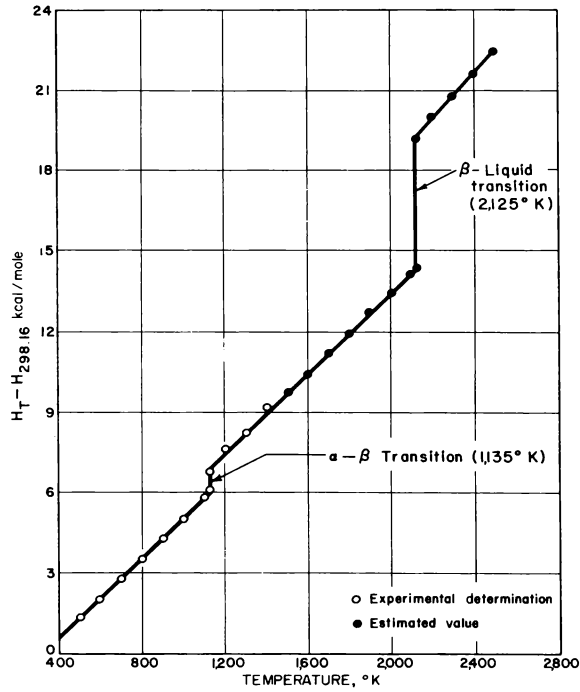
Figure 40.—Heat content of zirconium at elevated temperatures relative to heat content at room temperature *(per K. K. Kelley).*
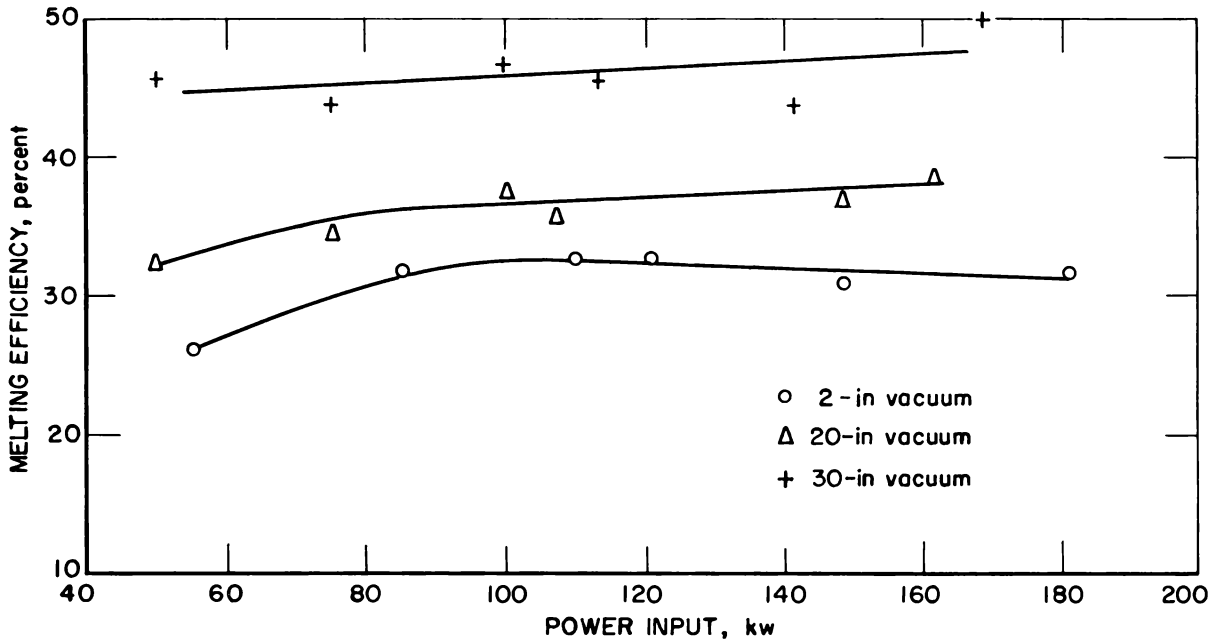
Figure 41.—Melting efficiency vs. power input, series 3 and 4 (straight polarity).
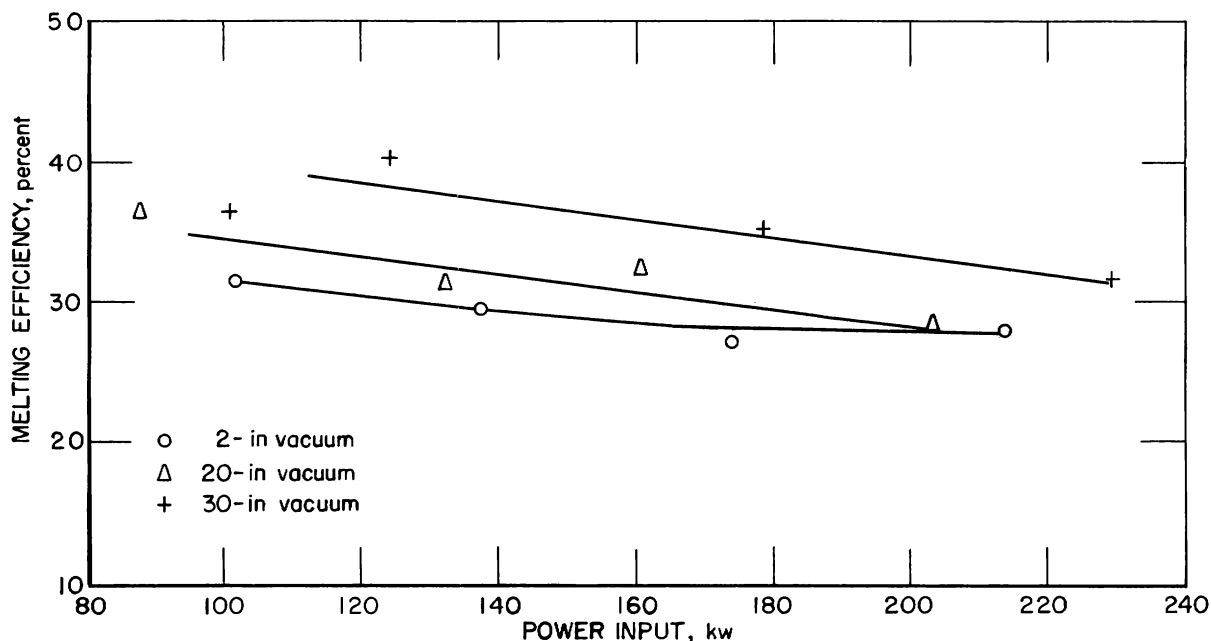
Figure 42.—Melting efficiency vs. power input, series 5 (reverse polarity).
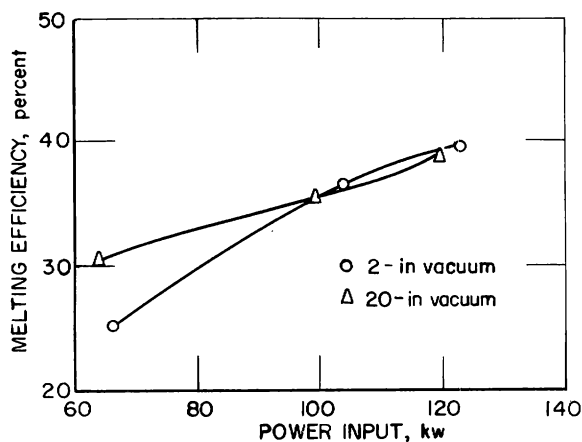
Figure 43.—Melting efficiency vs. power input, series 6 (alternating current).

efficiency. One may conclude from figure 44 that maximum metal efficiency is achieved with low pressures and high powers. As power input is increased, the 2- and 20-in vacuum runs approach the efficiencies yielded by the 30-in vacuum melts. Although the maximum efficiency (93.7 percent) is recorded on an ac melt, it is not felt that this figure is verified sufficiently by the other ac runs to indicate a trend.

The question has often raised as to whether or not the sidewall could be improved by de-creasing the rate of water cooling. If a single test can be considered to be conclusive, the answer is no. This is not surprising in view of the fact that the temperature differential between the ingot skin and the copper cup must be at least 800° C, and the differential inside the wall of the copper cup must be around 800° C. The change of water temperature from 20° to 90° C should not be expected to affect the ingot seriously.

Arc Stability

The study of arc stability or arc voltage and amperage fluctuations has a twofold interest. Violent power surges are hard on equipment; they tear loose flexible power conductors, shake bus connections, and may cause early deterioration of power sources. Secondly, the study of the fluctuations could lead to a better understanding of the mechanics of the metallic arc.

Superficially it has been noted that as the pressure is reduced in an arc-melting furnace, the fluctuations of the meters decreases. The operation at 30-in vacuum is steady and quiet. Figure 46 shows the variation of the voltage during three high current melts: D503 at 2-in vacuum, D510 at 20-in vacuum, and D513 at 30-in vacuum. The recording speed is 3 in/min. The "saw-teeth" in the D513 graph represent the changes in voltage as the electrode is
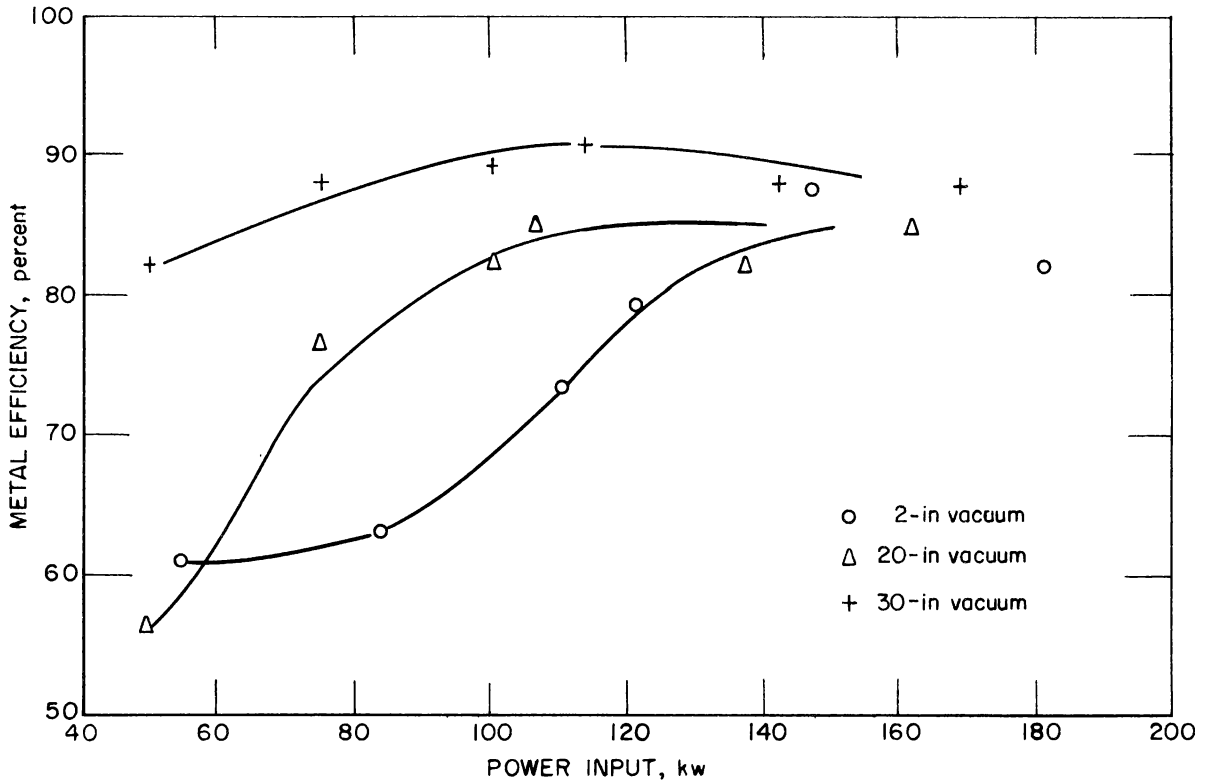
Figure 44.—Metal efficiency vs. power input, series 3 and 4.
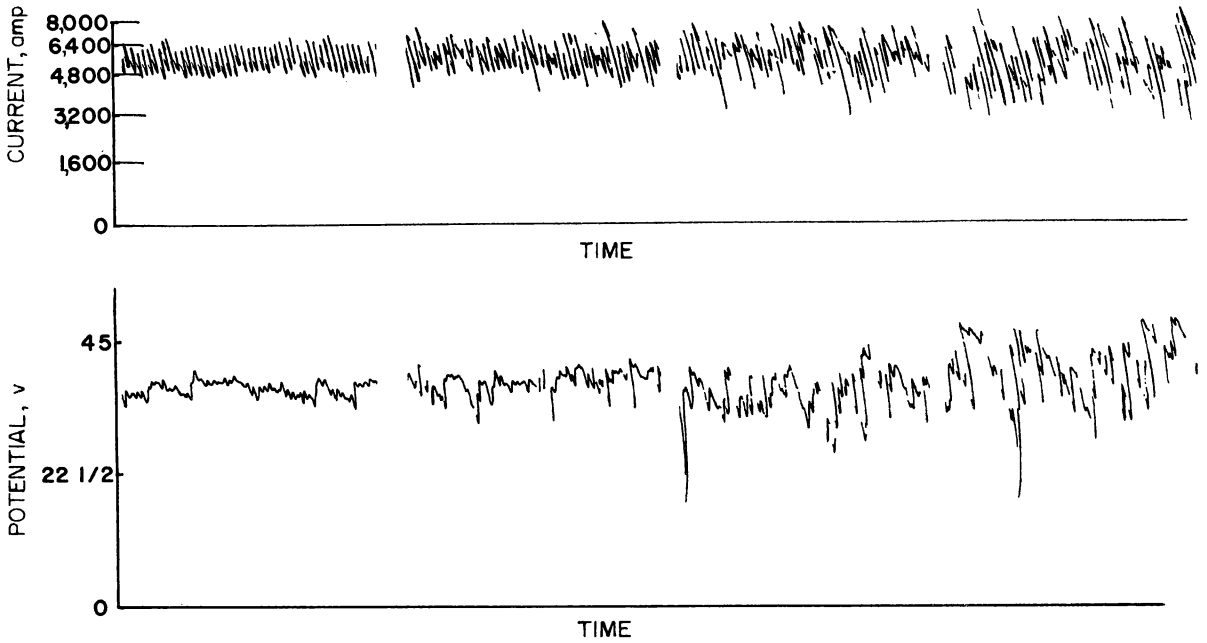
Figure 45.—Potential and current (recorded at 5 cm/sec).
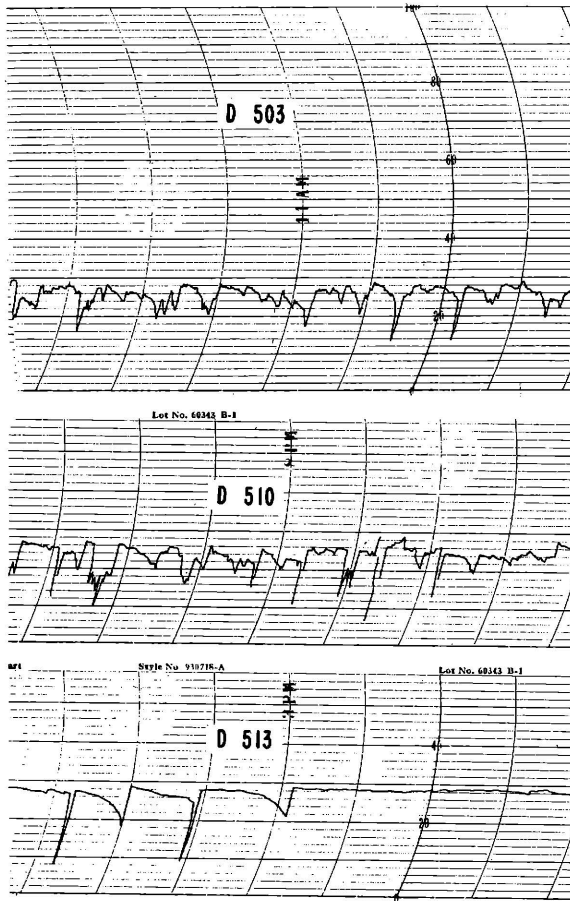
Figure 46.—Potential recordings at 2- 20-, and 30-in vacuum.

burned off and lowered. (Time is read from right to left.) With this speed recording, little, if any, improvement is to be seen between 2-in and 20-in vacuum operation.

Figure 45 shows four segments of a continuous high-speed recording of current and potential during a large consumable-electrode arc melt while the furnace was being pumped down from atmospheric pressure to 30-in vacuum (time reading from right to left). The change in character effected by the change in pressure is easily noted. The regular oscillation is considered to be 60-cycle leakage from the rectifiers. This recording was made at a rate of 5 cm/sec. The reasons for the great change in operation with a change in pressure are discussed by Wood and Beall [5]. Briefly, at atmospheric pressure, molten metal leaves the electrode in elongated drops, which often short across the arc gap and then explode from the heat evolved as they carry the surge of power. At reduced pressure, boiling and bubbling occur at the electrode and probably prevent the formation of elongated drops.

CONCLUSIONS

In this study, a number of ingots have been cast by the consumable-electrode arc process to study the effect of several variables of operation. The study has shown that molten pool volume is a function of both input power and furnace atmosphere. It has been shown that pool volume depends directly upon the rate of electrode consumption. Melting efficiency and metal-yield efficiency are improved by using reduced pressure and straight polarity. The quality of alloy ingots would be improved by deep molten pools, promoting mixing. Therefore, reduced pressure is recomended for production of zirconium and zirconium-alloy ingots.

5 Wood, F. W., and R. A. Beall. Studies of High-Current Metallic Arcs. BuMines Bull. 625, 1965, 84 pp.

CHAPTER 8.—HEAT TRANSFER TO WATER-COOLED COPPER CRUCIBLES DURING VACUUM ARC MELTING

By P. G. Clites and R. A. Beall

This chapter details the results of several experiments conducted with vacuum-arc melting equipment in which heat transfer from the molten charge to the cooling medium was studied. This work was sponsored by the Atomic Energy Commission under contract AT (11-1) 599.

Cooling of the crucible is characterized by high heat fluxes, and the use of water represents a potential safety hazard in that the crucible is occasionally ruptured during melting with the resultant mixing of molten metal with water. In rare instances, particularly during the melting of reactive metals, this mixing of water and molten metal has resulted in serious explosions in which a number of fatalities have occurred.

As a safeguard against this hazard, practically all large furnaces for melting reactive metals are now installed in vented explosion vaults and are extensively equipped with safety interlocks. Alternate coolants have also been investigated (2–4), but water has remained the primary coolant.

It is generally agreed that local overheating of the crucible causes crucible rupture, but the reasons for the local overheating are not fully understood. Suggested reasons include defects in the crucible wall, defects in the cooling system, localized wetting or alloying of the ingot and crucible wall, and irregularities in the arc discharge (12).

Little information is available on rates of heat transfer, crucible wall temperatures, and other criteria useful in designing cooling systems for the crucible. Most cooling-sytem design is based on theoretical assumptions regarding the mode of heat transfer to the crucible plus experience gained through years of melting. Theoretical aspects of cooling of the crucible during arc melting are contained in the work of Rossin (9), and some of the work in the field of continuous casting (10) is closely re-

lated. A more recent publication (3) was based on the solution by means of a computer of a mathematical model of heat flow during the consumable electrode arc melting of molybdenum.

In this report, experimental values of heat flux from the water-cooled copper crucible are presented, and the effects of some of the variables associated with the process are shown. The data presented were obtained during the consumable electrode arc melting of zirconium, titanium, and steel ingots up to 8-in diam using straight polarity (electrode negative) direct current.

Initial studies were conducted during non-consumable-electrode melting of $2\frac{5}{16}$-in-diam ingots. These heats were conducted in a six-piece crucible in which average values of heat flux over short increments of crucible length were determined. Small-scale, consumable-electrode heats were conducted in a two-piece, $2\frac{5}{16}$-in-diam crucible, and the technique developed was then applied to consumable electrode melting in a two-piece, 8-in-diam crucible. Data were also obtained on crucible wall temperatures and on the effectiveness of water jackets with very narrow annular spacing.

The information obtained in this study is considered representative of conditions existing during consumable electrode arc melting by industrial units, particularly for the reactive metals. The values of heat flux given are not intended to represent conditions that exist during the starting of a melting operation or when the ingot is very short. Determinations of heat flux during this portion of the melting cycle would be a study in itself. The values of heat flux given are intended to represent conditions after the ingot becomes at least one diameter in length. After this length has been achieved, melting has become relatively stable and the effect of heat transfer to the crucible bottom has diminished.

50

THEORETICAL PATTERN OF HEAT TRANSFER FROM INGOT TO COOLING WATER

Figure 47 represents the cross section of an ingot during consumable electrode arc melting in a water cooled copper crucible. During melting, the electrode (A) is consumed by heat of the direct current arc (B), which is maintained between the electrode and the molten pool (E). Normally, this molten pool extends nearly to the wall of the copper crucible (C), which is cooled by the water flow in the annular water jacket (4). The size and shape of the molten pool will depend on the conditions prevailing during melting, particularly on arc current and arc potential. The molten metal solidifies where it contacts the cold wall of the crucible and shrinks sufficiently to leave a gap (6) between the ingot (G) and the crucible wall.

The rate of heat transfer along the length of the crucible varies over a wide range of values with high values of heat flux near the top of the ingot where molten metal from the pool splashes against the crucible wall. High heat transfer rates also occur in an area just above the top of the ingot where molten spatter from the electrode strikes the wall to form a crown of metal. Bureau research on the effect of extremely long arcs indicated the existence of two areas of high wall temperatures above the ingot top (12). These two areas of high temperature concided with the excessively high crowns formed during melting under these arc conditions.
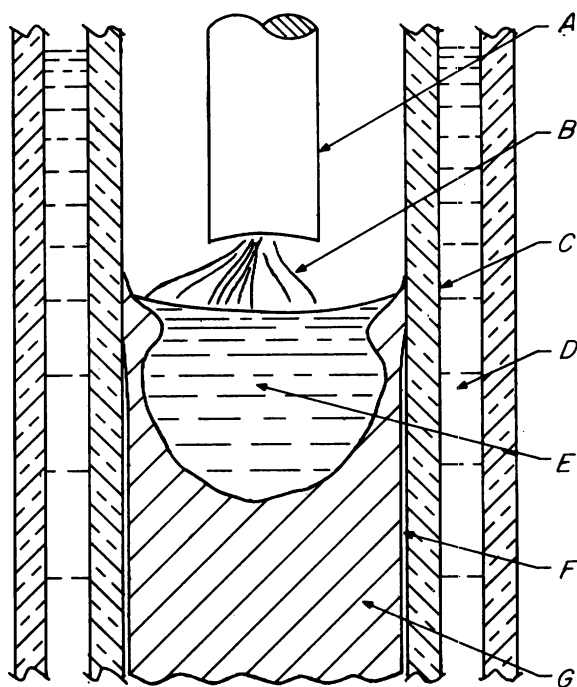
The rate of heat transfer is greatly reduced along the lower portion of the ingot where solidification and cooling of the ingot result in shrinkage of the ingot away from the crucible walls. Heat transfer rates are also relatively low a few inches above the ingot where radiation from the hot electrode, the arc, and the molten pool contribute heat to the crucible wall. Heat transfer rates through the bottom of the ingot are greatly reduced for the same reason heat transfer rates on the lower ingot sides are low. Solidification and cooling of the ingot result in shrinkage and poor contact with the bottom. One of the best evidences of this fact is the thin layer of solidified metal that remains in a casting ladle following a consumable-electrode casting heat. Such a skull of metal is shown in figure 48 and is typical of skulls obtained. On occasions, intimate contact occurs at a spot where the skull becomes welded to the ladle wall. When this happens, the skull thickens markedly at the point of good thermal content. In general, however, the thermal resistance between the ingot and crucible is relatively high along the lower surfaces of the wall and along the bottom.

In the experimental work conducted, it was assumed that uniform arc conditions existed throughout each run. In addition, it was assumed that after the ingot had developed to a length equal to one diameter, the heat flux profile did not change with increasing ingot length [1]. A mathematical study of the distribution of temperature and heat flow in arc-melted ingots is given by Wood (11).

A Electrode   B Direct current arc
C Copper crucible wall   D Water jacket   E Molten pool   F Shrinkage gap   G Ingot

Figure 47.—Cross section of ingot during consumable electrode arc melting in water-cooled copper crucible.

EXPERIMENTAL PROCEDURE AND RESULTS

The studies conducted were divided into three major areas: (1) Nonconsumable elec-

Figure 48.—Skull of zirconium remaining in the crucible of a consumable electrode are melting and casting furnace after pouring.

A 1/2-inch tungsten electrode
B Inlet and outlet pipes
C Mica insulation
D Thermocouple wells
E Ingot
F Water jacket
G Adjustable ingot support

Figure 49.—Six-piece crucible for heat transfer studies during nonconsumable electrode arc melting.

trode arc melting in a six-piece crucible, (2) consumable electrode arc melting in a two-piece crucible, and (3) the effect of narrow annular spacing for water jackets. The work with the two-piece crucibles received the greatest attention, since consumable electrode arc melting is of more commercial importance than is nonconsumable electrode arc melting. Melting studies were conducted in two-piece crucibles of $2\frac{5}{16}$-in diam and 8-in diam. The experiments on nonconsumable electrode melting and the study of water jackets with narrow annular spacing were conducted in $2\frac{5}{16}$-in-diam crucibles.

Nonconsumable-Electrode Arc Melting Studies

First attempts to measure the distribution of heat transfer rates along the length of the crucible were made with a nonconsumable tungsten electrode and a crucible divided into six increments of length. A diagram of the crucible is shown in figure 49. The crucible was divided into one 3-in length at the bottom, four $\frac{1}{2}$-in lengths, and one 1-in length at the top. These

sections were designated A through F from bottom to top. Section C was equipped with two iron-constantan thermocouples installed as shown in the insert of figure 49. Detail of the mica insulation between sections is also shown in the insert of figure 49. Each section was cooled by an individual water-cooling circuit. Water inlet and exhaust was by means of $\frac{3}{8}$-in-OD copper tubing which connected to a circumferential water jacket machined in each section.

The rate of heat transfer to each section was determined by measuring coolant flow rates and the temperature change of water for each section during melting of a zirconium ingot. For each run, the ingot was positioned with the top of the ingot at a selected level in the crucible and an arc was maintained between a $\frac{1}{2}$-in-diam tungsten electrode and the ingot. Recordings were made of arc current and arc potential for runs conducted at arc currents ranging from 750 to 1,200 amp. As soon as the run had reached equilibrium conditions, coolant flow rates and temperature changes were obtained for each of the crucible sections. Coolant flow rates were determined by weighing

samples of coolant taken over a 1-to 2-min interval during the run. Inlet and oulet temperatures of the coolant were measured by means of mercury thermometers. From these data, the heat transfer rates from the ingot to each of the crucible sections were determined.

Figure 50 summarizes data for a series of runs at various power levels from 19 to 36 kw. For these runs, the arc gap was 0.4 in, the furnace pressure was 400 torr of helium, and the ingot top was at the midpoint of section C of the crucible. The values plotted in figure 50 represent the average value of heat flux for each individual crucible section. Maximum heat flux occurred in section C for all power levels and was greatly reduced both above and below this section.

High values of heat flux occurred in section C because of direct radiation from the arc to the crucible and because of the proximity of the molten pool to the crucible wall. At the upper surface of the ingot, only a thin skin of solid metal separated the crucible wall from the molten pool, and portions of this skin were continually melted and reformed as the arc moved about the surface of the pool. Further down from the top of the ingot, heat transfer rates

decreased as a result of shrinkage of the ingot from the walls of the crucible.

With increased power input, the band of high heat transfer at the top of the ingot was increased in width. Heat flux to section B of the crucible increased markedly as the power was increased from 27 to 36 kw. Very little increase in heat flux to section B was noted with the power increase from 18 to 27 km because the band of high heat transfer had not been widened sufficiently to affect section B.

In addition to the information on the distribution of heat flux along the length of the ingot, data were obained on crucible wall temperatures during nonconsumable-electrode melting. For these tests, two iron-constantan thermocouples were imbedded in the wall of section C of the segmented crucible. These thermocouples were located at the midpoint of the $\frac{1}{2}$-in length of this section of the crucible as shown in the insert of figure 49, and provided a measurement of the temperature gradient through a portion of the crucible wall. The outputs from these thermocouples were recorded during nonconsumable-electrode arc melting of a zirconium ingot, the top of which was at the same level as the thermocouples.

The radial position of each of the two thermocouples was measured optically on a movable-stage metallographic microscope after sectioning the crucible at the thermocouple junctions. The temperature of the inside surface of the crucible wall was then calculated (6) from the relation-

$$t_i = t_1 + \frac{\Delta t \ln \dfrac{r_1}{r_i}}{\ln \dfrac{r_2}{r_1}} , \qquad (1)$$

ship where t_i was the temperature of the inside surface of the crucible wall, t_1 was the temperature indicated by the thermocouple nearest the inside surface of the crucible wall, and Δt was the temperature difference between the two thermocouples. The radial distance to the inside surface of the crucible, r_i, was 1.156 in; to the inside thermocouple, r_1, was 1.235 in; and to the outer thermocouple, r_2, was 1.352 in. Substituting these values in equation 1 yields the relationship:

$$t_i = t_1 + 0.725 \Delta t.$$

Table 8 lists data obtained at various power levels, and figure 51 is a plot of the calculated temperatures of the inside surface of the $2\frac{5}{16}$-in-diam crucible as a function of power input. Both
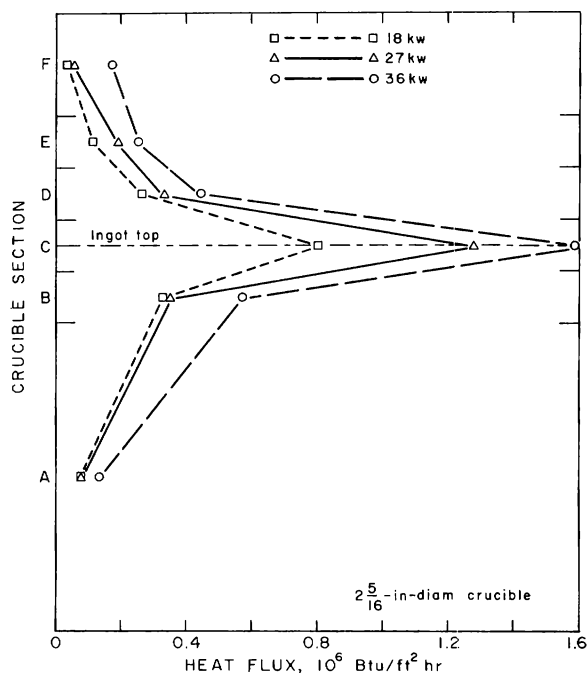
Figure 50.—Distribution of heat flux along length of crucible during nonconsumable electrode arc melting of zirconium.
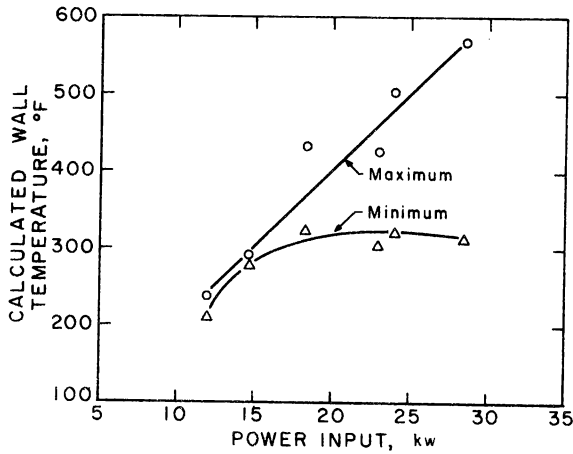
Figure 51.—Calculated temperatures of inside surface of crucible vs. power input. Nonconsumable electrode, 2-5/16-in zirconium ingot.

the maximum and minimum observed values are included in table 8 and in figure 51 to provide an indication of the variation in the wall temperature noted for any given power level. This variation was caused by movement of the arc and the subsequent nonsymmetry of the molten pool. At lower power levels, the differences between maximum and minimum temperatures were relatively small, but the differences became larger as the power input increased. The maximum values occurred when the arc was directed toward the side of the crucible containing the thermocouples. Table 8 also includes

values of heat flux calculated from the temperature gradient within the crucible wall.

The trends noted from these data are considered of greater significance than the actual numerical values reported. Precise determination of the short distance between the two thermocouples was impossible because of the uncertainty of the exact location of the junction within the thermocouple bead. The effect of removal of a portion of the wall for the thermocouple installation was an additional unknown which contributed to the uncertainty of the calculations. For these reasons, these data are presented to indicate trends in wall temperature and radial heat flux rather than precise values. Values of heat flux calculated from cooling-water data are considered more precise.

The experimental work conducted with non-consumable electrode melting in the six-piece crucible provided background information for the more important studies of heat transfer from the ingot to the crucible during consumable electrode arc melting. Consumable electrode studies were not conducted in the six-piece crucible because of the difficulty of instrumenting six separate cooling circuits to yield meaningful data and because of the limited cooling capacity of certain of the individual crucible sections.

Consumable-Electrode Arc Melting Studies

The study of heat transfer during consumable electrode arc melting was difficult because the length of the ingot, and consequently the posi-

Table 8.—Maximum and minimum calculated wall temperatures and radial heat flux

Power input, kw	t_1, °F	t_2, °F[1]	Δt, °F	t_1, °F	Radial heat flux,[2] Btu/ft²hr
12.0	Max. 212 Min. 187	180 158	32 29	235 208	0.71 x 10⁶ .64 x 10⁶
14.7	Max. 259 Min. 253	216 207	43 46	290 286	.95 x 10⁶ 1.02 x 10⁶
18.4	Max. 367 Min. 284	275 232	92 52	434 322	2.04 x 10⁶ 1.15 x 10⁶
23.0	Max. 374 Min. 270	293 226	71 44	426 302	1.57 x 10⁶ .98 x 10⁶
25.0	Max. 430 Min. 284	327 234	103 50	505 320	2.28 x 10⁶ 1.11 x 10⁶
28.6	Max. 484 Min. 275	354 226	130 49	578 311	2.88 x 10⁶ 1.09 x 10⁶

[1] t_2 was the temperature indicated by the thermocouple in the crucible wall farthest from the inner wall.
[2] Assuming k for copper is 215 Btu/ft² hr °F per ft.

tion of the top of the ingot, was continually changing. The dynamic nature of the process, both with respect to this change in length of the ingot and with respect to the characteristics of an arc, precludes any attempt at steady state conditions. One possible solution to this problem would be to use a bottom withdrawal mechanism with which the ingot top could be maintained at a constant level throughout the run. However, this approach was eliminated in favor of the one used because of expected difficulties in the mechanics involved in maintaining a constant ingot position.

Experiments with the 2-5/16-in-diam crucible. Figure 52 shows a cross section of the crucible that was designed to provide the data required. The 2$\frac{5}{16}$-in-diam crucible was divided into two, 4-in-long sections, each with its own integral water jacket. Water entered through a $\frac{3}{4}$-in copper pipe (I) at the bottom of the crucible, flowed upward along the walls of the lower section, over the lip of the cylindrical baffle (C), and out the exhaust of the lower section (H). The water was carried to the upper section through pipe (F). In the upper section an elliptical baffle (D) directed the water downward, under the lower lip of the cylindrical baffle (C), and the water then flowed upward

Figure 52.—Two-piece crucible for consumable-electrode arc melting studies.

along the wall of the upper section and exhausted through the outlet pipe (B).

Thermistor probes (A) were installed in the inlet and outlet pipes of the upper section. Signals from these thermistor probes were recorded as a measure of the outlet water temperature of the bottom section and the inlet and outlet water temperature of the upper section. The inlet temperature for the bottom section remained constant throughout the run and was measured by means of a mercury thermometer installed in the water supply line. An O-ring seal (G) between the two sections made the crucible vacuum tight and maintained a slight spacing between the two sections to reduce heat transfer from one section to the other.

Four iron-constantan thermocouples (E) were connected in parallel and imbedded in the crucible wall $\frac{3}{8}$-in above the joint between the upper and lower sections, and four more were similarly installed $\frac{3}{4}$-in above the joint. Each of the four thermocouples of the lower set were 90° apart, and the four thermocouples of the upper set were evenly spaced between them. These thermocouples yielded data on crucible wall temperatures at two levels $\frac{3}{8}$-in apart. They were radially located within the crucible wall to yield mean wall temperatures that were used to estimate the heat involved in any temperature change of the crucible itself.

Heat transfer data were obtained during consumable electrode arc melting of zirconium and titanium at various power levels and at furnace pressures ranging from 50 to 400 torr. The diameters of the consumable electrodes used were 1-in for titanium and 1$\frac{3}{8}$-in for zirconium. Power levels were varied from run to run as were relative values for arc current and arc potential.

The melting procedure for these runs was as follows:

1. The furnace was loaded with the consumable electrode of titanium or zirconium attached to the negative furnace electrode. A starting pad of sponge metal or, in some cases, a short length of ingot was placed in the bottom of the crucible which was the positive furnace electrode.

2. The furnace was closed and evacuated to the ultimate pressure of the system (10–15 millitorr). The desired furnace pressure was obtained by backfilling with helium.

3. The electrode was lowered until an arc was initiated between the lower end of the electrode and the base. Until a full pool of molten metal was formed in the crucible, arc current
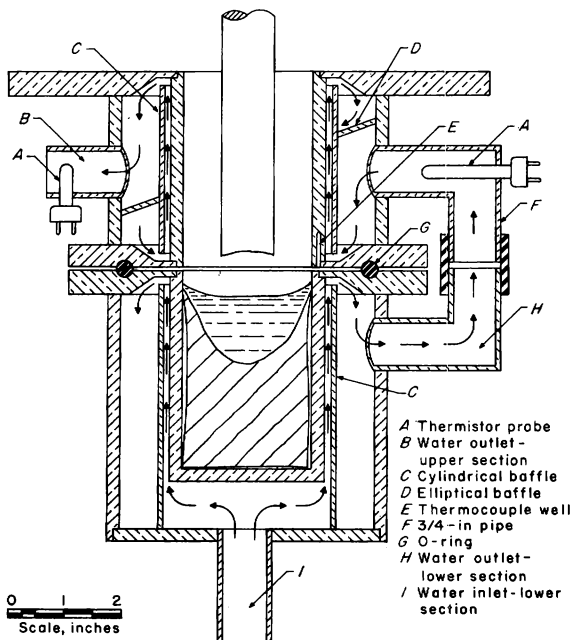
and potential were maintained at values which would cause melting of the base but at which no melting of the electrode took place.

4. The power level was then rapidly increased to the value at which the melt was to be conducted and was maintained at that level until a predetermined length of electrode had been melted.

5. Power was terminated and the ingot was allowed to cool at the pressure maintained during melting.

During the run, recordings were obtained of arc current, arc potential, temperature of the cooling water at the inlet and outlet of the upper crucible section, crucible wall temperatures, and electrode consumption rate. Direct readings of the inlet water temperature were taken, thus providing inlet and outlet water temperatures for both upper and lower sections of the crucible. Coolant flow rate was determined by taking periodic manometer readings of the pressure drop across a sharp-edged orifice.

Data from the two sets of thermocouples imbedded in the crucible wall are presented in figure 53. In this figure, temperature from both sets of thermocouples is plotted as a function of time. The dotted line at 200 sec represents the time when the ingot length was equal to the length of the lower crucible section or the time when the level of the ingot top moved past the division between the upper and lower crucible sections. Since the two sets of thermocouples are $\frac{3}{8}$-in and $\frac{3}{4}$-in above the division between the
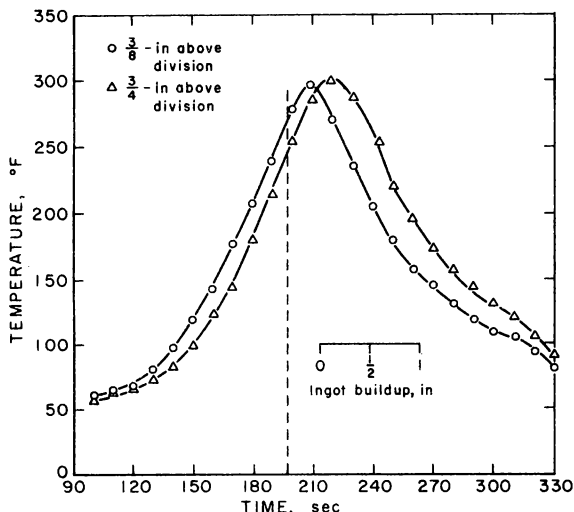
two crucible sections, they would be expected to reach their maximum values about the time the ingot was $4\frac{3}{8}$- and $4\frac{3}{4}$-in long. These data indicate that the wall temperature drops off rapidly on either side of the ingot top. Unfortunately, the two sets of thermocouples were not far enough apart to provide information on the change in temperature profiles for ingots much different in length.

Data from these thermocouples indicated that the amount of heat involved during changes in temperature of the mass of copper making up the crucible wall was only 0.9 percent of the total input. This figure was obtained by calculating the changes in heat content of 1-in increments of crucible length based on temperature changes obtained from the thermocouples. The maximum rate of change of the total heat content of the crucible was 970 Btu/hr when the ingot length changed from 4 to 5 in.

These figures were based on the supposition that the temperature profile was of the shape shown in figure 53 regardless of the length of the ingot. This supposition would not hold if the ingot were very short, and somewhat larger error would be expected during the first part of any melting operation.

Data on coolant flow rate and the temperature change of the coolant were used to calculate the heat absorbed by the cooling water to the upper and lower sections of the crucible as a function of time. Figure 54 is a typical plot of the rate of heat transfer to the water in the upper crucible section during the consumable-electrode arc melting of a $1\frac{3}{8}$-in-diam zirconium electrode. This particular run was made at a furnace pressure of 300 torr of helium, an arc current of 950 amp, and an arc potential of 34 v. The ingot formed was $6\frac{3}{4}$-in long and weighed 6.8 lb.

Measurements of the rate of electrode movement during these runs indicated that the electrode consumption, and consequently ingot buildup, was constant throughout the run. Distance along the abscissa thus is proportional to the length of the ingot at any time during the run. In the run represented in figure 54, 1 in of ingot formed every 50 sec. The dotted line at 200 sec represents the time at which the ingot was 4-in long, and the top was even with the division between the upper and lower crucible sections.

The rate of heat transfer to the upper crucible section was small during the early part of the run and increased gradually until the top of the

Figure 53.—Indicated wall temperatures $\frac{3}{8}$- and $\frac{3}{4}$-in above division of 2-5/16-in-diam crucible. Zirconium consumable electrode.
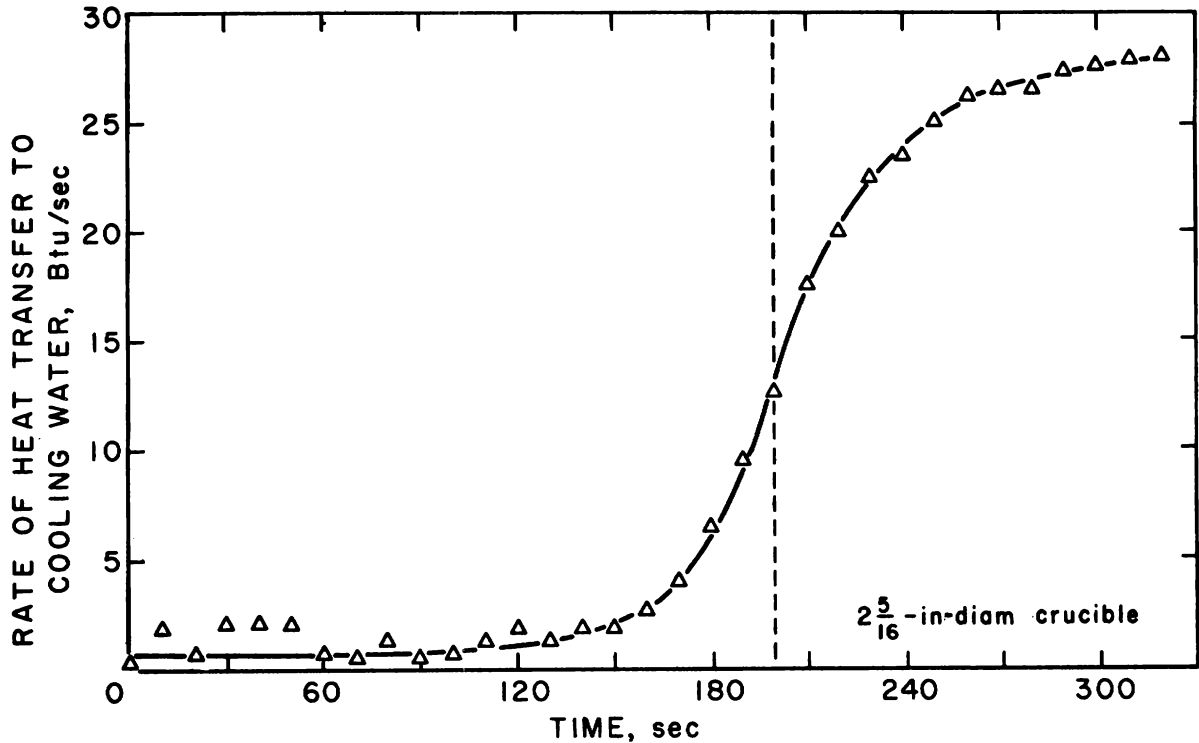
Figure 54.—Rate of heat transfer to upper crucible section during consumable electrode arc melting. Zirconium electrode.

ingot approached the division between the two crucible sections. The rate of heat transfer increased rapidly as the zone of high heat transfer near the top of the ingot moved into the upper crucible section. During the latter portions of the run, the rate of heat transfer increased only slightly with increasing ingot length.

The change in the rate of heat transfer observed during any interval of time during the run resulted from an increase in length of the ingot and movement of the heat flux profile relative to the upper crucible section. With each incremental increase in ingot length, the top crucible section was exposed to an additional increment of the heat flux profile. For example, during the time the ingot length changed from 4 to 4½ in the observed increase in the rate of heat transfer to the upper section represented the heat transfer from the upper ½-in section ingot. The average heat flux in Btu per square foot per hour for this ½-in section of ingot was determined by dividing the change in the rate of heat transfer by the sidewall area of the ½-in section of ingot. A similar calculation of heat flux can be made for any increment of ingot

length. Since the melting rate was uniform throughout the run, the slope of the curve in figure 54 is proportional to the change in the rate of heat transfer to the upper crucible section divided by the change in ingot length. The slope of this curve is therefore proportional to the heat flux.

Figure 55 is the graph of the slope of the curve in figure 54. The ordinate of figure 55 represents the distance in inches above and below the top of the ingot, and the abscissa is proportional to the slope of the curve in figure 54 and is expressed in Btu per hour per square foot of ingot surface. In figure 54, the slope of the curve to the right of the 200-sec line represents the heat flux for increments of ingot length below the ingot top, and slopes to the left of the 200-sec line represent the heat flux above the ingot top. Figure 55 thus represents the distribution of heat flux to the crucible during consumable electrode arc melting.

Data similar to that contained in figure 55 were obtained during the melting of zirconium and titanium under a variety of conditions; however, these data were greatly affected by the
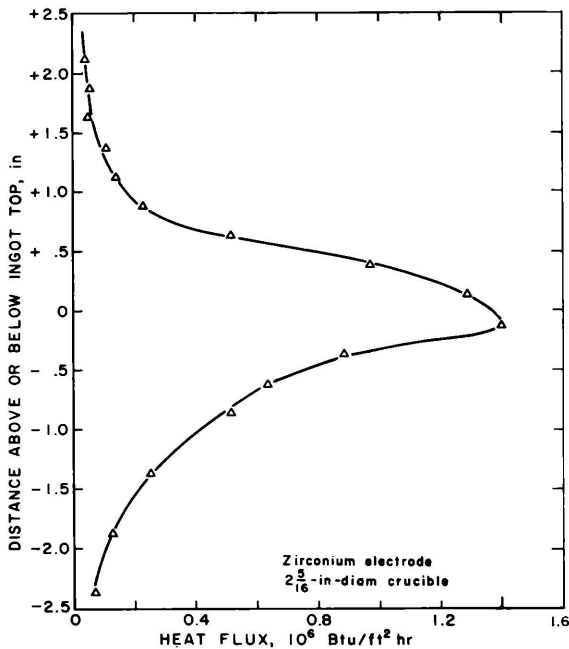
Figure 55.—Variation of heat flux to crucible cooling water along length of crucible.

Figure 56.—Eight-inch-diameter, two-piece crucible for heat transfer studies.

inherent instability of the arc during small-scale consumable electrode melting. As a result, the effects of many of the variables investigated were masked by variations in the arc characteristics caused by operational difficulties associated with small-scale melting. These difficulties were greatly increased at low furnace pressures, and consequently, no attempt was made to obtain data during melting at furnace pressures below 50 torr. Because of these limitations imposed by the small-scale equipment, similar experiments were conducted using an 8-in-diam crucible.

Experiments with the 8-in-diam crucible.— The crucible for this study was of the same basic design as shown in figure 52 and was installed in place of the ladle in an over-the-lip vacuum arc casting furnace. Figure 56 shows the crucible installed in the furnace, and figure 57 shows the crucible with the lower section separated from the upper section following a run.

The crucible was designed to produce an 8-in-diam ingot, 16- to 20-in long. The inside length of the lower crucible section was 8 in, and the upper section was 14-in long. The coolant flow pattern was the same as for the $2\frac{5}{16}$-in crucible; that is, water entered at the bottom of the lower section, cooled the lower section from bottom to

top, and then was directed to the upper section where it cooled the wall from bottom to top. Thermistor probes were positioned at the inlet and outlet of the upper section and thus provided the outlet temperature for the bottom section and inlet and outlet temperatures for the upper section. The inlet temperature for the bottom section was taken as the temperature of the water supply and remained constant throughout the run.

The coolant flow rate was determined by weighing four to six 1-min samples taken during the run. The coolant flow rate was relatively constant throughout each run and was maintained at approximately the same level for all runs conducted.

Nine heats were conducted in this crucible of which six were zirconium and three were steel. The electrodes for three of the zirconium heats were 6-in-diam, and three were $4\frac{1}{2}$-in-diam. All three steel electrodes were $4\frac{1}{2}$-in-diam. All of the ingots produced were 14- to 20-in long, and all the runs were conducted at furnace pressures in the range of 10^{-2} to 10^{-1} torr. Time for melting the individual heats varied from 13 to 22

Figure 57.—Eight-inch-diameter crucible with bottom section removed following a run.

Figure 58.—Effect of electrode diameter on heat flux to crucible wall.

min depending on power input and the material being melted. Table 9 summarizes the conditions which prevailed for the various heats.

The distribution of heat flux along the length of the ingot was determined by the same method outlined for the $2\frac{5}{16}$-in ingots. A significant difference in the maximum heat flux was noted for these 8-in runs as compared to that noted for the small-scale runs. For the 8-in runs the maximum heat flux was the range 0.4 to 0.5 x 10^6 Btu/ft² hr compared with 1.4 x 10^6 Btu/ft² hr for the $2\frac{5}{16}$-in runs described previously. This marked difference is not surprising. Experience indicates that the frequency of crucible burn-through is much higher for small diameter melts (less than 4-in-diam) than for larger melts.

Electrode diameter had a significant effect on the distribution of heat flux along the length of the crucible and on the maximum heat flux. Figure 58 shows the distribution of heat flux for two runs made under approximately the same operating conditions except for electrode diameter. For the 6-in-diam electrode, a higher maximum heat flux occurred, and the heat flux was concentrated over a shorter length of crucible.

The maximum heat flux for the larger diameter electrodes also occurred at a higher level than for the smaller electrodes.

These results are substantiated by previous Bureau work (1) related to the effect of electrode diameter on the yield of metal (percent of charge poured) during consumable electrode arc melting and casting operations. This previous research indicated that, while the electrode diameter did not affect the yield of metal, the shape of the molten pool changed significantly with electrode diameter. Small-diameter electrodes yielded skulls which were thin on the bottom and lower sides but which were thickened at the top. Large-diameter electrodes yielded skulls which were thick at the bottom and lower sides but which were thin at the top. The shapes of these skulls indicated that for the larger electrodes the heat in the molten pool was concentrated near the top of the pool, and for the small electrodes the heat was concentrated lower in the pool. Figure 59 represents the effect of electrode diameter on the shape of the molten pool during consumable-electrode are melting in which other furnace parameters were equal. The patterns of heat flux shown in figure 59 indicate the same distribution of heat within the molten pool.

Figure 60 shows a comparison of a $4\frac{1}{2}$-in-zirconium and a $4\frac{1}{2}$-in steel electrode melted at

Table 9.—Summary of 8-in-diam melts conducted

Number	Material	Electrode diameter, in	Nominal arc current, amp	Nominal arc potential, v	Coolant flow rate lb/min	Ingot weight, lb	Ingot length, in [1]
	Zirconium						
1	_____do_____	6	5,700	31	186	189	16.8
2	_____do_____	6	6,450	34	180	193	17.3
3	_____do_____	6	7,500	30	185	201	17.9
4	_____do_____	4½	7,500	30	187	191	17.0
5	_____do_____	4½	6,700	35	167	191	17.2
6	_____do_____	4½	7,200	32	180	186	16.8
7	Steel	4½	6,600	27	190	188	14.5
8	_____do_____	4½	6,500	31	183	186	14.5
9	_____do_____	4½	8,000	33	177	181	14.0

[1] Ingot length was measured from the ingot bottom to the top of the pool level and does not include the length of the crown.
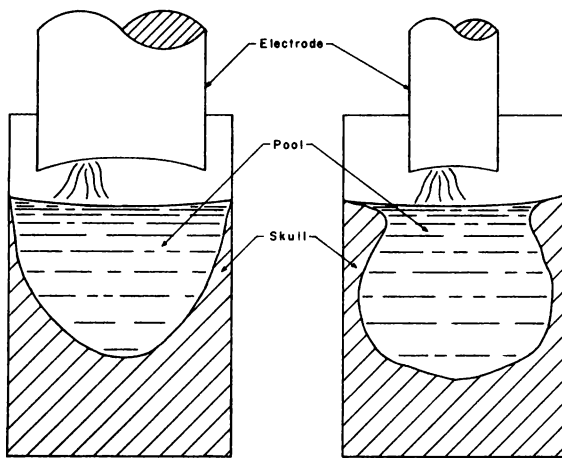
Figure 59.—Effect of electrode diameter on pool geometry.

Figure 60.—Effect of electrode material on heat flux to crucible wall.

approximately the same arc current and arc potential. In general, all of the steel melts yielded maximum heat flux at levels above similar runs with zirconium. The effect is believed to be the result of the manner in which the steel electrodes melt because af the gas content of the metal. Steels which have not been vacuum melted previously usually melt with very unstable arc characteristics because of the gas content of the electrodes. The electrodes of the steel runs were made from 4-in by 6-in bars of type 4340 steel which were forged to 4½-in-diam electrodes. Compared with mild steel, this material melted with relatively stable arc characteristics, but compared with the vacuum melted zirconium electrodes, the material melted with a considerably less stable arc.

The patterns of the heat flux for the steel runs indicate differences which can occur during the melting of dissimilar materials, but these runs would have to be supplemented by additional data obtained during the melting of a variety of materials before specific conclusions could be stated. Such data would be of particular interest for the more refractory materials such as molybdenum, tantalum, columbium, and tungsten. When melting these materials, cooling of the cold-mold crucible is often marginal, which indicates the possibility

of heat fluxes much greater than those cal-
culated for the zirconium and steel heats con-
ducted.

Materials other than steel and zirconium
were not melted in the 8-in crucible; however,
both titanium and zirconium were melted in
the $2\frac{5}{16}$-in crucible. The results of these small-
scale runs indicated little difference in the
maximum heat flux observed for the two
metals, but the maximum heat flux observed
for the titanium occurred further below the
ingot top than for the zirconium. The use of
smaller diameter electrodes for the titanium
runs would account for this shift in the loca-
tion of the maximum heat flux.

The effects of arc potential, arc current, and
power input were studied for a relatively nar-
row range of values at which normal operation
of the arc occurred. The effects of abnormally
high arc potentials or extremely high or low
arc currents were not observed. Consequently
the effects of these parameters were not as clearly
shown as would be desired. Figure 61 and
62 include data from the zirconium and steel
runs with $4\frac{1}{2}$-in-diam electrodes.

Figure 61 is a comparison of two runs at

Figure 62.—Effect of arc current and arc poten-
tial on heat flux to crucible wall during melt-
ing of steel electrodes.

Figure 61.—Effect of arc current and arc poten-
tial on heat flux to crucible wall during melt-
ing of zirconium electrodes.

approximately equal power input but with
different values of arc current and arc poten-
tial. The heat flux profile for the run made at
the higher arc potential was shifted upward;
that is, more heat was transferred to the wall
above the ingot top with increased arc poten-
tial. Melting experience substantiates this
effect; in fact, one way of maintaining a full
molten pool is to increase the arc potential.
This practice is especially effective in the re-
searcher's experience when melting and casting
tungsten. Higher heat losses by radiation from
the molten pool of tungsten often cause a skin
of metal to solidify from the sides inward across
the top of the pool. This skin can be elimi-
nated by operating at higher arc potentials.

Similar evidence of the effect of high arc
potential is shown by the heat flux profiles for
runs 7 and 8 in figure 62. These two runs were
made at approximately the same arc current
but with different values of arc potential. A
much larger percentage of the heat transfer for
the run at higher voltage occurred above the
top of the ingot.

When both arc current and arc potential
were increased as in run 9 of figure 62, the
peak value of the heat flux was increased as
would be expected, but the heat flux profile

was almost symmetrical with respect to the top
of the ingot. Increased heat flux below the top
of the ingot would be expected because of the
deeper pool formed with increased power in-
put. The higher arc potential and greater arc
length would also cause high values of heat
flux above the ingot top.

Run 6, which was not included in figure 61,
was run at 7,200 amp and 32 v, and the curve
for heat flux for this run falls between the
curves for runs 4 and 5 as would be expected.
The data presented in figures 61 and 62 are in
agreement with the experience gained during
melting; that is, for a given power input, a
high arc potential and low arc current will
yield a wide shallow pool while a low arc
potential and a high arc current will yield a
deeper, narrower pool.

The effects of arc potential were masked by
the effect of electrode diameter for the 6-in-
diam electrodes shown in figure 63, and the
results of run 1 of this series are not in agree-
ment with the results expected. Maximum heat
flux for run 1, which was made at 31 v and
only 5,700 amp, exceeds the maximum heat
flux for other runs conducted at both higher
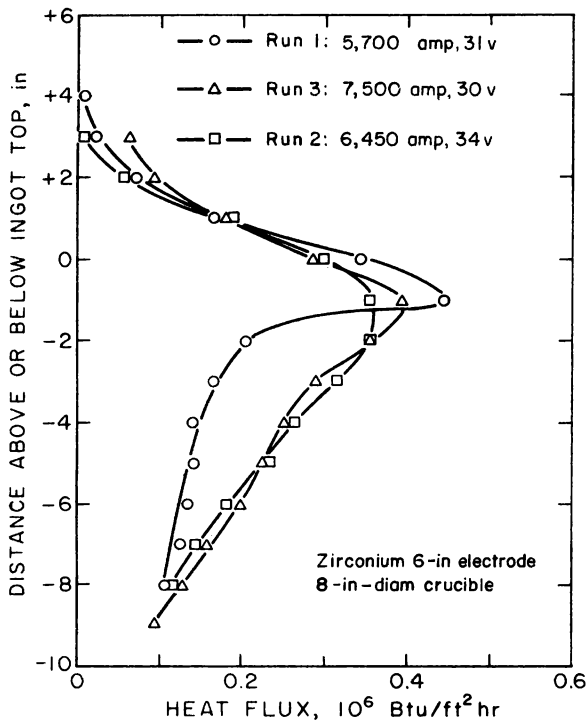
arc potential and arc current. The pattern of
heat flux for this run does indicate an extremely
shallow pool, however, and fits the general
trends outlined in this respect. An additional
study of the effect of extreme variations in arc
current should be conducted to determine
whether high heat flux can result under certain
conditions at low power input.

Effect of Narrow Annular Spacing for Water Jackets

Experiments were conducted to determine
the effectiveness of water jackets with a narrow
annular spacing during nonconsumable elec-
trode melting of zirconium in a $2\frac{5}{16}$-in-diam
crucible. The OD of this crucible was 2.750 in,
and the ID of the water jacket used varied from
2.770 to 2.850 in. The size of the annular spac-
ing of the water jackets studied was expressed
in terms of equivalent diameter which, for an
annulus, is defined as the difference between
the inside and outside diameters of the annu-
lus. Tests were conducted for five different
equivalent diameters of from 0.020 to 0.100 in.
Coolant flow rate was varied between 2,000 and
6,000 lb/hr for each equivalent diameter, and
the temperature of the crucible wall was re-
corded as a function of power input.

The primary purpose of these tests was to
determine whether water jackets with very nar-
row annular spacings could be used for arc
melting, and if difficulties would be experi-
enced with crucible expansion or the formation
of steam pockets. No such difficulties were en-
countered during tests conducted.

Figure 64 includes data obtained for 0.020-
and 0.100-in equivalent diameters at a coolant
flow rate of 4,000 lb/hr. Wall temperatures
were obtained with an iron-constantan thermo-
couple imbedded in the crucible wall approxi-
mately $\frac{1}{2}$-in below the top of a zirconium in-
got. The radial positon of the thermocouple
within the wall was not precisely determined;
therefore, the temperatures are considered only
a qualitative measure of the effectiveness of the
particular water jacket being studied.

The data in figure 64 substantiate the fact
that higher coolant velocities provide increased
rates of heat transfer. These data, plus experi-
ence gained through research on the melting
and casting of refractory metals at the Bureau,
indicate that more consideration should be
given to the design of water jackets that will
provide high coolant velocities. These design

Figure 63.—Effect of arc current and arc poten-
tial on heat flux to crucible wall during melt-
ing of 6-in-diam zirconium electrodes.
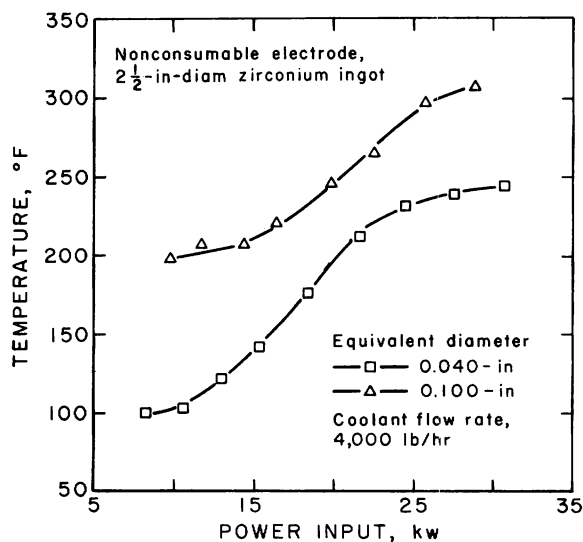
Figure 64.—Indicated wall temperatures vs. power input for two equivalent diameters.

considerations must be tempered by consideration of allowable pressure drops across the cooling jacket and mechanical problems of crucible and water jacket alinement.

DISCUSSION

The studies conducted with the two-piece crucible yielded values of heat flux from the ingot to the crucible wall that are believed to be representative of values encountered during consumable electrode arc melting of iron and steel and the reactive metals. These data, plus experience gained in the melting and casting of refractory metals, provide guidelines for the design of water-cooled copper crucibles and their water jackets. The following statements summarize the present Bureau thinking regarding such design.

Crucible Wall Thickness

One of the design considerations on which considerable disagreement exists is the optimum thickness for the crucible wall. For an assumed heat flux of 10^6 Btu/ft^2 hr and temperature drop through the crucible wall of 700° F, the wall of a copper crucible could be more than 1.5-in thick before conductance through the copper became a limiting factor. These assumed values of heat flux and temperature drop are conservative estimates based on the data obtained from these studies. It is be-

lieved that, up to 1.5 in, wall thickness is not a critical factor from the standpoint of heat transfer. Heavy walls offer the advantage of greater longitudinal heat transfer along the wall of the crucible and increased mechanical strength. It is recommended that crucible wall thickness be determined from consideration of mechanical strength. If wall thicknesses exceed 1.5 in, consideration must be made for heat conductance. Crucible walls less than $1/4$-in thick are not recomended.

Water Jacket Dimensions

An increase in the mass velocity, in pounds per hour per square foot of cross section, of a coolant will result in an increase in the coefficient of heat transfer from the crucible to the coolant. Thus, water jackets should be designed to provide optimum mass velocity of the coolant based on consideration of allowable pressure drop. Small-scale experimental work with very narrow annular water jackets yielded lower wall temperatures with increasing mass velocity, and no difficulty was encountered due to expansion of the crucible or the formation of steam pockets.

During visits at several industrial vacuum arc melting installations, it was noted that the use of a comon water jacket with several different sizes of crucibles is a common practice. The use of a small-diameter crucible in a water jacket designed for large crucibles results in a decrease in the mass velocity of the coolant for a fixed mass rate of flow. This practice evidently does not cause any difficulty, probably because of low rates of heat transfer involved. However, this practice may well prove unsatisfactory for melting more refractory metals when higher rates of heat transfer will be involved. In such cases, provisions should be made to provide increased coolant mass velocity by means of increased mass rate of flow, special water jackets, or inserts designed to reduce the annulus cross section.

The value of high coolant mass velocity has been demonstrated in vacuum arc melting and casting of tungsten by the Bureau. In this work, tungsten was melted in a 5-in-diam ladle using an arc current of 13,000 amp at an arc potential of 40 to 42 v. The annulus of the water jacket for this crucible had an ID of $5\frac{1}{2}$ in and an OD of 6 in. Coolant flow was maintained at 835 lb/min which was equivalent to a mass velocity of 1.6 x 10^6 lb/hr ft^2. The wall

thickness of the ladle was approximately $5/16$-in. No measure of the heat flux during tungsten melting has been attempted, but the heat flux is assumed to be much higher than any listed for melting studies included in this report.

These few aspects of equipment design are not intended to be all inclusive but represent areas of importance and about which questions have been raised. Such details of design as methods of grounding the crucible and the effects of nonsymmetrical magnetic fields set up by the arc have a great effect on the performance of vacuum arc furnaces but were not studied in this work.

CONCLUSIONS

During vacuum-arc melting in water-cooled copper crucibles, heat flux in excess of 10^6 Btu/ft^2 hr can occur. The effects of arc current, arc potential, ratio of electrode diameter-to-crucible diameter, crucible diameter, and electrode composition were studied and the following results were obtained:

1. The effects of arc current and arc potential were related. In general, increasing arc current increased the maximum heat flux. Increasing arc potential increased the maximum heat flux and shifted the location of the maximum heat flux nearer the top of the ingot. For a given power input, higher maximum heat flux will occur at high arc potential and low arc current.

2. For a given crucible diameter, higher heat flux will occur with larger diameter electrodes, and an increase in electrode diameter will shift the peak heat flux upward.

3. Melting on a small scale yields higher values of maximum heat flux because of instability of the arc during small-scale melting.

4. Electrode composition will affect values of heat flux because of differences in the thermal properties of the material melted and also because of gas content of the metal. An increase in gas content will shift the peak heat flux upward and increase the maximum heat flux.

5. Maximum values of heat flux observed during consumable-electrode arc melting of steel and zirconium electrodes were in the range of 0.2×10^6 Btu/ft^2 hr to 0.5×10^6 Btu/ft^2 for 8-in-diam ingots. Values up to 1.4×10^6 Btu/ft^2 hr were observed during small-scale melting of zirconium and titanium.

Studies on narrow annular water jackets indicated that the high mass velocity achieved with narrow annuli yield lower crucible wall temperatures.

Additional data should be obtained, particularly with respect to the effect of the metal being melted and the effect of furnace pressure. In the case of the effect of the metals being melted, it would be of interest to conduct similar experiments with the refractory metals, particularly molybdenum, tantalum, and tungsten. Much higher values of maximum heat flux would be expected with these metals, and valuable information could be obtained which is needed for designing furnaces for melting these metals.

The effects of furnace pressure were not studied in detail although the small-scale runs were conducted at furnace pressures ranging from 50 to 400 torr, and the 8-in-diam runs were conducted at a furnace pressure of approximately 5×10^{-2} torr. It is believed that it would be necessary to conduct melting studies at furnace pressures between 10^{-2} and 50 torr to cover the range in which the greatest changes take place.

The studies conducted were designed to measure the values of heat flux during normal melting conditions. It would be equally interesting to measure values of heat flux during abnormal arc conditions when maximum values of heat flux are undoubtedly much different.

A similar study should be conducted during electroslag melting. This method of melting is increasing in importance, and, based on examination of the ingots produced by this method, the patterns of heat transfer differ considerably from those during vacuum arc melting.

REFERENCES

1. Ausmus, S. L., F. W. Wood, and R. A. Beall. Casting Technology for Titanium, Zirconium, and Hafnium. BuMines Rept. of Inv. 5686, 1960, 31 pp.

2. Cooper, D. E., and E. D. Dilling. Liquid Metal Cooling for Consutrode Melting. J. Metals, v. 12, No. 2, 1960, pp. 149–151.

3. duManior, P., and C. M. Pierce. Computer Analysis of the Heat Flow in the Vacuum Arc Melting of Molybdenum. U.S. Air Force Tech. Doc. Rept. ML–TDR–64–308, October 1964, 13 pp.

4. Kirk, M. M., P. C. Magnusson, and G. L. Schmidt. Air Cooled Crucibles for Cold-Mold Arc Melting. BuMines Rept. of Inv. 5443, 1959, 23 pp.

5. Kroll, W. J. Production of Ductile Titanium. Trans. Electrochem. Soc., v. 78, 1940, pp. 35–47.

6. McAdams, W. H. Heat Transmission. McGraw-Hill Book Co., Inc., New York, 3d ed. 1954, 532 pp.

7. Moore, R. W. Preparation of Metallic Uranium. Trans. Electrochem. Soc., v. 63, 1923, pp. 317–328.

8. Parke, R. M., and J. L. Ham. The Melting of Molbdenum in the Vacuum Arc. Trans. AIME, v. 171, 1947, pp. 416–427.

9. Rossin, P. C. Arc Melting in High Vacuum. Paper in Vacuum Metallurgy. Pres. at the Vacuum Metallurgy Symp. of the Electrothermic and Met. Div., The Electrochem. Soc., Oct. 6–7, 1954; The Electrochemical Society, 1955, pp. 12–23.

10. Ushijima, K. On the Air Gap Between Billet and Mold. Report VI on Continuous Casting. Tetsu to Hagane, v. 48, No. 6, 1962, pp. 747–752; Brutcher Transl. S633.

11. Wood, F. W. On the Distribution of Temperature and Heat Flow in Arc-Melted Ingots. Thesis, Oregon State Univ., 1967, Arc-Melted Ingots.

12. Wood, F. W., and R. R. Lowery. Discharge Behavior in Vacuum Arc Melting. BuMines Rept. of Inv. 5749, 1961, 32 pp.

CHAPTER 9.—FABRICATION OF CONSUMABLE ELECTRODES

By R. A. Beall, F. W. Wood, and P. C. Magnusson [1]

Certain general qualitative requirements must be met for a consumable electrode, although quantitatively there may be a great variation for each application. The general requirements concern (a) strength, (b) conductivity, (c) purity, and (d) straightness. The chief point in regard to strength is that the electrode be able to support its own free weight. In some types of furnaces (3), the free weight is only a portion of the total weight of the electrode, since the electrode is supported at a point between the consuming end and the opposite or top end. In other equipment the electrode is supported at its top.

The electrical conductivity requirement is closely related to the exact application. In one instance, a $\frac{3}{8}$-in-diam solid rod was used as an electrode to form a 3-in-diam pool. The current required to maintain a pool of this diameter was excessive for the rod, and it collapsed from overheating caused not by the arc but by resistive heating. However, a much larger rod, perhaps with even lower specific conductivity, may have sufficed, because its conductance would have been greater. It is more accurate, then, to rate a given electrode on the basis of its overall conductance rather than its specific conductivity.

It is occasionally important to consider also the heat conductivity of an electrode. Where overheating by resistance is a problem, its ability to conduct heat from the rod to its fixture or suspension mechanism might provide some relief.

Purity is always important when one considers operations with the rare or expensive metals. Certainly the method of electrode production must not detract measurably from the purity of the final product. A welding method that adds much oxide or tungsten or a pressing technique that requires excessive die lubrication with oil or graphite is likely to be unacceptable.

The crucible wall will puncture quickly if the

energized electrode should touch it. As may be surmised, careful alinement of the electrode throughout the melting process is essential, and in practice this means that the electrode must be straight and remain so when heated. In some instances pressed electrodes have warped seriously during melting. This is thought to have been due to the variation of electrical conductivity in the cross section of the electrode, which caused uneven heating as the current passed through it. In a long flat pressing die the sponge fines tend to congregate at the bottom of the die and could easily cause a warped bar.

An additional consideration in the choice of method of electrode production is the case of alloy addition. It is common practice in many plants to add alloying ingredients to the sponge before pressing into an electrode.

Certainly no one electrode-production method is likely to handle all types of feed materials. Plate scrap and forging trim, which can be welded with ease, can be briquetted only if quite thin in section. Sponge naturally lends itself to pressing as an initial step to electrode formation. The experimental work reported will be classified as to the type of feed material used.

METAL-SPONGE ELECTRODES

The first method used at the Albany Metallurgy Research Center to produce a consumable electrode from sponge (1) utilized a steel sheath which was filled with pressed-sponge briquets, welded closed, and then hot-forged and rolled. The worked sponge was metallic in appearance and had good electrical and mechanical characteristics. The principal deficiency in the resulting bars was that the cross section lacked regularity; this prohibited the use of rollers or sliding contracts.

Sponge can be pressed to form long bars or electrodes directly. Many tons of zirconium were pressed at the Bureau of Mines Boulder City Met-

---

[1] Formerly electrical engineer, Albany Metallurgy Research Center, Bureau of Mines, Albany, Oreg.; now professor of electrical engineering, Oregon State Univ., Corvallis, Oreg.
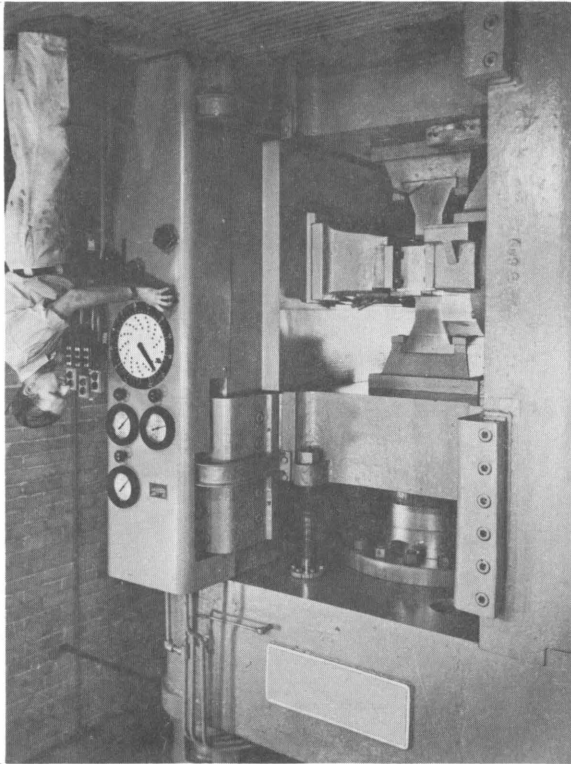
Figure 65.—Electrode briquetting press, Bureau of Mines, Boulder City, Nev.
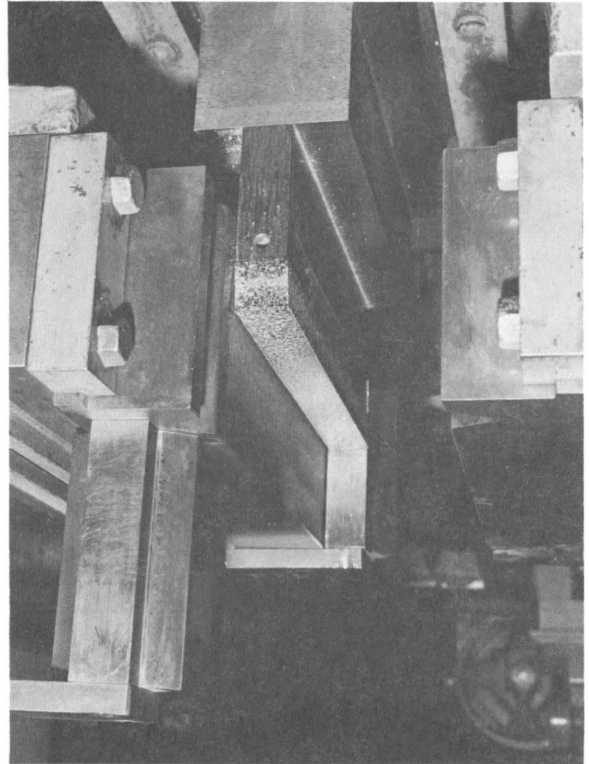
Figure 66.—Briquetting die for 2- by 2- by 20-in sponge electrodes.

allurgy Research Laboratory (Nev.). The equipment there consists of a large, triple-action, powder-metallurgy press, shown in figure 65. It was operated to form 2- by 2- by 20-in bars at 2,000 tons vertical pressure (50 tons/in²) and 1,500 tons holding pressure on the side ram. Figure 66 shows a pressed bar as the die is unloaded. Longer consumable electrodes have been continuously formed by welding the bars end to end in an inert atmosphere glovebox during melting (3).

A series of tests was performed to determine the resistivity and tensile strength of the "Boulder bars" at various compacting pressures. The data are shown graphically in figure 67. Of particular interest was the sharp increase in tensile strength as the forming pressure exceeded 40 tons/in². The density of the pressed bars (50 tons/in²) was approximately 87 percent that of metallic zirconium.

For smaller electrodes the equipment shown in figure 68 may be used. The side plates in this die are designed to float; that is, they do not touch the bottom of the large block when under pressure. The main block is made from 4140 steel, and the die components are of a nitrided steel. Pressures up to 250 tons or 25 tons/in² are used to produce a 1- by 1- by 10-in compact. Different sets of die parts may be used in the same block to produce smaller bars.

In addition to the methods for compacting sponge practiced at the Bureau of Mines, one other method deserves mention—that utilized for molybdenum by the Climax Molybdenum Corp. of Michigan (2), in which sponge or powder is fed continuously to a pointed reciprocating punch. The split die is arranged so that when the pressure reaches the desired level the briquet, a rod in this case, slips through. The rod is sintered before it enters the melting furnace.

SINTERING

Sintering is often used to strengthen compacts, and its effectiveness depends on the material used. The strength added to the compact is usually a function of time, temperature, and pressure used in the operation. The practice here has been to start with short cylindrical
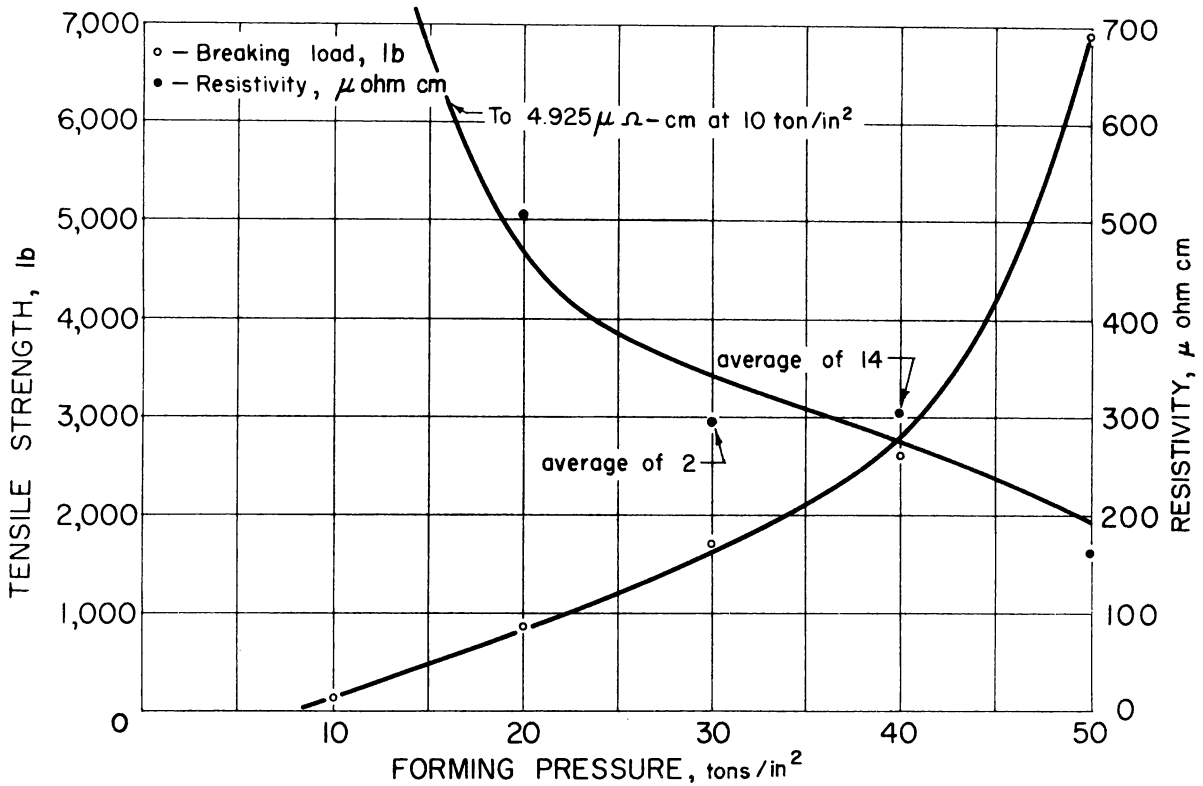
Figure 67.—Tensile strength and resistivity vs. forming pressure 2- by 2- by 20-in electrode compact.

briquets formed in a mechanical press at about 7 to 10 tons/in². At this pressure ½-in mesh zirconium sponge barely holds together. The briquets are sintered together by electrical-resistance heating in stacks to form cylindrical electrodes of usuable length. Figure 69 shows the equipment used and the resulting product made of machine chips.

The sintering equipment is a simple steel shell with a water-cooled copper base plate. The chamber is cylindrical, 14-in-diam and 18-in-high. Three stacks of zirconium briquets form the charge; they are short-circuited together at the bottom by the base plate. At the top, each stack is connected through a water-cooled, round copper plunger to one line of a three-phase power supply. Each stack of briquets is about 4-in-diam and 15-in-long; weighs about 14 kg, and in most instances consists of eight briquets. The stacks are arranged in an equilateral triangle with about 2-in clearance between pairs. The plungers pass through glands in the lid of the shell, and each makes contact with the center of one stack. A pressure of about 100 lbs is applied to each stack with a pneumatic cylin-der to assure motion of the plunger as the stack shrinks and to assist the sintering action.

The equipment is evacuated by a mechanical pump with a capacity of 13.1 cfm of free air, which maintains a vacuum of 40μ to 100μ during sintering. A viewport is provided for temperature measurement by optical pyrometer. Power is supplied from a tapped 300-kva transformer. In practice, the electrical resistance of the load drops during sintering to about one-seventh of the initial value.

Evaluations of sintered compacts were performed through the use of the flexure test with an anvil separation of 8½ in. Figure 70 shows graphically the relationship between this breaking pressure and the product of sintering time and sintering temperature. Generally speaking, a 7-min heating period with a maximum temperature slightly above 1,000° C will produce a satisfactory compact. Temperatures much above 1,100° C may give softening and severe warpage.

WELDED BRIQUETS

Welding is another method for fastening briquets together, and two general methods may
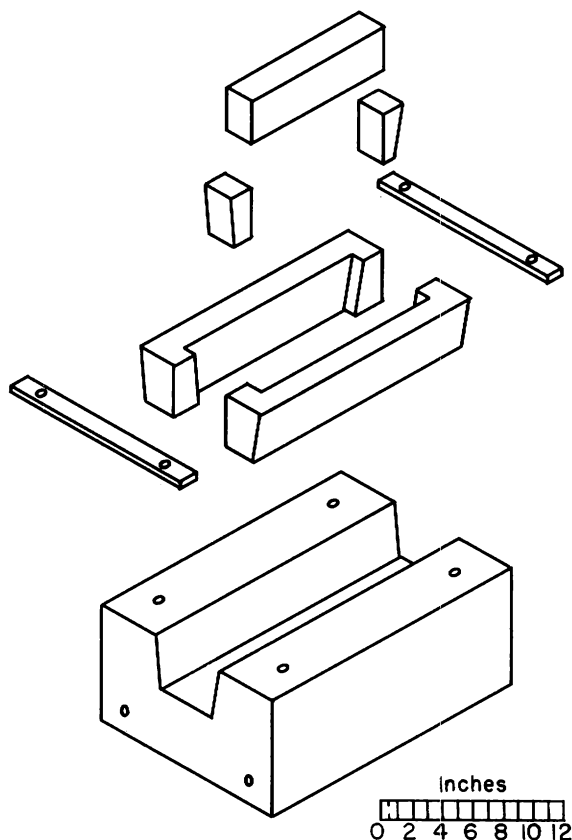
Figure 68.—Die for 1- by 1- by 10-in electrodes.

be used: Inert electrode welding, and consumable-electrode welding. Atmospheric contamination may be avoided by using inert-gas shielding or an inert atmosphere "dry box."

Unfortunately, no truly inert electrode has been discovered to date. When sponge that contains more than 0.05 percent chlorine is welded it is difficult, because of excessive spattering, to prevent electrode contamination. Thoriated tungsten (1 percent thoria) is the most satisfactory electrode used. Other electrode materials include pure tungsten, carbon, rhenium, and zirconium nitride (4). In view of this difficulty a minimum of welding gives the best results. Welding together a 5-ft stack of short cylindrical briquets of low-grade sponge, with its contained chlorides, leads to severe electrode contamination, because several end-to-end passes are required.[2] On the other hand, a pressed compact of the same material 5 feet long, made of three 2- by 2- by 20-in bars, could be welded with four

2-in tack welds, and electrode contamination would be relatively small.

Two general types of inert-atmosphere dry boxes are in regular use at this time. For welding small, light compacts, the type shown in figure 71 is used. In this equipment the operator holds by hand a suitable device having a $\frac{1}{8}$- to $\frac{1}{4}$-in-diam thoriated-tungsten electrode. Foot pedals control a high-frequency starter to initiate the welding arc and the arc-power source. Currents between 180 and 250 amp are typical. A second method utilizes a mechanically operated welding head, as shown in figure 72 and schematically in figure 73. In this equipment higher currents may be used. Motion is given to both the work and the electrode to allow several different types of welding operations. For dry-box operation, evacuation to 150μ with a mechanical pump is considered adequate, provided that the leak rate of the equipment is less than 20μ/min. Operation in the glove-type apparatus requires a nicely balanced pressure for maneuverability. In the remotely operated gear a negative pressure is maintained to secure the flanges tightly against leakage. A more detailed description of this equipment was reported previously (5).

As mentioned welding may be done with a consumable electrode rather than with an inert electrode. With the consumable electrode an inert-gas shield is used more commonly than a dry box. Commercial machines are available that automatically feed a wire which is consumed in the arc. Two general types of equipment are available. The simpler and cheaper machine has provision for manually controlled and preset wire speed. In the highest cost equipment the wire feed speed is electrically controlled by the arc conditions.

As to the use of inert-gas shielding compared to dry-box operation, the shield, at best, is never as good as a dry box at its best. The degree to which a compact is contaminated by the atmosphere in shielded welding depends upon the efficiency of the shield, the length of weld, and the rate of cooling.

Because of the difficulty of installation and operation of a wire-type machine in a dry box and the flammable nature of zirconium sponge, this technique has not been studied in detail in this laboratory. It is understood, however, that at least one commercial titanium melter is producing electrodes from sponge by consumable wire welding.

A very limited investigation has been made

---

[2] Use of plasma torches or electron-beam welding by industrial groups have assisted in the elimination of contamination.
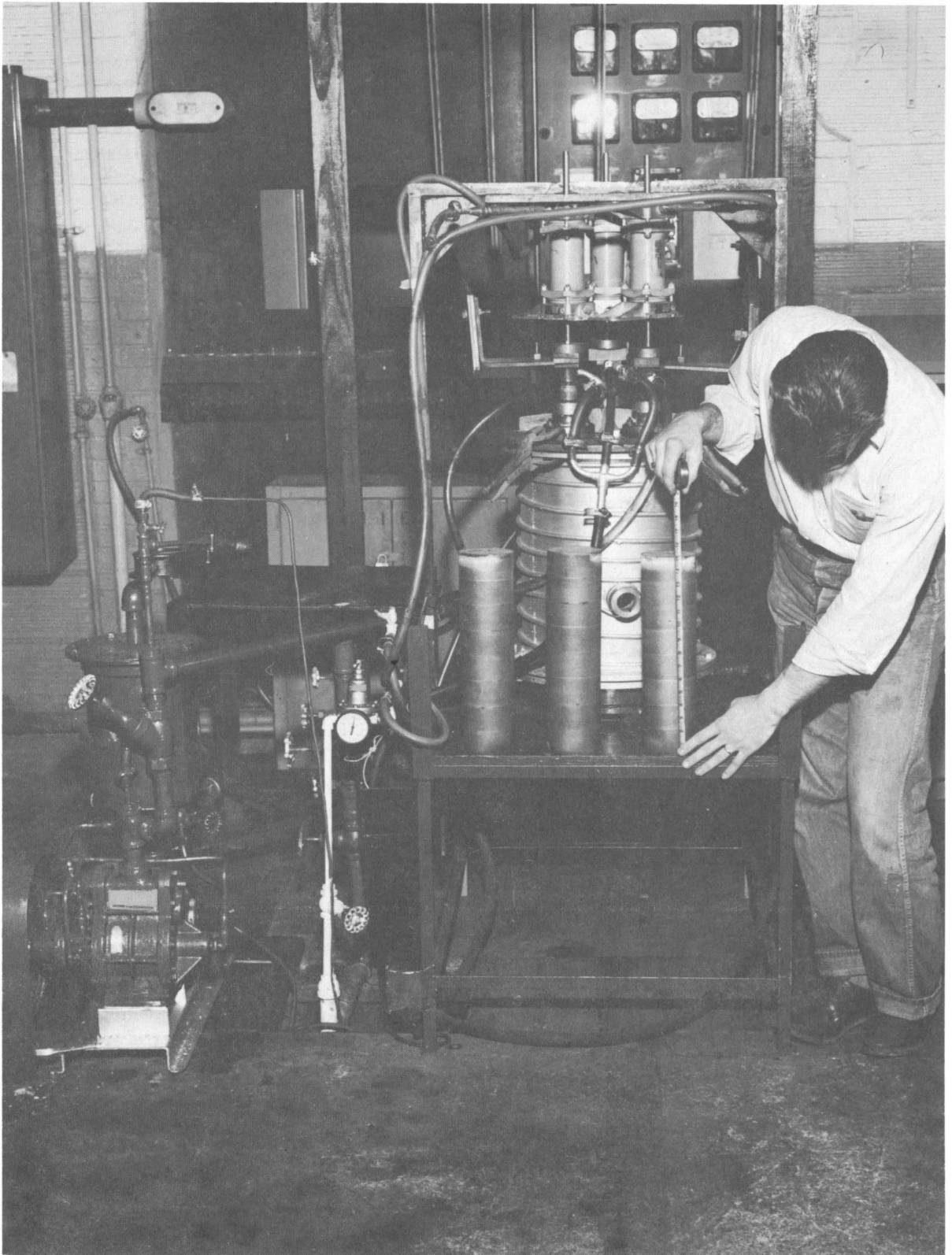
Figure 69.—Electrode sintering furnace.
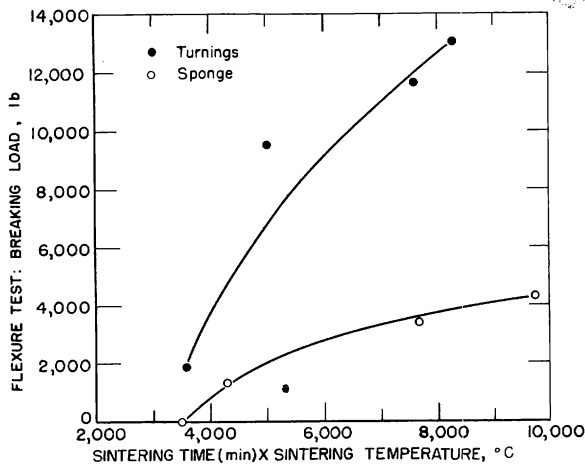
Figure 70.—Strength of electrodes vs. sintering time and temperature (4-in-diam compacts; 8½-in anvil separation).

on the feasibility of flash welding as a method of connecting compacts of sponge. The few tests conducted indicated that the system could be used. Some trouble was caused by chlorides (or other volatiles) blowing the molten or welded metal away from the joint during the flash cycle. The need for a very secure grip of the soft compacts, and the relatively high cost of the equipment, were the main reasons for not pursuing this mode of fabrication further.

In conclusion, little trouble has been experienced with welding bars. The use of jigs has eliminated earlier difficulties with crooked bars. Conductance, however, has regularly been a problem. As a general operating rule, the welding bead or beads must have enough cross section to carry the entire arc current without overheating and melting. Purity is difficult to control when one operates a tungsten electrode on a spattering material.

MACHINE CHIPS

Before machine chips or turnings can be handled with any degree of ease, they should be crushed. At this laboratory they are found to be readily reduced in size by passing them through a hammer mill. Figure 74 shows a mill with the product. When the chip material is reduced to usable form, the possibilities of treatment to yield consumable electrodes are as manifold as they are for sponge.

In general, turnings require a higher pressure than sponge to form a briquet of comparable strength. Satisfactory 4-in-diam sponge briquets may be produced in an 80-ton-capacity mechanical press, but turnings of the same dimensions require at least 200 tons total pressure to yield a briquet of equal quality. This amounts to about 16 tons/in^2. Figure 69 shows turnings briquets when sintered, and figure 75 shows welded turnings briquets. Spot welding is not as satisfactory as strip welding, since less strength and less conductance are obtained.

Figure 70 shows the breaking strength of sintered bar electrodes from machine chips compared with those from sponge for several values of the product of sintering time and maximum temperature.

MASSIVE SCRAP

The chief problem in handling scrap is due to the irregular shapes involved. Figure 76 shows electrodes made from plate and casting scrap. Plate scrap usually must be hand-fabricated by welding in a dry box. The prime requisite is straightness. Conductance and strength requirements are met without difficulty. Tungsten-electrode arc welds seldom give spattering problems with this type of material. Regular shape castings may be lined up and welded in an automatic box, as shown at the right in figure 76. Hollow sections may be filled with light scrap and tack-welded.

No attempt is made here to discuss the problems of cleaning, or alloy separation in handling scrap. Needless to say, any oxide, nitride, oils, or ordinary dirt left on an electrode will affect the resultant ingot.

INGOT ELECTRODES FOR REMELT

It is common practice with the rare metals and their alloys to melt at least twice by the consumable-electrode process when prime ingot quality is desired. That is, if a first melt is made in a 3-in-diam cup, the 3-in-diam ingot serves as an electrode for remelting into a larger, that is 4-in-diam cup. Routinely, a ½-in clearance on the radius is sufficient on sizes up to 5-in diam, and 1-in clearance on other sizes up to 10-in diam.

Since the final ingot is shorter than the initial ingot and since other considerations behoove one to keep length to diameter ratios above 4, it is often necessary to form the second electrode from two or more ingots. This may be accomplished in at least two ways: By welded joint or by threaded nipple, and sometimes by both.
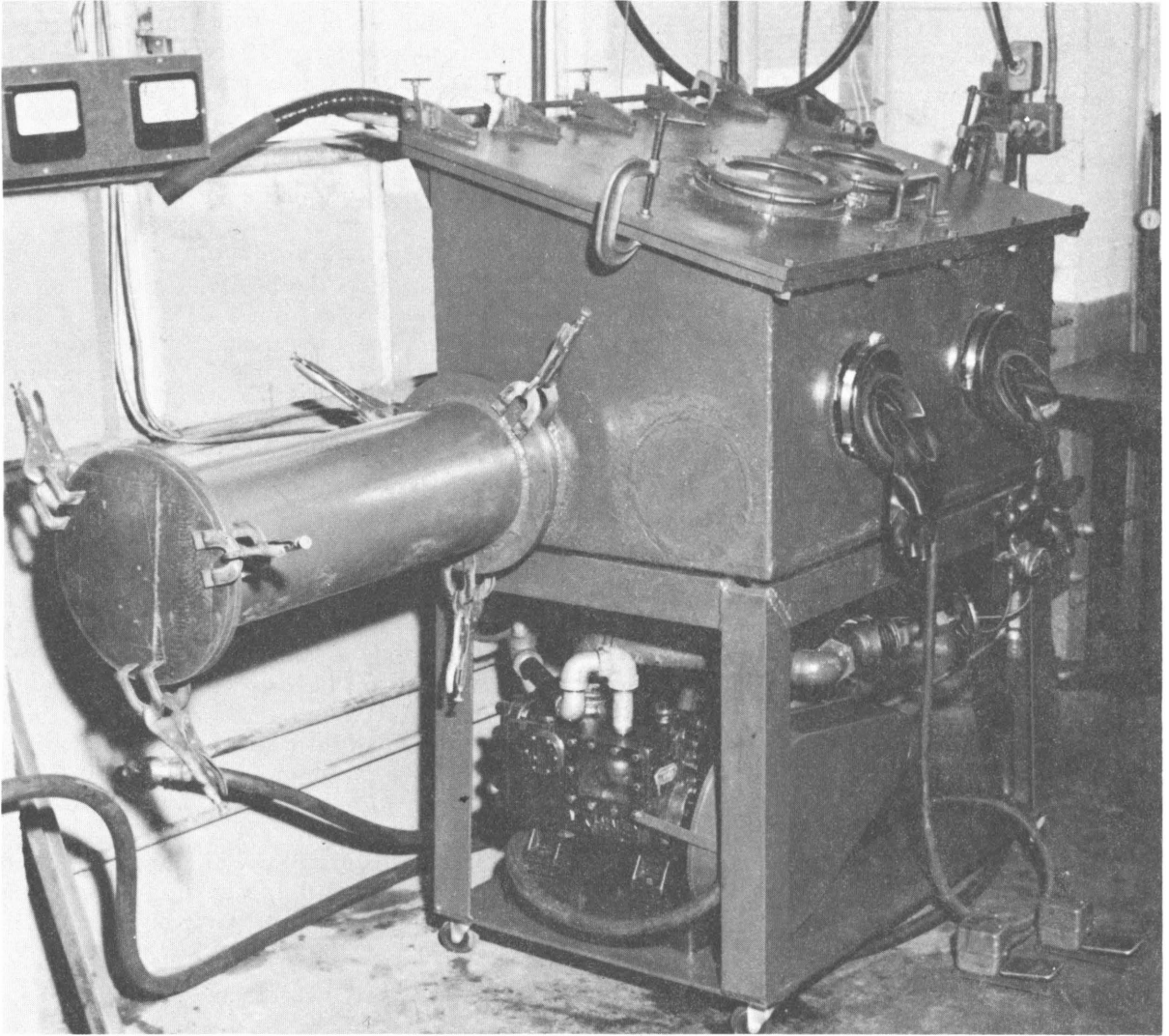
Figure 71.—Inert atmosphere hand welding box.
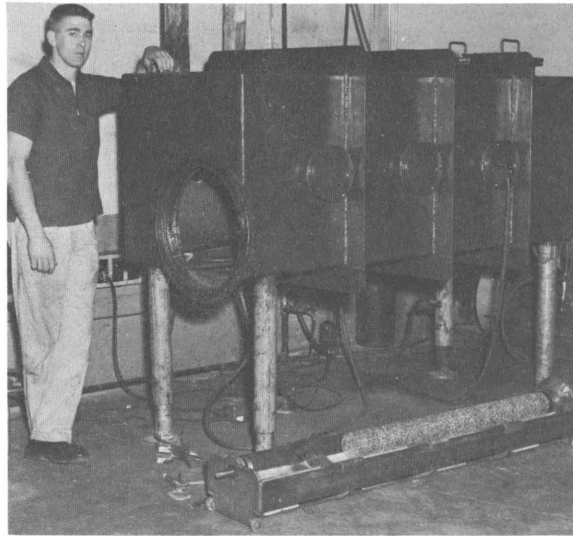
Figure 72.—Inert atmosphere automatic welding box.
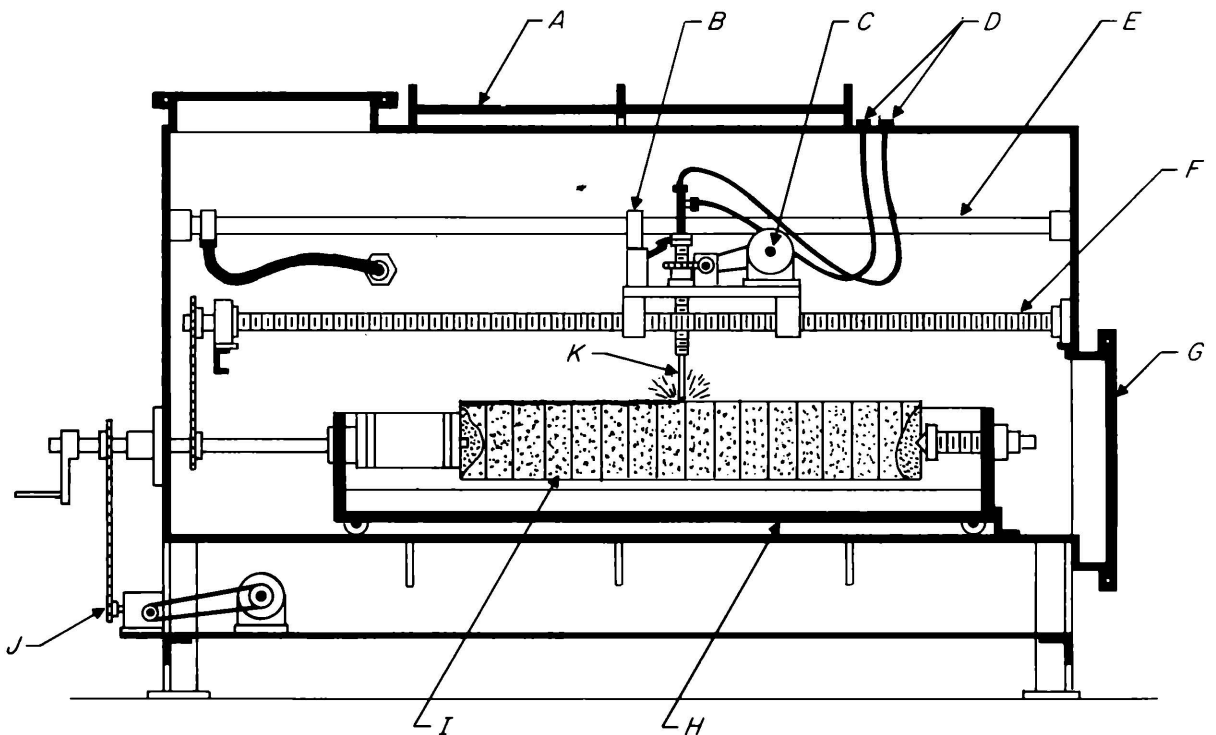
A Water jacket   B Power sliding contact   C Raise and lower drive motor   D Water leads   E Power contact   F Lead screw   G Manhole   H Water jacket   I Electrode compacts   J Lead screw drive   K Tungsten electrode

Figure 73.—Schematic view of inert atmosphere automatic welding box.
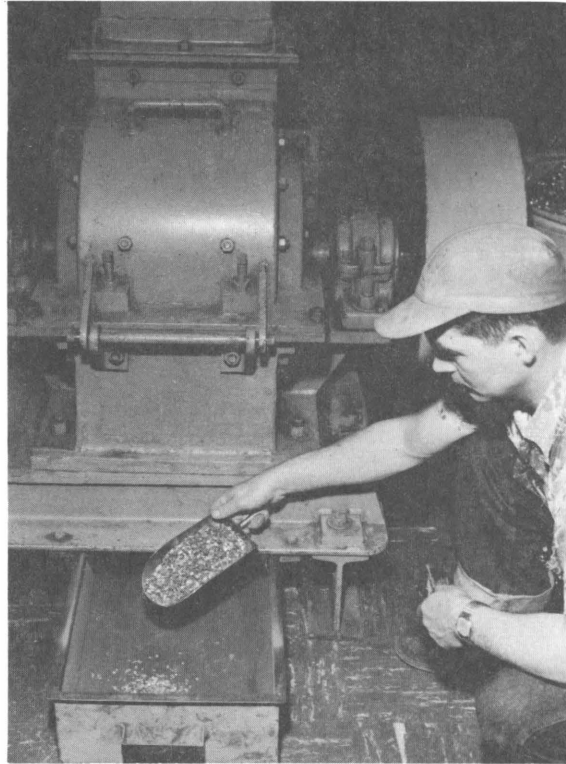
Figure 74.—Hammer mill for processing
machine chips.
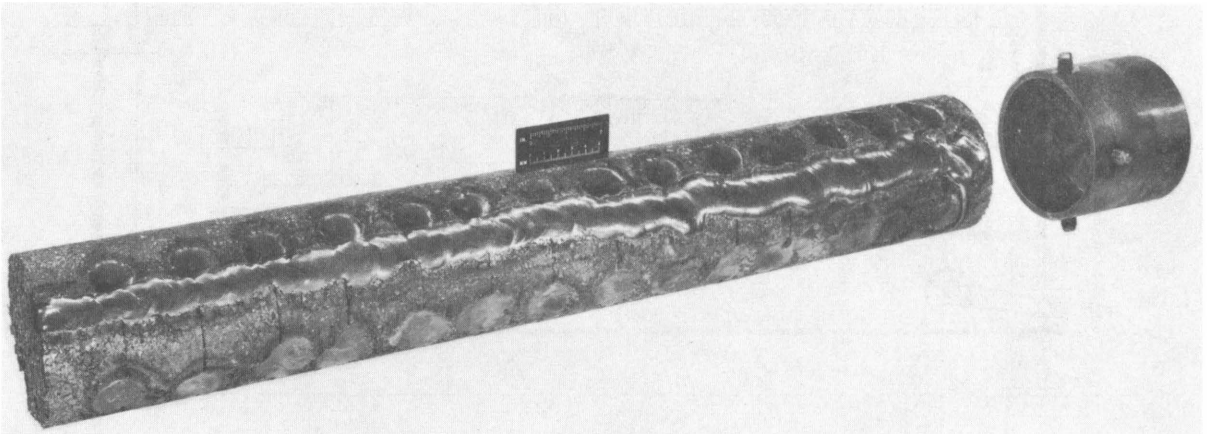
Figure 75.—Electrode of welded briquets.
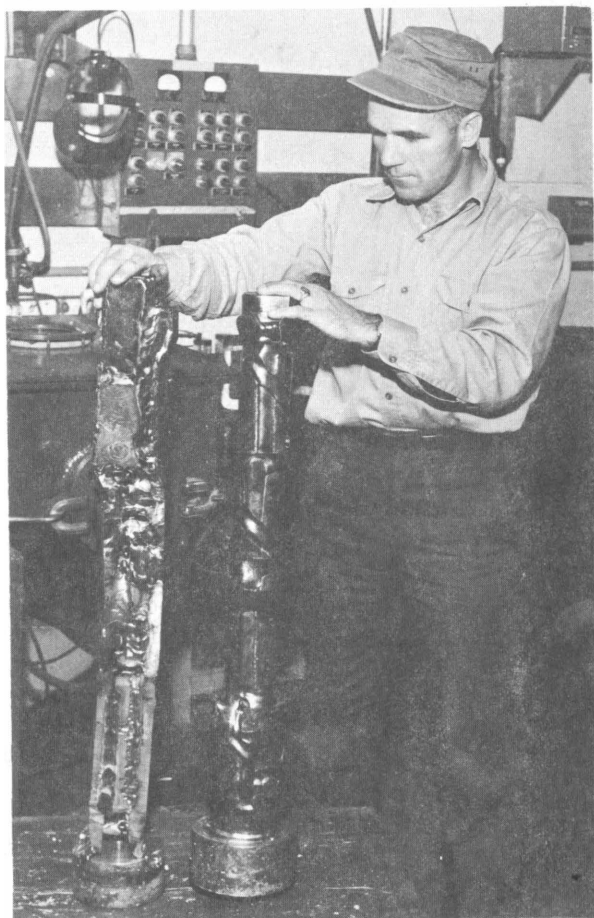
Figure 76.—Electrodes of welded plate and casting scrap.

Figure 77.—Electrodes of welded ingots.

As a general rule for joining electrodes, at least 1-in² area of contact should be allowed for every 1,000 amp of arc current. Figure 77 shows the equipment for welding 7-in-diam ingots to produce an electrode for remelting in a larger cup.

Regular practice at this laboratory is to tap the faced ends of first-melted ingots and to screw them together with short nipples of the same metal (1-in N.C. thread). The chief objective is to achieve face-to-face contact of the ingots, as the nipple alone could not conduct the required arc current without overheating and melting.

In conclusion, it must be stated that no one method for producing consumable-electrode compacts is satisfactory for all applications. Pressed bars have advantages over cylindrical briquets in length-to-width ratios and dimensional consistency. Sintered bars may be produced in quantity with low capital investment. Welded fabrications are easily made by hand or machine and help to utilize scrap that would otherwise be difficult to handle.

REFERENCES

1. Gilbert, H. L., W. A. Aschoff, and W. E. Brennan. Arc Melting of Zirconium Metal. J. Electrochem. Soc., v. 99, May 1952, pp. 191–193.
2. Parke, R. M., and J. L. Hamm. The Melting of Molybdenum in the Vacuum Arc. Trans. AIME, v. 171, 1947, pp. 416–427.
3. Stephens, W. W., H. L. Gilbert, and R. A. Beall. Consumable-Electrode Arc Melting of Zirconium Metal. Trans. ASM, v. 45, 1953, pp. 862–871.
4. Wood, F. W. Electrode for Melting and Welding Zirconium Metal. U.S. Pat. 2,892,924, June 30, 1959.
5. Wood, F. W., J. O. Borg, and R. A. Beall. Arc-Ingot Conditioning by Sidewall Fusion. BuMines Rept. of Inv. 5149, 1955, 11 pp.

CHAPTER 10.—ULTRASONIC INSPECTION OF ARC-CAST ZIRCONIUM AND ZIRCONIUM ALLOYS

By F. W. Wood and J. O. Borg

Although limited experience has been gained with a variety of alloys, ultrasonic testing techniques have been applied extensively to two zirconium alloys as well as to zirconium. The effect of alloying additions has been slight and required no modification of testing practices.

ULTRASONIC PROPERTIES

From the values of Young's modulus and density reported by Boulger (1) calculated velocity of longitudinal sound in zirconium is about 12,500 fps as compared with some 17,000 to 20,000 fps in most steels. Therefore, a 5-Mc wave would have a wave length in zirconium of about 0.030 in and in steel of about 0.045 in. Similarly, a 2.25 Mc wave would have wave lengths of about 0.067 in and 0.10 in in zirconium and steel, respectively. Although not strictly true, the cross-sectional area of the smallest detectable flaw is generally considered equal to the wave length of the test wave. Pulse frequencies of 2.25 and 5 Mc have been used exclusively in the routine straight-beam testing of ingots. Generally, better resolutions and narrower pips are obtained with 5 Mc. On the other hand, the 2.25 Mc pulse results in less interference. When a 5-Mc test pulse is applied to normal-quality, arc-cast, Bureau of Mines zirconium, the limit of effective penetration is 3 to 4 ft.

EQUIPMENT

The instrument employed by the Northwest Electrodevelopment Laboratory for ultrasonic testing is a Sperry type UR, style 50E401 reflectroscope. The principle of the reflectroscope and the history of its development have been presented in more detail elsewhere (2–3, 5). Briefly, however, the equipment used has three components: a pulse generator, an oscilloscope, and a crystal searching unit. The combination constitutes a pulsed echo-ranging system in which the searching unit alternately acts as a transmitter and a receiver. The pulses originate electronically in the pulse generator, are converted to mechanical vibrations, and are transmitted to the test piece by the piezoelectric searching unit. Upon reflection from a discontinuity or opposite test-piece face, pulses are received by the searching unit and transformed into an alternating voltage, which is fed into the oscilloscope as the vertical sweep signal. This vertical signal may be superimposed upon either linear or square-wave horizontal sweep signals at the discretion of the operator.

Visible evidence of reflected pulses appears as vertical deflections or pips on the oscilloscope screen. The resulting pattern may be visually observed and photographed by using a camera attachment on the reflectoscope. The origin of the oscilloscope trace is a fixed point on the screen, and the position of the searching unit is represented by a pip at this origin. The distance from the trace origin to a pip representing a reflected pulse is proportional to the distance from the searching unit to the point of reflection. The frequency of the square-wave signal is variable through a wide range. Thus, this signal may be used as a marking scale to estimate the position of a discontinuity.

The width of the first pip on the reflectogram, indicating the position of the searching unit, is determined by the pulse-length adjustment. In tests of ingots of zirconium and its alloys, the settings required are such that a portion of the oscilloscope trace, representing 4 to 8 percent of the ingot length, is obscured. Consequently, when an ingot is examined from the top face, the shrink-pipe pip may not be resolved from the searching unit pip. Accordingly, special emphasis has been given to examination of ingots from their bottom faces. Telescoping the horizontal sweep causes successive orders of reflection to appear on the oscilloscope screen. Detection of flaws in close
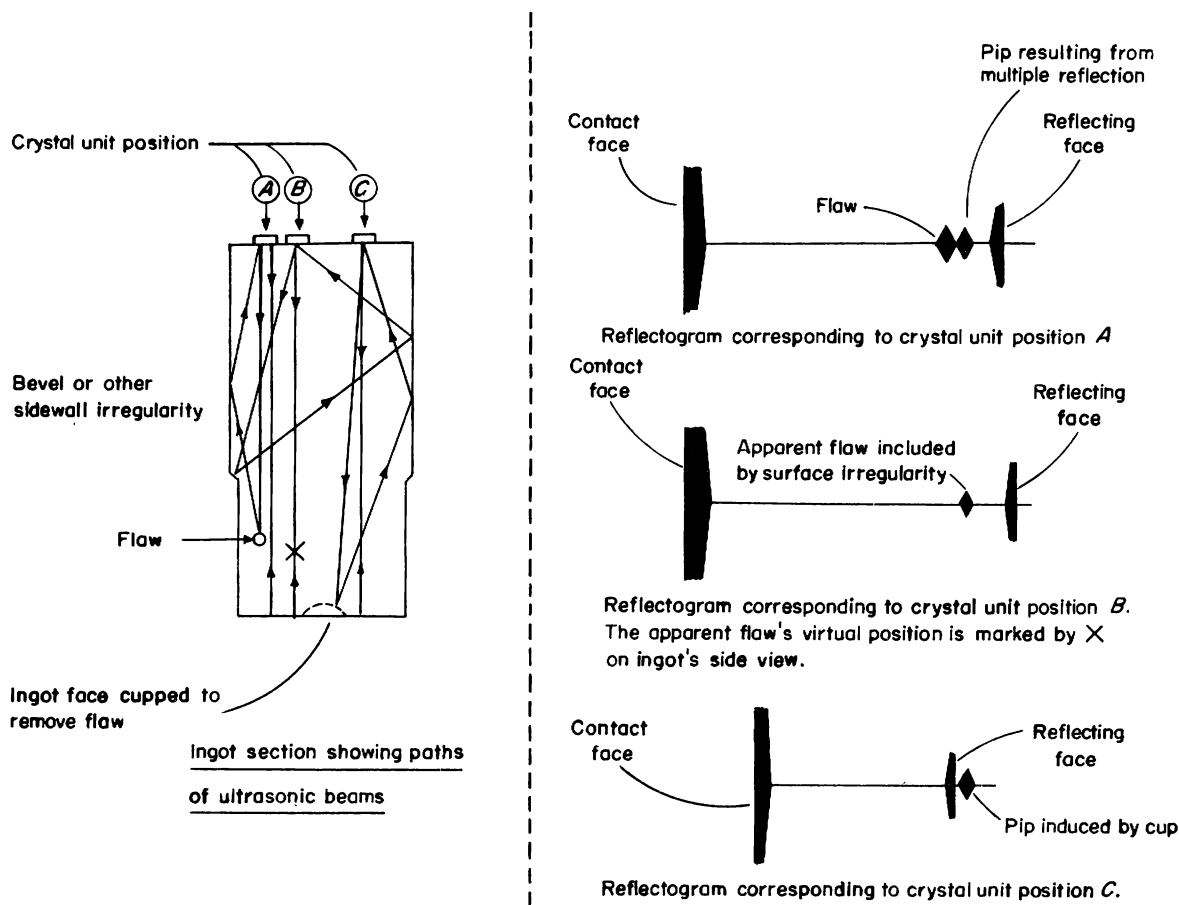
Figure 78.—Cross section of ingot, showing possible flaws and resulting reflectograms.

proximity to the crystal unit and examination of thin pieces of metal are sometimes simplified by using the second order of reflection.

Because of beam divergence and absorption, detection of small flaws in ingots over 30-in long is sometimes difficult. The use of a stronger ultrasonic pulse is limited because increasing the pulse amplitude or length intensifies the interference as well as amplifying the pips indicating specific flaws. This confuses or even obscures the true picture, and the application of too much power is as apt to lead to misinterpretation as is the use of insufficient power. Therefore, moderate power is used with careful observation of the trace.

A metallic object is examined for internal discontinuities by contacting the metal surface with the searching unit and moving it very slowly and carefully, covering the entire test surface several times. It is advisable to apply a heavy layer of oil to the metal surface for lubrication and coupling. Best results are obtained when the contact surface is flat and polished, although satisfactory results may be obtained on a flat or slightly curved, lathe-finished surface.

Special techniques, such as immersion testing (4), have been developed for use when irregular surfaces are involved. Immersion testing involves placing both the piece under test and the searching unit in a liquid medium. However, the use of special techniques has not been necessary in the work under discussion.

The most common discontinuity encountered in ingots is the shrink pipe formed near the top. A certain amount of interference, absorption, or both, is always present in a reflectogram, the magnitude depending upon such things as grain size, impurities, the quantity of metal penetrated, and the geometry of the
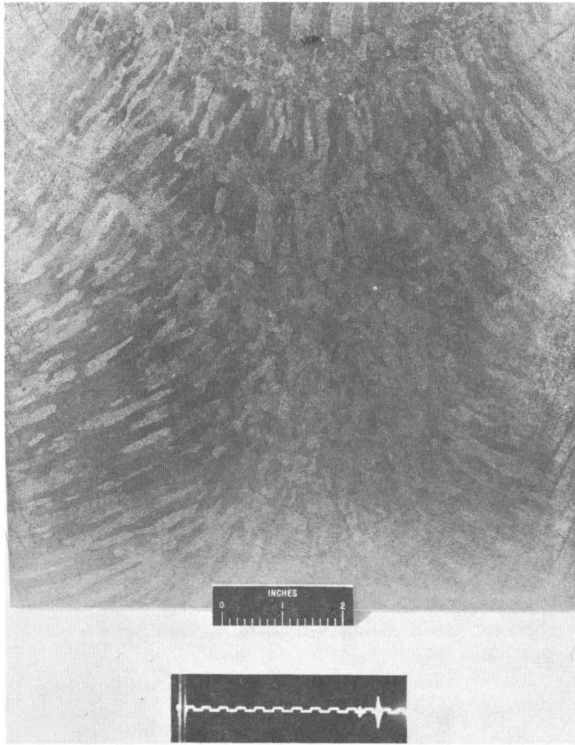
Figure 79.—Ingot containing shrink hole and typical square-wave sweep signal used in locating similar flaws.

5 mc signal   2.25 mc signal

Figure 80.—A concentration of porosity near the top of this ingot was delineated in the reflectograms shown.

object under test. A lack of symmetry or the presence of geometrical irregularities can produce misleading effects. Figure 78 illustrates the effects of surfacec irregularities and internal flaws by typical reflectogram patterns. The trace from position *A* is typical for a void where the beam is reflected from several faces. Surface irregularity, position *B,* results in a trace that normally would indicate a flaw at X. However, when a transverse measurement is made from the opposite end and the trace does not indicate a flaw, it is concluded that the distortion of the wave is the result of a surface imperfection. The pattern resulting from position *C* is typical for a surface imperfection on the opposite end of an ingot.

INGOT TESTING

Ingots are tested after the ends and sides are dressed in a lathe. In some instances, where the sidewalls are unusually smooth, machining may not be necessary.

The smooth bottom surface of the ingot is covered with machine oil and the examination

completed. Generally, the search from one end is sufficient to delineate the defect. However, if any uncertainty exists, transverse measurements are made to locate the defect more precisely. Following the examination, the defect is removed either by machining, if the area is within 1 in from the end, or by sawing off a section of the ingot.

Figure 79 shows a shrink hole in an ingot and a typical square-wave sweep signal used in locating similar flaws. The large pip at the left represents the position of the crystal searching unit (bottom ingot face), and the pip farthest to the right represents the position of the reflecting face. The third and smallest pip indicates the presence and position of a discontinuity. The ingot was 22½-in long. Consequently, the frequency of the square wave was adjusted so that there were 22½ half-cycles between the pips representing the contact and reflecting faces of the ingot (one-half cycle is obscured by

the pip on the left). Thus, the position of the discontinuity was determined to be about $1\frac{7}{8}$ in from the reflecting face. The test-pulse frequency was 5 Mc.

In gaging the general soundness of ingots, failure of a 5-Mc pulse to penetrate at least 30 in of metallic zirconium or zirconium alloy has been taken as evidence of excessive porosity. Ingots with a general distribution of porosity and ingots with localized porosity replacing or accompanying the usual shrink pipe have been encountered. The ingot shown in figure 80 contained porosity, particularly in the top half, as indicated by the accompanying reflectograms.

Routine testing does not depend on the availability of highly skilled personnel. Entirely satisfactory results may be obtained with only a few hours of testing experience. With reasonable care, very little maintenance or internal adjustment is required. Ultrasonic inspection has the added advantages of being nondestructive and is readily applicable to a variety of shapes and sizes of zirconium without preparing special test specimens.

REFERENCES

1. Boulger, F. W. The Properties of Zirconium. U.S. AEC Rept. AECD-2726, 1949, p. 83.
2. Delano, R. B., Jr. Supersonic Flaw Detector. Electronics, v. 19, January 1946, pp. 132–136.
3. Firestone, F. A. The Supersonic Reflectoscope for Interior Inspection. Metal Prog., v. 48, No. 3, September 1945, pp. 505–512.
4. Hitt, W. C. Douglas Detects Flaws by Underwater Testing. Machinery, v. 59, No. 2, October 1952, pp. 212–214.
5. Kelman, D. M. Nondestructive Flaw Detector. Westinghouse Eng., v. 9, No. 4, July 1949, pp. 115–118.

CHAPTER 11.—THE DEVELOPMENT OF THE SKULL CASTING METHOD

By R. A. Beall, F. W. Wood, J. O. Borg, and H. L. Gilbert [1]

THE PROBLEM AND A BASIS FOR ITS SOLUTION

In the early summer of 1953, the Bureau of Mines was requested by the Department of the Army through Watertown Arsensal to explore the possibility of conducting research on casting titanium metal. The objective of the program was "to develop a technique for producing formed castings of titanium metal not less than 40 pounds in weight and without introduction of deleterious contamination."

In essence, the problem of producing a casting of any metal is threefold: (1) Heat some of the metal to the liquid state, (2) transfer it to a mold, and (3) hold it while it cools and solidifies. The solution is, of course, never as simple as the statement. The obstacles implied by each phase of the problem are determined by the quality of product required and the character of the particular metal involved.

Molten titanium (mp, about 1,660° C) reacts with all common refractories and alloys with most metals. At temperatures far below its melting point, titanium is severely attacked by the active atmospheric components. Furthermore, the presence of some contaminants in minute quantities can be detrimental to titanium. Hence, merely to contain a quantity of molten titanium may lead to possible contamination.

Although consumable-electrode arc melting makes it possible to produce titanium ingots uncontaminated by either crucible or electrode, it has previously yielded only cylindrical shapes. This is satisfactory as a starting shape for forging, but it does hinder the designer in total utilization of titanium.

Considerable work has been done on the shape-casting problem. Kroll and Gilbert (4) announced in 1949 a method of shape-casting zirconium and titanium utilizing a graphite

crucible heated by a graphite resistor. Sutton, Gee, and DeLong (9) demonstrated the use of induction heating in the same type of crucible. In neither instance would the carbon content meet present standards.

Lang, Kura, and Jackson of the Battelle Memorial Institute reported (6) the operation of a tilt-pour, tungsten-electrode, graphite-hearth skull furnace. The Rem-Cru Titanium Research Laboratories also operated an inert-electrode skull furnace (7) which was later enlarged to accommodate a 100-lb pour. In December 1952, Kuhn (5) utilized a water-cooled hearth plate and tungsten electrode to precision cast several small parts. Simmons, Edelman, and McCurdy (8) developed a bottom-pour, tungsten-electrode arc furnace. By the last of 1953 the development of the inert electrode skull furnace had progressed so that a 10-lb casting unit was placed on the market (10).

This was the situation when the Bureau of Mines began titanium-casting research. Consumable-electrode increment melting had reached an advanced state of development. Casting was confined to inert-electrode skull-type melting involving the use of one or several arc electrodes.

At the Bureau of Mines laboratory at Albany, Oreg., production requirements for consumable-electrode zirconium ingots had relaxed slightly, and the variables of the process were being studied, particularly the shape and volume of the molten pool during various melting conditions. It was discovered, and subsequently reported (1), that for zirconium the pool volume was a direct function of the rate of melting. A second conclusion of this study was that the melting rate for a given power input was enhanced at furnace pressures slightly above that at which glow discharge occurs. Under these circumstances it was shown that molten-pool volume approached 50 percent of the volume of the ingot. Because this indicated for the first time the feasibility of producing castings of refractory metals by the consumable-elec-

trode arc process, the Bureau investigators obtained a patent (2).

FURNACE DEVELOPMENT

Initiation of Project

Approximately 900 lbs of commercially pure titanium in the form of hot-forged billets was received for use in initial stages of the work. The first point to be determined was whether titanium could be melted to form deep pools, as in zirconium melting. Employing the same arc-melting equipment used in zirconium melting, a series of 10-in-diam ingots was cast. When the melting had progressed to the desired limit, the arc current was terminated, and a small amount of alloying material was dropped into the pool simultaneously. A typical ingot of the series was 15½-in long. Upon sectioning and etching this ingot, the pool was found to be more than 14-in deep; its volume was estimated to be 746 cubic inches and its weight 115 lbs. This was 62 percent of the ingot. Figure 81 shows the cross section of the ingot and the pool.

Next, attempts were made to transfer the molten metal to a mold. For convenience it was decided to try a bottom-pour technique to fill a machined graphite mold. A standard arc-melting furance was modified by adding a mold box below a 14-in-diam copper crucible and water jacket, as shown in figure 82. The new crucible was furnished with a pouring hole stoppered with a water-cooled copper plug.

Having produced a deep pool in a titanium skull, it was expected that, when the water cooling was removed from an area of the skull bottom, the skull would be melted and tapped at this point by conducting heat from the pool. This proved to be the case, and figure 83 shows the appearance of the mold-box interior at the time of opening. Both the sidewall and interior of the cylindrical casting were of good quality.

A series of 79 heats was made in this furnace. In all, 58 heats were poured, and 52 castings were produced. The average reliability (66 percent) is not necessarily representative; the reliability for the last 40 heats of the series was 75 percent and the last 20, 76 percent. The improvement in performance is accounted for by increased experience and enlargement of the pouring hole from 1½ to 3-in. The term "reliability" in percent indicates the ratio of the number of poured castings to total heats.
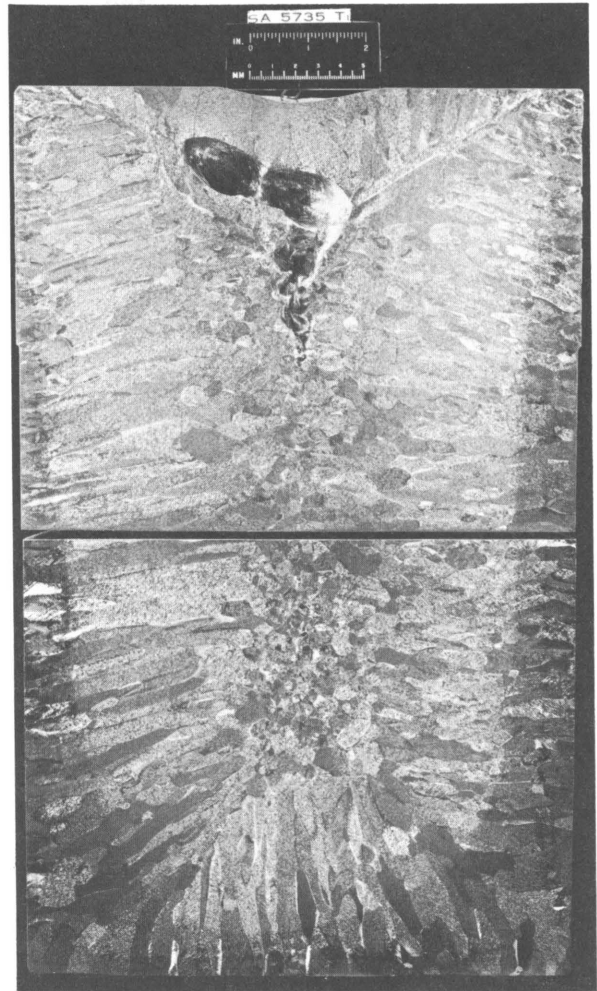
Figure 81.—Longitudinal section of a titanium ingot, showing deep pool.

Lack of success may have been due to a stuck plug, too thick a skull, or other reasons.

A variety of castings was produced with untrimmed weights ranging from 12 to 61 lbs: 33 percent weighed between 10 and 20 lbs; 41 percent between 20 and 30 lbs; 16 percent between 30 and 40 lbs; and 10 percent over 40 lbs. Many of the castings were simple cylinders, but others were shapes such as those shown in figure 84.

It soon became apparent that the size of the initial mold box imposed serious limitations, so construction was begun on a new bottom-pour furnace with interchangeable 14- and 10-in-diam crucibles and a mold box that measured roughly 6 ft wide by 6 ft deep by 4½ ft high. Later, because of certain inherent disadvantages of the bottom-pour technique, it was decided to explore
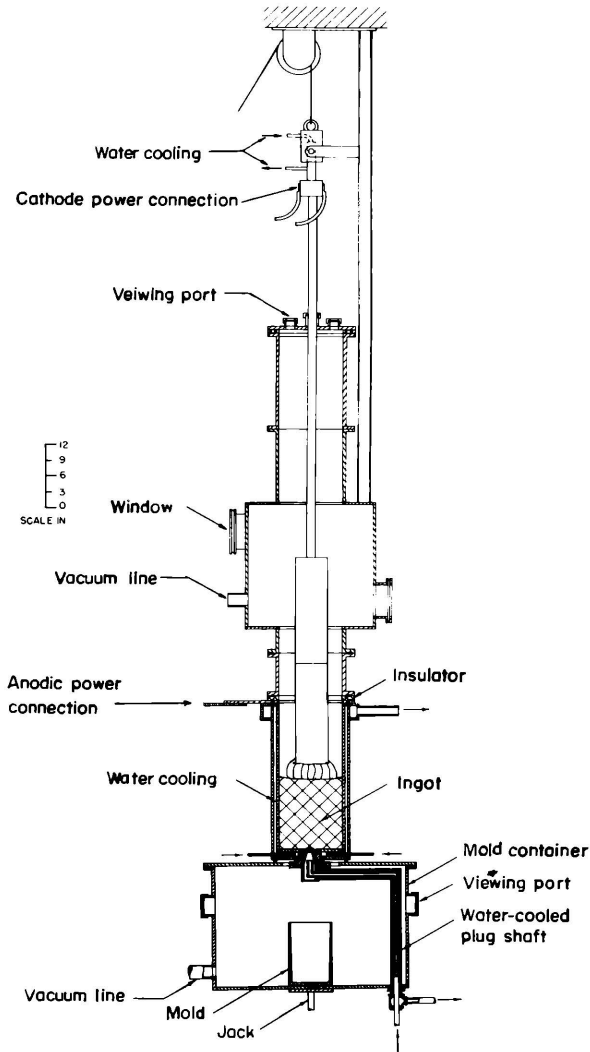
Figure 82.—Consumable-electrode arc-melting furnace, with modification for bottom tapping.

Figure 83.—Crucible and mold box, bottom-pour furnace.

concurrently the possibility of pouring over the lip of a water-cooled copper ladle.

Improved Bottom-Pour Casting Furnace

The enlarged version of the bottom-pour furnace is shown in figure 85. In this instance, instead of moving the mold box under the crucible, the crucible was placed upon the mold box, the latter being stationary and strong enough to support the weight of the upper portions of the furnace. As before, the electrode was connected mechanically and electrically by a water-cooled copper shaft, which enters the top of the furnace through an O-ring gland.

The mechanism for removing the water-cooled copper plug underwent many modifications, partly because it occasionally stuck to the skull. Originally the plug was drawn by a manually operated shaft, but it became necessary to utilize a heavier and more positive drive. The final improvement was a 5-in-diam, double-acting, pneumatic piston operated by helium at 100 psi. The plug was withdrawn vertically; then the plug mechanism was drawn to the side on a roller track. The mold, also on a roller track, was attached to the plug mechanism and was drawn under the pouring spout.

The design of the plug was changed also. Initially, a hollow, water-cooled, truncated cone of copper sealed a 3-in-diam hole. This was succeeded by a similarly designed plug that sealed a 4-in-diam hole. The final modification was a 6-in-diam, cylindrical plug and hole.

Two mechanical pumps, each rated at 110 cfm free air displacement and working in parallel on 2-in lines, constituted the vacuum system.

The mold box was ¾-in steelplate with reinforcing H-beams to prevent deformation under vacuum. Several ports and two manholes were provided for visibility and entry in addition to the main door, which was nearly the full end dimension of the box. The bottom was double-walled for water-cooling.
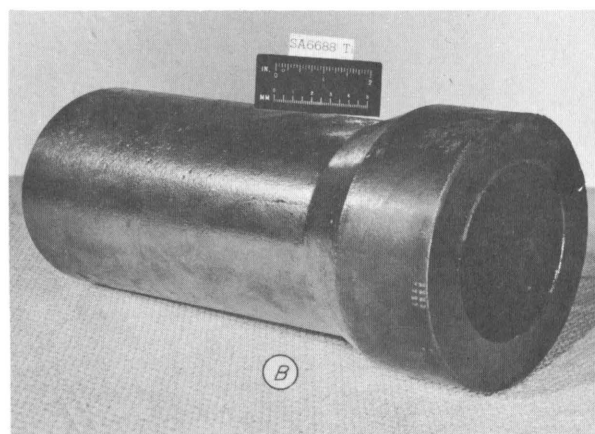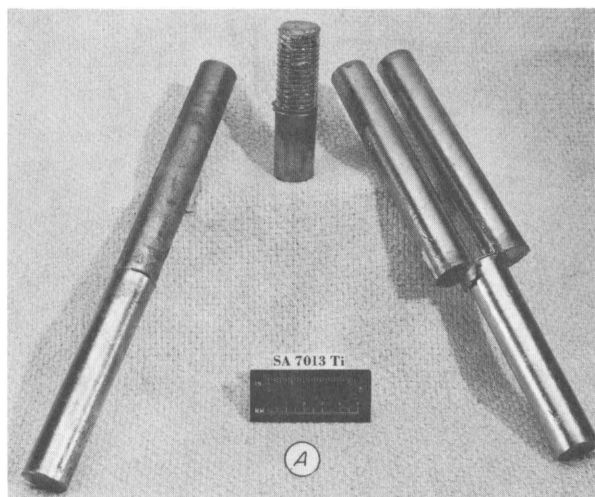
Figure 84.—*A*, cast titanium tools; *B*, cast titanium breech liner.

Figure 85.—Large-scale bottom-pour casting furnace.

The operational cycle finally adopted for the equipment was as follows:

1. Assemble furnace (approximately 30 min).
   A. Charge starting pad in crucible.
   B. Load electrode.
   C. Assemble and place mold.
2. Pumpdown (approximately 50 min).
   A. Final vacuum, 150μ.
   B. Check leak rate (to be less than 5μ/min).
3. Preoperation inspection (5 min).
   A. Make final check of power connections.
   B. Check water pressure and flow readings.
   C. Check alinement of electrode.
   D. Check helium pressure to pneumatic cylinder.
4. Melt (15 min for a full-capacity pour).
   A. Backfill to 1-in of Hg with argon and/or helium.
   B. Initiate arc of 3,000 amp, 33 v.
   C. As soon as a pool of molten metal has been established open the valve to the vacuum pumps for the remainder of the melt.
   D. Stabilize potential at 30 v and raise current to 8,000 amp in 500-amp increments at intervals governed by observation of exit temperature of copper-plug cooling water.
   E. Melt to desired point, then raise to a maximum available current of 12,500 amp.
5. Pull plug, 1 min.
   A. Cut power when pouring begins.
6. Cool, 50 min.
7. Disassemble, 30 min.
Total cycle: About 3 hr.
Procedure 4D requires elaboration: A simple bulb thermometer was mounted in the outlet line carrying cooling water from the copper plug. The closest convenient location happened

Table 10.—Bottom-pour casting heats

Heat No.	Electrode cross section, in^2	Skull OD, in	Weight poured, lb	Resultant skull weight, lb	Ratio: pour/electrode consumed	Ratio: pour/net charge
SA8127	38	14	101.7	44.1	[1] 1.01	0.68
SA8266	38 to 50	14	20.3	10.4	[1] .92	.66
SA8293	38	14	22.5	10.8	[1] .99	.63
SA8305	38 to 50	14	40.4	29.8	Unknown	Unknown
SA8315	38 to 50	14	38.8	48.7	1.09	.44
SA8335	38	14	46.7	4.6	[1] 1.28	.91
SA8346	38	14	17.6	11.5	.88	.61
SA8393	38	14	17.2	14.8	.73	.53
SA8464	50	10	33.1	10.4	[1] .89	.76
SA8490	50	10	44.1	9.3	[1] .98	.82
SA8492	19 to 50	10	37.0	11.0	1.02	.75
SA8730	38	14	50.7	26.2	[1] .78	.65
SA8753	38 to 50	14	104.7	28.7	[1] .85	.77
SA8788	38 to 50	14	100.5	32.4	[1] .86	.76
SA8958	38	14	72.3	26.0	[1] .85	.74
SA8977	38	14	82.7	27.3	.99	.75
SA9053	38 to 50	14	62.4	28.7	[1] .80	.68
SA9113	38	14	88.6	34.4	Unknown	.72
SA9187	38	14	75.0	27.8	[1] .81	.72
SA9203	38	14	74.7	26.5	[1] .84	.73
SA9303 [2]	38	14	47.4	30.9	[1] .73	.60
SA9336	38	14	80.7	50.3	.83	.61
SA9398 [3]	38	14	67.3	26.0	[1] .86	.72
SA9410	38	14	75.0	44.5	1.05	.63
SA9422	19 to 38	14	75.6	41.9	1.22	.64
SA9444	78	14	75.6	46.7	.96	.61
SA9501 [2]	38	14	76.3	30.0	1.01	.72
SA9504 [3]	38	14	78.1	38.6	.92	.67
SA9508	50	14	71.9	28.4	[1] .87	.75
SA9547	38	14	94.8	46.7	[1] .75	.65
SA9672	19 to 50	14	63.1	31.3	[1] .84	.68
SA9791	38	14	77.6	27.3	[1] .88	.74
SA9819	50	14	71.0	31.8	[1] .84	.69
SA9842	50	14	113.8	38.8	.99	.73
SA9853	50	14	108.0	42.3	1.05	.72
SA9876	38 to 50	14	112.0	46.7	1.03	.74

[1] Charge did not include a skull from an earlier heat.
[2] Ti + 8Mn.
[3] Ti + 7Mn.

to be about 4 ft from the plug, and about 8 gal of cooling water was circulated through ½-in copper tubing each minute. Upon establishing a molten pool with 3,000-amp arc and evacuating the furnace, the arc power was increased to 4,000 amp at 30 v. Within 2 min this normally resulted in penetration of the skull or other crucible charge, and consequently the thermometer reading began to rise. If this did not occur, the power was advanced in 500-amp increments until either a temperature rise was detected or the current reached 8,000 amp. The minimum time between incremental power advances was considered to be 45 sec. When the indicated temperature did begin to increase, the arc power was maintained constant until the temperature rise slowed. As temperature leveled off, the arc current was increased by 500 amp. This procedure continued until arc current reached 8,000 amp, keeping the power input just high enough to cause a gradual, steady increase of temperature. The maximum temperature attained during a heat was commonly 100° to 110° F, but the reading usually dropped to about 85° or 90° F by the time the plug was withdrawn.

Some type of control technique is essential to successful operation, since excessive application of power at any time during a heat may cause the plug to be wet, preventing withdrawal. On the other hand, if the skull thickness over the plug exceeds 1 in at any time during latter stages of the heat, the skull cannot be pene-

trated. This was determined by sectioning and etching sections of the metal remaining in the crucible. Surprisingly, attempts to effect control with a thermocouple mounted in the plug failed. Presumably this was because (1) the entire plug was subject to considerable mechanical shock, (2) the sensitivity of the thermocouple used made it difficult to distinguish between general temperature trends and spurious fluctuations, and, possibly, (3) induction of extraneous voltages in the thermocouple leads.

Table 10 is a chronological listing of general information pertaining to 36 successful bottom-pour heats made in the enlarged furnace. In addition to these, 48 attempts failed—26 because the skull was not penetrated, 14 because the plug became stuck, and eight because of miscellaneous mechanical, electrical, or other failures. More than one reason was found for sticking of the plug. In addition to wetting, if the plug and taphole diameters were permitted to differ by more than $\frac{1}{16}$-in, molten metal would flow into the gap, freeze, shrink, and securely lock the plug in place. Near conclusion of the work it was established that the practical pouring capacity of the furnace was about 110 lb. Attempts to exceed this limit were responsible for failure to penetrate the skull in several instances.

Still referring to table 10, the 4-in-diam plug was installed at heat SA 8293; the 6-in-diam plug and pneumatic withdrawal mechanism were installed at heat SA 8730; at heat SA 9187 the operating procedure based on plug-cooling water temperature was adopted; and starting with heat SA 9398, no attempts were made to exceed 110 lb. Overall, 43 percent of the heats were successful; after the final operating procedure was adopted, 69 percent were successful; and after recognition of the furnace capacity, 78 percent succeeded.

Although many successful castings were made with this equipment, the operation cannot be considered satisfactory or ready for industrial application. Chief among the unsolved problems are (1) control of the moment of pour and (2) quick recycle. Using a consumable electrode, it is quite important that the instant of pouring be controlled; that is, if the pour occurs before or after the desired time, the quantity of molten metal will be less or greater than desired. The former could ruin the casting; and the latter, if excessive, could ruin a mold by overflowing and certainly waste expensive metal. The greatest uncertainty is in the thickness of skull formed over the pouring spout. The thicknesses of pene-

trated skulls have varied from $\frac{1}{16}$ to 1 in, owing to the freedom of the arc to cover the entire bottom of the crucible. Slight differences of cooling rate are bound to occur, depending upon the base material and the exact geometry of the previously used skull. In contrast to those instances when even maximum power failed to penetrate the skull, there were instances when the pour occurred before the plug was entirely removed or the mold was in place. Figure 86 is a cross section of a chilled heat with flow lines and cold shuts tracing the history of a 14-in-diam skull.

The second disadvantage of the present bottom-pour furnace is the inability to replace the plug in the crucible to allow a subsequent melt and pour. This prevents using multiple molds and attaining normal production rates. The drips of metal that were always present following a pour and that froze in the pouring spout made it necessary to remove the skull after each heat for trimming. Formation of these stalactitic impediments is encouraged by the flow of vapors through the taphole and by the inevitable vortical flow of molten metal through a hole. Hot metal, either molten or solid, in the skull or mold is a source of vapor. Since vacuum operation is essential, the skull and mold regions are zones of relatively high vapor pressure. Being water-cooled and comparatively remote from the source of vapor, the taphole is a zone of lower pressure. The consequent vapor currents impinging on and constricted by the taphole cause a turbulence that disrupts the even flow of liquid metal. This situation was relieved slightly in heat SA 8464 (see table 10) when the practice of maintaining the arc during metal pouring was abandoned.

With the 3- and 4-in-diam tapholes, the objectionable drips were invariably found to be against the taphole walls, further complicating their removal. This was avoided, at least part of the time, by enlarging the taphole to 6 in, for it was found that the diameter of the opening in the skull was normally only 2 or 3 in. With the larger hole the drips tended to hang from the skull itself without directly contacting the taphole walls. However, the point at which the skull was pierced was not subject to control, and the drips still clung to the taphole walls too frequently.

Efforts were made to facilitate reinsertion of the plug by manually grinding and cutting the drips away while the skull remained in the crucible. Chisels, chippers, gouges, various grinders
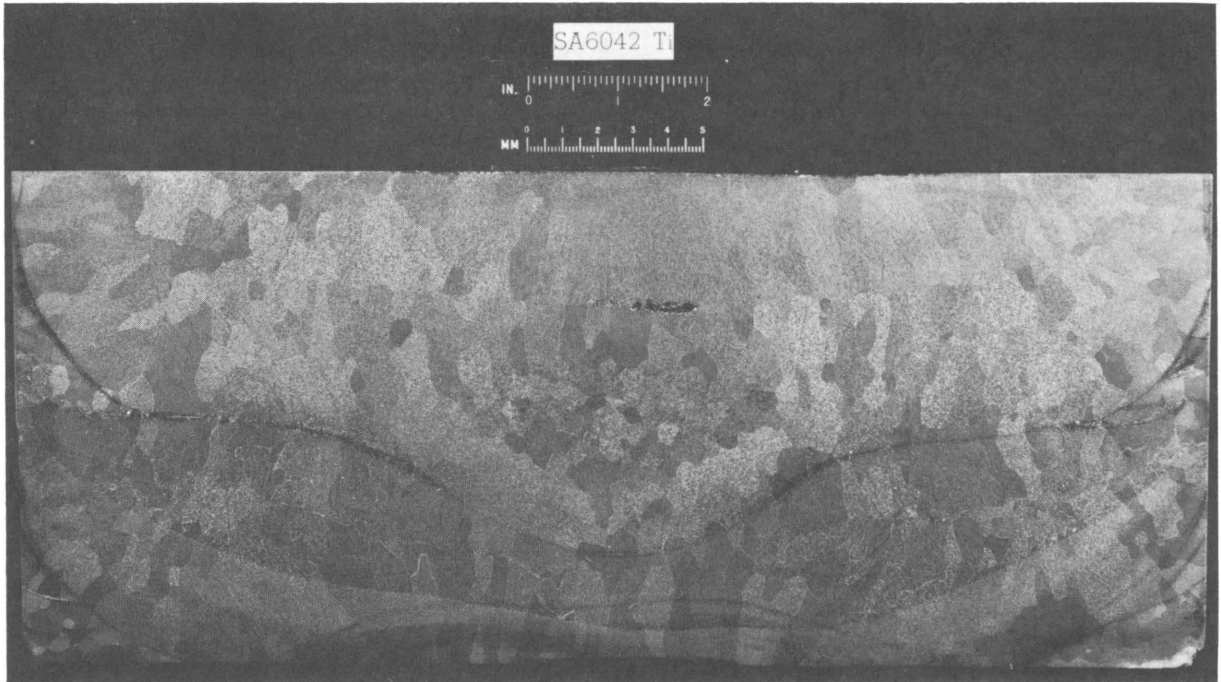
Figure 86.—Longitudinal section of a chilled ingot.

and abrasive cutters, and both oxyacetylene and electric torches were employed. In no instance was the removal effected cleanly enough to permit the plug to be reinserted without raising the skull slightly, and in addition the taphole was frequently damaged.

In another approach to the problem, it was reasoned that perhaps complete removal of the drips was not necessary or possibly a water-cooled plug was not needed. In the first instance, either the plug must be partly inserted or the skull must be lifted from its contact with the crucible bottom. If the plug is only partly inserted, the skull thickness over the tapholes is increased, reducing the furnace capacity and probability of success accordingly. When the skull is raised it is readily pierced, and part of its molten content drains into the gap between skull and crucible. This metal quickly freezes, and both the metal and its heat content are lost for practical purposes. Again, the probability of a successful pour is reduced because of a thicker skull.

To test the second proposed method of operation, a special series of heats tested the feasibility of pouring without a cooled plug. Heats SA 8305, SA 8315, and SA 8335 listed in table 10 were included. In this case, either a titanium plug must be used or the rate of electrode consumption must be high enough (on the order of 100 lb/min is estimated) to permit direct casting. The maximum consumption rate attained with available rectifying capacity was about 11 lb/min. This proved insufficient to produce sound castings directly. When a titanium plug was used, premature tapping was common, since essentially no control could be exercised over the moment of pour.

It is undoubtedly possible to install in the mold box remotely operated cutting or trimming machinery to remove troublesome drips, perhaps while the casting cools. However, the complexity of such auxiliary apparatus under the conditions of vacuum and temperature suggested the need for an entirely different concept for pouring.

It was the increasing awareness of these problems that prompted and hastened the exploratory work with the pour-over-the-lip technique.

Pour-Over-The-Lip Casting Furnaces

The first objective of the pour-over-the-lip method of casting was to construct a small furnace to explore the feasibility and to determine whether larger scale equipment could be justified. Accordingly, in April 1954, an available

A   Power connection
B   O-ring
C   Consumable electrode
D   Viewing ports
E   Tilting lever
F   Tilting crucible
G   Mold
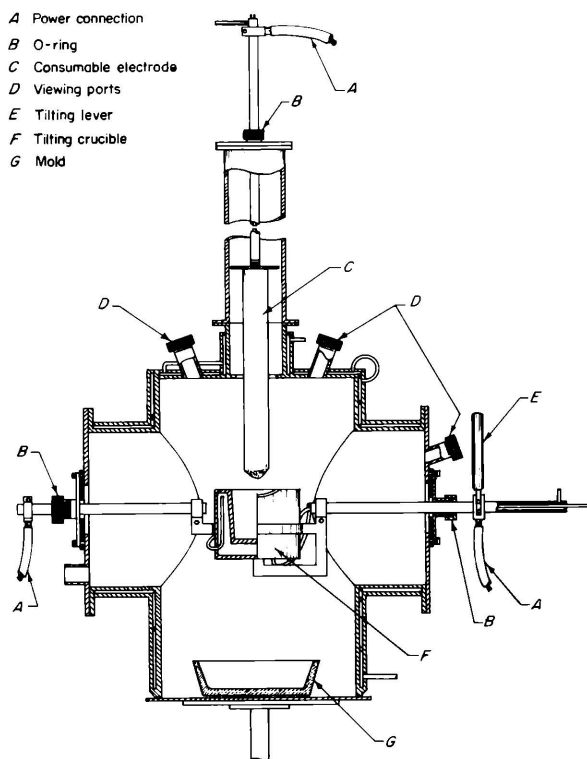
Figure 87.—Schematic diagram of pour-over-the-lip furnace.

Figure 88.—Pour-over-the-lip furnace.

water-cooled shell was modified to accommodate a pouring ladle. Figure 87 shows the furnace construction schematically, and figure 88 shows the equipment in operation.

Initially, provision was made for only one power lead to the ladle. Apparently this L-shaped current path, possibly in conjunction with the steel furnace shell, produced a magnetic field that deflected and tended to fix the arc in the plane of and at about 135° from the legs of the L, causing local overheating and burn-through. At any rate, addition of another power lead to yield an inverted T configuration resolved the difficulty.

The shape of the ladle underwent several changes, the most satisfactory shape being a cylinder that was slightly tapered to facilitate skull removal. Figure 89 shows a cup and a skull.

Availability of only 4,000 amp at the first furnace location limited the ladle to 160 in³, with a 6-in diam. As much as 16.5 lb could be poured under these conditions, but castings were consistently unsatisfactory with respect to surface quality. Cold shuts, flowlines, and unconsolidated spatter were much in evidence. The flow

of cooling water (about 5 gpm) required to protect the ladle from arc damage was capable of rapidly quenching the relatively small ladle charge, and fluidity suffered.

Relocation of the furnace near a more powerful source of current, permitted upscaling limited only by dimensions of the furnace shell. Through the use of a 550-in³, 8-in-diam ladle and arc currents of 5,000 to 5,500 amp, a successful series of castings was produced. These castings included a fluidity spiral series and a group of 6- by 6- by ½-in test plates of titanium, 8-percent manganese alloy, illustrated by figures 90 and 91. At this point the pouring capacity of the furnace was about 26 lb.

A total of 74 heats was made in the pilot-scale equipment. Pours resulted from 37 of 41 heats at the first furnace location and from all of 33 heats at the second location. This experience made it possible to conclude the following:

1. With fixed electrode-ladle geometry and a uniform operating procedure, the skull weight tended toward an equilibrium value that depended primarily on arc current, total ladle charge when ready for pouring, and the time

Figure 89.—Tilting crucible and skull.
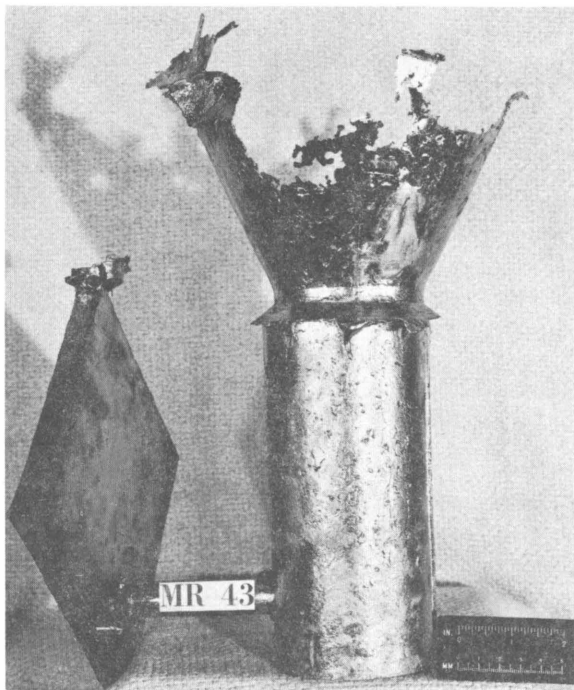
Figure 91.—Cast titanium plate.
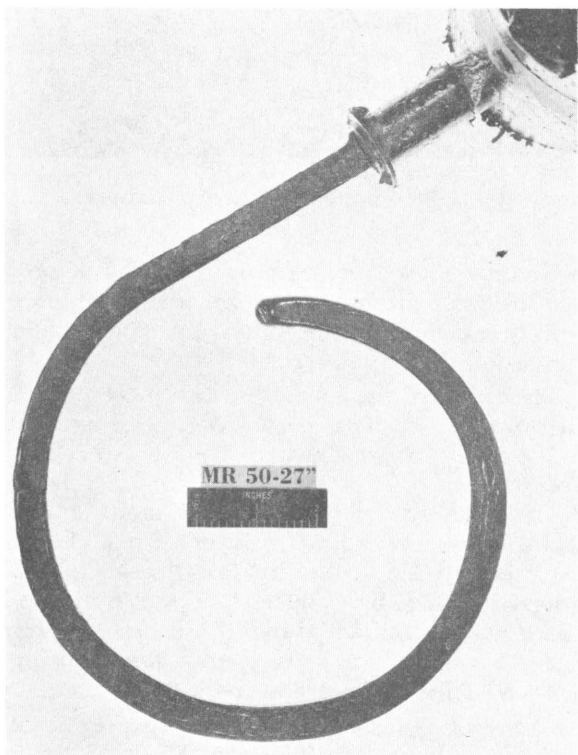
Figure 90.—Fluidity spiral showing 27-in flow.

interval between arc termination and completion of the pour. If conditions were maintained on succeeding heats, there was no significant increase of skull weight beyond the equilibrium value.

A Electric hoist cable
B Pneumatic lift to withdraw electrode
C Water-cooling lines
D Power connectors
E Vacuum glands
F Water-cooled stinger
G Consumable electrode
H Water-cooled ladle
I Tilting mechanism
J Vacuum line
K Water-cooled shell
L Graphite mold
M Windows
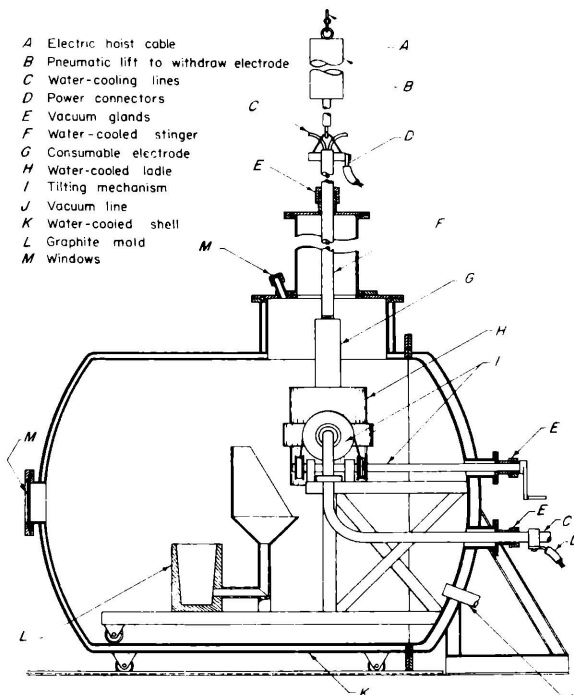
Figure 92.—Improved over-the-lip casting furnace (schematic).

2. Although the skull weight did not change significantly, metal froze around the rim of the skull, particularly in the pouring lip, and the skull shape changed slightly. However, a skull could be used at least 10 times before trimming was necessary.

3. Casting surfaces of die-cast quality were obtained.

4. The furnace could be cycled rapidly, yielding a heat every hour.

5. Reasonable fluidity could be expected. From 16 to 27 in of flow was recorded in a spiral with ½-in-square cross section when arc current of 5,000 amp was employed.

6. Optical pyrometer readings inconclusively indicated temperatures in the range 1,900° to 2,300° C for metal flowing over the lip of the ladle.

7. Indications were that several pours could be made with one furnace assembly and pump-out, if enough room was provided for changing molds.

These features encouraged construction of a larger lip-pouring furnace. Designs were begun in November 1954, and by February 1955 trial runs had begun. Figure 92 shows the schematic details.

This furnace resembles a bell-jar and matching dome, the bell being mounted horizontally, on casters and rails. The crucible, tilting mechanism, vacuum lines, power connectors, and mold floor are all attached to the stationary dome. The electrode drive equipment is mounted to an I-beam rail parallel to the rails on which the bell travels. The consumable electrode, shaft, and gland are mounted on the bell. The electrode drive has in addition to an electrically operated cable winch, a pneumatic cylinder to provide quick removal of the electrode before pouring.

The cup construction is shown in figure 93. A novel feature is the use of an eliptical deflector tilted to distribute the water flow evenly around the crucible. The 825-in³ crucible is made from 8-in ID seamless copper tubing tapered slightly by a lubricated steel mandrel forced into the straight-walled pipe with a press. Heating is unnecessary for the operation. The top lip of the cup is spun to eliminate the possibility of a weld failure at this point.

The ladle is tilted by a drum and cable, as shown in detail in figure 94. Cooling water is led to the cup by two rotating unions gasketed with Teflon. Current is conducted into the furnace by the copper water pipe and led around
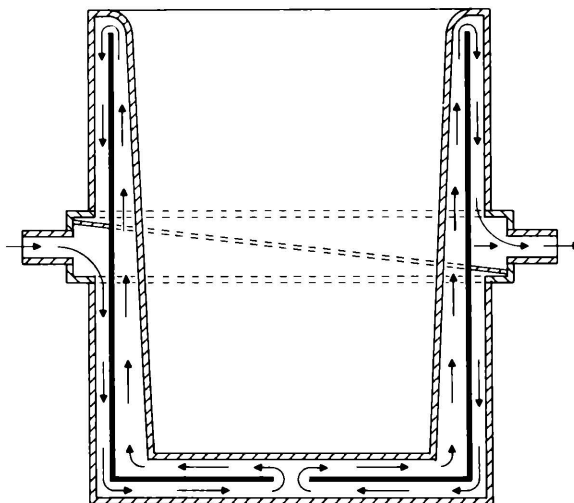
Figure 93.—Schematic of water-cooled cup.
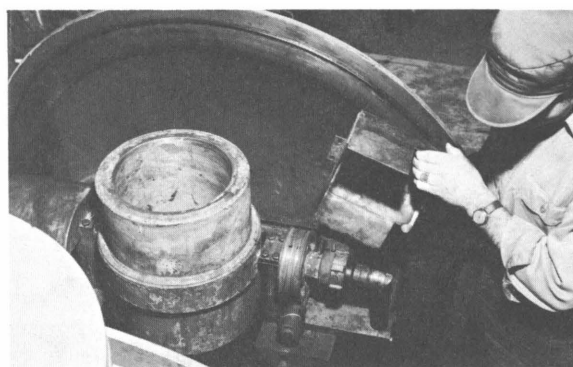
Figure 94.—Mounting and tilting mechanism.

the unions with a solid copper shorting bar, the final contact being the trunnion bearings of the cup. The axis of ladle rotation passes through the geometrical center of the ladle.

The furnace is evacuated by a mechanical pump having a free air displacement of 110 cfm. Figure 95 shows the furnace as installed.

In operation the travel of the electrode or its suspension shaft is limited by a micro switch that simultaneously activates the pneumatic cylinder to remove the electrode, activates the tilting mechanism, and cuts the arc power. The time lapse between the contact of the electrode limit switch and the completion of the pour is about 4 sec. The angle of ladle rotation is likewise limited by micro switches, although optional provision is made for manual control of each pouring step. The instrument and control
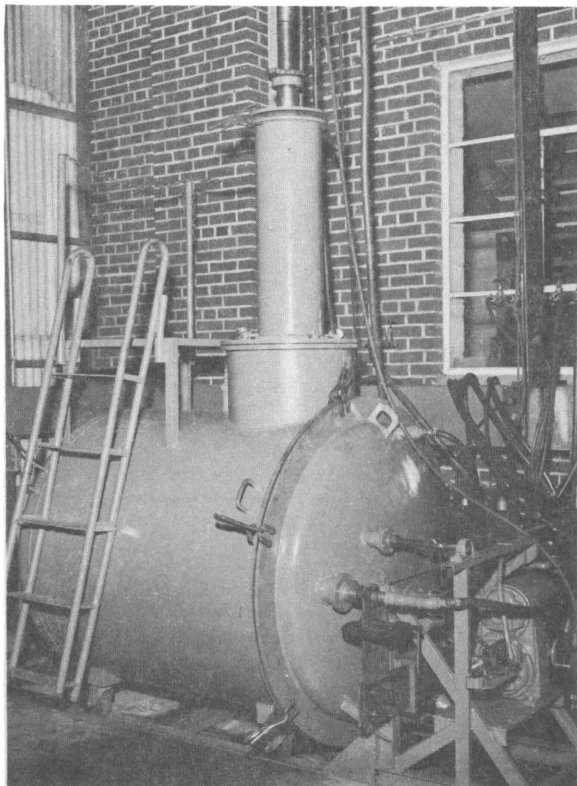
Figure 95.—Improved over-the-lip casting furnace (as installed).

panel is remotely situated as a safety precaution. Most of the construction details are designers' choices based on expediency, and the same results can undoubtedly be achieved through a variety of engineering approaches.

The following operating procedure has been evolved.

1. Assemble furnace (15 min).
   A. Charge starting pad or skull into ladle.
   B. Load electrode.
   C. Assemble and place mold.
   D. Preset limit switch arm on the electrode suspension shaft.
2. Pumpdown (30 min).
   A. Final vacuum: About 120μ registered on the thermocouple gage, about 10μ registered on the McLeod gage.
   B. Leak rate: About 2μ/min on the thermocouple gage.
3. Preoperation inspection (5 min).
   A. Make final check of power connections.
   B. Check cooling-water pressure and flow readings.
   C. Test limit switches.

D. Check alignment of electrode.
E. Check air pressure and test pneumatic cylinder.
4. Melt (15 min for full-capacity pour).
   A. Leave vacuum valve open.
   B. Strike a 4,000 amp, 30 v discharge.
   C. Immediately raise power to 5,000 amp, 30 v.
   D. In 1,000-amp increments at 30-sec intervals, raise arc current to 9,000 amp maximum. Advance the electrode to maintain a potential of 30 v.
   E. Maintain the melt at 30 v until the pour is begun automatically.
5. Cool (40 min for 90-lb casting).
6. Disassemble furnace and mold (15 min).

Total time: About 2 hr.

Relative to procedure 1A, when a skull is available for charging, up to about 10 percent of the weight to be poured can be placed in the skull as loose scrap without causing an increase of skull weight.

The thermocouple gage pressures are measured at a point about 3 ft from the cup, and the McLeod gage is about 10 ft from the cup. McLeod-gage pressures are normally 5μ to 15μ at the beginning of a melt and rise to a value of 150μ to 500μ by the time the pour is made. A glow discharge may be expected to result from procedure 4B, and procedure 4C is necessary to establish true arc conditions. Care must be exercised in keeping the arc potential at 30 v or slightly less to avoid recurrence of the glow.

As an acceptable alternative melting procedure, the vacuum valve may be closed and the furnace backfilled with argon to a mercury manometer pressure of about 30 mm before executing procedure 4B. Then the vacuum valve should be opened when the 5,000-amp current level is reached. In this instance the final pressure is much the same, but it is approached from higher rather than lower pressures.

It appears that the average time required per casting could be reduced appreciably. Time required for furnace evacuation could be reduced by installing higher capacity pumping equipment, and a 20-min cooling period is actually adequate if blue oxide contamination of the casting surface can be tolerated. Of still greater significance, however, is the possibility of enlarging the furnace chamber to accommodate several molds, a mechanism for moving them into place under the ladle, and enough electrode to fill the molds. In this way only the

melt procedure need be repeated for each casting.

In trial operation 2 failures were followed by 23 consecutive successful heats, as listed in table 11. An 80- to 90-lb pour normally involves a total furnace charge of about 165 lbs. Except in those instances marked by footnote 1 in table 11, the total charge has included about 77 lbs carried over from a previous heat in the form of a skull and an electrode stub. Ten consecutive heats, SA 10029 through SA 10208, were made in a single skull before the skull was abandoned because of a buildup of metal at the rim of the ladle. Figure 96 shows the cross section of a typical skull. Abandoned skulls can be reclaimed by removing the heavy rims and reusing them as skulls or by filling them in the usual way but chilling the heat without pouring. In the latter case, forging or sectioning of the resulting ingot permits recycling as electrode stock.

Safety Consideration [2]

Remote operation is considered essential in arc casting because of the incidence of disastrous explosions in industrial titanium-melting furnaces. To protect the operating crew, the entire melting and pouring cycle was controlled from a remote location. Because of the non-routine nature of most operations, researchers considered it essential to provide visibility into the furnace. To achieve this, an optical system was installed to project images of the molten metal and the arc on a ground-glass screen in the control room.

The furnace schematic diagram in figure 92 shows that two view ports are mounted over the crucible. Angle-mounted first surface mirrors were installed over the view ports, aiming the image of the crucible horizontally toward the control booth. Immediately outside the booth are two three-lens optical systems which projected the two images through a 2-in-thick plastic window to a ground-glass screen inside the booth. The two images, each showing about one-half of the crucible, are projected side by side, giving effectively a full view of the crucible.

The chief advantages of this three-lens unit are possible wide variability in installation dimensions and small variation required to focus on a changing pool level. A further convenience is that the ground glass can be moved manually to focus rather than moving one of the lenses. Lens movement would require a complex remote-operated mechanism. Figure 97 depicts the optical diagram of the unit.

CENTRIFUGAL CASTING

Cast tubes of reactive metals have been produced by centrifugal casting using conventional practice. Figure 98 is a picture of the inside of the furnace shown in figure 81. The spin-casting apparatus consists of a duplicate set of three spindles: The top one is spring loaded, driven by a jackshaft and chain; the shaft passes through a vaccuum gland in the furnace wall. Molten metal is poured into graphite cylindrical mold backed by a steel pipe. Hardened steel rings, which match the trunnion wheels and prevent lateral drifting, are mounted on the exterior of the pipe. The ends of the casting mold are also graphite with steel backing. The trunnions are mounted so that their spacing can be adjusted to fit molds 4- to 18-in-diam, and the chain drive permits lateral adjustment.

In operation the metal was poured through a large funnel into a vertically placed graphite tube. The metal flowed into the mold through a 1½-in-diam sprue. Speeds of 400 to 1,200 rpm have been used, resulting in centrifugal forces on the order of 70 to 100 times gravity. Figure 99 shows some of the castings produced from a titanium alloy and one of the molds disassembled.

The apparent surface contamination due to graphite is very slight. This suggests again that the metal was in contact with the mold walls
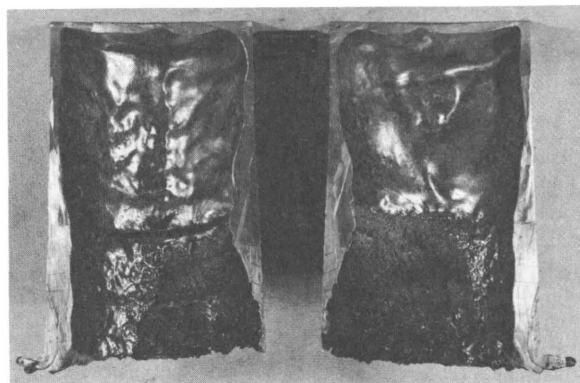
Figure 96.—Longitudinal section of skull.

Table 11.—Over-the-lip pour-casting heats

Heat No.	Graphite mold shape	Weight poured, lb	Resultant skull weight, lb	Ratio: pour/electrode consumed	Ratio: pour/net charge
SA 9865_____	14- by 14- by 1-inch plate__	45.2	41.9	[1] 0.58	0.52
SA 9877_____	_____do_____	59.5	43.7	.99	.58
SA 9917_____	6-inch-diameter cylinder__	68.4	52.9	.86	.56
SA 9963_____	_____do_____	76.7	57.3	.93	.57
SA 9978_____	_____do_____	82.2	62.4	.93	.57
SA 9979_____	_____do_____	69.7	57.8	1.01	.55
SA 10029_____	_____do_____	83.8	68.4	[1] .71	.55
SA 10190_____	_____do_____	76.7	57.3	1.19	.58
SA 10196_____	_____do_____	76.7	58.2	.95	.57
SA 10197_____	_____do_____	77.2	59.8	.97	.56
SA 10198_____	_____do_____	78.9	52.0	1.05	.59
SA 10201_____	_____do_____	92.6	52.9	1.03	.65
SA 10202_____	_____do_____	85.1	53.4	1.10	.62
SA 10205_____	_____do_____	77.6	52.9	1.07	.58
SA 10207_____	_____do_____	79.4	52.9	1.05	.60
SA 10208_____	_____do_____	54.0	57.8	1.12	.52
SA 10210_____	_____do_____	90.4	45.9	[1] .71	.66
SA 10238_____	_____do_____	92.2	42.8	1.09	.68
SA 10993 [2]_____	18- by 18- by 1-inch plate__	93.9	40.4	[1] .72	.70
SA 11026 [2]_____	_____do_____	84.5	33.7	1.09	.71
SA 11027 [2]_____	10-inch-diameter dome___	56.0	32.8	1.00	.63
SA 11276 [3]_____	18- by 18- by 1-inch plate__	93.9	47.6	[1] .73	.66
SA 11328 [4]_____	_____do_____	101.4	41.9	[1] .78	.71
Average_____					.61

[1] Ratios low because new skulls were formed.
[2] Ti + 6Al, 4V.
[3] Ti + 3Fe–Cr, 3Fe–Mo.
[4] Ti + 3Al, 5Cr.
Note: Average OD of tapered skulls was 8½ in all cases. Electrode cross sectional areas ranged from 12 to 40 in [2], but 28 in [2] electrodes predominated.
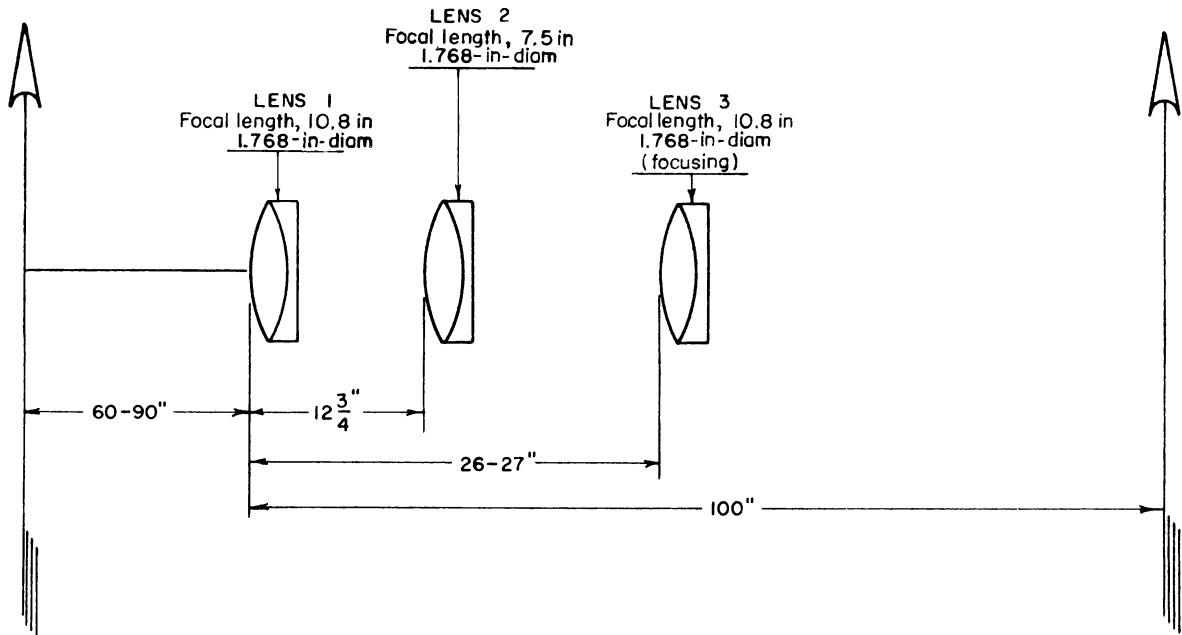
Figure 97.—Optical diagram for arc furnace projection system.
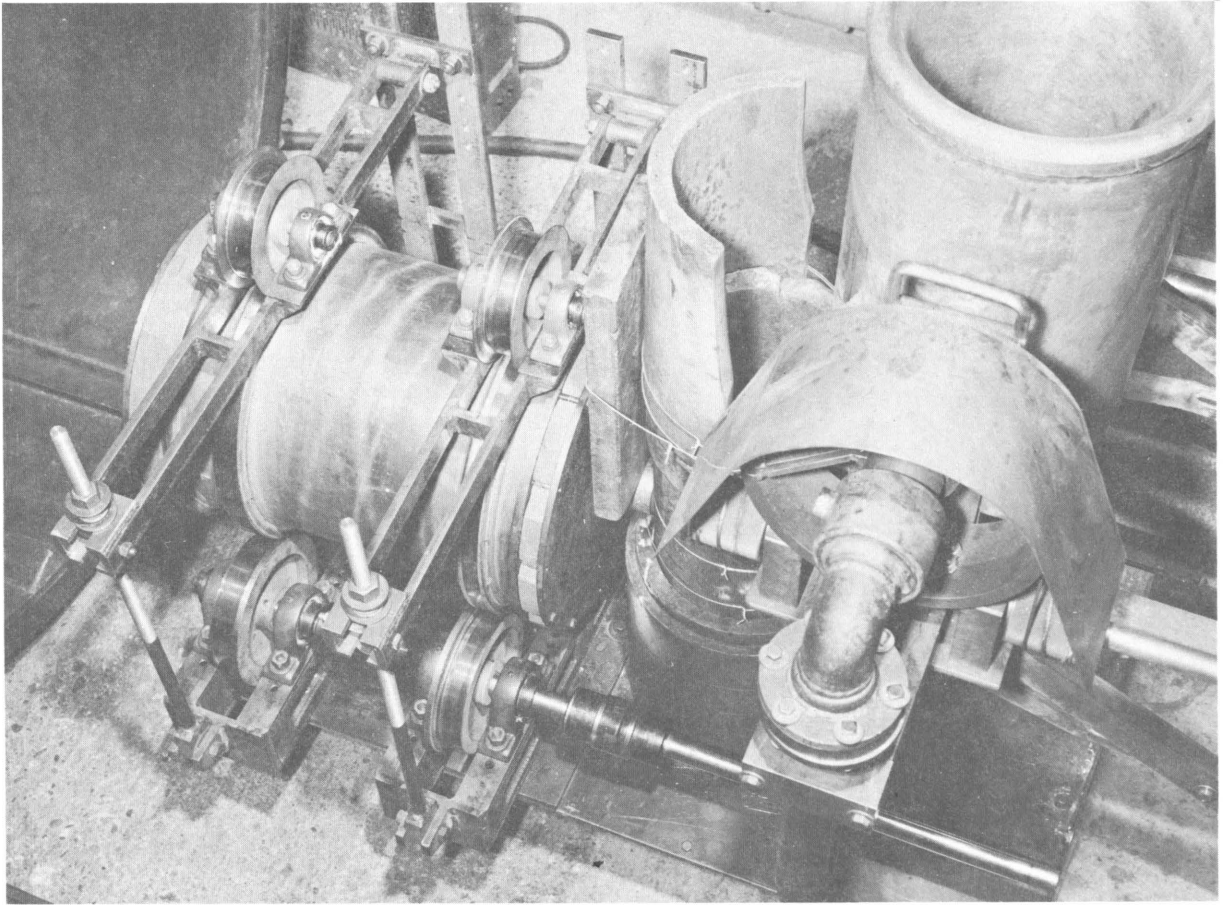
Figure 98.—Spin casting mechanism, showing crucible and pouring funnel on right.

for only a short time before it froze and shrank away. Of interest was the relatively fine-grain sructure of these castings compared with the large grains in the conventional cold-mold ingot. The surface finish on the interior was usually of excellent quality, except in instances where very short castings were made. It is presumed that this roughness was due to excessive turbulence during pouring.

Originally, porosity was evident in some castings. This has been eliminated to a large extent by the use of good-grade melting stock and by more careful control of energy input. As an example of the soundness obtained, two cylindrical castings of hafnium, 12-in long by 1½-in ID by 2¾-in OD, were gamma-graphed by another agency, which reported an area of sponginess near the end of one casting and a few spots of porosity near the exterior surface, the largest being about 1/16-in-diam.

Figure 99.—Typical centrifugal castings of titanium produced in mold on right.

In commercial extrusion practice, zirconium and titanium arc-melted ingots must be forged to break up the gross grain structure. For tube production, then, sponge must be double
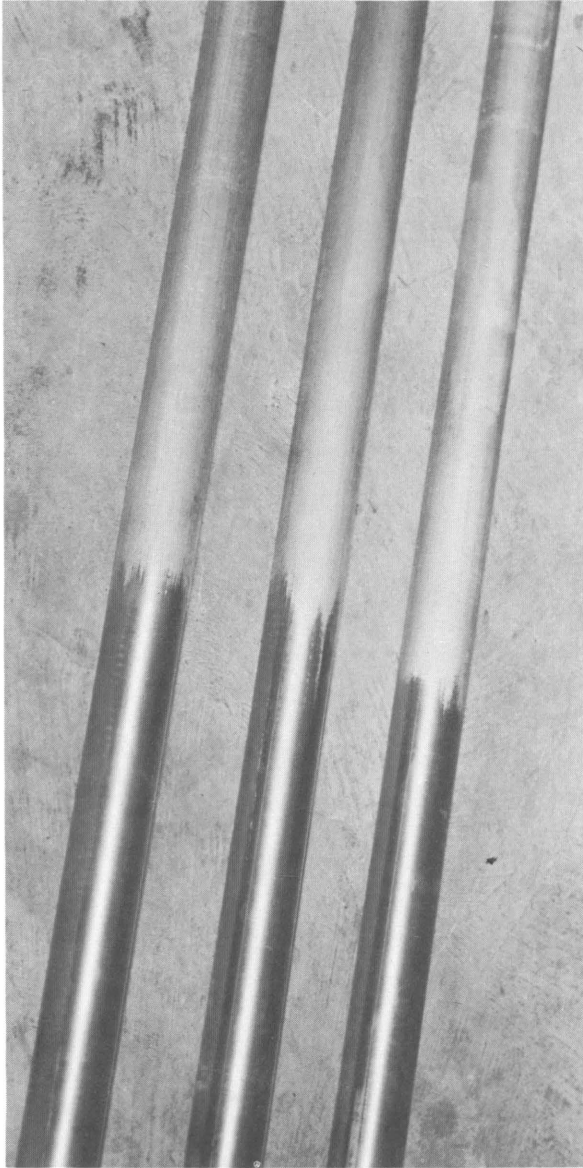
Figure 100.—Extruded Zircaloy-2 tubing directly from as-cast billet, showing original surface and ground finish.

melted, conditioned, forged, conditioned, and bored or pierced. As an alternative, the proposal was to double melt, spin cast, and machine to final size, eliminating two steps and improving the yield. Another advantage can be realized when the cost of drilling or boring becomes prohibitive because of hardness of the alloy.

Three Zircaloy-2 blanks were produced during 1957 and shipped to Chase Brass and Copper Co. for extrusion. All outside surfaces of

one tube were left in the as-cast condition; the surfaces of the remaining two tubes were conditioned by machining.

From original dimensions of 6.73-in OD by 1.82-in ID by approximately 9 in, each blank was successfully extruded to tubes of $2\frac{1}{16}$-in OD by $1\frac{5}{8}$-in ID by about 17 ft long. Results for the blank with as-cast surfaces were particularly pleasing, perhaps because an inferior product was anticipated. Actually, all tubes produced appeared to be satisfactory, and only a relatively light finish grinding was required. Figure 100 shows the tubes with part of each still in as-extruded condition and the remainder as-ground. Table 12 shows the material yield.

Extrusion was followed by a group of bench-drawing and stretch-straightening tests. The following items summarize the results of the tests:

1. Centrifugally cast blanks of Zircaloy-2 can be successfully extruded directly from the as-cast state without intermediate conditioning other than light machining of surfaces.

2. The oustide surfaces of extruded tubes are commensurate with the surface finish of the starting blanks but otherwise are normal for Zircaloy-2.

3. Extrusion without prior machining of cast surfaces results in unexplained surface stringers but is otherwise satisfactory.

4. The inside surfaces of extruded tubes are somewhat rougher than normally expected for Zircaloy-2 but are still acceptable.

5. Extrusion can be followed by bench drawing to achieve additional reduction in area up to a total of at least 25 percent in about 10- or 15-percent increments. Vacuum annealing, recoating, and mainte-

Table 12.—Material-yield data on extrusion, percent

	Casting number		
	SA 16,929	SA 17,159	SA 17,171
Extrusion number____	390	391	392
Rough to finished blank _____	92.5	86.3	87.0
Finished blank to half-conditioned tube _____	88.8	88.5	86.3
Overall yield _____	82.2	76.3	75.1

nance of small plug clearances may permit reductions in area by drawing up to a total of about 50 percent, but this possibility must be tested further.

6. Relatively slight stretching of extruded Zircaloy-2 tubes results in a significant increase of 0.2 percent offset yield strength without comparable changes of other tensile properties.

PHYSICAL PROPERTIES OF CAST MATERIAL

In October 1957, a series of the gate valves shown in figure 101 was placed in industrial service to establish performance characteristics when subjected to (a) water containing 2,300 ppm chloride at 284° F (140° C), (b) 65 percent nitric acid at 230° F (110° C), (c) 15 to 16 percent sodium hypochlorite at 194° F (90° C). The same valves were hydraulically tested, and all seats and gasket seals withstood at least 500 psi of sustained pressure. This was the upper limit of the hydraulic testing equipment. After 1 year of operation as specified above, the valves appear to be unchanged.

A group of 25 Zircaloy-2 brackets of the type shown in figure 110 was fairly typical of static castings produced in machined graphite molds. A discussion of their properties will be used to illustrate the normal quality to be expected in reactive metal castings. Surfaces were generally smooth, but there were occasional superficial folds or wrinkles caused by the high rate of heat loss to the graphite mold. The surface ranged from bright to light shades of tan or gray. Metallography of surface sections revealed that carbon contamination extended to a maximum depth of 20 mils (0.020 in). Analysis of samples collected from the first 5 mils under the surface indicated 400 to 600 ppm carbon, and analysis of samples from the entire 20 mils of surface contamination indicated 200 to 400 ppm carbon. Above 500 ppm, carbon contamination causes a slight increase in the corrosion rate of zirconium in chloride solutions, but this increase does not become serious until the contamination level exceeds 1,000 ppm (3).
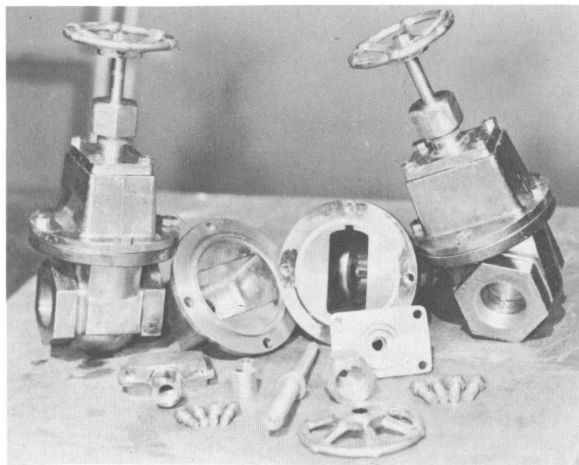
Internally, the bracket casting contained scattered porosity, mostly pinhole variety; but in a few instances porosity approached $\frac{1}{8}$-in. The soundness was adequate for normal corrosion service but would fail to meet the usual aircraft-type specifications. However, there is no reason to believe that aircraft quality could not be obtained through the improved design of static molds or by resorting to centrifugal casting techniques. In 1959 the Air Force was sponsoring research in several phases of this problem.

Several brackets were subjected in their entirety to corrosion by steam at 750° F and 1,500 psi for 3 days. The result was a normal lustrous black oxide layer. No white corrosion products were formed. Standard corrosion coupons were also collected and subjected to 750° F steam at 1,500 psi for a total of 98 days. The results are compared in table 13 with typical behavior of wrought metal.

The average 0.2 percent yield strength was 49,600 psi, average tensile strength 66,600 psi, and reduction in area at the fracture averaged 36 percent. These values are typical of hot-rolled metal of the same composition. The thin wall sections of the cast brackets necessitated a substandard Charpy V-notch test, and a special series of specimens from wrought metal was tested for comparison. The cast specimens possessed about one-half (6 ft lb) the impact resistance of wrought metal (10 ft lb) both at room temperature and at 200° F. Testing of the cast brackets was performed by the Atomic Power Division of Westinghouse Electric Co.

PROCESS VARIABLES [3]

Largely as a result of intuition, practical casting techniques have been developed, but there are several areas of potential improvement.

Figure 101.—Cast titanium gate valves.

Table 13.—Corrosion rates of cast and wrought
Zircaloy

Time, days	Weight gain, mg/cm²	
	Average of cast brackets	Typical of wrought metal
14	2.80	3.5
28	3.97	4.5
42	4.50	5.5
56	6.22	6.5
70	6.84	7.5
84	8.07	8.5
98	9.39	9.5

Table 14.—Metal yield as function of
electrode diameter

Heat No.	Electrode diam, in	Residual skull weight, lb	Weight poured, lb	Yield, percent
75-LB HEATS				
SA 11,366	8	39.2	75.0	65.5
SA 11,367	6	34.0	75.0	68.8
SA 11,370	4	34.4	71.0	67.3
40-LB HEATS				
SA 11,557	6	15.9	40.1	71.6
SA 11,558	4⅜	13.2	40.6	75.4
SA 11,559	3	13.2	40.6	75.4

The need has been shown for further development of mold designs and materials or other changes leading to reduced costs, improved casting soundness. and a wider range of process application. Also, the use of vacuum techniques has not been fully exploited for maximum improvement of produce quality. Progress toward these objectives is continuing, but there is a real need for a clearer understanding of process control and the influence of various operating parameters. Of special interests are variations in the yield of metal (percent of charge poured), the distribution of heat, metal temperatures, and melting rates as functions of arc current, pressure, alloy composition, and casting sizes.

The Bureau has conducted two separate series of zirconium casting heats to study the influence of electrode diameter on the yield of metal. The first series consisted of three heats, all without benefit of initial skulls, in a 9½-in-diam ladle, at nominal currents of 8,000 amp, and at nominal pressures of 100μ to 200μ. The only deliberate variable between heats was the electrode diameter. As an extra precaution, all electrodes were fabricated from the same ingot stock to minimize variation of metal composition. The second series of three heats used the same procedure, except that the ladle was 8½-in-diam, pressures were more nearly 400μ, and the electrode sizes were smaller. Table 14 tabulates results of both series.

The variation of the yields in each series has no significant order in relation to electrode size. The minor differences observed are no more than might be expected to result from such things as cooling irregularities. However, it is not standard practice to generate a new skull in each heat, as was done in the experiments. Accordingly, a conclusion that electrode

size has no bearing on yield must be qualified by the admission that when a skull is retained through a series of successive heats its weight usually increases slightly to some equilibrium value over the first several melts. This weight increase is principally a buildup at the upper rim of the skull, and it is suspected that the ultimate buildup is greater for smaller electrodes

A larger series of experimental heats with titanium alloys furnished information on yields, metal temperatures, melting rates, and mold reactions. This series included six levels of arc current, three distinct ranges of pressure, three ladle sizes, and four alloy compositions. Each of the various water-cooling loops associated with the casting furnace was equipped with a flow-meter and iron constantan thermocouples for continuous recording of coolant volume and temperature. These data were used to calculate the relative distribution of heat to the various furnace components as a function of time. Strip-chart records of current, potential, and time supplied a total energy input figure for each heat, and this was proportioned and assigned in accordance with the heat distribution derived from the volume and temperature of cooling water. Average molar heat contents and metal temperatures were deduced from the partition of energy between the molten and solid portions of the charge. As standard practice, weights were obtained that allowed the calculation of metal yields and average melting rates. Each pour was made into a network of cubical mold cavities ranging in size from 1 to 8 in. Most molds were of machined graphite,

but in several instances sizes up to 4 in were duplicated with mold components of rammed graphite furnished by Frankford Arsenal. Thus, direct comparison was possible between the various sizes and between the two mold materials. Rammed mold materials are being constantly improved, and the relevant results of this study typify only the rammed materials available in June 1957. Operating data are summarized in tables 15–18.

The choice of method for temperature estimation may be criticized, but the method was selected because the temperature are too high for conventional probe measurements, and optical or radiation pyrometry is complicated by ionized vapors and reflection of an electrode image from the molten pool surface. In addition, the investigators decided that an average temperature has more significance than a localized temperature.

Table 15.—Variable arc-current series, operating data [1]

Heat No.	Nominal intended current, amp	Average recorded current, amp	Power, kw	Energy, kwhr	Average pressure, μ	Weight poured, lb	Residual skull weight, lb
SA 17,299	8,000	7,320	251	72.2	142	157.8	114.9
SA 17,285	9,000	7,620	248	79.7	292	181.9	106.7
SA 17,230	10,000	8,700	288	78.2	119	191.7	80.7
SA 17,469	11,000	9,188	312	75.0	160	179.8	74.1
SA 17,397 [2]	11,000	10,017	348	82.6	126	137.9	55.8
SA 17,604	12,000	11,039	415	96.2	89	193.8	115.8

[1] Ti–6Al, 4V alloy ; 11-in ladle.
[2] No initial skull.

Table 16.—Variable pressure series, operating data [1]

Heat No.	Nominal intended current, amp	Average recorded current, amp	Power, kw	Energy, kwhr	Average pressure, μ	Weight poured, lb	Residual skull weight, lb
SA 17,604	12,000	11,039	415	96.2	89	193.8	115.8
SA 17,469	11,000	9,188	312	75.0	160	179.8	74.1
SA 17,540	11,000	11,200	364	92.5	164,000	162.6	97.5
SA 17,563	11,000	10,133	348	92.1	527,000	145.3	106.7

[1] Ti–6Al, 4V alloy ; 11-in ladle.

Table 17.—Variable ladle-size series, operating data [1]

Heat No.	Ladle diam, in	Average recorded current, amp	Power, kw	Energy, kwhr	Average pressure, μ	Weight poured, lb	Residual skull weight, lb
SA 17,774	8½	10,062	361	56.6	91	104.7	70.1
SA 17,469	11	9,188	312	75.0	160	179.8	74.1
SA 17,604	11	11,039	415	96.2	89	193.8	115.8
SA 17,653	14½	10,387	353	70.1	101	135.2	90.4

Table 18.—Variable alloy series, operating data

Heat No.	Alloy	Ladle diam, in	Average recorded current, amp	Power, kw	Energy, kwhr	Average pressure, μ	Weight poured, lb	Residual skull weight, lb
SA 17,397 [1]	Ti–6Al, 4V	11	10,017	348	82.6	126	137.9	55.8
SA 17,774	Ti–6Al, 4V	8½	10,062	361	56.6	91	104.7	70.1
SA 17,798	Ti	11	10,160	365	77.5	166	125.0	57.8
SA 18,011 [1]	Ti–4Al, 4Mn	8½	8,710	293	62.4	121	39.0	83.6
SA 18,066 [1]	Ti–8Mn	8½	9,310	302	30.2	190	28.0	36.6
SA 18,080 [1]	Ti–8Mn	8½	9,420	319	76.1	133	58.9	114.0

[1] No initial skull.
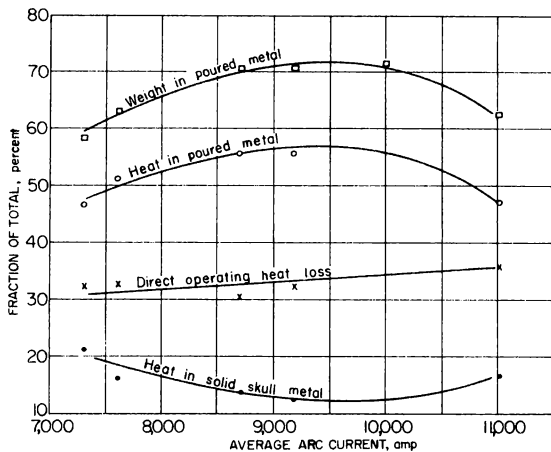
Figure 102.—Heat distribution and metal yield as functions of arc current.
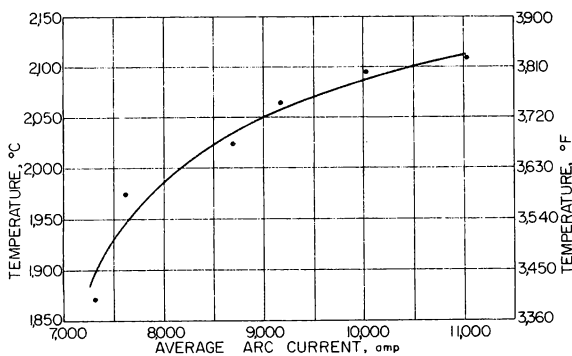
Figure 103.—Temperature of poured metal as function of arc current.

Figures 102 and 103 present some effects of arc-current variation. These graphs are associated with the operating data of table 15. Although the effciency of operation reached a maximum at some optimum center near 10,000

amp, the temperature of the molten metal continued to increase at higher currents.

Are current is also a major factor in determining melting rates. That the melting rate is directly proportional to arc current has been recognized by those who engage in dc arc welding with a consumable rod (11) and in production of simple ingots by consumable electrode arc melting. This is also true of consumable electrode arc casting, but care must be exercised in defining melting rate. In arc melting ingots, where a skull is not formed, the melting rate is the same as the rate of electrode consumption. Skulls are involved in arc casting, and researchers found that any loss of weight by a skull must be added to electrode consumption to yield a melting rate proportional to arc current. If a skull gains weight, the increase represents metal acquired from the electrode and is already included in the electrode consumption rate. The ratio of melting rate to current in the experiments under discussion was about 1.2 lb/min/kiloampere. No ordered dependence of melting rates, temperatures, or operating efficiencies on arc power were discovered. The influence of current was independent of electrical potential.

Ladles of different sizes were used with results shown in figures 104 and 105. The diameter of each ladle was 1-in smaller at the bottom than at the top. The resulting taper facilitated removal of residual skulls but necessitates the use of an average diameter as an index of size. The scatter of data corresponding to the 11-in ladle size is disturbing at first glance, but more detailed inspection reveals that the spread of values reflects the effect of uncontrollable arc-current variations. Since the ladle size can be fixed rigidly, the scatter did not appear in figures 102 and 103, but since arc current cannot be precisely controlled, its variation must be
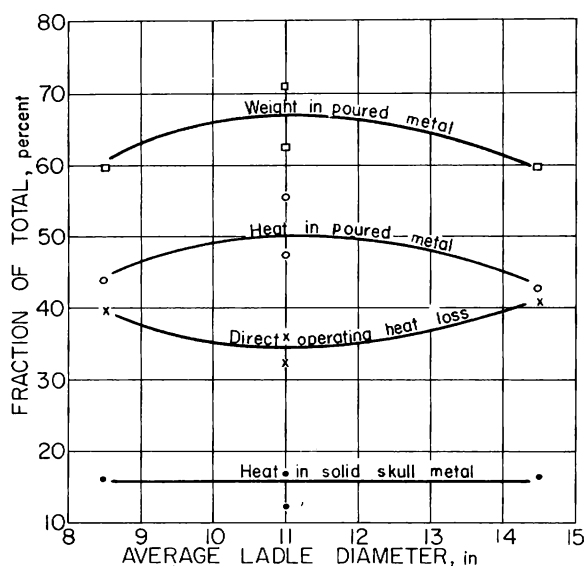
Figure 104.—Heat distribution and metal yield as functions of ladle diameter.
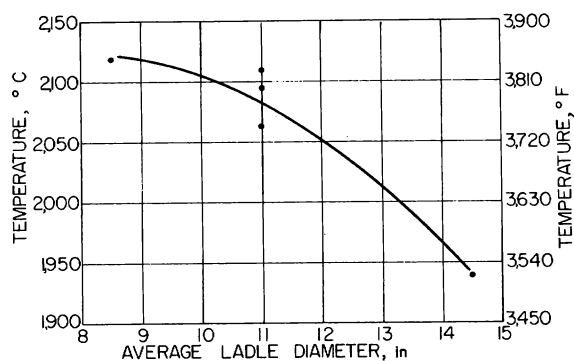
Figure 105.—Temperature of poured metal as function of ladle diameter.

taken into account in evaluating figures 104 and 105. Within the range of conditions specified by tables 15–17, the relation between current and ladle size with regard to molten-metal temperature can be expressed by the empirical quadratic approximation:

$T = 430 (1 + 0.51\ I - 0.0231\ I^2) (1 + 0.0655\ d - 0.003367\ d^2)$, where T is average temperature in °C, I is arc current in kiloamperes (Ka), and d is the mean ladle diameter in inches. A variety of other empirical approximations could have been used. The agreement between values as calculated above and the calorimetrically measured temperatures is shown in table 19. The most serious disagreements

Table 19.—Comparison of measured and calculated values of average molten-metal temperatures

Heat No.	T_m, measured, °C	T_c, calculated, °C	$\dfrac{T_m - T_c}{T_c} \times 100$, percent
SA 17,299 [1]	1,870	1,922	−2.71
SA 17,653 [2]	1,940	1,927	+ .67
SA 17,285 [1]	1,975	1,950	+1.28
SA 17,230	2,025	2,029	− .20
SA 17,469	2,065	2,055	+ .49
SA 17,540 [3]	2,070	2,098	−1.34
SA 17,397	2,095	2,085	+ .47
SA 17,604	2,110	2,098	+ .57
SA 17,563 [3]	2,115	2,100	+ .71
SA 17,774 [4]	2,120	2,107	+ .62

[1] Low current.
[2] Large ladle.
[3] High pressure.
[4] Small ladle.

occur at currents below 8,000 amp and high pressures.

Attempts to approximate metal yields with equations of similar form have been unsuccessful. Unfortunately, the nature of the relationship between arc current and ladle diameter is more complex when yields are considered, and it appears that a logarithmic or exponential term may be involved. In any case, the utility of such empirical approximations is limited. There is a real need for a practical, but simplified model of the molten pool during arc melting that will allow a theoretical deduction of equations for temperature and volume.

On the basis of earlier studies (1), there is little doubt that furnace pressure constitutes a third interacting variable, but variable-pressure-series results as shown in table 20 indicate that the effect is subordinate to the influence of current and ladle size and less significant than the estimated error of temperature measurement. Thus, to define the role of pressure, more precise methods of arc-current control and of temperature measurement would have to be devised.

Table 20 also compares results for the various alloys that were available. Probably the most significant facts that may be inferred from these data are that molten-metal temperatures were generally higher and operating efficiencies were lower for alloys containing manganese. On the basis of previous routine experience, the lower efficiencies were expected, but the investigators had assumed that this was caused by an excessive loss of heat by vaporization of

Table 20.—Heat distribution, variable-pressure and variable-alloy series

Heat No.	Alloy	Average pressure, μ	Melting rate, lb/min	Molten metal temperature		Skull temperature		Fraction of total charge poured, percent	Fraction of heat in molten metal, percent	Fraction of heat in skull, percent	Direct operating heat loss, percent
				°F	°C	°F	°C				
VARIABLE-PRESSURE SERIES											
SA 17,604	Ti–6Al, 4V	89	14.6	3,831	2,110	2,951	1,625	62.5	47.3	16.9	35.8
SA 17,469	Ti–6Al, 4V	160	12.6	3,750	2,065	2,588	1,420	70.8	55.6	12.2	32.2
SA 17,540	Ti–6Al, 4V	164,000	12.3	3,759	2,070	2,552	1,400	62.6	40.9	12.9	46.2
SA 17,563	Ti–6Al, 4V	527,000	9.7	3,840	2,115	2,705	1,485	58.6	37.1	15.0	47.9
VARIABLE-ALLOY SERIES											
SA 17,397	Ti–6Al, 4V	126	13.2	3,805	2,095	2,779	1,525	71.3	39.1	9.0	52.0
SA 17,774	Ti–6Al, 4V	91	11.9	3,849	2,120	2,760	1,515	59.9	43.8	16.3	39.9
SA 17,798	Ti	166	13.7	4,342	2,395	3,002	1,650	68.4	40.8	10.3	48.9
SA 18,011	Ti–4Al, 4Mn	121	9.9	4,425	2,440	2,589	1,420	31.8	16.6	16.7	66.8
SA 18,066	Ti–8Mn	190	7.2	4,460	2,460	2,930	1,610	43.3	18.1	12.4	69.5
SA 18,080	Ti–8Mn	133	11.5	4,139	2,280	2,617	1,435	34.1	19.0	15.4	62.6

manganese. The existence of higher temperatures and the pressure levels maintained (see table 18) completely contradict this notion. Instead, it now appears that the explanation of lower efficiencies for manganese alloys goes much deeper and involves a basic influence of manganese on the arc-discharge mechanisms whereby the heat directly received by the arc cathode decreases and that received directly by the anode (in this instance the molten pool) increases.

The temperature of skull metal was remarkably uniform throughout, regardless of operating conditions. Variations were random and could not be related to operating conditions. Values ranged from 2,523° F to 3,002° F (1,385° C to 1,650° C), and averaged 3,731° F (1,500° C). The one 3,002° F (1,650° C) value was obtained with commercially pure titanium and is probably too high, since the melting point is only 3,020° F (1,660° C). The estimated error for all reported metal temperatures is ±90° F (±50° C).

The similarity between the fraction of the total charge poured and the fraction of total heat contained by molten metal may be noted in figures 102 and 104. Although the similarity seems perfectly logical, it could not be anticipated. The heat content of molten metal certainly must depend to some extent on the volume or mass of molten metal, but not necessarily on the fraction of total charge represented by that mass.

The heat lost during arc operation and not appearing in either cast metal or the residual skull varied widely from about 30 to 70 percent of the total heat input. The manner in which direct heat losses were dissipated was fairly consistent, however. Of this direct loss, 80 to 88 percent was included in the heat content of cooling water from the ladle. Another 10 to 20 percent represented heat generated in water-cooled electrode components, including friction brushes used to apply power to the stinger shaft. Less than 1 percent appeared as miscellaneous losses through furnace walls.

REFERENCES

1. Beall, R. A., J. O. Borg, and F. W. Wood. A Study of Consumable-Electrode Arc Melting. BuMines Rept. of Inv. 5144, 1955, 21 pp. (See chapter 7, this bulletin.)
2. Gilbert, H. L., R. A. Beall, and J. O. Borg. U.S. Pat. 2,825,641, Mar. 4, 1958.
3. Golden, L. B., I. R. Lane, Jr., and W. L. Acherman. Embrittlement of Zirconium and Tantalum in Hydrochloric Acid. Ind. and Eng. Chem., v. 45, No. 4, April 1953, pp. 782–786.
4. Kroll, W. J., and H. L. Gilbert. Melting and Casting Zirconium Metal. J. Electrochem. Soc., v. 96, No. 3, September 1949, pp. 158–169.
5. Kuhn, W. E. Titanium and Zirconium Castings Now Practicable. Mat. and Methods, v. 36, No. 6, December 1952, pp. 94–95.
6. Lang, R. M. Shell Molds for Titanium Castings. Am. Foundryman, v. 25, No. 3, March 1954, pp. 60–62.
7. Rem Cru Titanium, Inc. The Design, Construction, and Operation of a 25-Pound, Bottom-Pour, Skull, Arc-Melting Furnace. Interim Tech. Rept. 1 to Watertown Arsenal, Jan. 22, 1953, 59 pp.; DDC, AD 18475.
8. Simmons, O. W., R. E. Edelman, and H. McCurdy. A Bottom-Pour Arc Type Furnace for Melting and Casting Titanium. Frankford Arsenal Rept. R–1165, September 1953, 22 pp.; Light Metals, v. 18, No. 1, January 1955, pp. 11–12.
9. Sutton, J. B., E. A. Gee, and W. B. DeLong. Casting and Forging of Titanium. Metal Prog., v. 58, No. 5, November 1950, pp. 716–720.
10. Steel. Titanium Castings. V. 133, No. 26, Dec. 28, 1953, p. 88.
11. Wilson, F. L., G. E. Clausen, and C. E. Jackson. The Effect of I^2R Heating on Electrode Melting Rate. Weld. J., v. 35, No. 1, January 1956, pp. 1s–8s.

CHAPTER 12.—MOLDS FOR SKULL CASTING

By S. L. Ausmus,[1] F. W. Wood, and R. A. Beall

THEORETICAL CONSIDERATIONS

The requirements for a "perfect" or ideal mold material are both physical and economical. Physically, the mold must be strong enough to support its weight and withstand moderate handling without breakage. It must have a hard enough surface to withstand the washing action of the molten metal as it impinges on the interior mold surfaces and upon the core. Economically, the material must be adaptable to other-than-laboratory situations.

The thermal conductivity of the mold must be sufficient to hold the temperature of the metal-mold interface below the temperature of chemical reaction. Unfortunately chemical reaction does not begin or end at a discrete temperature; thus, the resaerchers are forced to select arbitrarily, a reasonable compromise as to surface contamination.

Permeability is a physical property and is again related to chemical reactivity; that is, whatever gas or gases are released by metal-mold reaction and/ or from the heated mold itself, must be eliminated from the mold cavity. This, of course, can be accomplished with vents as well as by a permeable mold material.

Because of the broad range of application for cast parts and because the physical requirements of the castings are determined by the application, the establishment of standards for surface appearance and internal soundness is difficult. Changes in mold material and design will affect the appearance and structure of the casting and will also affect the economics of the operation. For the purposes of this study a cast surface finish of 250μ to 500μ in, RMS, which is roughly comparable to that obtained by conventional sand molding, was considered satisfactory.

To fully evaluate a mold it is necessary to evaluate a cast metal product. For the purposes of this development, the number of items cast and the variations of gate-riser arrangements have been held to a minimum. In the future, a worthwhile study could be made on the relationships between mold material and configuration.

As a general guideline for this research, it was determined that the equipment must be reasonably conventional to foundry practice. One could produce by a long exposure at high temperature a shaped graphitized mold equal to or better than a machined graphite mold. As a matter of fact, it is possible that shaped compacts could be delivered to a manufacturer of graphite for firing with reasonable economy. However, the time involved in such a cycle would probably not appeal to the foundryman. Further, one could require a 2,000° C treatment at high vacuum; this, however, would be completely foreign to the conventional foundryman.

PERMANENT MOLDS

When the reactive-metal casting technique was first satisfactorily developed in 1955, three mold materials were available; namely, machined artificial graphite, rammed powdered graphite, and massive and/or water-cooled copper or aluminum. This choice of materials has not yet been extended, although considerable refinement has been achieved, particularly in expendable rammed graphite.

Dense graphite was an early choice as a mold material for zirconium and titanium casting. The ease with which this material is machined, its reasonable strength, high thermal conductivity, and low reactivity with the molten metal, make graphite suitable for a permanent mold material for many casting applications (5)

One of the greatest problems in designing machined graphite molds is how to prevent the casting from binding the mold when it shrinks. For example, the conventional flanged valve will have two flat flanges parallel to one another and connected by a straight section. On cooling, the shrinkage of the straight section will cause
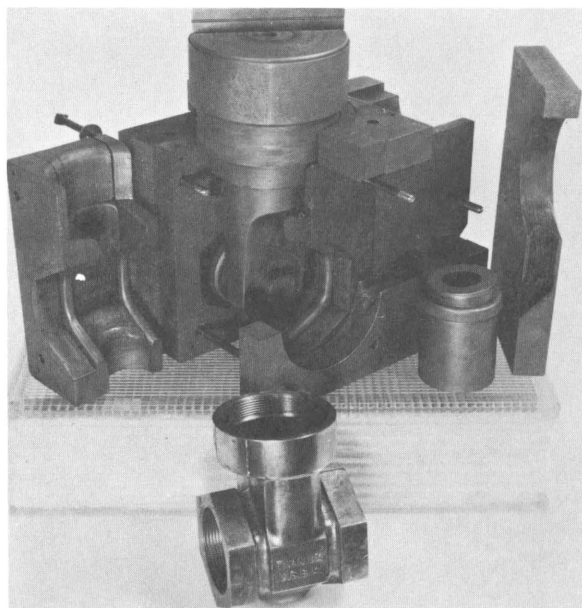
Figure 106.—Laminated mold for titanium gate valve.
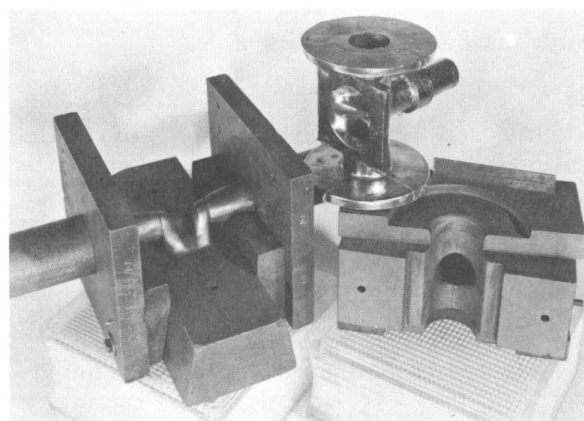
Figure 107.—Laminated mold for titanium diaphragm valve.

the flanges to pinch tightly against the mold parts, making it difficult if not impossible to save the "permanent" mold for reuse. To solve this problem, a system of laminar construction with tapered key sections has been worked out. Figures 106 and 107 show typical laminated molds. The laminar construction reduced the breakage and simplified the machining of deep cavities. Cores also can be made of multisection units with a key block, as shown in figure 108. Figure 109 shows the resultant casting.

It is necessary to obtain fine-grain dense graphite, (1.65 g/cc or more) to realize the best surface finish on the casting. Care in preparing radii and in smoothing mold faces was essential to good castings and good mold life. The Bureau has not had occasion to produce any single part in enough quantity to determine the average mold life of a properly designed unit. However, several patterns have been used eight to 12 times with negligible deterioration.

Inspection of a casting poured in graphite makes it apparent that the molten metal was in contact with the graphite for only a fraction of a second before it froze and shrank away from the mold surface. In some instances reaction and washing were observed where a heavy flow of metal impinged on a graphite surface.

EXPENDABLE MOLDS

Early Bureau Work

The possibility of producing expendable-type molds for reactive metal casting was first explored by the Bureau in 1955. This was a pioneering study and involved only a limited program; however, certain significant conclusions were reached. Twenty-five titanium and zirconium casting heats were made in rammed graphite molds of various compositions. Of the molds used in this program none of those which contained silicates, ceramic materials, molasses, lamp black, or paraffin proved satisfactory, whereas molds which contained raw linseed oil or core oil as a liquid binder and none of the above ingredients produced castings of fair to good quality.

Curing and firing of the molds were accomplished chiefly with the aid of a vacuum resistance-heated furnace (2) and a carbide-production furnace (3). Temperatures went to 850° C in the vacuum furnace and to 1,850° C in the carbide furnace.

The limited chemical values recorded, indicated a carbon pickup to 250 ppm for the castings over the electrode stock used. Oxygen increased 150 ppm, but nitrogen showed no noticeable change. One of the better castings produced, a zirconium torsion-bar bracket, is shown in figure 110.

Among the interesting alternate materials tested was zirconium silicate formed into molds by the frozen-mercury investment technique. Figures 111 and 112 indicate that mold reaction is severe except on the thin casting sections.
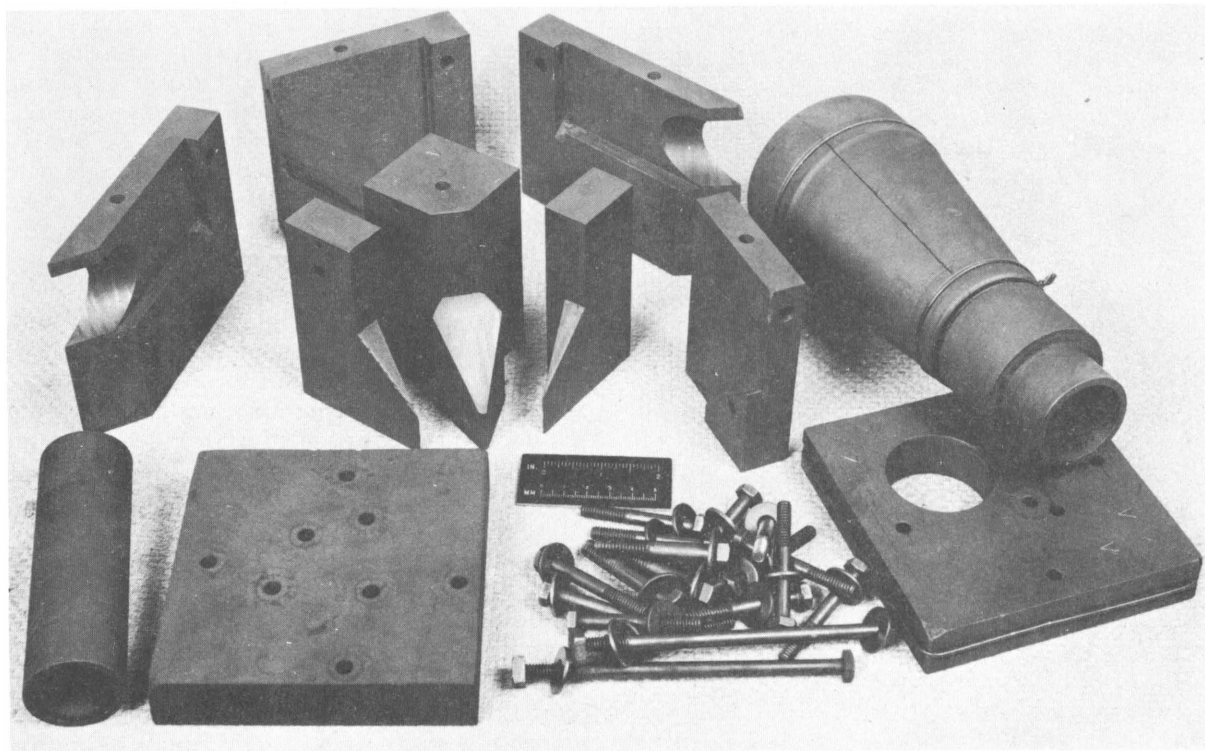
Figure 108.—Machined graphite mold with laminated core, disassembled.

Oxygen contamination on the thin sections was less than 0.03 to 0.04 in deep.

Investigations in this field were discontinued until 1957. At that time the present full-scale development and evaluation program was initiated.

The basic problems confronting the investigators at the initiation of the program were (1) to develop one or more mold materials, with pulverized graphite as a base, capable of containing molten titanium with a minimum of mold-metal reaction, (preparation of these materials had to be adaptable to foundry practice wherever possible); (2) to evaluate the physical characteristics of the molds; and (3) to evaluate the castings produced from these molds on the basis of soundness, surface quality, and mold-metal reaction.

Formula Development

Pioneering studies, as noted earlier, indicated that raw linseed oil offered a good potential as a fluid binder in any water-free formula which might be developed. Thus a series of mold formulas was prepared in which powdered graphite and linseed oil were the primary ingredients, and various other binder materials were added. In this series the primary factor considered was green strength. Those formulas which proved to have adequate green strength were further evaluated for cured and fired strength, dimensional stability, permeability, and ultimately casting characteristics.

The formulas developed in this first series are listed in table 21. In addition, experiments utilizing water-free tar as a fluid binder were conducted but were signally unsuccessful. Of the 36 formulas thus investigated, only four exhibited characteristics promising enough to merit further investigation. These formulas, BW, S, T, and TY, appear in table 22 in their final form.

In addition to the mixes listed in table 21, a series of molds was made in which powdered sugar was subsituted for dextrin in formulas BW, S, T, and TY. This substitution was unsuccessful. The resultant molds and cores exhibited extremely poor releasing characteristics when stripped from the patterns.

From the many variations tried, three significant factors were apparent:
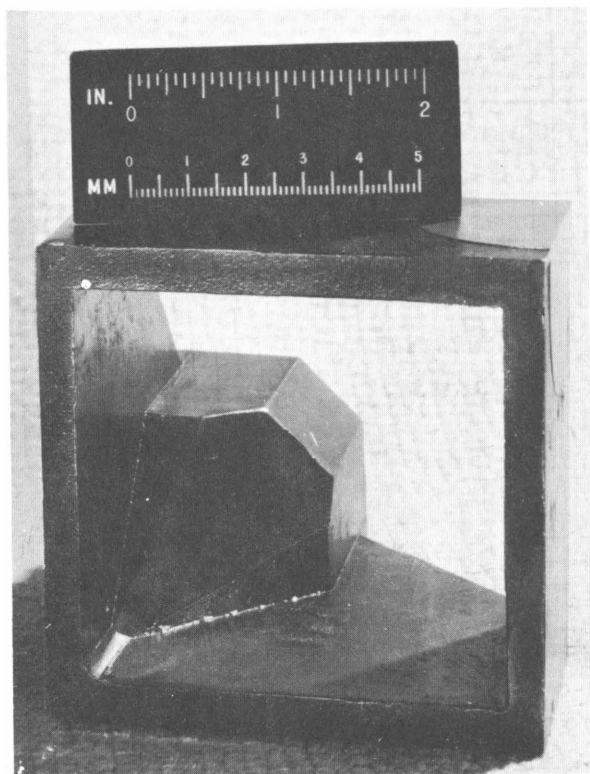
Figure 109.—Cast zirconium reactor part from mold shown in figure 108.

Figure 111.—Titanium castings from frozen mercury molds provided by Alloy Precision Casting Co.
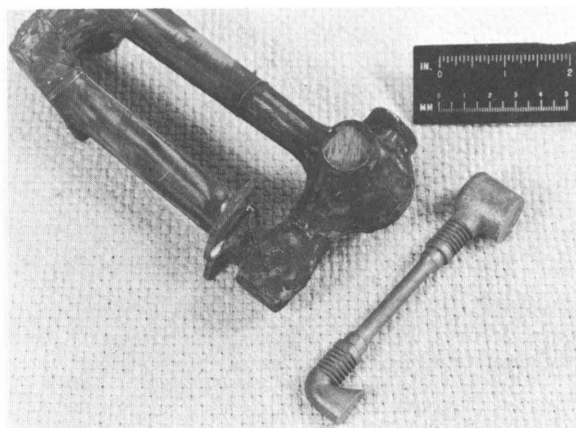
Figure 112.—Titanium castings from frozen mercury molds provided by Kolkast, Inc.

Figure 110.—Zirconium torsion-bar bracket.

1. The graphite powder used must not contain particles larger than −20 mesh.

2. The amount of cornstarch must be closely controlled. (Later evaluation proved that the cornstarch content should be held to 6 percent.) No substitutes for cornstarch were discovered.

3. Cereal binder and dextrin can be freely substituted and mixed with no apparent effect. In later work it was determined that improved green strength, better definition, and greater dimensional stability were achieved when the

Table 21.—Experimental mold formulas—series I

Mix designation	Materials	Remarks
A through E_____	Graphite powder (machine fines). Cornstarch. Linn oil. Carbowax–4000.[1]	Screen analyses of graphite varied from mix to mix; 100 percent minus 20 mesh to 50 percent minus 8 plus 16 and 50 percent minus 20. Cornstarch varied from 10 to 12 percent of dry ingredients. Linn oil (a commercial core oil of raw linseed oil). Carbowax–4000[1] added to oil up to 10 percent. Mix B was fair.
F through G_____	Same as A–E with water added in form of hydrolyzed starch.	These materials failed completely during firing cycle.
H through O_____	Graphite powder. Cornstarch. Pulverized pitch. Water glass. Linn oil plus 10 percent Carbowax–4000.[1]	Graphite powder screened to minus 20 mesh. The materials in these mixes were added in varying amounts with no successful products resulting.
P through Y_____	Same as A–E with the addition and substitution of cereal binder and dextrin.	Graphite powder screened to minus 20 mesh. Silicon was added to mix U which reacted severely with cast titanium. Mixes S and T offered sufficient promise to be investigated further.
BW_____	Graphite. Cornstarch. Dextrin. Linn oil plus 10 percent Carbowax–4000.[1]	A combination of mixes B and W with dextrin and cornstarch each 6 percent of dry mix. Very favorable results.
TY_____	Same as BW with addition of cereal binder.	Cornstarch and dextrin increased to 9½ percent each and cereal binder added 6½ percent. Satisfactory on initial trials.

[1] Trade name, Union Carbide Chemicals Co., a high-molecular-weight polyethylene glycol wax.

Table 22.—Mold formulas of promise as chosen from series I

Ingredient	BW	S	T	TY
Dry, weight-percent:				
Powdered graphite_____	8	78	78	78
Cornstarch _____	6	12	17	8
Pitch _____		5		
Dextrin _____	6	5	5	14
Fluid (Linn oil plus Carbowax–4000)[1][2] per 100 g dry ingredients, ml_____	25	29	27	26

[1] 20 g Carbowax/100 ml oil.
[2] Carbowax–4000 was found satisfactory for this particular application. Since no other commercial products were tested, no special endorsement of Carbowax is implied.

Carbowax–4000 was increased to 20 g/100 ml of oil in the fluid binder.

An evaluation shows that the physical properties of the molds that appear in table 22 were improved with the use of a graphite powder of uniform quality and particle size distribution. Excessively fine powder, −150 mesh, caused decreased permeability and at the same time caused a greater tendency of the mold to warp and crack during the curing and firing cycles. In addition, the flowability of the material (an important feature in core blowing) was reduced, mold stripping was hampered, and physical strength was lowered.

Careful screening of machine fines could produce a powder with a satisfactory particle size distribution; however, commercial powders of guaranteed screen analyses are available, and their use is recommended. The average distribution of machine fines screened through a 20-mesh sieve is compared with that of a recommended commercial powder in table 23.

General Mixing Techniques

In the development of the mold formula, the mixing procedures did not differ significantly from standard foundry techniques. The dry ingredients were mixed thoroughly in a double cone-type blender and then transferred to a ribbon mixer. The fluid binder, heated to permit the incorporation of the Carbowax −4000, was added slowly to the dry ingredients. After the materials were thoroughly mixed, they were transferred to the molding flask or core blower cartridge for mold preparation. A more detailed description of the process will be given in the section "Present Molding Practice."

Development of Curing and Firing Cycles

Curing Techniques.—Generally speaking, the techniques applied to the curing of green molds and the firing of dried molds are equally as important to the finished product as the mold formula.

The basic process consists of a low temperature air cure (38° C), a high temperature air cure (93° C), and a firing cycle in a reducing atmosphere at 960° C. This basic technique required from 300 to 400 hr. Most of this time represented the extended period at 38° C necessary to promote oxidation. If this low temperature air dry were omitted or shortened, the molds would warp and crack during the 93° C air cure, and evolution of volatiles at the higher temperatures of the firing cycle would cause distortion and perforation of the molds.

Table 23.—Particle size distribution of graphite powders in the minus 20-mesh fraction

Sieve size, mesh/in	Weight-percent retained	
	Machine fines	Recommended grade
35	33.8	(²)
65	25.6	62.0
80	3.8	(²)
100	6.3	29.0
150	(²)	7.0
200	14.0	1.0
Pan	16.5	1.0

¹ Commercial powders of guaranteed screen analyses are recommended; one such powder, Graphite Number GP–BB5, available from National Carbon Co., was found satisfactory; other commercial powders were not tested.
² Not screened at this level.

In an effort to reduce the time involved in curing the molds, a precuring process was developed. This process did significantly shorten the total time involved, and it also reduced the time period between the actual formation of the mold and the completion of the firing cycle. Although later work demonstrated a better method of achieving much the same end, a brief description of the precuring process will be given.

The mold material was prepared in the usual manner. After the liquid binders were mixed into the dry material, the moist mass was permitted to cure at 38° C for 88 hr. This time was determined by trial and error. After the material had been sufficiently precured, it was necessary to cool it to room temperature before attempting to blow or ram a mold. The formed mold would then go directly to the 93° C oven for 72 hr or until the mold attained a hardness approaching that desired for the finished product. The total time involved for this process was approximately 50 percent of that for the standard method, which involved no precure.

The principal objection of this technique is that unless extreme care is taken, the material will overcure and will become useless for molding. In some applications, however, this process may be of value.

Firing Cycle.—The final processing step in the preparation of expendable graphite molds and cores involves the high-temperature firing cycle. It was arbitrarily decided to hold firing temperatures below 1,000° C and avoid vacuum curing

and firing in an effort to produce a product and an art that would lend itself more nearly to conventional foundry practice and be economically attractive to the steel industry as well as for reactive metal casting.

In the establishment of proper techniques in this regard there were two primary considerations: (1) Temperature and time-temperature gradients and (2) media.

Concerning the first consideration, it remained to be established at what temperature below 1,000° C satisfactory molds and cores could be produced, and how long that temperature should be maintained. To determine this, a series of small molds and cores was formed, cured, and placed in a steel box filled with pulverized charcoal. The box was placed in a muffle furnace and the temperature raised by 100° C steps. At each step the furnace temperature and reactions were allowed to stabilize for 1 hr before proceeding. Evolution of smoke and fumes from the box at around 500° C was an indication that carbonization of the mold material binders was occurring, and the furnace was held at this temperature until visible smoking had ceased.[2] All molds were elevated to at least 750° C, and some were taken to 960° C.

The furnace was allowed to stabilize at the peak temperature before being shut off. The box remained in the furnace until it had cooled to at least 300° C, after which the molds were removed from their beds.

Casting trials of molds and cores fired at 750° and 960° C indicated that removal of volatile mold material components was not sufficient at the lower temperature. The volatiles remaining in the molds fired at the lower temperature were driven off during the casting operation and caused the castings to have greater mold-gas porosity, as shown in figure 113. As can be seen in figure 114, castings from the molds fired at the higher temperature exhibited a much lower degree of porosity.

It was speculated that a longer "soak" at 750° C might remove the volatiles, but the success afforded with molds fired at 960° C decided the researchers on this course, and this is now the standard practice.

With regard to the firing media or mold bedding material, the three considered were charcoal, powdered graphite, and pulverized coke, in that order. Charcoal was used for a time but did not give uniform results. Reaction be-

Figure 113.—Titanium casting from mold fired to 750° C.
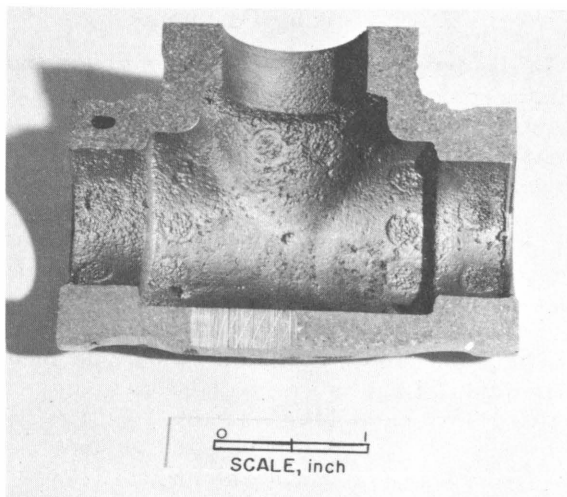
Figure 114.—Titanium casting from mold fired to 960° C.

tween the molds and the bedding would often result in an unusable mold. Graphite was substituted, but with this material insufficient protection against oxidation was afforded. The oxidation was apparently concentrated on the binder materials and resulted in an extremely soft and crumbly mold. Commercially available pulverized petroleum coke provided adequate oxidation protection and at the same time did not react with the molds themselves. The firing

---

[2] The smoke produced contained dangerous quantities of carbon monoxide gas. Particular attention must be paid to proper ventilation and personnel protection.

box was initially fitted with a steel lid, but this was later replaced by a graphite cover that provided additional oxidation protection.

It is recommended that conditioned or recycled coke be used rather than new calcined coke. The conditioning is apparently helpful in reducing the sulfur content. Conditioning may be accomplished by baking the coke in the firing furnace before using it to bed the molds.

Physical Evaluation

The four mold formulas listed in table 30 were selected for further evaluation because they exhibited the most favorable properties in the green state and because they could be cured and fired without appreciable distortion. Each formula was rejected when failure was observed, but only after ascertaining whether a slight modification in either formula or technique would correct the situation. Results from this further evaluation showed clearly that formula BW was the only one worthy of further examination.

The physical property evaluation of the mold materials involved tests for tensile strength, compressive strength, permeability, density, and shrinkage. In the tests AFS and ASTM specifications were complied with wherever applicable.

At the conclusion of the general evaluation program, mold material formula BW was subjected to additional tests to ascertain the effects of certain changes in the mold preparation and curing techniques. For the purpose of clarity, the latter evaluation will be reported in the section, "The Material of Choice."

Early in the evaluation program, test specimens were prepared from each formula by three different methods. These methods were blowing, hand ramming, and pressing. The pressed specimens were formed at pressures of 40, 80, and 120 psi and were evaluated for tensile strength, compressive strength, shrinkage, and permeability at each forming pressure. Later in the program the pressed specimens were eliminated to simplify the evaluation; however, sufficient evidence was obtained to demonstrate that a very hard, smooth, and dimensionally stable product could be formed by this means.

Comparison of Formulas BW, S, T, and TY

Tensile Test.—Tensile tests were performed on specimens conforming to ASTM specification C-190-49. (See fig. 115.) The cross sectional area in the reduced section was 1 in.[2] Overall length of
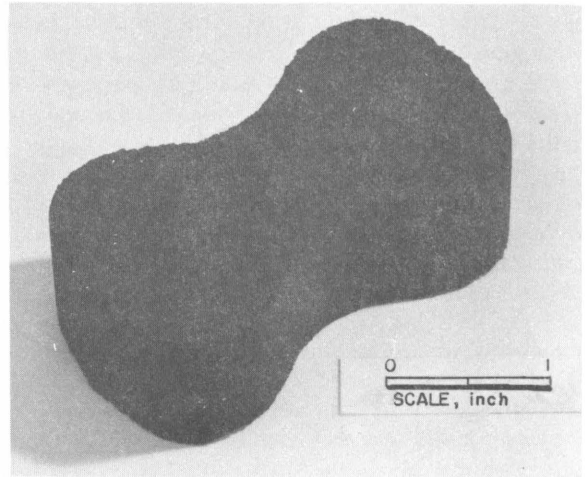
Figure 115.—Tensile test specimen ASTM–C–190–49.

the specimen was 3 in. The tensile specimens were formed in a standard AFS twin tensile core-box and were pulled with special grips in a universal testing machine.

Four series of specimens were made from each mold formula. The values obtained from these tests were badly scattered. This scatter was attributed in part to the lack of uniformity of the graphite machine fines used; therefore, an additional series of tests was conducted on specimens formed from the commercial graphite powder. Mold material formula S was not included in the latter series. The results of these tests are listed in table 24.

Averages of tensile-test values obtained in all series for each of the four formulas are as follows, in psi: BW, 89; S, 48; T, 61; TY, 72. These values indicate that the UTS of material BW

Table 24.—Ultimate tensile strength determined for three expendable graphite mold materials formed from a commercial grade graphite powder,[1] psi

Method of preparation	BW	T	TY
Blowing	40	27	40
Hand ramming	45	53	99
Pressed:			
40 psi	94	68	94
80 psi	85	72	106
120 psi	107	92	100

[1] All values are averages of 4 tests.
Cross head travel = 0.05 in/min.
Load rate = 120 lb/min.
Testing temperature = 20° C.

is 24 percent greater that that of the next strongest material.

Compressive Strength Test.—The strength of a foundry mold material may be determined by tensile, shear, or compressive tests. For the purpose of this investigation it was decided to include both tensile and compressive strength determinations; a 2-in-diam, and 2-in-high, cylindrically shaped specimen was used throughout this investigation.

Four series of test specimens were formed in each mold-material formula for 80 specimens. Tests were performed on the universal testing machine used in the tensile testing program. Lower platen speed was 0.05 in/min (average strain rate 0.025 in/in/min). Average values for compressive strength as determined by this series are given in table 25.

Averages of compressive strength values obtained for all specimens from each of the mold material formulas are listed below. A striking similarity to the tensile averages given previously is noted in psi: BW, 97; S, 57; T, 49; TY, 61. Mold formula BW has a compressive strength value 57 percent higher than TY, the second strongest material.

Table 25.—Compressive strength of four expendable graphite mold materials, psi

Method of preparation	BW	S	T	TY
Blowing_____	35	34	16	29
Hand ramming_____	81	56	32	51
Pressed :				
40 psi_____	82	60	60	69
80 psi_____	136	76	86	92
120 psi_____	150	77	53	74

Permeability.—Permeability of a mold material is that physical property that allows a gas to pass through it. According to AFS specifications, mold permeability is determined by measuring the rate of flow of air through a standard 2-in by 2-in-diam specimen. Because in reactive metal casting only completely baked and fired molds can be used, fired permeability (*1*) was the only value sought for in this material.

Permeability is expressed as a number according to the following formula:

$$P = \frac{Vh}{p\,a\,t},$$

where P = permeability number;
where V = volume of air passing through the specimen, cc;

where h = height of specimen, cm;
where p = pressure of the air, g/cm^2;
where a = cross-sectional area of specimen, cm^2; and
where t = time, min.

The apparatus used in this investigation for the determination of permeability was a permmeter. Permeability may be determined in the following ways with this equipment: (1) The automatic-clock method which permits direct reading from the dial but is accurate only to ±10 percent and (2) the AFS standard method, which is the procedure used in this determination and requires the calculation of the permeability value. The latter method will permit accuracy to ±1 percent if care is taken in the time measurement.

When using the AFS standard method, the formula above is employed. All factors are constant except time, which is measured by a stop watch. The volume of air is maintained at 2,000 cc ±1 percent, the standard specimen is 2 inches (5.08 cm) in height and has a cross-sectional area of 3.1416 in^2 (20.268 cm^2). The pressure of the air is maintained at 10 g/cm^2. Thus the formula becomes P = 50.12t, when time is measured in minutes, or P = 3007.2t, when time is in sec; therefore, the higher the resultant figure, the greater is the permeability of the material.

Permeability values for the four mold formulas are listed in table 26. There is a scatter of data which is the result of the nonuniformity of the graphite powder used during this early phase. Later values obtained on specimens prepared from mold-material formula BW and a graphite powder of uniform particle size are higher and are much more consistent. Permeability values were increased as much as three times over previous levels, as may be seen in table 27, without sacrificing tensile or compressive strength.

Density.—Density measurements were made on fired 2-in-diam by 2-in-high compressive strength and permeability specimens.

The values listed in table 26 indicate the direct relationship between forming pressure and density. When the density is plotted against permeability, figure 116, it can be seen that permeability varies inversely with density.

Density and permeability values for the blown BW specimens listed in table 27 indicate that the use of commercial graphite powder with the resultant elimination of large volumes of the −150-mesh fraction has reduced the density and simul-

Table 26.—AFS permeability and density of four mold materials [1]

Method of preparation	AFS permeability				Density, g/cc			
	BW	S	T	TY	BW	S	T	TY
Hand rammed_____	123	67	102	69	1.00	1.03	0.94	1.03
Blown_____	26	35	54	45	1.16	1.11	1.09	1.09
Pressed:								
40 psi_____	9	23	23	16	1.18	1.11	1.13	1.15
80 psi_____	6	14	12	10	1.26	1.14	1.19	1.17
120 psi_____	4	11	12	10	1.29	1.17	1.19	1.20

[1] All values are averages of 4 tests.

Table 27.—AFS permeability and density of blown specimens of mold material BW prepared from commercial graphite powder

	Series I, no precure	Series II, precure
Number of specimens_____	10	6
Average permeability number___	337.4	356.9
Average deviation_____	9.98	22.9
Standard deviation_____	16.65	23.05
Average density, g/cc_____	0.890	0.979
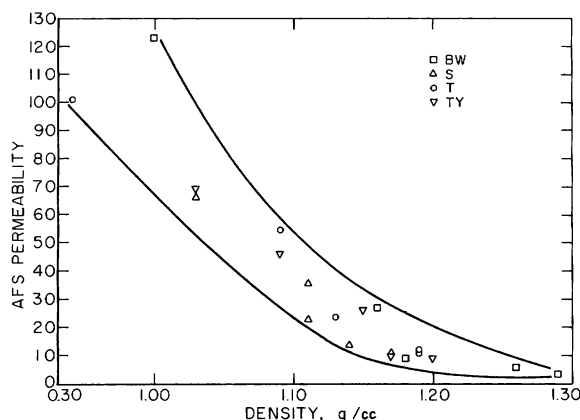
Figure 116.—Density vs. permeability of four mold material formulas.

taneously increased the permeability compared to the values obtained on specimens listed in table 26 which were prepared from machine graphite fines.

Mold Shrinkage.—The amount of the shrink which a specimen of any given mold material will undergo during the curing and firing process must be consistent and uniform if sound dimensionally accurate castings are to be made. To determine this shrinkage factor for the four mold material formulas, measurements were made on four series of tensile test specimens of each material before and after processing. Specimens were formed in each of the five ways described previously. Four measurements were made on each specimen for 80 measurements per mold formula. Average values for the entire four series appear in table 28.

Table 28.—Average shrinkage values of four series of tensile test specimens

Method of preparation	Shrinkage expressed as percent [1]			
	BW	S	T	TY
Blowing_____	2.03	3.37	4.24	4.33
Hand ramming_____	2.54	1.27	4.31	4.11
Pressing:				
40 psi_____	1.69	1.14	3.62	3.28
80 psi_____	1.19	1.60	2.89	3.07
120 psi_____	1.44	.53	2.55	2.49

[1] These values are expressed as the percentage shrink of the original dimensions. A value of 100 percent is equivalent to 0.120 in/ft.

From the values in table 28 it would appear that formula S exhibits the lowest shrinkage factor of the four; however, considerable variance from specimen to specimen and from dimension to dimension of the same specimen makes this material particularly unattractive. The apparently low shrinkage of the S material, particularly in the specimens pressed at 120 psi, is a result of swelling and distortion of the specimen.

The consistency of shrinkage of the BW specimens may be seen in table 29, which is a tabulation of the average of four measurements per specimen of four batches of mold material BW. More recent improvements in mixing and curing techniques have further reduced the shrinkage and improved the consistency of material BW. This will be discussed in the following section.

Material of Choice.—From comparative physical evaluation of the four mold materials it became clear that material BW exhibited more favorable characteristics than the other three; therefore, the remainder of the research effort was concentrated on this basic mix. Time and temperature control during the wet mixing operation, carbon dioxide addition, and strict attention to the quality of the powdered graphite used were the most significant factors that led to further improvements of the product.

As mentioned previously, a study was made to determine the effects of precuring the material in an effort to reduce total curing times. From the evaluation data it was clear that although curing times could be reduced, the product often exhibited inconsistent physical properties. (See table 27.) Even so, some physical properties of both standard cured and precured BW specimens will be given, since most of the final evaluation program was concerned with this study of the variables in the mixing and curing process.

Table 29.—Shrinkage of BW tensile test specimens, percent [1]

Method of preparation	Series I	Series II	Series III	Series IV
Blown	2.63	2.94	2.91	3.64
Hand rammed	2.93	1.97	2.50	2.74
Pressed:				
40 psi	1.24	1.76	1.67	2.07
80 psi	.96	.94	.93	1.91
120 psi	1.43	1.19	1.18	1.96

[1] Each value is the average of 4 measurements per specimen.

For purposes of clarity at this point in the investigation, each batch of BW material which was prepared was assigned a lot number. This number was prefixed by the letters XM. By this mean is was possible to maintain the identity of a given set of molds prepared under a variety of conditions from their preparation to the ultimate casting. In an effort to improve the BW mix and the final product, several lots were prepared in which the following factors were varied and the results noted: (1) Mulling time, (2) carbon dioxide versus air that was introduced during the mixing operation, and (3) precure versus cure. In all of the variations, the properties of tensile strength, permeability, density, and shrinkage were measured on specimens both hand rammed and blown.

Mixing time variations were narrowed to 8

and 10 min, and the precuring time cycles were established by a series of experiments on molds and cores prepared from lots XM–50 through XM–63.

At the conclusion of the study of these 14 lots, hand rammed and blown tensile test specimens, permeability specimens, and molds and cores for test castings were prepared from lots XM–64 through XM–90.

Tensile strength determinations were made on 32 standard mold tensile specimens produced from XM–86 and XM–87. The effect on UTS of the three mixing variables and the one forming variable was noted. Table 30 lists the average values of all specimens within each series. It is obvious from these data that optimum conditions of preparation exist. To obtain either blown or hand-rammed cores and molds of superior quality, the green material must be mixed for 8 min in a flow of CO_2 and cured directly.

Permeability determinations were made on the blown specimens only. Values ranged from AFS 231 to 345 for the direct-cured specimens and from AFS 190 to 320 for the precured material with an average deviation of 38 and 59, respectively. The greater deviation observed in the precured specimens verifies the earlier finding that a product of lesser uniformity results when the precuring technique is used. Table 31 lists the permeability values obtained on the specimens in the direct-cure series.

Shrinkage determinations were made on 16 tensile test specimens from XM–86 and XM–87. Measurements were made of the neck width and overall length of each specimen, and were taken after the completion of the firing cycle.

Because of the nature of the material and the shape of the specimen (see fig. 115), a slight variation in measurements was to be expected. This variation shows itself prominently in the shrinkage values which are expressed as percent decrease in dimenion in table 32.

In spite of the variations, certain trends are obvious. The variable which most affects the shrinkage of the material is the molding method. In general, the hand-rammed specimens shrink about 0.5 percent less than the blown specimens. Somewhat less prominent is the trend toward dimensional instability in the precured series. The mulling time and atmosphere appear to have little if any effect upon ultimate shrinkage.

Comparison of these values with those given in tables 28 and 29 indicates a substantial reduction in shrinkage.

Table 30.—Average values obtained on
32 tensile test cores [1] with four major variables

Major variables	Ultimate stress,[1] psi
Mulling atmosphere:	
CO_2	164
Air	119
Curing technique:	
Direct cure	152
Precure	131
Mulling time:	
8 min	149
10 min	134
Molding method:	
Hand rammed	199
Core blowing	84

[1] Average of 16 specimens.

Table 31.—AFS permeability values for direct
cured BW blown specimens

Mulling time, min	Mulling atmosphere	AFS permeability
8	CO_2	334
10	CO_2	231
8	Air	295
10	Air	345

Density determinations were made only on the blown permeability specimens from XM–65 and XM–71. These two mixes were mulled under CO_2 for 8 min. The following values were obtained:

Mix	Shrinkage, percent	Density, g/cc
XM–65—precure	2.56	0.867
XM–71—no precure	2.36	.931

Comparison of the density of these specimens with that of the earlier material which was not mulled under CO_2 (table 27) indicates a slight increase in density. A comparison of tables 27 and 31 shows that this increase in density was achieved without an accompanying loss in permeability.

Determination of the volume of mold gas, residual after firing, was made on hand rammed and blown 2- by 2-in cylindrical specimens [3] from mix XM–90. The test temperature was 1,850° F. The volume of gas to be generated during the casting operation must be determined if the molds and cores are to be properly vented to prevent "blowing" the casting.

Table 32.—Shrinkage as determined on 16 tensile test mold specimens, percent

Mulling atmosphere	Mulling time, min	Direct cure		Precure	
		Length	Width	Length	Width
Blown specimens:					
CO_2 mulled	{ 8	2.65	3.14	2.26	1.97
	{10	2.65	2.36	2.40	2.36
Air mulled	{ 8	2.52	2.36	2.80	2.36
	{10	2.65	1.97	2.26	2.36
Hand-rammed specimens:					
CO_2 mulled	{ 8	1.98	1.97	2.26	2.36
	{10	2.25	1.97	2.26	2.36
Air mulled	{ 8	1.98	1.58	1.98	1.97
	{10	1.98	1.58	1.87	.39

[1] Specimen swelled after ramming, resulting in increased dimension.

In figure 117 the volume of gas in cubic centimeters per gram of mold specimen is plotted against time. The lower volume obtained from the hand-rammed specimen is attributed to its higher density and lower permeability, rather than a lower residual gas content.

Present Mold Practice

Since the initial development of the formula for the BW mix, improvement in the quality of the mold and the resulting casting has been

[3] These determinations were made through the courtesy of Dan L. Smith, ESCO Corp., Portland, Oreg.
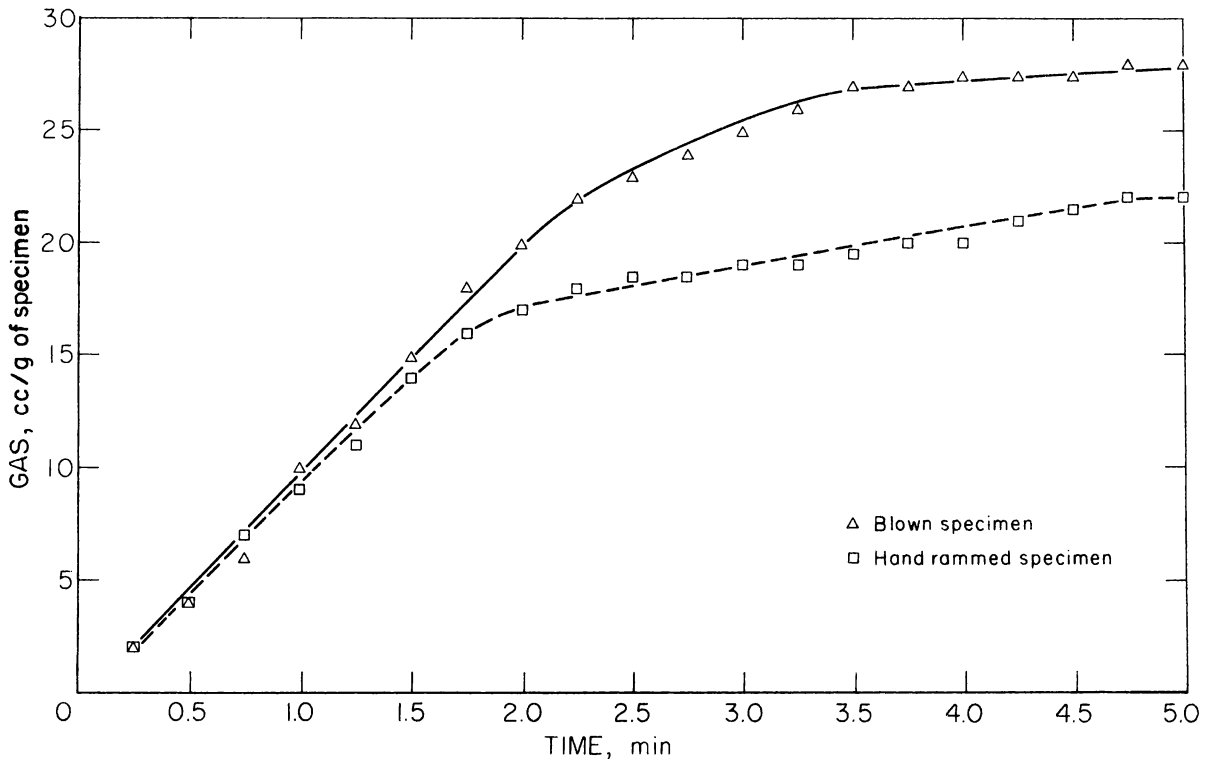
Figure 117.—Mold gas evolution of blown and hand rammed specimens of mold material
XM–90 at 1,850° F.

effected. The use of a powdered graphite of uniform quality and specific sieve analyses, the introduction of a carbon dioxide atmosphere during the mulling operation, and the elimination of the precure cycle have cut curing times and resulted in a consistent and uniform product. Careful attention to temperatures during the mixing and forming steps has further enhanced product uniformity.

The present molding process for mold formula BW is given below.

Material Preparation.—In preparation of the dry ingredients, the starch, dextrin, and/or cereal binder are sifted to remove any lumped material. Careful and complete blending of the dry mix is essential to good mold preparation. A double-cone type blender is quite satisfactory for this purpose.

The fluid binder is prepared by heating a core oil of a raw linseed-oil base and incorporating into it the required amount of Carbowax–4000. The liquid binder should be heated to a point just below the boiling temperature, or about 240° C. This permits a partial polymerization of the linseed oil, hastens the curing process, and

strengthens the resultant green molds. The heated oil should be cooled below 100° C before being blended with the dry mix in the ribbon mixer.

The oil and wax mixture may be prepared several days in advance. Repeated heating and cooling, however, gradually causes the polymerization to advance, and in time the liquid will become too viscous for use. When this occurs, it will be observed that the mold material that comes from the mixer will not have the proper amount of adhesiveness to compact and hold a shape when pressed into a ball in the hand. To test for proper consistency the material is pressed lightly into the ladle and then removed. This is shown in figure 118. A stickiness or reluctance to release is an indication of too much liquid binder, and the inability of the material to hold its shape is an indication of too little.

After the fluid binder is prepared and cooled below 100° C, it is transferred to the ribbon mixer where the dry materials have previously been placed. Carbon dioxide gas is introduced during the mulling operation that is timed for 8 min. The flow of CO_2 need be only sufficient
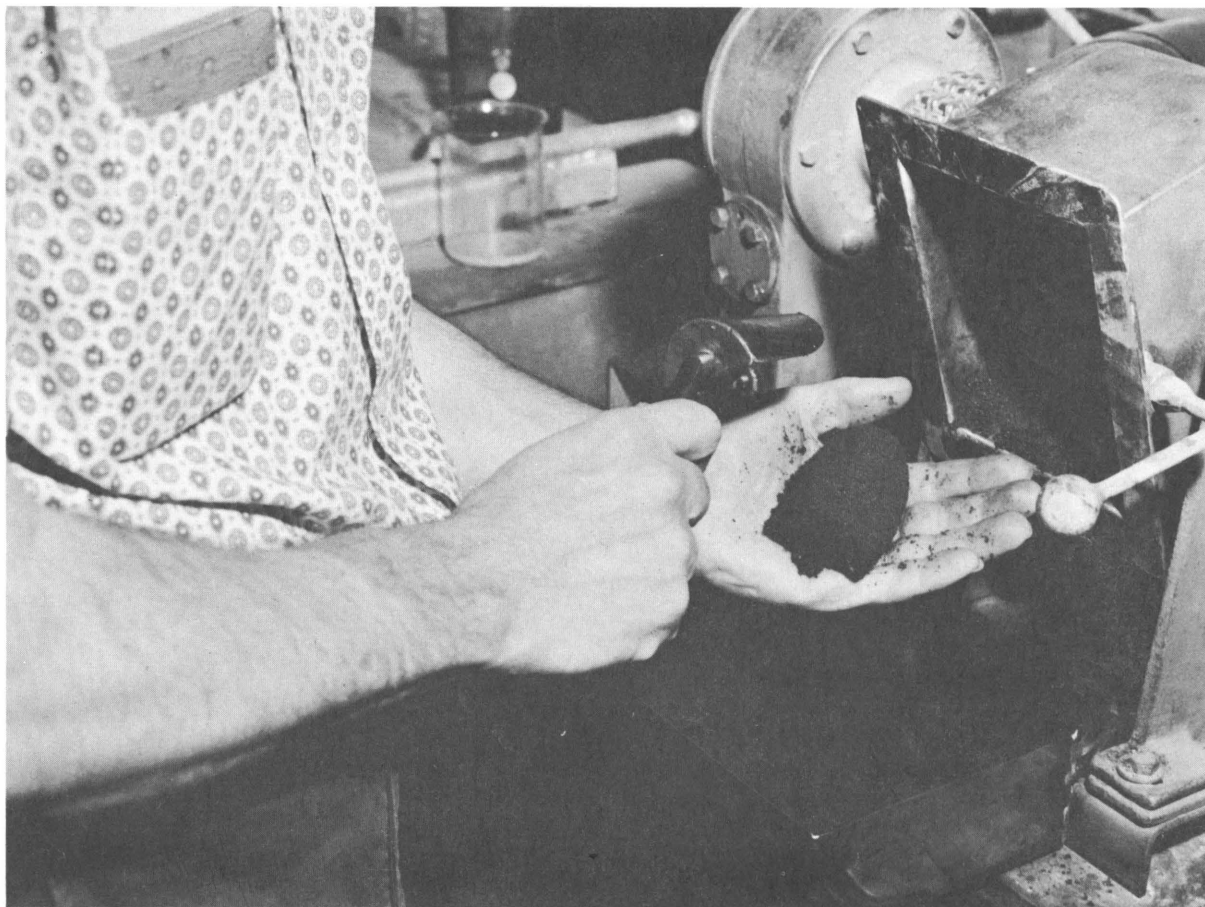
Figure 118.—Test of mold material moist consistency.

to assure the exclusion of other atmospheric gases. The mulling time must be controlled closely to achieve the most satisfactory product. It is expected, however, that some variation in time will be noted when scaling up to pilot plant or commercial scale.

The mulled material must be allowed to cool to room temperature before it is used in core-blowing operations since the warm material will not flow properly. It may be hand rammed somewhat above room temperature, but again, if it is too warm, difficulty will be experienced in stripping the mold.

In the production of molds by means of hand-ramming techniques, conventional foundry equipment and procedures may be used with the exception that parting powders and sands are not suitable. Flasks and patterns should be coated with a good grade of silicon parting liquid or lard oil. In place of parting sand between the cope and drag, a 0.005-in

layer of shim stock is used as shown in figure 119.

The primary advantage of the material developed in this investigation is its ability to flow, thus making it adaptable for core blowing applications. The material should be somewhat more moist for blowing than when used for hand ramming. The skill and art of the molder will be a factor in controlling the final fluid content of the mix.

For the purposes of this investigation a cartridge-type core blower was obtained. Standard core boxes, produced from magnesium by a commercial pattern shop, were used. Magnesium is the material of choice for these boxes, but aluminum may be used for mold patterns and flasks.

Venting of the core blow boxes for material BW is similar in requirements to that for more conventional sand-core blowing. In general, the vents are placed to lead the material and per-
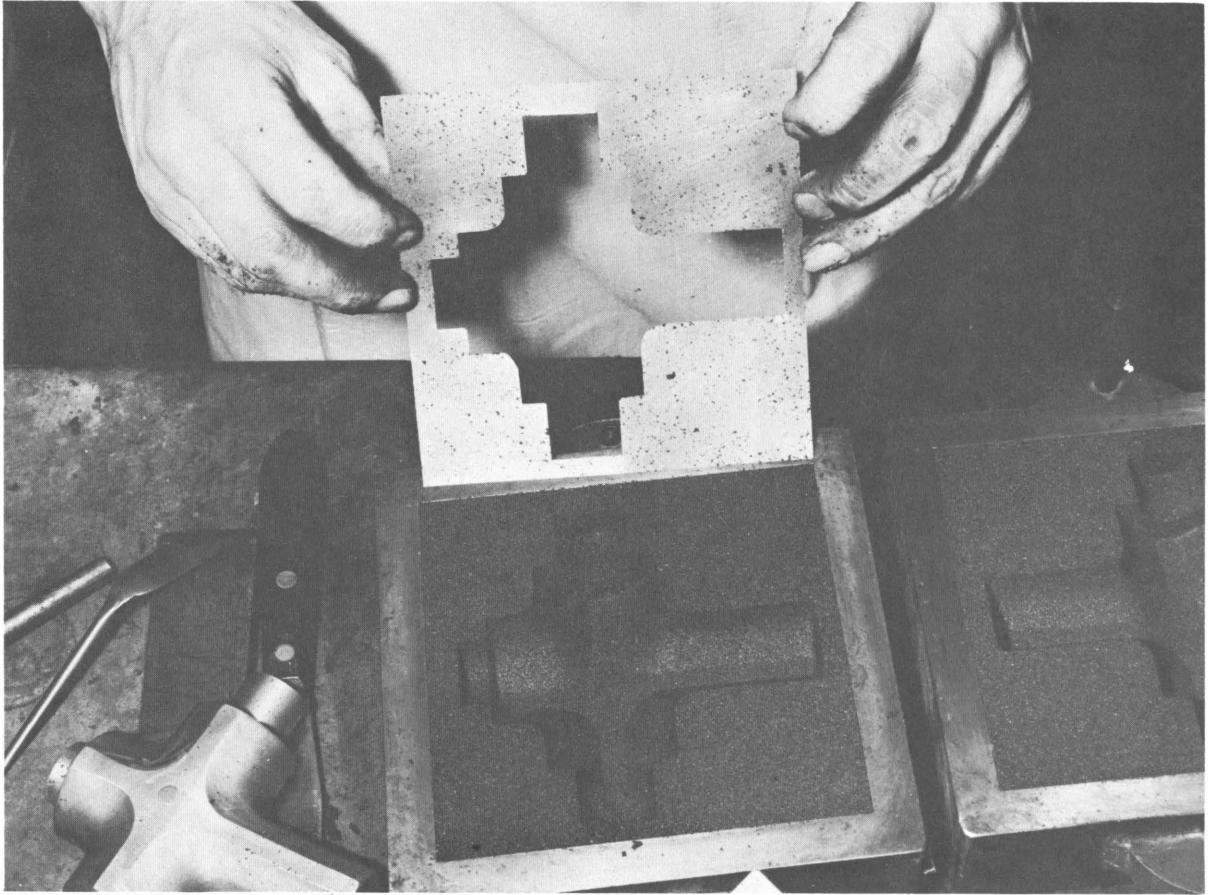
Figure 119.—Metal shim stock is removed after the mold has been rammed.

mit uniform compaction. Each core shape will have its own particular venting requirements. The vent placement in two typical cores produced in this study are shown in figures 120 and 121.

Curing and Firing.—Once the molds and cores are formed, they are stripped and placed on drying boards in the oven with the temperature set at 93° C. Drying boards may be of graphite or metal to which a parting agent has been applied. If graphite is used, a single layer of waxed paper may be placed between the mold and the drying board to prevent sticking. After the molds have set sufficiently to permit handling, they may be removed from the boards.

Blown cores are cured in the same manner, but the dryers should be designed for their particular shape. The cores may be transferred from the blow box directly to the dryer (fig. 122), thus eliminating the chance of damage due to handling. These dryers should be made of aluminum or magnesium and coated with a parting agent. Plaster dryers were tried but were badly cracked by the 93° C temperature. The time required for curing at 93° C varied with the size and thickness of the molds or cores. It varied from 70 to 80 hr for small blown cores to as much as 300 hr or more for massive items. The hardness of the mold is the index of curing. Blown cores must have durameter readings in the high 70's and hand-rammed molds in the low to mid-90's before they are considered ready to be fired. The fired mold or core will have hardness values of 2 to 6 durameter points over the cured item.

To facilitate the curing of thick sections of hand-rammed molds, holes may be drilled into the material. This will not only reduce curing times but will prevent cracks and distortion from developing when the mold is fired.

When it is determined that the molds are sufficiently cured, they are removed from the
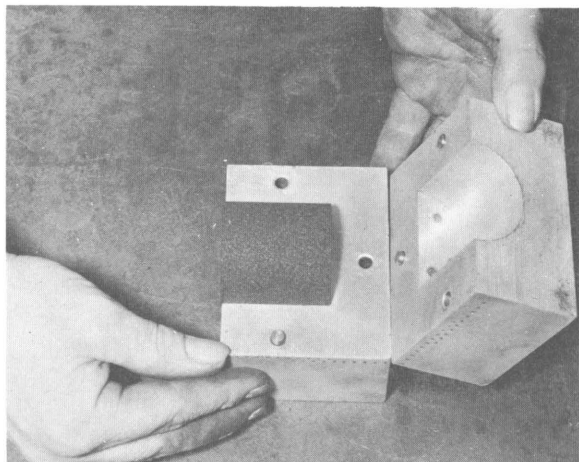
Figure 120.—Core blow box and core for 2- by 2-in permeability specimen.
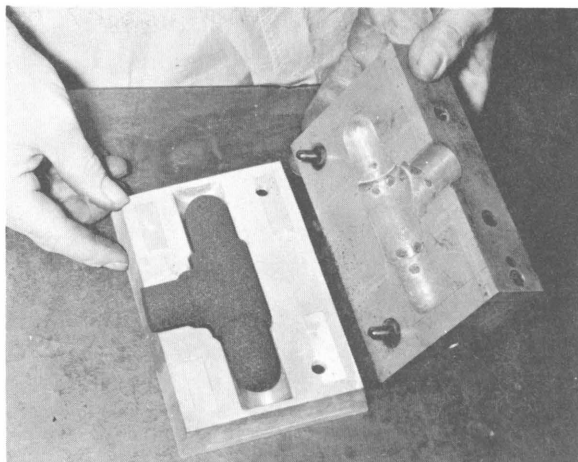
Figure 122.—Blown core stripped from core box onto dryer.
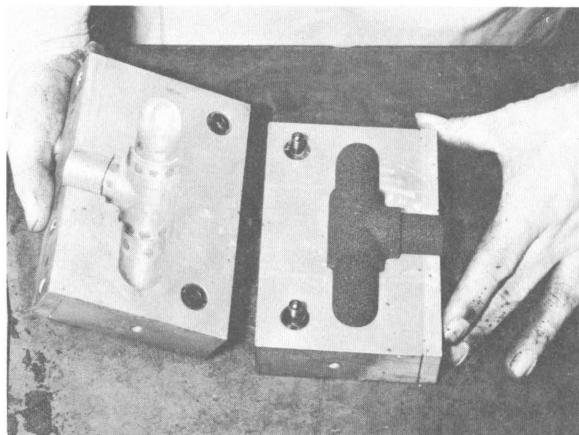
Figure 121.—Core blow box and core for 1-in pipe tee.

oven and placed in the coke bed in which they will be fired. (See fig. 123.) For maximum protection all surfaces should be covered by at least 1 in of pulverized coke and the firing box fitted with a graphite cover.

The bedded molds are placed in the furnace at 200° C, and the temperature is raised gradually in 100° stages. At each step the temperature is permitted to stabilize before proceeding. At about 500° C the molds begin to smoke, an indication that carbonization and violatilization of the binder materials are beginning. Smoke is evolved over a 200° C range (500° to 700° C), and in this range the temperature is held until no further smoking is evidenced. When the evolution of smoke has ceased, the temperature

is again elevated stepwise to a maximum of 960° C. This temperature is held for 1 hr, after which the furnace is shut off and allowed to cool. When the system has cooled to a temperature below 300° C, the molds are removed.

Mold Assembly.—Typical assembly of the 1-in pipe tee mold with blown core as used in this development program is shown in figure 124. Not shown in the figure, but of vital importance to the quality of the casting produced, is the venting of the mold and core to allow the escape of residual mold gas and prevent its entrapment within the casting. To accomplish this, holes approximately $\frac{1}{32}$-in diam are drilled through the mold and into the core as illustrated by the schematic drawing pictured in figure 125. The effect of proper venting is dramatically illustrated by comparing the castings in figures 126 and 127.

In some instances it is necessary to repair or build up a section of mold. This may be accomplished by the use of a paste made of powdered graphite and a core adhesive, providing the repaired surface does not come into extensive contact with the molten metal. A typical application would be to repair to the parting face. The repair paste is applied to the fired mold and is oven dried until hard. It need not be refired.

Casting Evaluation

Titanium.—Evaluation of the four basic mold formulas began early in the investigation with a series of cast titanium 1-in pipe tees. Several
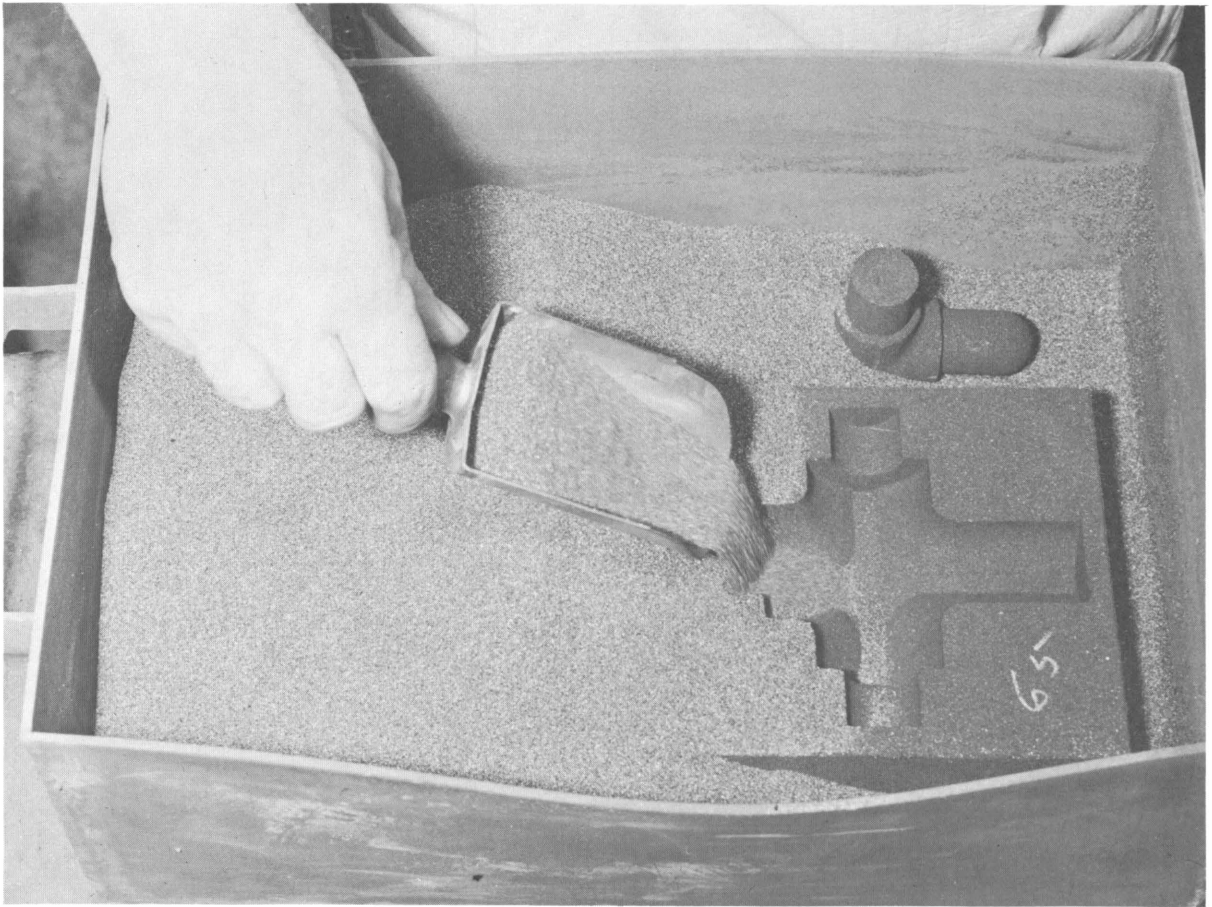
Figure 123.—Mold and core bedded in coke prior to firing.
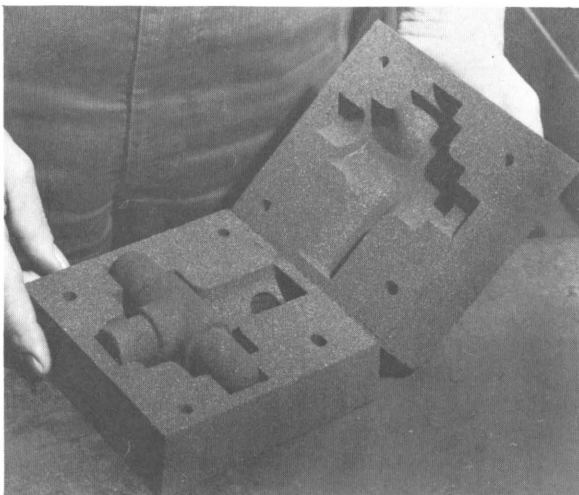
Figure 124.—Mold assembly with core
in position.
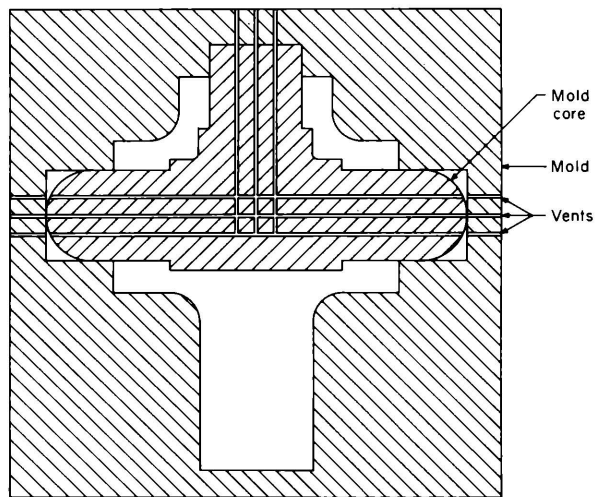
Figure 125.—Vent placement in expendable
mold assembly.
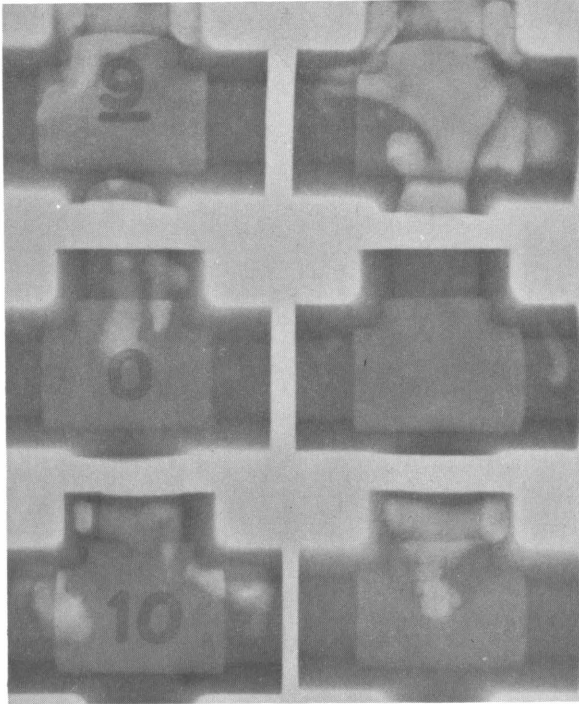
Figure 126.—Radiograph of castings from unvented molds.
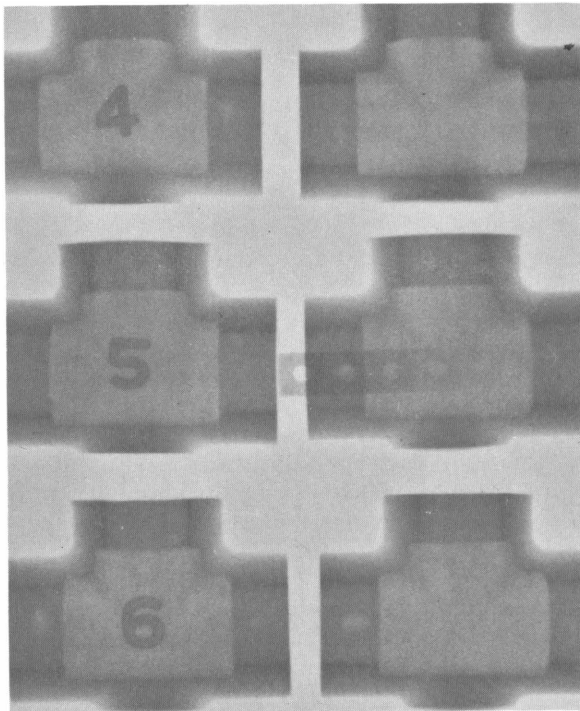
Figure 127.—Radiograph of castings from vented molds.
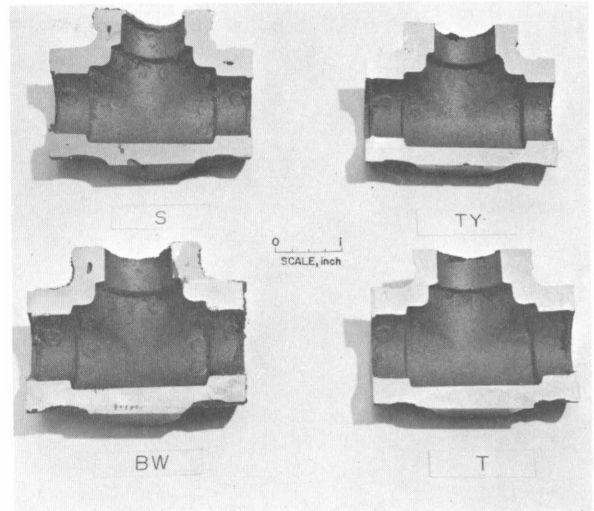
Figure 128.—Sectioned cast titanium pipe tees produced in four basic expendable mold formulas.
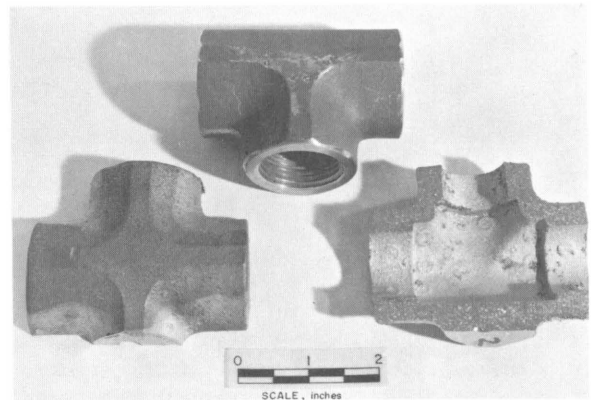
Figure 129.—Sectioned cast titanium pipe tees (SA 22,511) from CO_2 mulled expendable mold material XM– 64.

series of test castings were produced before proper venting practices were established which would prevent casting defects. Patterns and core boxes were produced by a commercial pattern shop.

Casting trials demonstrated that there were no significant differences in the as-cast surfaces obtained from the four formulas. Sectioned castings produced in each of the four mold formulas are shown in figure 128. Casting evaluation data as it pertains to formulas S, T, and TY will not be given inasmuch as formula BW demonstrated superiority in all mold evaluation tests.
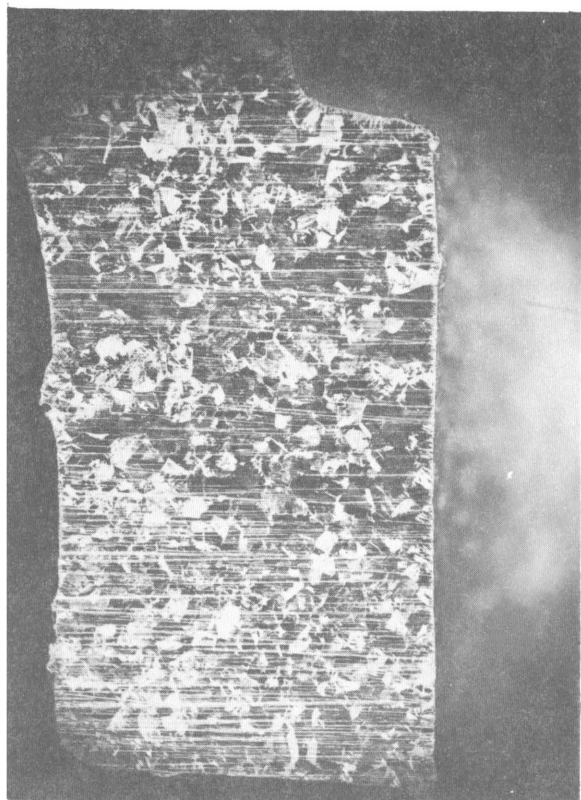
Figure 130.—Grain structure of cast titanium in mold material XM–64. Etch: 45 H_2O, 45 HNO_3 10 HF ($\times$ 10).

Figure 131.—Microstructure of casting SA 22,511 in area of Knoop traverse. Knoop hardness indentations made with 1 kg load. Etch: 45 H_2O, 45 HNO_3, 10 HF ($\times$ 50).

Improvement in the physical properties of the mold material inevitably resulted in an improved cast product. Typical of the titanium castings produced in the improved CO_2 mixed material is the pipe tee shown in figure 129. It will be observed in the photomacrograph ($\times$ 10) of a section of this casting, which appears in figure 130, that an extremely uniform grain structure exists from the cast surface inward. The grain structure near the as-cast surface can be seen in the photomicrograph in figure 131. The Knoop hardness indentations appear at 0.004-in increments from the cast surface inwards to a total depth of 0.024 in and thereafter at 0.020-in increments to a depth of 0.64 in. A surface-hardening effect due to strains produced by rapid chilling and some solution carbon can be seen to a depth of about .013 in. No visible carbon contamination can be observed.

Larger titanium castings, such as the one appearing in figure 132, were made so that the effect of pouring larger quantities of metal into the rammed material could be observed. This particular casting, SA 22,596, consisted of two 3- in-diam, 6.5-in-high, cylindrical sections connected by a thin flat section 6.5-in square by about 0.12-in thick. Several of these castings were produced in BW CO_2 mixed material in an effort to reduce the thickness of the plate section. Partial filling of the thin section occurred as low as 0.07 in, but complete filling was not possible below 0.100 in. From the excellent appearance of these larger castings it was apparent that castings of larger cross section and mass could be made with success in this particular mold material.

In addition to the 1-in pipe tees, test blocks 2-in thick and 4-in square were cast in molds formed from each of the final series of evaluation batches according to the schedule in table 33. From the block castings, specimens were obtained for tensile tests, microscopic studies, hardness traverses, and chemical analyses to determine the depth of carbon contamination.
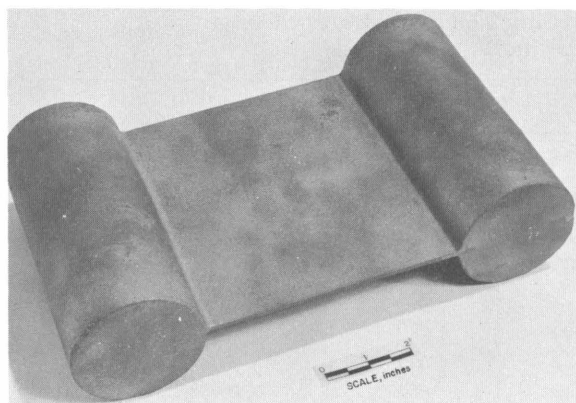
Figure 132.—Cast titanium flow plate, SA 22,596 from XM-72.

Table 33.—Schedule of mixing and curing variables of eight expendable BW mold material mixes

Mold mix number	Mixing time, min	Mixing atmosphere	Cure	Casting produced
[1] XM-68	8	CO_2	Direct___	SA 22,548
XM-76	8	CO_2	Precure__	SA 22,826
XM-85	8	Air	Direct___	SA 22,826
XM-84	8	Air	Precure_	SA 22,826
XM-75	10	CO_2	Direct___	SA 22,706
XM-73	10	CO_2	Precure_	SA 22,641
XM-70	10	Air	Direct___	SA 22,679
XM-74	10	Air	Precure__	SA 22,635

[1] XM-68 was prepared according to the procedure demonstrated to produce the most acceptable molds.

The electrode stock varied from casting to casting; therefore, to evaluate the analyses from one to another, the amount of increase or difference from an established base value has been plotted rather than an actual value. This base value was obtained by analyses of drillings removed from the center of each cast block. The same procedure is used in comparing the hardness of the metal at various levels below the cast surface.

Carbon and nitrogen analyses were obtained on samples taken at 0.015-in increments below the surface. The samples were taken from several areas of the casting and blended to assure a representative sample. The results of the analyses are shown in table 34. The values for carbon in excess of that contained in the base metal are given in table 35. The average values are plotted against depth in figure 133.

The hardness base line was established by obtaining an average Knoop hardness of the
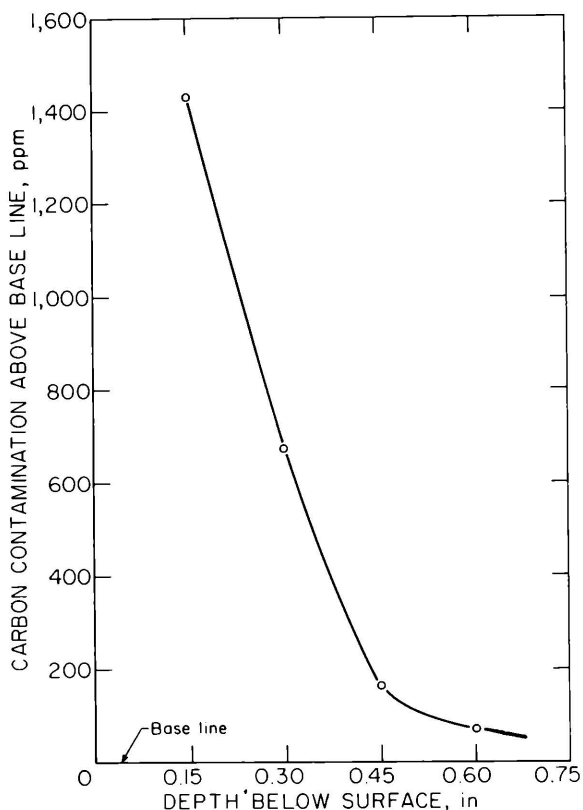
Figure 133.—Average depth of carbon contamination in eight titanium castings.
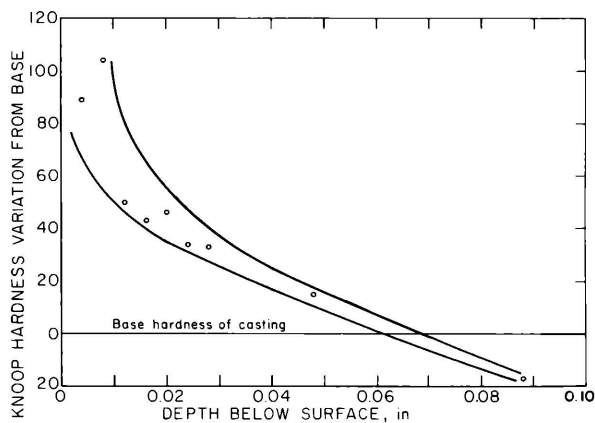
Figure 134.—Average depth of surface hardening effect in eight titanium castings.

interior metal of the casting. A Knoop hardness traverse using 1-kg load was made for each casting at 0.004-in intervals to a depth of 0.028-in beneath the casting-mold interface, then two additional readings at depths of 0.048-in and

Table 34.—Carbon and nitrogen analyses of eight titanium castings produced in expendable graphite BW molds, ppm

Casting	Mold mix number	Depth below surface				
		0.015 in	0.030 in	0.045 in	0.060 in	Base line
		CARBON ANALYSES				
SA 22,548	XM-68	1,450	560	490	360	380
SA 22,826	XM-76	1,500	1,250	870	670	560
SA 22,826	XM-85	2,200	1,350	860	750	600
SA 22,826	XM-84	1,950	1,450	870	770	610
SA 22,706	XM-75	2,100	1,500	750	770	620
SA 22,641	XM-73	2,200	930	410	350	310
SA 22,679	XM-70	2,300	1,250	800	730	710
SA 22,635	XM-74	1,950	1,300	570	370	400
		NITROGEN ANALYSES				
SA 22,548	XM-68	150	160	130	140	110
SA 22,826	XM-76	200	200	190	170	200
SA 22,826	XM-85	260	220	230	260	250
SA 22,826	XM-84	210	250	200	220	210
SA 22,706	XM-75	170	200	190	200	170
SA 22,641	XM-73	120	130	130	120	110
SA 22,679	XM-70	240	220	230	220	220
SA 22,635	XM-74	130	150	170	110	140

Table 35.—Carbon contamination above the base line in BW titanium castings [1]

Casting	Mold mix number	Depth below surface				
		0.015 in	0.030 in	0.045 in	0.060 in	Base line
SA 22,548	XM-68	1,070	180	110	0	380
SA 22,826	XM-76	940	690	310	110	560
SA 22,826	XM-85	1,600	750	260	150	600
SA 22,826	XM-84	1,340	840	260	160	610
SA 22,706	XM-75	1,480	880	150	130	620
SA 22,641	XM-73	1,890	620	100	40	310
SA 22,679	XM-70	1,590	540	90	20	710
SA 22,635	XM-74	1,550	900	170	0	400

[1] Carbon contamination is given in parts per million above that established for the interior metal of a given casting.

Table 36.—Knoop hardness values of eight titanium castings produced in expendable graphite BW molds

Casting	Mold mix number	Knoop hardness values [1]				Base value [2]
		Depth below surface				
		0.004 in	0.024 in	0.048 in	0.088 in	
SA 22,548	XM-68	262	207	201	168	170
SA 22,826	XM-76	378	222	217	237	222
SA 22,826	XM-85	253	273	291	215	232
SA 22,826	XM-84	328	322	269	225	244
SA 22,706	XM-75	307	213	210	239	228
SA 22,641	XM-73	207	218	204	193	189
SA 22,679	XM-70	307	291	227	136	223
SA 22,635	XM-74	366	218	198	181	188

[1] The anomalies that appear in the table are attributed to the effect of grain orientation on individual Knoop hardness values.
[2] Base values are averages of 4 determinations.

0.088-in. Selected values obtained from these traverses as well as the base value appear in table 36. The average difference between the values of the eight castings and their respective base line is shown in figure 134. The values that appear below the base line are the result of the extreme variation in Knoop readings from one grain to another in any one casting.

The significant feature is the curve that indicates that the surface-hardening effect of carbon contamination is negligible below 0.040 in, although there is analytical evidence of slight carbon contamination below this level. A photomicrograph (fig. 135) taken in the area of the hardness traverse of casting SA 22,635 XM-74, shows the depth of significant contamination to be less than 0.028 in. This is further evidenced in figures 136 and 137.

Figure 136.—Microstructure of titanium cast in XM–75 near cast surface. Etch: 45 ml H_2O, 45 ml HNO_3, 10 ml HF ($\times$ 50).

Figure 135.—Microstructure of titanium cast in XM–74 near cast surface. Etch: 45 ml H_2O, 45 ml HNO_3, 10 ml HF ($\times$ 50).

The surface hardening is caused primarily by the carbon contamination and the strains induced by the rapid chill typical of cold-mold castings. Nitrogen causes a much greater hardening effect on titanium than does carbon (4), but analyses of the cast block indicate very little increase in this contamination over the base metal level as shown earlier.

From the data obtained by chemical analyses, visual observation, and hardness tests it is evident that when using this mold material, the reaction between the titanium metal and the mold wall is considerably greater than when machined graphite is used. The amount of contamination falls off rapidly with depth, however, and below about 0.04 in, little if any effect is observed.
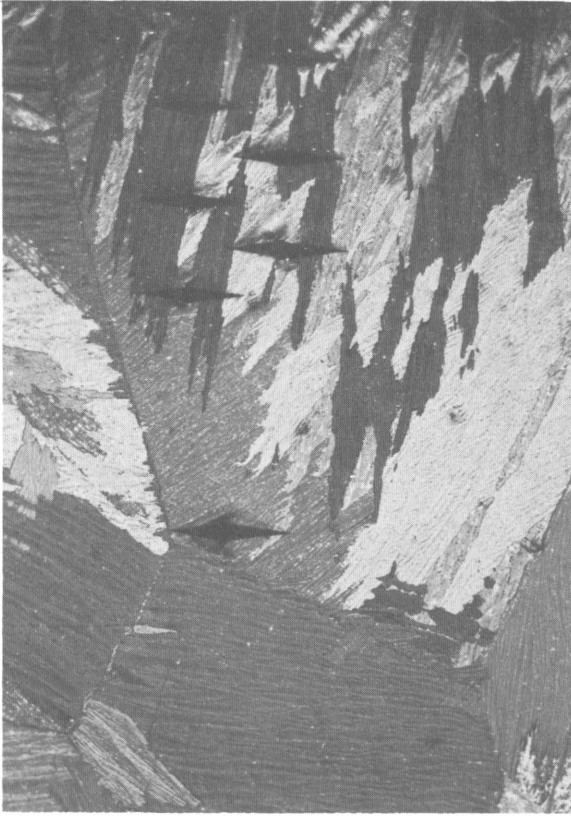
Figure 137.—Microstructure of titanium cast in XM–76 near cast surface. Etch: 45 ml H_2O, 45 ml HNO_3, 10 ml HF ($\times$ 50).

Figure 138.—Hafnium cylinders cast in expendable mold material BW.

Mechanical tests were performed on standard 0.250-gage-diam tensile test specimens machined from the test block castings. Two specimens were prepared from each casting, one from near the center and the second from as near the cast surface as possible. Without exception, the specimen nearest the cast surface gave ultimate tensile strength values of from 1,000 to 2,500 psi greater than did the central specimen. Data from the specimens nearest the cast surface are listed in table 37. The variation in values is a result of the nonuniformity of metal composition from casting to casting rather than differences in mold-preparation techniques. Referring again to table 41, the castings from XM–76, SM–85, and XM–84 were poured from the same casting heat and, therefore, contain metal of uniform composition. The mechanical properties listed in table 37 for these castings are very similar even though the mold preparation techniques varied for each.

The yield stress, tensile strength, and elonga-

tion of these castings are well within the specifications for commercial titanium [4] and are equivalent to castings produced in machined graphite molds.

Zirconium and Hafnium.—Zirconium and hafnium castings were poured into a series of expendable molds of material BW for the purpose of evaluating the effect of the higher pouring temperature of these metals on the resultant castings.

Hand-rammed cylindrical molds, $2\frac{1}{2}$-in-diam by 3-in-high, were used for both zirconium and hafnium. Figure 138 shows two such hafnium castings and half of the mold for each. The molds were bottom gated. In addition to the cylindrical castings, five zirconium pipe tees were cast, two of which (fig. 139) were cast in the improved material XM–71 which was mulled for 8 min under CO_2 and cured directly. The success with which zirconium may be cast in this material is demonstrated in figure 140. The finished pipe tee shown here has been sandblasted to give an excellent surface both inside and out prior to the thread-cutting operation.

[4] Tentative Specification for Titanium and Titanium Alloys Castings. ASTM Designation B 357–61T, issued 1961.

Table 37.—Mechanical properties of cast titanium produced in expendable graphite BW molds

Mold mix number	Yield stress, 0.2 percent strain, psi	Tensile strength, psi	Elongation, percent per inch	Reduction in area, percent	Hardness, Bhn kg/mm ^{2}
XM–68	67,550	72,650	22	32.6	197
XM–76	90,600	98,900	18	28.7	243
XM–85	89,500	97,700	16	28.7	239
XM–84	87,500	97,700	19	30.0	255
XM–75	80,500	92,000	18	28.0	229
XM–73	57,890	64,770	22	29.9	168
XM–70	88,900	99,400	18	31.5	250
XM–74	56,320	64,820	22	34.7	180
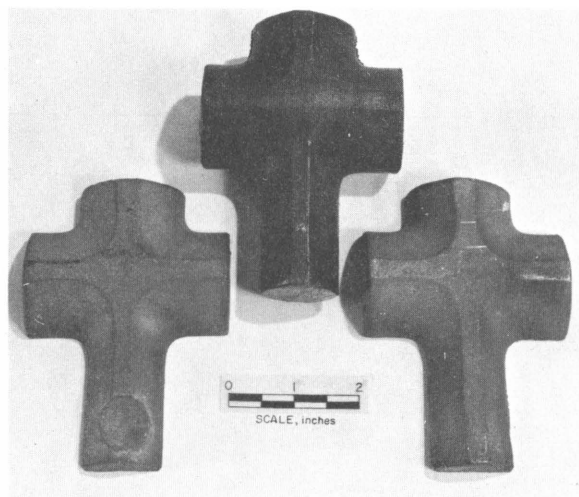
Figure 139.—Zirconium pipe tees cast in mold material XM–71.

Evaluation of the cylindrical molds was limited to chemical analyses of the casting and the ingot stock from which it was made, hardness traverses, and comparative micrographs to examine the cast structure. The cast zirconium pipe tees were sectioned and examined for soundness and microstructure. Comparative evaluation data of the zirconium and hafnium cylinders are given in table 38. Microscopic examinations of specimens cut from each of the cylindrical castings shows no carbon inclusions or other mold-metal reaction. (See figs. 141 and 142.) The zirconium casting show a fine Widmanstätten structure throughout, which is the same structure observed in the ingot stock from which it was produced. (See fig. 143.)

Knoop hardness traverses on specimens from both castings show the surface hardening effect to be very slight. Below about 0.016 in, the hardness is equivalent to that of the center of the casting.
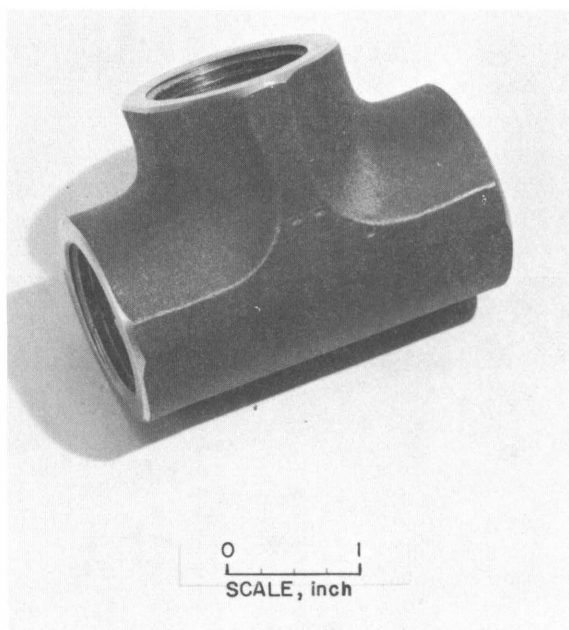
Figure 140.—Finished zirconium pipe tee with sandblasted surface, cast in mold material XM–71.

Several attempts were made to utilize this mold material for molybdenum casting but without notable success. Severe surface reaction and blowing of the casting occurred in each case.

The results of the casting evaluation of expendable mold material BW, particularly of improved CO_2-treated material, show that satisfactory titanium, zirconium, and hafnium castings can be produced where some compromise in surface finish can be afforded. Less deleterious surface effects are noted with zirconium and hafnium than with titanium, in spite of their higher melting points.

Table 38.—Carbon content and hardness of zirconium and hafnium cast in expendable graphite mold material BW

Casting	Depth below surface, in x 10⁻³	Brinell hardness number	Weight-percent	
			Carbon	Nitrogen
SA 21,674 (zirconium):				
Mold 1 _____	{1–15	212	0.068	0.011
	{15–30	192	.030	.011
Mold 2 _____	{1–15	212	.068	.011
	{15–30	190	.028	.011
Base metal _____	----------------	197	.031	.012
SA 21,709 (hafnium):				
Mold 1 _____	{1–15	281	.021	.003
	{15–30	277	.006	.004
Mold 2 _____	{1–15	255	.034	.004
	{15–30	285	.016	.004
Base metal _____	----------------	283	.008	.004

Figure 141.—Microstructure of hafnium cast in mold material BW, near cast surface (SA 21,709). Etch: 45 ml H_2O, 45 ml HNO_3, 10 ml HF ($\times$ 100).
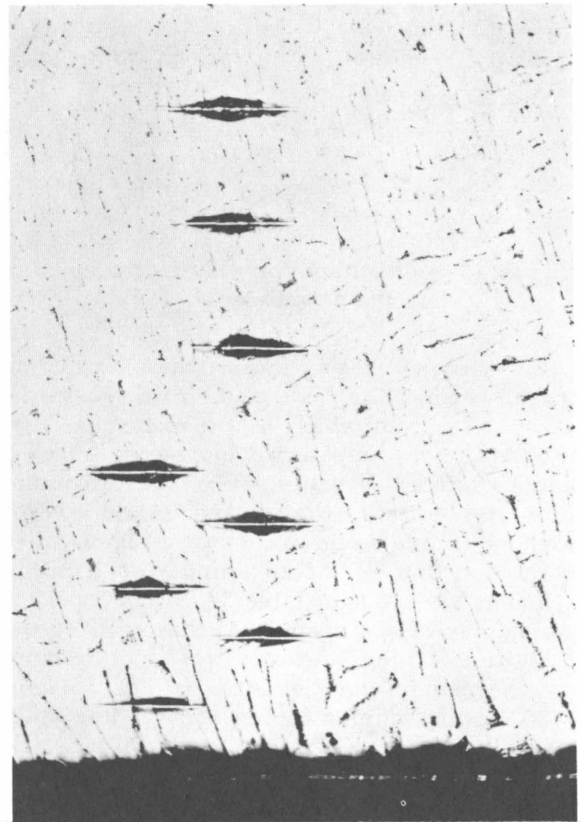
Figure 142.—Microstructure of zirconium cast in mold material BW near cast surface (SA 21,674). Etch: 45 ml H_2O, 45 ml HNO_3, 10 ml HF ($\times$ 100).
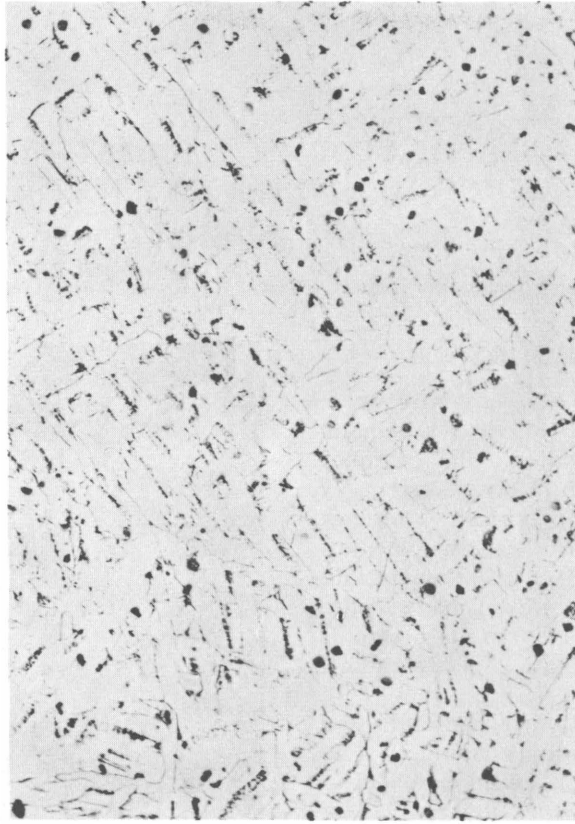
Figure 143.—Microstructure of zirconium ingot used as feed material for casting SA 21,674. Etch: 45 ml H_2O, 45 ml HNO_3, 10 ml HF ($\times$ 100).

REFERENCES

1. American Foundrymen's Society. Foundry Sand Handbook. 1952, p. 65.
2. Kroll, W. J., C. T. Anderson, H. P. Holmes, L. A. Yerkes, and H. L. Gilbert. Large Scale Laboratory Production of Ductile Zirconium. J. Electrochem. Soc., v. 94, No. 1, July 1948, p. 16.
3. Kroll, W. J., W. W. Stephens, and J. P. Walsted. Graphite-Rod Hairpin-Resistor Radiation Furnace for High Temperatures. Trans. AIME, v. 188, 1950, pp. 1394–1395.
4. McQuillan, A. D., and M. K. McQuillan. Metallurgy of the Rarer Metals. V. 4. Titanium. Academic Press Inc., New York, 1956, p. 341.
5. Wood, F. W., and R. P. Adams. Molds For Titanium Castings. Light Metal Age, v. 15, Nos. 7–8, August 1957, pp. 18–20.

CHAPTER 13.—LABORATORY-SCALE CASTING FURNACE FOR HIGH-MELTING-POINT METALS

By P. G. Clites and E. D. Calvert [1]

DESCRIPTION OF FURNACE

Figure 144 is a view of the laboratory-scale casting furnace, and figure 145 is a schematic cross section. The water-cooled ladle chamber (*A*) and the mold chamber (*F*) were originally designed to fit the body of an existing, 4-in ingot furnace, and thus utilize the existing vacuum system and controls for the casting operation. Numerous modifications have been made to the furnace since it was installed, but its design is still such that it is an adaptation of a standard ingot furnace.

Figure 146 is a cross section of the ladle, the ladle chamber, and the mold chamber. The inner wall of the ladle chamber is a 7¼-in length of 9-in copper pipe; the outer wall is an equal length of standard 10-in copper pipe. The two walls are joined at the ends with flanges of ½-in copper plate. Inlet and outlet fittings for the cooling water are standard ⅝-in water-hose fittings brazed to holes in the outer jacket. These fittings are 1-in above and below the bottom and top flanges, respectively. The two openings for the ladle arms are 180° apart and 3½-in below the top flange. Two-inch lengths of stand- and 1½-in copper pipe are threaded on the outer end to accommodate brass nuts for effecting an O-ring seal, as shown in the figure. The standard 1¼-in copper pipe used for the ladle arms fits easily within these ports.

Details of the ladle design are also included in figure 146. The ladle is supported on two 12-in lengths of standard 1¼-in copper pipe (*C*) that serve as the electrical connections to the ladle and the inlet and outlet for cooling water. One end of each arm is threaded, and the arm is screwed into the ladle to provide the mechanical and electrical connection. These arms are the supporting members for the ladle and are free to rotate within the ports of the ladle chamber when the ladle is tipped. An O-ring provides the vacuum seal between the
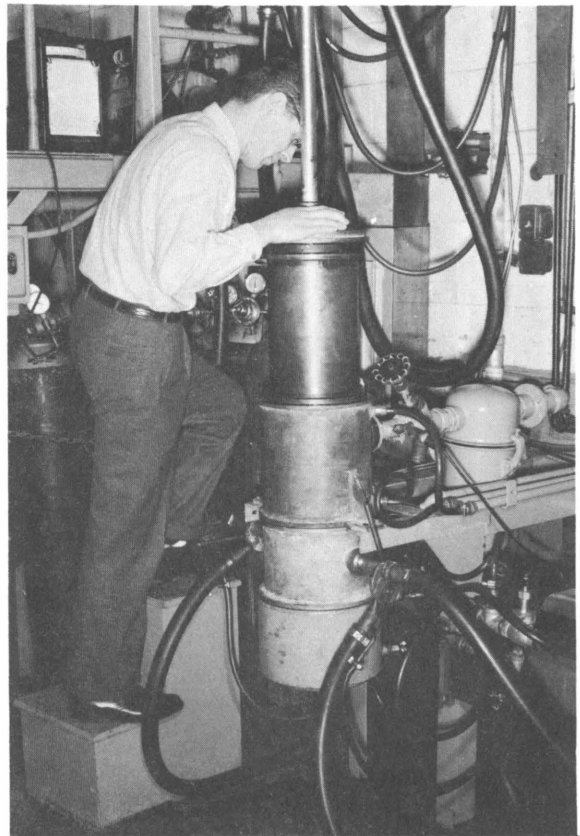
Figure 144.—Overall view of casting furnace.

water flowing into the ladle and the interior of the furnace.

The outer wall of the ladle is a 4¾-in length of standard 5-in copper pipe with a ¼-in copper plate brazed on the bottom. The sockets for the arms are machined from 2½-in copper rod. The two arms insure good electrical contact by tightening against a shoulder machined on the inner surface of these sockets.

The inner liner (*G*) is fabricated from a length of standard 3-in copper pipe. The lip of the liner is spun so that the brazed joints are

[1] Supervisory research chemist, Albany Metallurgy Research Center, Bureau of Mines, Albany, Oreg.

A Electrode drive
B Pneumatic cylinder
C Power connections
D Water-cooled electrode
   support
E Observation port
F Consumable electrode
G Water-cooled ladle
H Water-cooled tilting
   mechanism
I Vacuum outlet
J Water-cooled mold
   chamber
K Graphite mold
L Water line
M Tilting handle
N Water-cooled ladle
   chamber

0   10   20
Scale, in
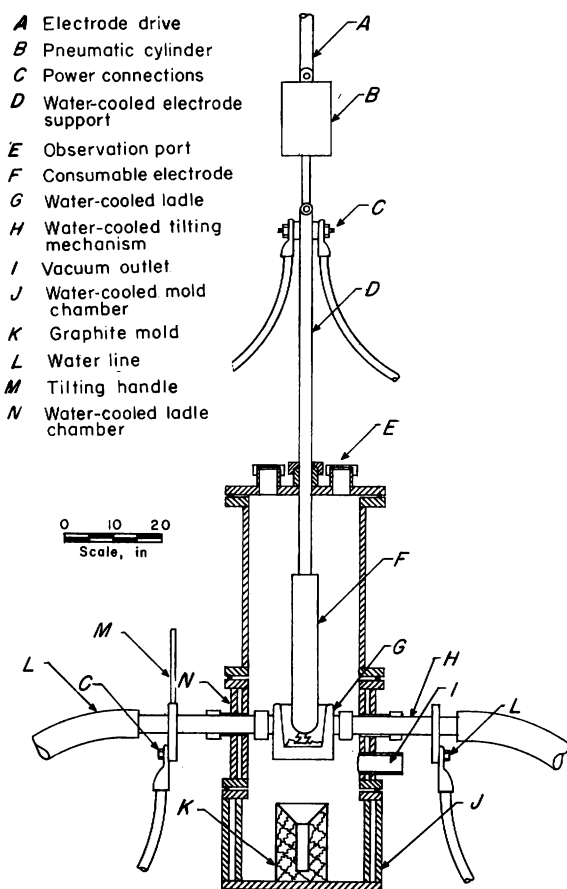
Figure 145.—Laboratory-scale casting furnace.

not exposed to the arc during melting. The ladle is 4-in deep, and the sidewalls are tapered from approximately a 3-in diam at the bottom of the ladle to a 3½-in diam at the top. This taper facilitates removal of the skull from the ladle after a heat. The bottom is ¼-in copper plate brazed in position. These liners must be replaced frequently when work involves high temperature metals. No problem has been encountered in machining the brazed joint between the lower surface of the lip and the outer wall of the ladle in order that new liners can be installed.

Experience in producing the inner liners has shown the following procedure to be the most satisfactory. A length of 3-in pipe sufficient to produce several liners is mounted in a lathe, and the lip for one liner is spun. A length sufficient for one liner is then removed, and the lip for a second ladle is spun. In this way, heating the end to be spun does not soften the end of the pipe held in the lathe chuck as it would if the pipe stock were cut to length before spinning

the lip. Following the spinning operation, a steel mandrel is pressed into the partly completed liner to form the tapered sides. This operation is performed cold. The raw edges of the liner are then machined, and the bottom is brazed into position.

Arrows in figure 146 indicate the coolant flow through the ladle. Water enters one arm of the ladle and is directed by baffles (I, J) so that it impinges on the bottom surface of the inner liner and flows upward along the liner walls. The elliptical baffle is set at an angle with the centerline of the arms so that it is above the inlet arm and below the outlet arm. This baffle forces the inlet water downward between the cylindrical baffle and the outer wall of the ladle, and on the outlet side it directs the water out the opposite arm. The opening between the baffle and the inner surface of the spun lip is held to approximately one-eighth inch to assure adequate coolant flow at this critical part of the ladle.

The mold chamber, located directly below the ladle, is a 8-in-deep double-walled steel chamber with 10-in ID. The chamber provides enough space for molds used in most of the research work with this furnace; however, a larger chamber would be desirable for molds required for the production of small, shaped castings.

The copper electrode shaft consists of two coaxial copper pipes which permit end-to-end circulation of cooling water. Water, which enters at the top, flows through the inner pipe to the bottom of the electrode shaft, then upward between the inner and outer pipes to the top of the shaft, where it is exhausted. Flexible, water-cooled power leads are bolted to the upper end of the electrode shaft for the cathodic connection of the electrical power circuit.

The power supply for the furnace consists of 18 selenium rectifiers connected in parallel. Open-circuit voltage for the network is 70. Arc current available to the furnace is limited to 8,000 amp by the shunt used for metering. By motor-driven tap changers, the arc current can be controlled from a minimum of 200 amp to the maximum.

A 5-hp vacuum pump with a capacity of 110 cpm produces an ultimate furnace vacuum of 15μ with a leak rate of less than 3μ/min. This pump is more than ample for the system.

FURNACE OPERATION

The melting and casting operation begins with the selection and fabrication of an elec-

A Water-cooled ladle
    chamber
B O-ring seal
C Water-cooled ladle
    arm
D Power connection
E Vacuum outlet
F Water-cooled mold
    chamber
G Ladle liner
H Tilting handle
I Cylindrical baffle
J Elliptical baffle
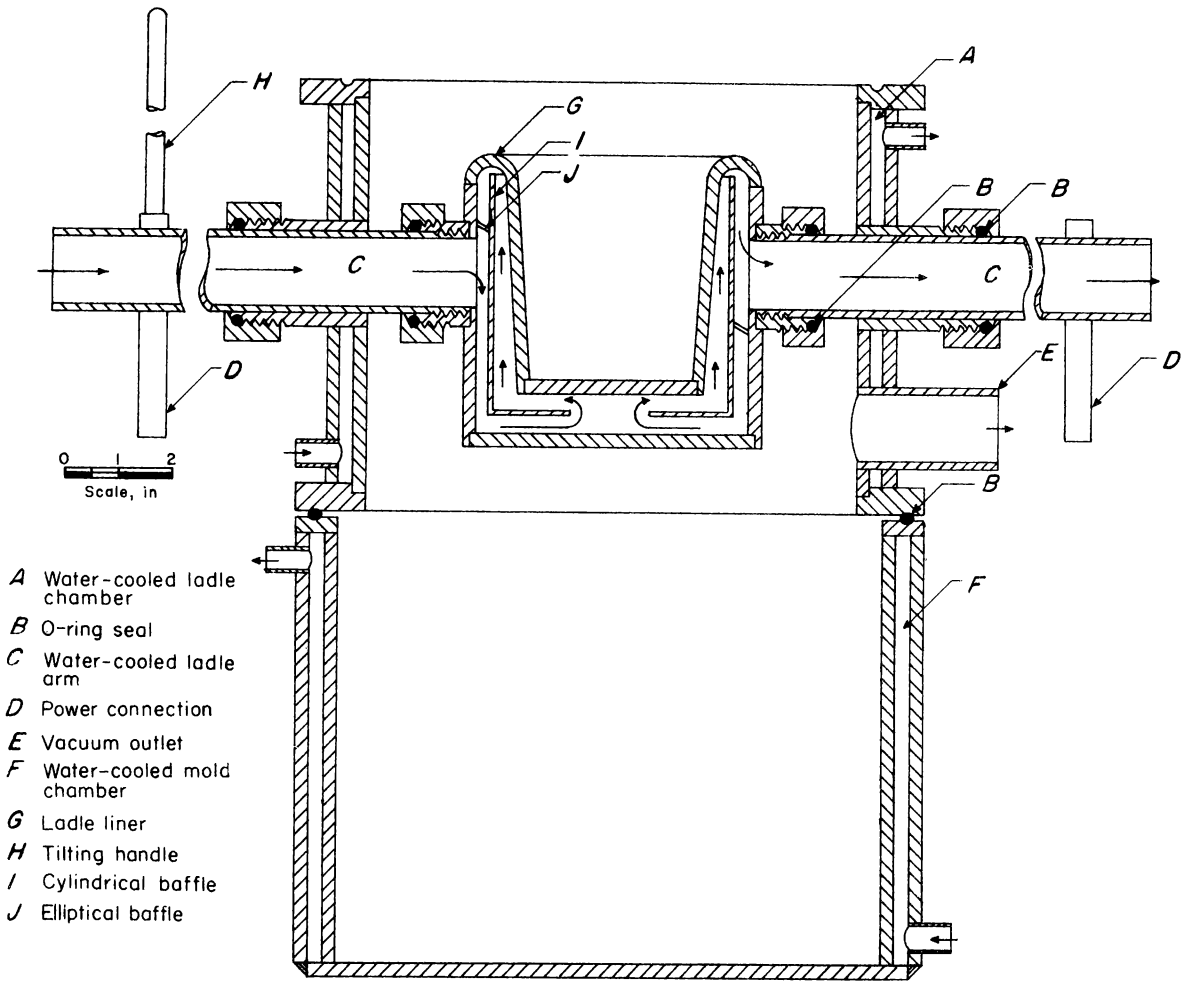
Figure 146.—Ladle, ladle chamber, and mold chamber (laboratory-scale casting furnace).

trode. Castings have been made with electrodes prepared from sponge, scrap turnings, sintered powder, sintered and forged powder, and previously melted material. Electrodes with a very small cross section and those fabricated from material containing volatiles result in a low ratio of the metal poured to the metal melted. Electrodes fabricated from pressed bars of sponge metal containing large amounts of residual salts and from iron containing appreciable quantities of dissolved gases result in a particularly low ratio.

A ¾-in male thread is machined on one end of the electrode stock. For material that cannot be machined, a suitable stub of metal with this thread is welded to one end. The thread screws into the water-cooled copper shaft and provides the mechanical and electrical connection between the shaft and the electrode. It is impor-

tant to machine a square shoulder on the electrode so that good metal-to-metal contact is made between the electrode and the shaft to assure an efficient electrical connection.

The length of the electrode is determined by the length the furnace body will accommodate and the amount of metal required for the castings. A 3-in-diam electrode 20-in long will provide ample metal for a series of three or four runs and can be accommodated easily by the furnace described.

For all heats it is necessary to provide a starting pad in the bottom of the ladle on which to initiate the arc. If the skull from a previous melt is available, it is placed in the ladle, and a few chopped turnings are placed in the bottom of the skull to facilitate striking the arc without having it adhere to the skull. Figure 147 shows the ladle with a skull in position.

Figure 147.—Furnace interior showing skull in position.

When no skull is available, more turnings are placed in the bottom of the ladle to serve as a starting pad. The amount varies with the metal being melted, but usually it should be sufficient to cover the bottom of the ladle to a depth of approximately half an inch. For example, heats of titanium and zirconium are started with 150 g of base, whereas heats of tantalum require 450 g. (The densities of zirconium and tantalum are respectively 6.5 and 16.6 g/cc.)

When the electrode and base have been loaded into the furnace and the molds placed in position, the furnace is closed and evacuated. Most metals are melted and cast with the furnace evacuated to the ultimate vacuum of the system at the beginning of the heat and with the vacuum valve of the furnace open throughout the run. The thermocouple gage, located in the vacuum line between the furnace and the main furnace valve, normally indicates an absolute pressure of 150μ to 500μ during the heat. The casting of chromium provides an exception to the practice of operating in the micron range. The high vapor pressure of chromium makes it necessary to melt it in a pressure of about one-third of an atmosphere of helium. This practice would be necessary for other metals with high vapor pressure and with alloys when one or more of the alloy additions has a high vapor pressure.

When the proper furnace pressure has been attained, the electrode is lowered until an arc is initiated between the electrode and the starting pad. Starting electrical power requirements vary with the metal but should be high enough to melt the starting pad and low enough to pre-

vent rupture of the ladle. A typical starting arc current for a zirconium melt would be approximately 1,500 amp. Typical values for arc current and the potential for various metals are given in table 39.

As soon as the base has been consolidated into a molten pool, the power is raised to the desired level. So that a uniform arc potential is maintained, the electrode is fed downward by a motor-driven rack and pinion as it is consumed. When the required quantity of metal has been melted, the arc is terminated. This quantity can be determined by observing the melting of a pin placed at predetermined point on the electrode or by watching the level of the molten metal in the ladle. The instant the arc is terminated the electrode is withdrawn from the ladle by the air cylinder mounted in the electrode drive mechanism. This cylinder is actuated by a hand lever near the pouring station. The ladle is then tipped, and the contents are poured into the mold. The entire operation from the time the arc is extinguished until the metal is poured generally is completed in 2 sec.

After the pour, the furnace is allowed to recover to a pressure approaching the ultimate attainable and is backfilled with helium to an absolute pressure of 15 in Hg. This speeds cooling and helps prevent contamination of the hot metal. Cooling time ranges from 20 to 30 min.

Table 39 summarize the results of several typical runs. In general, maximum casting efficiency results from a proper balance of electrical power and water cooling; however, other factors, such as electrode composition and arc potential, also influence the casting efficiency. Casting efficiency, as used in this report, refers to the ratio of the weight of metal poured to the weight of the total charge (weight of electrode melted plus weight of skull or base). For metals with higher melting points, higher power levels and increased coolant flow are required.

OPERATION WITH SPECIFIC METALS

The following paragraphs briefly outline the results for the various metals melted in this furnace. In addition to the work with individual metals described in subsequent paragraphs, research has been conducted on the relationship of the operating variables to skull casting. Fluidity spirals, similar to those shown in figures 148–150, have been cast to determine the effects of arc current, arc potential, and coolant flow to the ladle. These variables affect casting efficiency and the fluid life of the metal, measured

Table 39.—Results of casting heat

Heat No.	Material	Arc current, amp	Arc potential, v	Cooling water to ladle, gpm	Weight poured, lb	Resultant skull weight, lb	Casting efficiency, percent
REACTIVE METALS								
1	Titanium _____	2,200	30	9	1.71	2.02	44
2	_____do_____	3,000	32	4	2.69	1.27	59
3	_____do_____	3,500	32	[1] 3	3.59	1.10	55
4	_____do_____	3,000	30	8	2.55	1.05	68
5	_____do_____	3,000	28	16	2.23	1.98	53
6	_____do_____	4,000	28	12	2.98	1.23	69
7	_____do_____	3,500	28	18	2.67	1.73	45
8	Zirconium _____	2,600	30	10	2.70	3.20	45
9	_____do_____	3,500	32	15	2.94	3.09	48
10	_____do_____	3,500	30	15	3.22	2.54	53
11	_____do_____	4,000	30	15	3.84	2.13	62
12	_____do_____	4,500	30	15	3.95	2.16	64
13	_____do_____	5,000	30	15	3.64	2.20	59
14	_____do_____	5,000	32	15	3.53	2.37	57
15	_____do_____	4,500	32	15	3.85	2.09	63
16	_____do_____	4,000	32	15	3.09	2.65	53
17	Hafnium _____	3,000	30	9	4.24	3.48	52
18	_____do_____	3,000	30	8	5.34	3.40	76
19	_____do_____	3,500	30	7	7.54	3.20	77
20	_____do_____	4,000	30	7	5.31	3.03	68
REFRACTORY METALS								
1	Columbium _____	3,500	31	10	4.16	2.77	56
2	_____do_____	3,500	28	10	3.57	3.04	54
3	_____do_____	3,500	28	9	3.99	3.46	52
4	_____do_____	5,000	30	26	5.56	1.70	73
5	Molybdenum _____	3,500	44	30	2.36	3.33	40
6	_____do_____	3,500	35	30	3.42	4.05	45
7	_____do_____	4,500	38	30	5.07	3.55	57
8	_____do_____	5,500	38	30	4.60	2.99	59
9	_____do_____	5,500	38	30	4.19	3.57	54
10	Tantalum _____	6,000	25	[2] 15	6.44	7.57	45
11	_____do_____	5,000	26	[2] 15	7.51	6.36	53
12	_____do_____	4,500	30	25	4.95	3.20	57
13	_____do_____	7,000	26	25	6.01	4.74	55
14	_____do_____	5,500	30	[1] 32	4.96	8.63	35
15	_____do_____	5,500	28	30	5.47	5.31	49
16	_____do_____	6,000	25	35	9.52	6.60	58
17	Tungsten _____	6,000	27	32	2.64	7.77	25
IRON, IRON–URANIUM, AND CHROMIUM								
1	Iron _____	3,000	23	9	2.78	2.82	47
2	_____do_____	3,500	28	7	2.93	3.23	44
3	_____do_____	3,500	29	7	3.41	3.50	57
4	_____do_____	3,500	28	7	3.37	3.71	41
5	Iron-uranium alloy__	3,000	30	9	3.56	1.74	70
6	_____do_____	3,000	20	9	3.17	1.73	55
7	_____do_____	3,500	20	9	3.74	1.60	69
8	_____do_____	3,200	27	11	3.71	2.92	44
9	_____do_____	3,000	25	10	3.37	1.45	41
10	Chromium _____	3,500	31	8	2.05	1.85	47
11	_____do_____	3,500	31	8	1.78	1.25	43
12	_____do_____	3,500	31	8	2.54	1.41	56

[1] Inner liner of ladle failed and water was admitted to the melt.
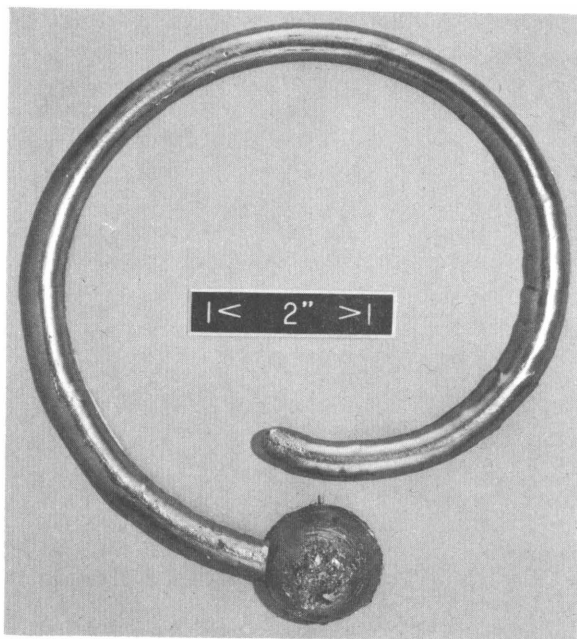[2] Approximate.
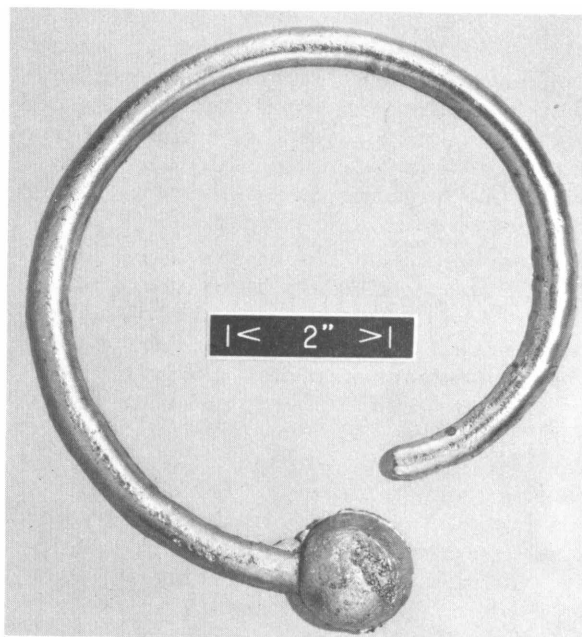
Figure 148.—Fluidity spiral of titanium.

Figure 150.—Fluidity spiral of columbium.
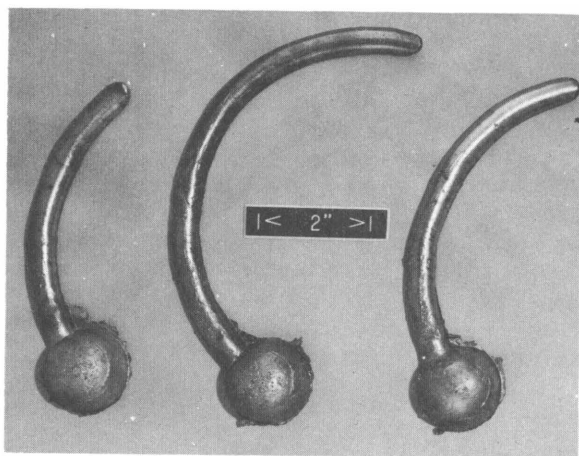
Figure 149.—Three fluidity spirals of zirconium run (left to right) at 3,500, 4,500, and 5,000 amp.

by the length of the fluidity spiral. Data are insufficient to draw conclusions as to the interrelationship of these variables; however, the values stated for the arc current, arc potential, and coolant flow for each of the following metals have produced the best results.

Titanium.—Titanium can be satisfactorily melted and cast using 8 to 10 gpm cooling water to the ladle, an arc current of 3,000 to 3,500 amp, and an arc potential of 30 v. From table

39 it will be noted that run 3 was made with only 3 gpm of water on the ladle and that at this low value the ladle failed. A comparison of runs 1 and 4 indicates that an increase in arc current from 2,200 to 3,000 amp produces a greater increase in casting efficiency than is achieved by decreasing the coolant flow from 8 to 4 gpm as in runs 2 and 4.

Figure 148 shows the surface markings of a fluidity spiral of titanium produced in titanium heat 7 of table 39. The runner length is 21 in. The mold for this casting was machined graphite, as were all the molds used for the heats described.

Zirconium.—Zirconium is melted and cast satisfactorily under nearly the same conditions as titanium; however, high arc currents (3,500 to 4,500 amp) are required for melting and casting zirconium. Figure 6 shows three fluidity spirals cast at arc currents of 3,500, 4,500, and 5,000 amp. Maximum casting efficiency and fluidity were obtained with an arc current of 4,500 amp. Arc potential was maintained at 32 v and coolant flow at 15 gpm for all three runs. These three are included as zirconium heats 9, 15, and 14 of table 39.

Hafnium.—Because of the scarcity of hafnium metal, few heats have been made, and these have used electrodes formed from bars of

pressed turnings. When these runs were undertaken, 4,000 amp was the limiting arc current available. Experience with other metals indicates that casting efficiencies can be increased by operating at higher arc currents, but no such heats have been attempted with hafnium even though the furnace is now equipped to operate at arc currents up to 8,000 amp.

Columbium.—Columbium shows considerable promise as a metal to which this casting process can be applied. Columbium heat 4 of table 39 indicates the excellent casting efficiency obtained when columbium is melted at higher power levels. Figure 150 is a photograph of the fluidity spiral cast in this run. The runner of this spiral was 18-in long—only 3-in shorter than the best titanium runner produced. The electrode for this heat was a sintered and forged powder metal compact. The cast columbium was ductile, and the surface of the casting was excellent. Additional casting heats are necessary to verify reproducibility of the results obtained in this run.

Molybdenum.—Molybdenum can be readily arc melted and cast, but the resulting castings are extremely brittle. Centrifugal castings produced in a larger casting furnace were reported to be more ductile.[2] Fluidity spirals of molybdenum have been produced with 11-in runners. Higher arc potentials are needed to produce high melting rates and, hence, high casting efficiencies. An arc current of 4,500 amp and an arc potential of 38 v results in satisfactory casting efficiency.

Tantalum.—Of seven attempts to cast tantalum, five were successful. Table 39 summarizes the results of six of the runs. The maximum length achieved in a fluidity spiral was 12 in. These castings show that shape casting of tantalum is feasible; however, additional work on both crucible design and mold materials is necessary to decrease the possibility of crucible failure and to improve casting quality.

Tungsten.—Nearly all of the numerous attempts to cast tungsten have ended in failure of the crucible liner. Only one run yielded a sample of poured metal. (See chapter 15.)

Chromium.—A limited number of chromium castings have been produced in the furnace to check the applicability of the process to this metal and others of high vapor pressure. All of the castings have been melted and cast in a

helium atmosphere at an absolute pressure of 10 in Hg. Chromium heats 10–12 of table 39 give the results of three chromium runs. The castings produced in these heats were not evaluated, but it was noted that their grain size was smaller than that of arc-melted ingots.

Copper.—Copper is difficult to melt and cast in a water-cooled copper crucible because the high heat conductivity of copper causes a very heavy skull to be formed; hence, casting efficiencies are low. In numerous heats a graphite liner was placed in the ladle. The walls and bottom of this liner are one-fourth inch thick and insulate the molten copper from the cold walls of the ladle. With this arrangement, all of the metal can be poured from the ladle and no skull remains. An arc current of 3,000 amp and an arc potential of 25 v provide satisfactory copper castings. The main difficulty in casting copper is the lack of control of the rate at which the metal is poured, as any delay in the pouring cycle causes the metal to solidify in the ladle.

Iron.—A number of mild steel castings have been produced using electrodes fabricated from commercially available hot-rolled steel rod. This rod is not a satisfactory material for electrode stock because its high content of dissolved gases causes low casting efficiencies and porous castings.

Iron heats 5–7 of table 39 utilized electrode stock prepared from iron-uranium alloys which had been vacuum arc melted before the casting heat. Heats 8 and 9 were run using electrode stock of identical composition; however, the stock had not been vacuum melted before the casting heat. A comparison of casting efficiencies for these five heats indicates that efficiency is higher when the electrode stock has been vacuum melted.

DISCUSSION

Experience with this furnace has shown the need for numerous improvements to increase its usefulness and ease of handling. The ladle and ladle arms have already been modified from the original design to provide increased waterflow to the ladle. The original arms were constructed of 1-in copper pipe; the arms described in this paper are 1¼ in and give a flow of 50 gpm with a line pressure of 60 psi.

This flow provided adequate cooling for melting tantalum, but ladle failure occurred on nearly every tungsten heat attempted. It is questionable if increased waterflow would prevent ladle failure during tungsten heats, but this fac-

[2] Calvert, E. D., S. L. Ausmus, S. A. O'Hare, and A. H. Roberson. Molybdenum Casting Development. BuMines Rept. of Inv. 5555, 1960, 16 pp. See chapter 14 of this bulletin.

tor should be considered if additional attempts are made to cast tungsten.

A suggested improvement for the furnace is the enlargement of the mold chamber. The chamber has been adequate for much of the research, but on several occasions the small size of the chamber has seriously limited the versatility of the equipment. A larger chamber would provide the necessary room for properly designed molds. It would also be convenient if access to the mold could be gained from the front of the furnace, so that the molds could be positioned and removed without lowering the chamber from the furnace body.

The furnace could be improved by the use of a one-piece liner for the ladle. The brazed joint between the bottom of the liner and the walls was a weakness. On several occasions the ladle failed during a tungsten heat, but no holes have been found in the liner after the melt cooled. It is possible that the brazed joint parted during the melting and sealed when the run was terminated.

In conclusion, design and operational techniques have been presented for a laboratory-scale arc-casting unit. The versatility of the equipment has been demonstrated by the form and variety of material melted. The equipment should be particularly useful for producing metallurgical specimens where homogeneity in cast material would be beneficial. As many industrial and college laboratories have or plan to install cold-mold arc furnaces, the fact that the casting equipment can be only a modification of a conventional furnace is a definite advantage.

CHAPTER 14.—MOLYBDENUM CASTING

By E. D. Calvert, S. L. Ausmus, S. A. O'Hare,[1] and A. H. Roberson

Molybdenum, with a melting point of 2,620° C and superior creep strength at 1,600° F and above, has been the object of much attention by metallurgists in the past few years. These advantages have been offset by certain limitations in fabrication, however, and the preparation of cast shapes has not been possible until recently. Classically, the metallurgy of molybdenum depended on pressing powdered metal into suitably shaped blocks and sintering them in a vacuum furnace to about 2,000° C. These sintered bars could be forged or rolled into plate or sheet and drawn to wire. Sizes were limited, and uses were confined mostly to small electrical parts.

The application of consumable-electrode arc melting for the preparation of sizeable ingots as announced by Parke and Ham (7) in 1946 was a turning point in molybdenum metallurgy. Arc-cast molybdenum ingots were forged into usable commercial shapes, and the use of molybdenum as a structural material advanced rapidly. Applications of the consumable-electrode vacuum arc melting technique spread rapidly to many of the reactive metals, and today it is the standard method for melting titanium, zirconium, and hafnium.

PROCEDURE

The basic techniques used to produce cast molybdenum shapes were the same as for any of the reactive metals. Vacuum arc-melting and casting practices as established for titanium, zirconium, and hafnium were followed insofar as equipment and general procedure were concerned. The basic differences between the casting of molybdenum and these other metals were in controlling the major variables such as arc current, arc potential, and coolant flow. Figure 151 shows the setup used in the skull furnace for molybdenum.

The actual mechanics in preparing for a molybdenum casting heat do not differ drastically

from those of any other metal. The arc is established by lowering the electrode against a starting pad of molybdenum chips or turnings placed in the bottom of the crucible. As soon as a molten pool is established, power is increased, and melting proceeds as rapidly as possible. If a skull from a previous melt is available, it may be reused to advantage. The use of a starting pad of turnings is useful in establishing the arc, since the pad melts from under the electrode and prevents the electrode adhering to the skull.

Maintaining the proper arc length is especially critical when molybdenum is being melted. When the distance between the electrode and pool is small, a collar may form around the electrode and finally short against the side of the crucible. Excessive spacing results in a diffuse arc that may result in arcing between the electrode and crucible and a possible puncture of the crucible wall. The melting rate is reduced drastically in either case.

Experience has shown that the arc potential should range from 36 to 40 v with a dc current of 10,000 amp for a pouring crucible 10-in-diam. These parameters will vary with both crucible geometry and composition of the electrode, but in all likelihood the most satisfactory arc potential will be found to be higher with molybdenum than with other metals such as titanium, zirconium, and hafnium.

Pour efficiency is defined as ratio of metal poured to total metal melted from the electrode, plus starter pad, expressed as percent. Pouring efficiency for these four heats ran from 30 to 74 percent. The higher ranges are reached when a skull from a former heat is used, since the skull must be left behind when a pour is made. This is evident in table 40 where the first two pours were made from bare crucibles, while the last two utilized skulls from former melts, and more than 70 percent of the metal melted from the electrode was poured into the mold. The efficiency of the casting operation is increased by a close control of the crucible-coolant flow rate and by the adjustment of total energy input to

[1] Research physical metallurgist. Albany Metallurgy Research Center, Bureau of Mines, Albany, Oreg.
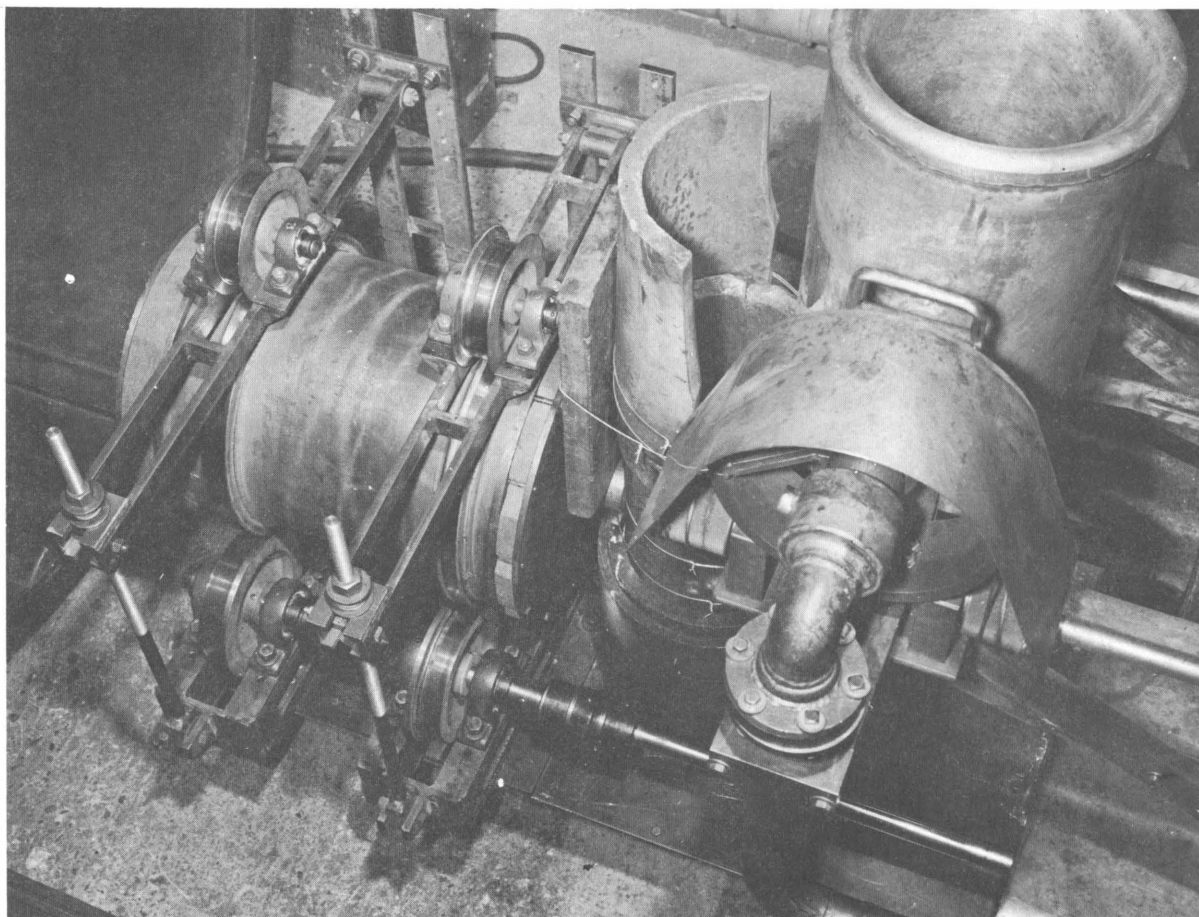
Figure 151.—View of casting equipment. Rotating mold on left, water-cooled copper crucible, upper right.

an optimum which will promote maximum pool depth. A high rate of melting is assumed to be an indication of this optimum level of energy input.

Four successful molybdenum castings have been made. These include two centrifugally cast tubes, one multiple static casting consisting of two pipe tees, a 1- by 2- by 8-in plate, and a Ruff fluidity runner. Details of the four casting heats are presented in table 40.

The two centrifugally cast tubes were poured into a graphite-lined steel drum rotating around a horizontal axis at 826 and 1,028 rps, respectively. These speeds produced forces of 45 and 75 times gravity, respectively, at the periphery of the 4½-in molds.

The first static casting produced from molybdenum was Ruff's-type fluidity test runner (fig. 152). The mold was constructed from machined graphite, according to the specification listed in

the Metals Handbook (1). The metal flowed through the $\frac{7}{16}$-in diam channel a distance of 8 in. A similar casting of titanium produced under comparable conditions ran 16 in.

The pouring arrangement of the multiple static casting is shown in figure 153. The assembly included two pipe tees—one cast in a machined graphite mold and the other in a rammed mold of graphite powder and a suitable binder. The plate was cast into a machined graphite mold. The sprue and runner molds also were machined graphite.

EVALUATION

The centrifugal casting shown in figure 154 exhibited a dimpled surface that was eliminated by a $\frac{1}{32}$-in lathe cut. The casting was removed from the mold without evidence of sticking, and the bright surface discounted any suspicion of

Table 40.—Molybdenum casting heat

| Heat No.	Casting	Weight of metal poured, kg	Pouring efficiency, percent	Arc current, amp	Arc potential, v
SA 19,946_____	Centrifugally cast tube— 4⁷⁄₁₆-in OD, 4-in ID, 7³⁄₁₆-in length.	14.10	30.45	9,500	18–22
SA 20,380_____	Ruff's fluidity runner____	21.10	57.03	9,000	38–40
SA __20,432_____	Centrifugally cast tube— 4⅜-in OD, 2⅜-in ID, 8-in length.	23.10	73.80	9,600	36–40
SA 20,505_____	Multiple static casting___	21.60	71.40	9,500	34–38
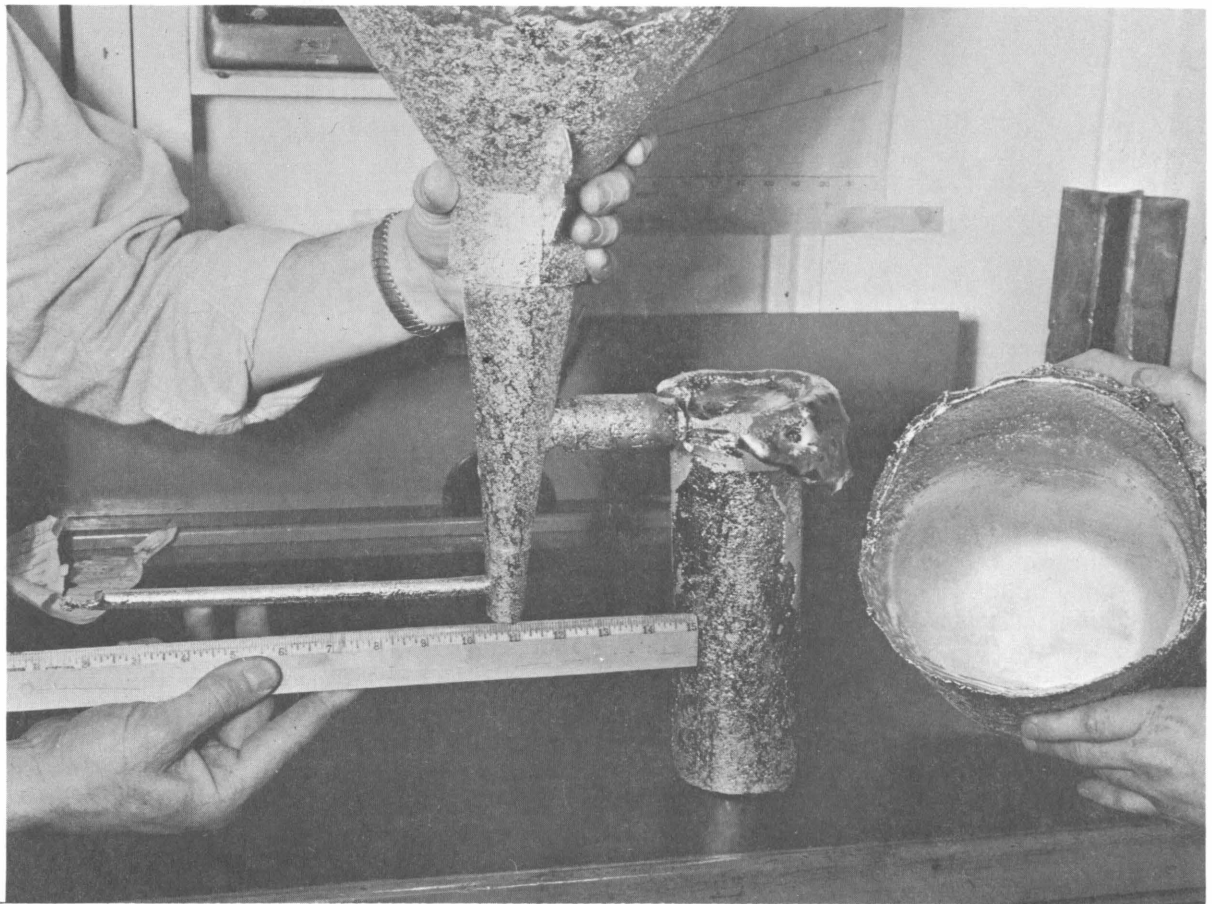
Figure 152.—Fluidity test runner and melting crucible skull, both of cast molydbenum.
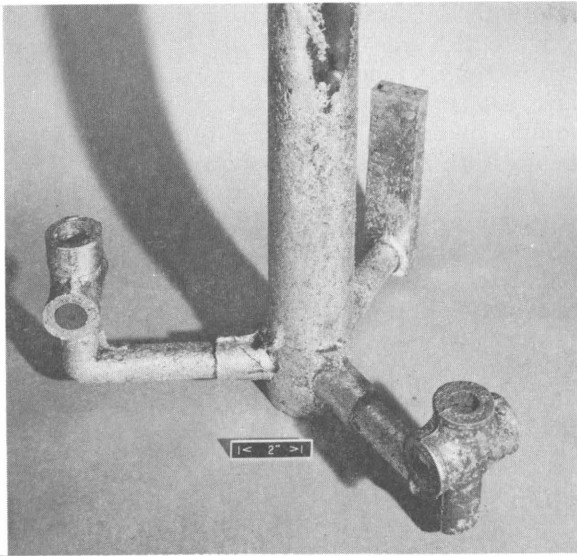
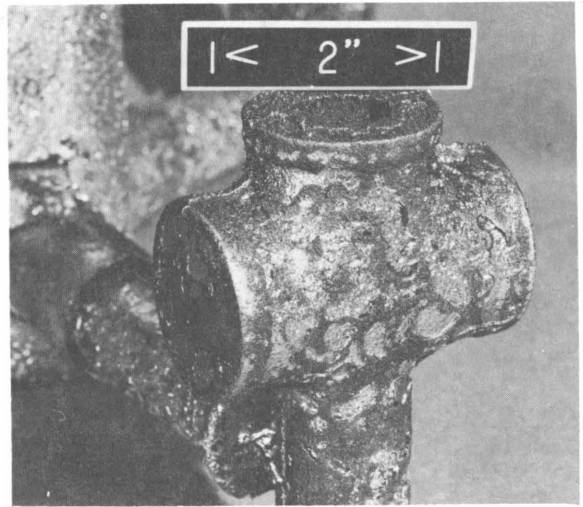Figure 153.—Multiple static cast molybdenum.

Figure 155.—Molybdenum pipe tee, cast in expendable graphite.
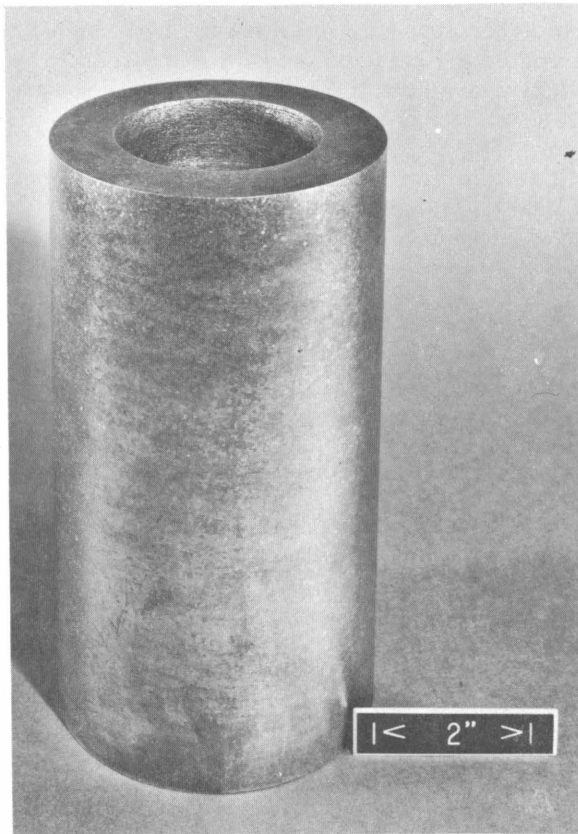

Figure 154.—Centrifugal casting.

metal-mold reaction. The interior surface was clean, bright, and fairly smooth; here, again, only a light lathe cut was required to remove surface imperfections.

The multiple static casting assembly is shown in figure 3. Both of the pipe tee castings were excessively porous, due to mold gas, as well as turbulence, and rapid chilling. The 1- by 2- by 8-in plate was more nearly sound than was expected. A normal shrink cavity was present in the upper 20 percent, and one small void occurred near the bottom in the area of the gate. The lower cavity could be anticipated in any bottom-poured casting with a gate of sufficiently large cross section to act as a heat sink.

In the expendable graphitic mold (the same material used in casting titanium), the molten molybdenum severely attacked and reacted with the mold material, producing a heavy carbide on all casting surfaces. Figure 155 illustrates the appearance of the shape cast in the expendable mold. The blackened, mottled surface shows evidence of severe mold reaction. This is marked contrast to the bright, clean surface of the same shape cast in machined graphite (fig. 156). The rough surface of the latter casting should not be confused with a mold reaction. This unattractive appearance was a surface defect, and probably was caused by metal low in superheat that solidified the instant it came into contact with cold surface of the mold. Besides the excessive carbide reaction that occurred in the expendable mold, a severe case of porosity resulted from the mold
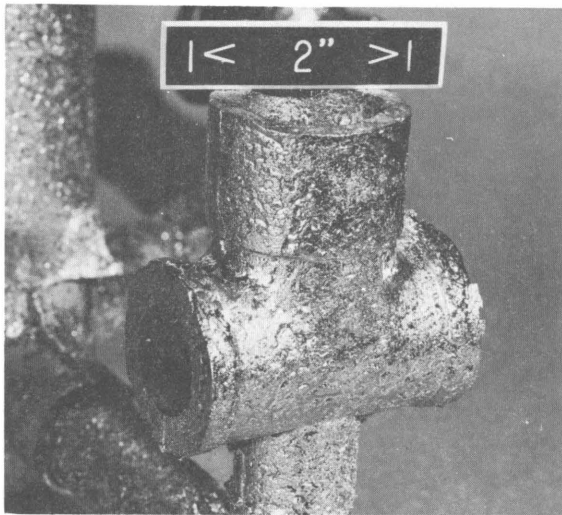
Figure 156.—Molybdenum pipe tee, cast in machined graphite.

2-¼-in-diam tensile specimens taken at 3 locations— 120° apart

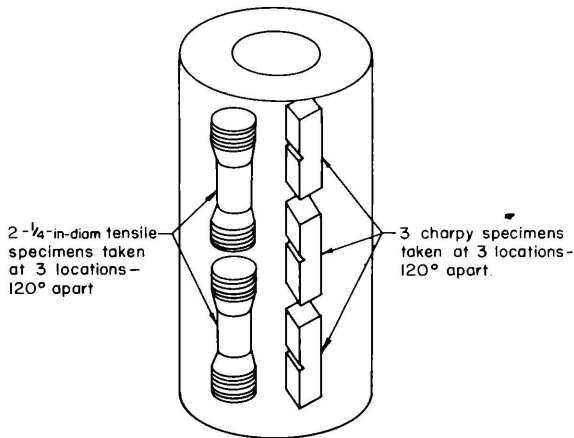3 charpy specimens taken at 3 locations— 120° apart.

Figure 157.—Location of test specimens.

gases generated at the moment of pour. This mold gas is a result of volatiles remaining in the mold and core after firing at 960° C in CO. Vacuum firing of the expendable mold parts at 1,000° C may overcome the gas evolution, and the carbide reaction might be solved by the use of a graphitic wash applied to the mold surfaces before firing.

All castings, both centrifugal and static, produced in machined graphite indicate practically no carbide reaction. Most of the molds could be reused, although occasional areas of heat checking or slight metal attack were noted.

One centrifugally cast tube, 4½-in-diam, 8-in-

long, with 1-in walls, similar to the one shown in figure 154, was inspected by radiography and then sectioned longitudinally to provide tensile bars, Charpy impact specimens, and metallographic specimens. The location of test specimens within the casting is shown in figure 157.

A cobalt-60 radiographic survey of the casting was made by suspending a 220-mc source at the center of the tube; the surface was covered with type M film. At the closest point, the source was about 2½ in from the film. A molybdenum penetrameter with a sensitvity of 0.5 percent was used as a calibration. The examination failed to delineate porosity or casting defects or show any variation in density from end to end.

Tensile properties were determined on six standard ASTM specification E857T, 0.250-in-round specimens. The nominal tensile strength lies between 37,800 and 41,700 psi, with an observed average of 39,800 psi. The yield strength, 0.1 percent offset, lies between 31,700 and 39,000 psi with an observed average of 35,300 psi. There was no measurable reduction in area or elongation in a 1-in gage length.

One 0.250-in-diam tensile specimen, machined from the static cast fluidity run, had a tensile strength of 57,800 psi and a yield strength by 0.1 percent offset of 52,500 psi. An $\times$ 6 macrograph of a cross section of the rod is shown in figure 158.

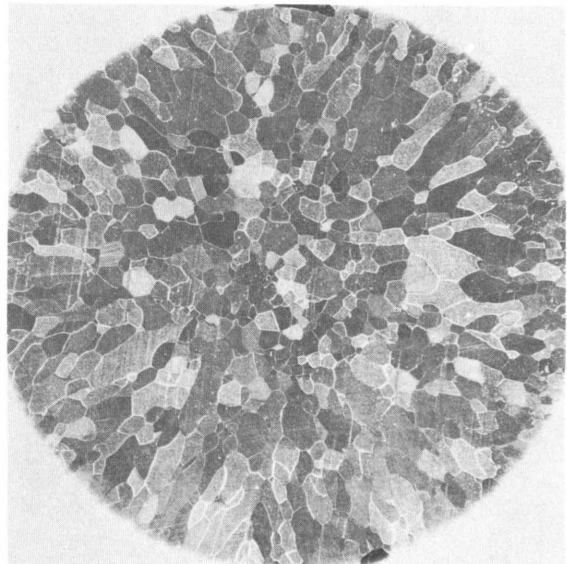The uniformity of grain size, as well as a finer

Figure 158.—Cross section of fluidity runner ($\times$ 6).

grain size, probably explains the variation of tensile properties between this bar and samples taken from the cylinder.

Nine V-notched Charpy impact specimens prepared according to ASTM specification E23–56T were used for impact testing. All nine specimens broke with an impact value of 2 ft lb. Before the impact specimens were notched, electrical resistivity measurements were made on them. The average value obtained was 5.39μ ohm cm. The highest value obtained was 5.60μ ohm cm, and the lowest value was 5.35μ ohm cm. There appears to be a significant difference in the electrical resistivity between portions of the casting. The Bureau is analyzing the values statistically.

A section was taken from each end of the sample for metallographic examination. A small amount of grain boundary constituent is evident, as well as scattered angular islands. The structure is identical to one reported as carbide by other investigators (6). Chemical analysis of the casting supports this contention. Diamond pyramid microhardness with a 1-kg load was taken from inside to outside on both ends of the casting. Values varied from a maximum of 194 to a minimum of 171, with an average value of 180. No major difference was noted between ends.

Rockwell "A" hardness taken on the inside and outside of three sections of the casting averaged A49. There was no apparent systematic difference in the observed hardness between the inside and outside of the tube or from end to end.

Figure 159 illustrates the extremely large grains as well as the wide variation in grain size in the cylindrical casting. Inadvertently, the identifying marks that would permit identification of the pouring end of the cylinder were destroyed, and it was not possible to orient the casting. The average grain size is 500 gr/in², with a maximum diameter of 0.091 in, and a minimum of 0.032 in.

Measurements on machined specimens showed a density of 10.208 by gravimetric determination and 10.213 ± 0.06 by X-ray methods. Mechanical and physical properties are summarized in table 41.

Three 1-in-cube pieces were rolled from a furnace temperature of 600° C without severe edge cracking. Reductions of 10 percent per pass were made through unheated rolls. The original thickness, final thickness, and reduction in area are presented in table 42.

Similar rolling schedules have been described
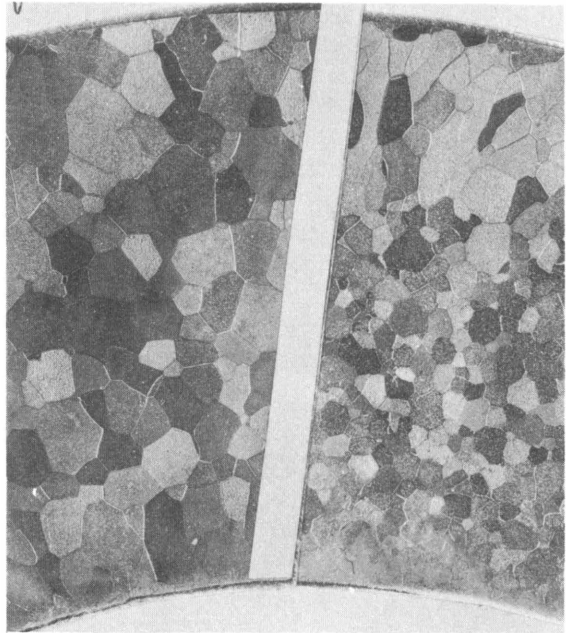
Figure 159.—Sections taken from opposite ends of cylinder, showing variation in grain size (× 6).

by Bruckhart (2), although the temperatures that he used were somewhat higher.

DISCUSSION

Mechanical properties are somewhat lower than values reported for sections taken from bars rolled from arc-cast ingots. This can be attributed to grain refinement caused by working. The variation in tensile strengths between the bars taken from the cast cylinder also can be explained by the difference in grain size between various specimens.

Spacil and Wulff (9) have reported a marked variation in tensile properties that may be correlated with grain size. They report tensile and yield strengths of 65,500 and 42,500 psi, respectively, in specimens annealed at 2,100° C and slow cooled. The 0.04-in-diam wire with which they worked showed one to three grains in the cross section. Marden and Wroughton (4) reported tensile strengths averaging 50,000 psi, with considerable variations from the mean, in 0.505-in tensile bars cut from 1-in-square bars prepared by pressing and sintering, and Freeman (4) stated that the strength of unworked sintered bar or cast ingot varied between 45,000 and 70,000 psi.

Table 41.—Mechanical and physical properties of arc-cast molybdenum

Ultimate strength _____psi	39,800
Yield strength (0.1 percent offset)____psi	35,300
Elongation _____	Nil
Reduction in area _____	Nil
Charpy impact _____ft lb	2
Hardness:	
DPH, 1-kg load _____	180
Rockwell A _____	49
Density, g/cc at 22° C:	
Gravimetric _____	10.208
X-ray _____	10.213±0.06
Resistivity _____μohm cm	5.39
Grain size _____No./in²	500

Table 42.—Rollability of molybdenum casting

Original thickness, in	Final thickness, in	Reduction, percent
0.720	0.091	87.4
.440	.091	79.3
.359	.090	74.9

Grain size in the as-cast tubes is large compared to the more familiar cast metals, but much smaller than in arc-cast molybdenum ingots where single grains, ¼-in in cross section and 2 to 3 in long, are common.

The reported electrical resistivity of 5.39μ ohm cm approaches Fink's (3) value of 5.6, established for hard-drawn wire, and Freeman's (4) reported value of 5.21μ ohm cm in annealed metal. The density approaches the theoretical, 10.22 at 68° F.

Diamond pyramid hardness values show no marked variation from center to outer edge, which is further evidence that no reaction occurred between the liquid metal and the graphite mold in the extremely short interval between contact and solidification. The average hardness value of 180 coincides exactly with the figure listed for arc-cast ingots (8), and shows that the hardness of commercial grade metal is not entirely dependent on grain size.

REFERENCES

1. American Society for Metals. Metals Handbook. Cleveland, Ohio, 1948, p. 201.
2. Bruckhart, W. L. The Working of Molybdenum and Its Alloys. Ch. 6 in The Metal Molybdenum, American Society for Metals, Cleveland, Ohio, 1957, pp. 109–142.
3. Fink, Colin S. Ductile Tungsten and Molybdenum. Trans. Electrochem. Soc., v. 17, 1910, p. 229.
4. Freeman, R. R. Properties and Applications of Commercial Molybdenum and Molybdenum Alloys. Ch. 2 in The Metal Molybdenum, American Society for Metals, Cleveland, Ohio, 1957, pp. 10–30.
5. Marden, J. W., and D. M. Wroughton. Effect of Working on the Physical Properties of Molybdenum. Trans. Electrochem. Soc., v. 89, 1946, p. 217.
6. Olds, L. E., R. B. Fischer, and J. H. Jackson. A Metallurgical Study of Molybdenum. Battelle Memorial Institute 12th Qtrly. Status Rept. to Office of Naval Research, Navy Dept., June 1, 1952 (Project NR 034–402), pp. 73–99.
7. Parke, R. M., and J. L. Ham. Melting of Molybdenum in the Vacuum Arc. Trans. AIME, v. 171, 1947, pp. 416–430.
8. Semchyshen, M. Development and Properties of Arc-Cast Molybdenum Alloys. Ch. 14 in The Metal Molybdenum, American Society for Metals, Cleveland, Ohio, 1957, pp. 281–329.
9. Spacil, S. H., and J. Wulff. Effects of Oxygen, Nitrogen and Carbon on the Ductility of Wrought Molybdenum. Ch. 13 in The Metal Molybdenum, American Society for Metals, Cleveland, Ohio, 1957, pp. 262–265.

CHAPTER 15.—CENTRIFUGAL CASTING OF TUNGSTEN

By E. D. Calvert and R. A. Beall

Tungsten, having the highest melting point of any metal, has long been required for high temperature uses in lamp filaments and tool bits. More recently, however, designers have demanded tungsten and tungsten alloys in novel and difficult-to-produce shapes. Conventional powder metallurgy techniques have been satisfactory for production of many of the required shapes and have been particularly useful for composites such as the silver tungsten transpiration cooled devices. Cold-mold ingots have met requirements where high density or large sizes cannot be realized by powder metallurgy. Shape requirements can often be met through machining or possibly forging. Beyond all this, there is still a need for high density shapes that can best be filled through casting by the vacuum-arc skull-casting method.

Reference is made to the developments at Oregon Metallurgical Corp.[1]

EQUIPMENT

A medium scale skull-casting furnace specifically designed for tungsten casting is pictured in figure 160 and shown schematically in figure 161. The horizontal axis and vertical axis spin casting mechanisms are interchangeable and, when installed, form an integral part of the furnace chamber. Figure 161 shows the vertical axis spin mechanism installed.

The electrode assembly, which consists of a water-cooled copper shaft to which the consumable electrode is attached, and a pneumatic cylinder, is suspended by a solidly mounted rack and pinion. The pneumatic cylinder is an important link in the mechanism; it rapidly withdraws the electrode from the ladle when the arc is terminated. Delays are thus avoided in pouring the molten metal from the ladle to the mold.

Water-cooled copper blocks with copper impregnated graphite inserts deliver electrical

[1] Hardy, R. G., Joseph L. Gunter, and Thomas A. Hamm. Centrifugal Casting of Tungsten and Molybdenum Alloys. Metal Prog., v. 82, No. 2, August 1962, pp. 72–77.
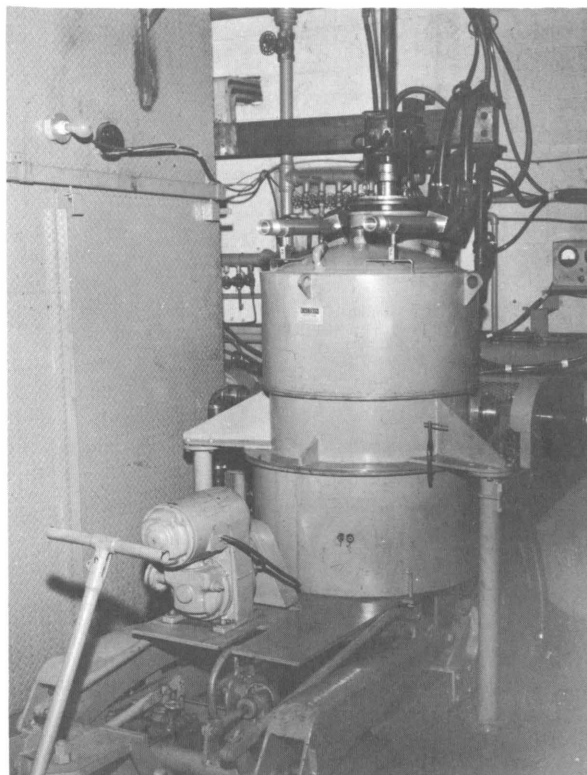
Figure 160.—Skull casting furnace.

power to the electrode shaft. Water cooling for the crucible as well as the positive power connections to the system are provided through the crucible arms. Electrical contacts are copper blocks fitted with copper-impregnated graphite bushings similar to those used for the electrode shaft. The crucible is similar to that described in chapter 11 and has a volume of approximately 150 in³. The crucible cooling water is held at a minimum of 95 gpm at 115 lb pressure. Sufficient cooling is provided to allow tungsten castings to be made without the use of preformed protective skulls. The maximum pour of unalloyed tungsten achieved was about 15 kgs.

Figure 161.—Skull casting furnace, schematic representation.

Figure 162.—Vertical axis casting mechanism.

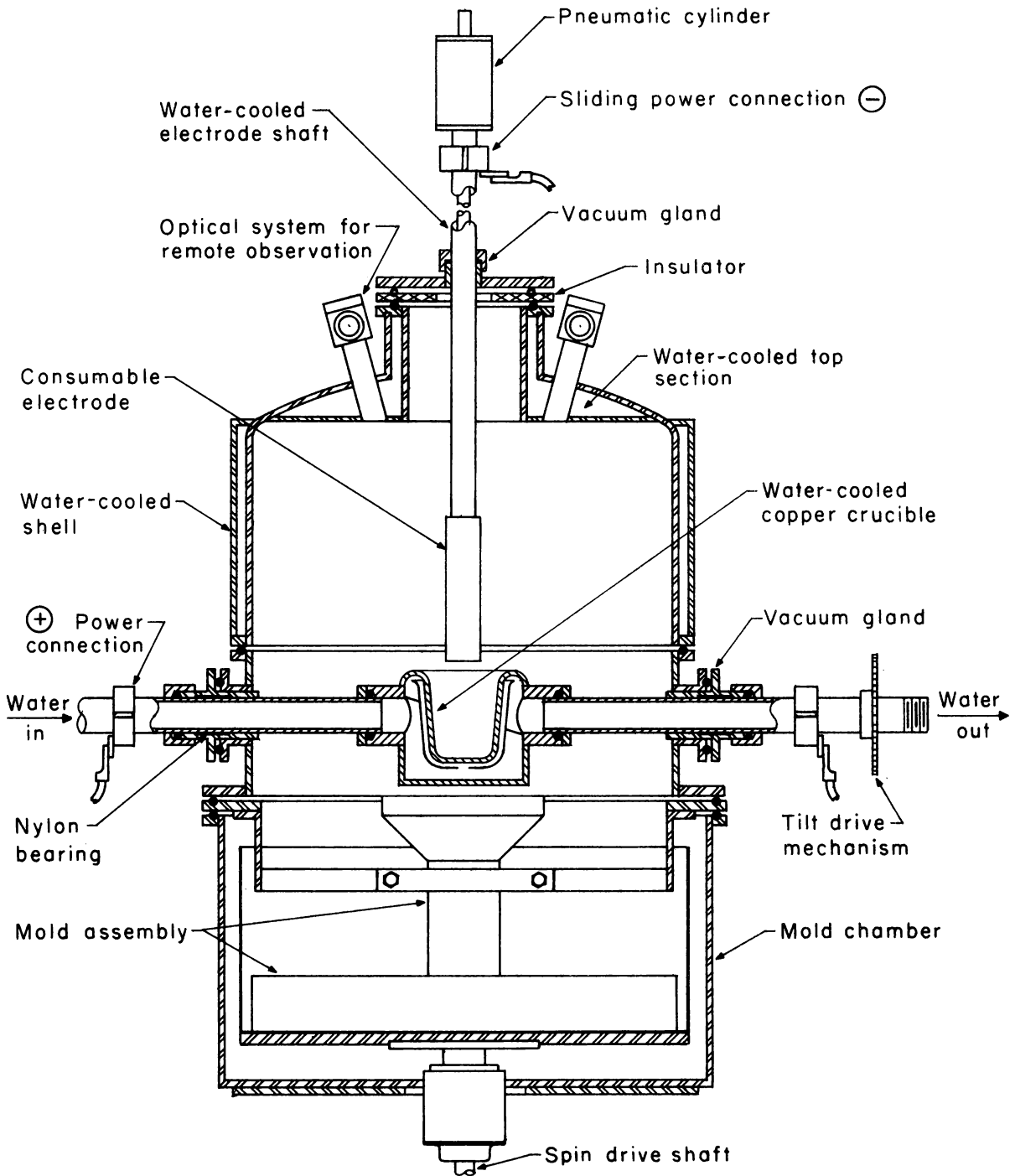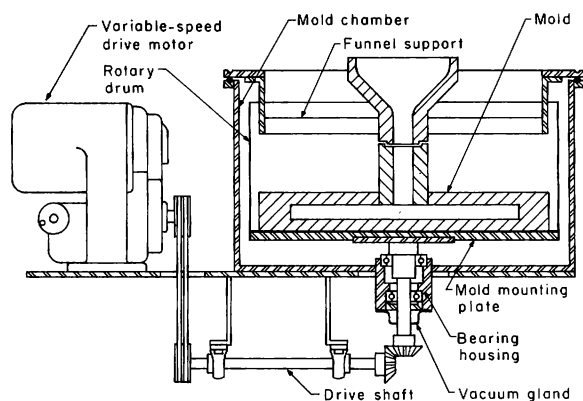Figure 162 shows a schematic drawing of the vertical axis spinning mechanism. The rotary drum, which houses the mold, is 30-in-diam and can be driven up to 700 rpm maximum. A force of 200 g can be imparted to castings which are gated to the periphery of the drum. Vertical axis spin casting is useful in the preparation of complex shapes, rods, bars and solid cylinders, as well as hollow cylindrical tubes.

Figure 163 is a schematic drawing of the horizontal axis spinning mechanism. It shows the mold chamber, spinning drum, and placement of funnel and sprue. The steel drum is graphite lined to provide a mold for the preparation of hollow cylindrical castings. Tubes up to 8-in diam and 12-in long can be cast in this mechanism. The drum can be rotated at a maximum speed of 2,000 rpm; this speed will cause a centrifugal force of about 390 g's on the casting.
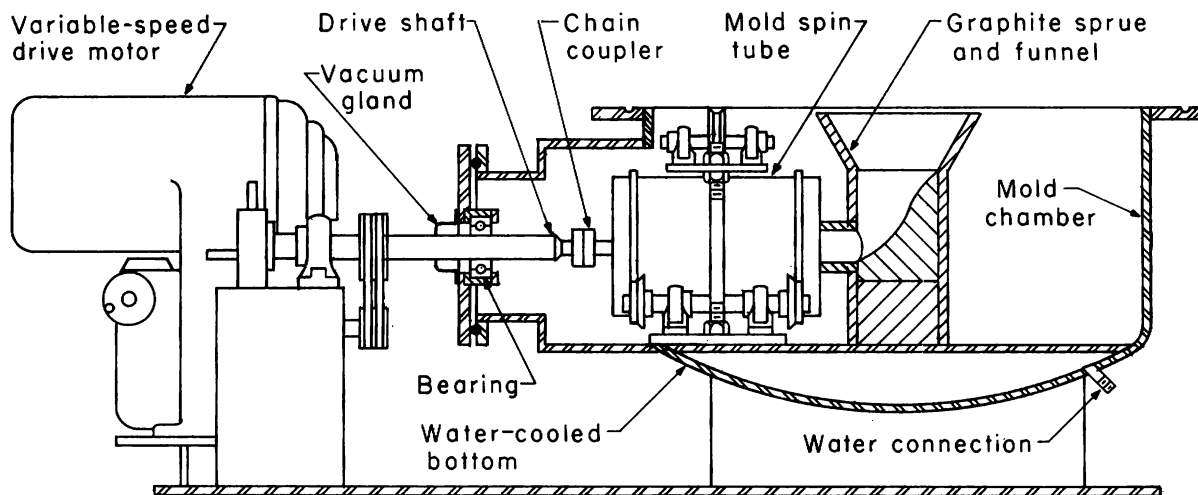
The vacuum system consists of a blower of 1,250 cfm displacement which is backed by a mechanical pump of 140 cfm displacement. An ultimate vacuum of less than 1×10^{-3} torr can be readily attained. The pressure during melting is maintained at approximately 2.5×10^{-2} torr.

Melting power is provided by 23 dc, selenium rectifiers connected in parallel to a common bus-bar. A maximum current of approximately 13,000 amp at 40 v can be delivered to the melting furnace. Open circuit potential is 70 v.

PROCEDURE AND RESULTS
Electrode Preparation

Electrodes for tungsten casting are prepared from a variety of source materials including arc-melted ingots, welded scrap tungsten, and isostatically pressed and sintered tungsten powders. The most satisfactory electrodes are pressed powder compacts which are sintered to a density of approximately 85 percent of theoretical. These compacts can be readily produced to desired lengths and diameters which eliminate the necessity for welded joints which often are detrimental to electrode soundness and which sometimes result in highly resistive zones. The electrode adapter or stub is normally made from a machineable tungsten base alloy such as W-2 Mo. This is joined to the consumable electrode by TIG welding and to the electrode shaft with a threaded stud.

Melting and Casting Operation

To begin melting, a 4,000-amp arc is initiated. The arc potential is held at approximately

Figure 163.—Horizontal axis casting mechanism.

20 v, which indicates an extremely short arc gap, until all of the base material has been consolidated. The arc current is then adjusted to the maximum capability of the power supply. The potential is allowed to increase to around 40 v and is maintained at this level to achieve the maximum electrode consumption rate, approximately 4 kgs/min, until the desired amount of metal has been melted. The spinning mechanism is then started and brought to full speed, after which, the arc power is shut off. Opening the switch to turn off the melting current simultaneously activates electrode withdrawal and the pouring cycle. Approximately 2 sec elapse from the moment of arc termination to the time that the crucible is completely tilted.

As the volume of liquid metal is of primary concern, every effort is made to maintain it at the highest possible level. The operation is carried out at as high a power input and as high a melt rate as is possible, and the metal is poured as fast as is practical. Solidification begins immediately when the power is turned off and progresses very rapidly owing to heat transfer by conduction to the cold copper crucible and to loss by radiation.

Molds

Because of the high melting temperature of tungsten, mold materials have of necessity been limited to graphite. Of available grades of graphite, only the most dense and those with the lowest ash contents have been satisfactory. To minimize carbon pickup, the runner entrance and exit are chamfered to a smooth radius to promote laminar flow and minimize washing to sharp corners. Recently, gates and mold surfaces have been coated with tungsten by plasma flame spray applications, and runners have been lined with tungsten sheet. These practices have virtually eliminated mold-metal reaction.

Resultant Castings

The versatility of centrifugal skull casting is being thoroughly investigated. Both vertical and horizontal axis centrifugal tungsten casting techniques have been studied to determine necessary parameters to prepare sound castings and to control locations of shrinkage cavities and solidification interfaces. Major controlled variables are the amount of applied force in excess of that exerted by gravity (spinning speed) and mold design, particularly the location and geometry of gates and runners.

Vertical Axis Castings.—The applications of vertical axis spin casting techniques have been investigated with centrifugal castings. The true centrifugal castings were poured to prepare cylindrical tubes in which the outside diameter is determined by the confines of the mold and the inside dimensions and the geometry are determined by the volume of metal poured and by rotational speed.

The cavity within a vertical axis casting tends to be parabolic in shape. The faster a vertical axis casting is spun the less pronounced will be the bore taper or parabolic geometry of the cavity and the more nearly will the bore become a true cylinder. It can be seen, therefore, that the lower limits of speed are governed by the amount of taper tolerable in the casting. The upper limits of speed are dictated by the need to avoid excessive stresses on the outer solidified casting skin and the risk of forming hot tears. Figure 164 shows a group of centrifugally cast hollow cylinders which were cast into molds rotated on the vertical axis at varying speeds. Those castings upon which insufficient force was applied can be recognized by the slumped appearance of the bore, especially apparent near the top of the casting. The shallow parabolic cavities seen on other castings in this group are indicative of relatively low centrifugal forces
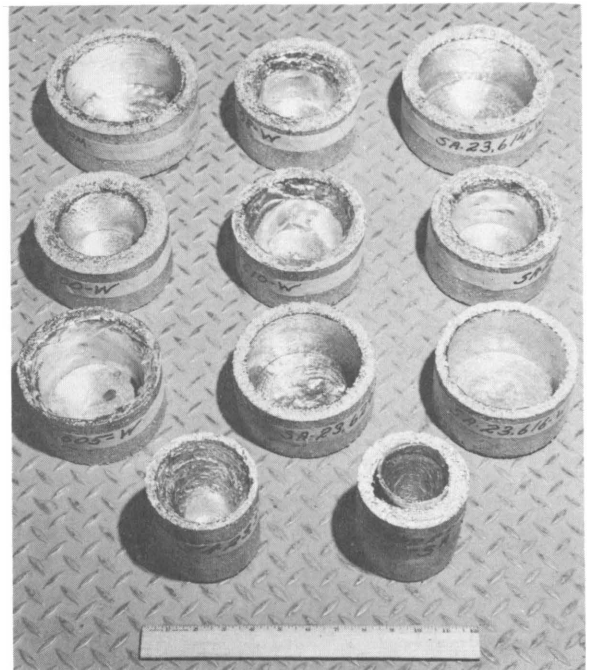

Figure 164.—Group of spin castings: Note the differences inside the bores of the cylinders.

Figure 165.—Group of spin castings: Note the indications of hot tearing on the inner walls, bottom left.

which were sufficient to prevent slumping but not enough to form straight walls. The nearly vertical wall castings were spun at higher speeds but were within the limits necessary to avoid hot tearing. The cylinders shown at the bottom in figure 165 were rotated at speeds sufficient to impart excessive hoop stresses on the partially solidified outer skin. An indication of hot tearing is seen on the interior wall of the casting shown at the bottom left of the picture. For the most part the grain structure is essentially equiaxed, and the locations of shrinkage cavities and interfacial structures are very near to the inside walls of the castings. It is presumed that this means that the metal as received by the mold does not exceed its liquidus temperature by very much and that most of the heat of fusion is extracted at the mold-metal interface. Radiation losses from the inside diameter appear to be relatively unimportant. It has been found that locations of porosity, shrinkage cavities, and solidification fronts are also directly influenced by spinning speed. The faster speeds tend to move defects closer to the bore of the casting.

Vertical axis spin casting techniques have been applied to prepare a variety of pressure fed or centrifuged castings. In some instances specific structural sound shapes were prepared; in other cases, specimens were made for evaluation and fabrication experiments. Plates, rods,
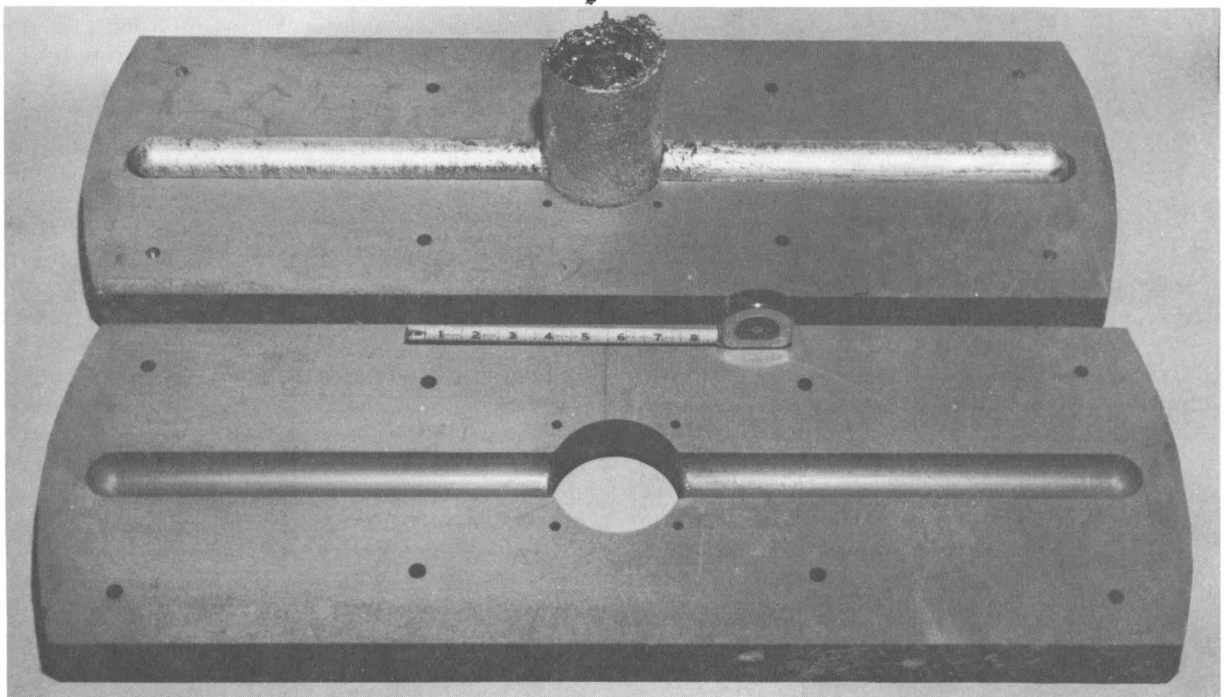

Figure 166.—Pressure casting tungsten rods.

Figure 167.—A typical horizontal-axis casting, as removed from the mold.

bars, and cylindrical billets for fabrication, as well as complex shapes, have been prepared. Reliable reproducibility of shape, structure, and properties has been achieved. Figure 166 shows a typical example of pressure-cast rods produced by vertical axis spin casting.

The major contaminant encountered in castings produced by this method is carbon. Analyses indicate that normally pickup of carbon is limited to less than 25 ppm with most of this being confined to casting surfaces adjacent to the mold walls. Removal of about 25 mils from casting surfaces, as a rule, reduced the carbon level to that of the feed material. A higher level of carbon is generally found at the rod ends.

Horizontal Axis Centrifugal Casting.—Only hollow cylinders with straight inside walls have been formed by horizontal axis centrifugal casting techniques. The outside walls are always governed by the confines of the mold and are, as a rule, straight. Contoured wall castings have been made on occasion, however, to demonstrate the capability of the process. A much higher spinning speed is employed for horizontal axis casting than for vertical axis castings because of the possibility of liquid metal slumping or raining down from top dead center when the applied centrifugal force is not adequate to hold it in place. As already noted, locations of defects such as porosity and shrinkage cavities due to nondirectional solidification are a function of spinning speed.

In general, nearly complete directional freezing can be achieved in horizontal castings by spinning at a fast enough rate and by selection of a length 'to diameter ratio which will minimize heat loss by radiation to the open ends of the cast cylinder. Crystallization at the inside diameter of the casting is thus retarded and the major body of heat is conducted through the mold wall. Solidification then proceeds from the outside wall, presenting a continuous liquid front nearly to the inside surface of the casting.

Figure 167 shows a typical horizontal axis centrifugal casting as removed from the mold. The porosity and roughness can usually be completely eliminated by removal of about $\frac{1}{16}$-in of metal from the casting wall, and this will, as a rule, also eliminate carbon contamination resulting from contact with the mold wall.

Centrifugally cast tungsten tubes, whether produced by vertical axis or horizontal axis spinning techniques, are highly stressed in the as-cast condition. It is advisable to stress-relieve the tubes at about 1,100° C prior to machining, especially those having relatively thin walls and large diameters.

CHAPTER 16.—THE FUTURE OF COLD-MOLD MELTING AND CASTING

By R. A. Beall

To conclude the thesis of cold-mold melting properly, comment should be made about potential development and limitations for the future. Although the writer holds no brief as a soothsayer, certain trends seem to have gained sufficient momentum so that some extrapolations can be made safely.

To begin with, it is fairly certain that use of cold-mold vacuum-arc-melting will continue to expand for steel alloys. In chapter 3 it was suggested that the national capacity for vacuum-melted steel is around 100,000 tons/yr. Recently, Dr. S. G. Fletcher, President of ASM, was reported (13) to have remarked that total vacuum-melted products will exceed 100,000 tons/yr in 1970. Since cold-mold vacuum-arc furnaces are seldom operated at full capacity, this suggests that a marked increase in installations is ahead. With the increased demand for titanium, one can anticipate a parallel increase in installed capacity for this metal.

More interesting than prognosticating statistics, however, is anticipating changes in technology. Whereas in the work reported herein, the open electric arc alone is considered as a heat source for cold-mold melting, this is not the sole means of heating. Among the others to be considered are submerged-arc, electron-beam, ion-beam, plasma, and induction heating. The Hopkins Process or submerged-arc melting in a cold-mold crucible was first announced in 1939 when R. K. Hopkins published details of a technology for melting steel alloy under a slag cover by a technique similar to the consumable-electrode arc method. The developments were summarized in an AIME session devoted to the "Kellogg Process" (10).

More recently, the rights to this process were assumed by the Firth Sterling Corp., which is deeply involved in exploiting the benefits thereof.

In the U.S.S.R. the "electroslag process," as the technique was termed, received a great deal of attention first as a welding method, than as a steel-alloy melting technique. In 1965, Mischler commented on the work of Gurevich and Mischenko on the use of submerged-arc or elec-troslag welding for titanium (14); in 1961 Morozov (15) published details of electroslag melting of titanium; in 1963 Gurevich (8) covered significant developments in shaped ingots by electroslag melting.

The Bureau of Mines melting-research group is engaged in a program to evaluate this development with domestic titanium. The results of the first year's work are now available (4). In addition, preliminary studies are in process on the use of a slag cover for melting refractory metals.

The advantages claimed for slag melting over vacuum are (1) improved sidewall, (2) removal of impurities, and (3) consistent grain orientation. Possible disadvantages are the retained gas content and the resultant microporosity.

In contrast to slag-melting, which eliminates the vacuum, electron-beam melting accentuates the vacuum. (An electron beam can be made to protrude a distance in the atmosphere or in partial atmospheric pressure through use of suitable orifices and pumping stages. However (to the author's knowledge) no application of the principle has been utilized for melting). Whereas metal arcs by their very nature require a modicum ion population—and resultant pressure, electron beams need no ion population and operate best at very low pressures.

The prime virtue of electron-beam melting is associated with the low pressure, for it is possible to eliminate many gases and volatile compounds from metals and as a result obtain highly purified products. The Bureau's contributions in the field of electron-beam melting have been reported earlier (2–3, 16). This method heating in the cold-mold crucible has undergone a rapid expansion since 1958, primarily for tantalum and columbium production, and can be expected to be applied to other commodities for exploitation.

Hayashi reported (9) on the use of electron-beam heating for a skull furnace and showed photos of titanium castings he had made.

Efforts have been made to combine the benefits of induction heating with the cold-mold crucible. The copper crucible unfortunately is

located so that it collects all the eddy currents from an applied electromagnetic field. There are several schemes which have more or less overcome the problem. The earliest used a pancake coil which was let down over the surface of the melt. A second used a laterally slit crucible. Recent announcements have been received on the use of a silver water-cooled "basket" crucible which contains the melt through surface tension.

The Bureau development, described in a report by Clites (which cites the above earlier schemes) requires the cold-mold to be integral with a horizontal axis intensifier and induction coil (7). This unit is a highly versatile laboratory tool, but whether or not it can be scaled-up to meet an industrial need is the present subject of investigation.

Beyond the use of the cold-mold crucible for melting, there is a largely unexplored field of high-temperature chemical reactions which can be contained in a cold-mold crucible. In a restricted sense, the electroslag or Hopkins-process melting technique, noted above, is an opening wedge into this field. For instance, careful selection of the slag composition makes it possible to eliminate or reduce impurity concentrations in steel. This "liquid-liquid" reaction conducted in a nonreactive cold-mold, at high temperature, has a wide potential for use for both common and exotic metals.

Solid-liquid reactions in the cold mold were the subject of investigations involving carbides (1, 6). This Bureau work showed that metal-carbon reactions could be conducted with an arc as a heat source; further, the resultant carbide could be melted and cast into shapes.

Gas-liquid reactions in the cold-mold crucible have not been studied. There are several interesting possibilities immediately apparent, such as hydrogen reduction of oxides, preparation of carbides with a metal-methane reaction or with an oxide-carbon tetrachloride reaction, or preparation of nitrides with a gas-metal reaction.

Thermal decomposition in an arc confined in a cold mold was the subject of an early investigation by Jaffe and Pitler (11) who claimed a method of obtaining titanium from decomposition of the chloride. Molybdenum has been prepared by the decomposition of MoS_2 in an arc furnace at the Bureau laboratories.

Another likely area of extension of cold-mold melting is the variation of the shape of the crucible. Nearly all of the work to date has been with round cold molds simply because copper is most easily obtained in tubing. How-

ever, as far as ingots are concerned, round is far from the most desirable shape. Bureau work in 1956 showed that cold molds could be rectangular shaped (12) when three consumable electrodes were used. In more recent work (4), slabs were prepared with a single slab-shaped consumable electrode. In the U.S.S.R., slab-shaped titanium ingots have been described (8). Doubtless, as titanium (and steel) ingots of increasingly larger sizes are produced, there will be stronger incentives toward slab shapes for ease in forging and rolling.

While on the subject of crucibles, comment may be made on the use of metals other than copper for cold crucibles. Copper is particularly undesirable in steel; therefore, there is incentive for a substitute crucible material. Buehl describes in a patent (5) the use of low-carbon steel as a cold-mold for arc-melting.

A final and inevitable extension of the present cold-mold operations will be in size. As the demands for high-grade metallurgically clean metal increase, it will be necessary to increase not only the number of melting units, but also the capacity per unit. The ultimate limit in size of cold-molds has probably not yet been realized. At this time one questions whether the limit will be dictated by strength of materials, by power supply, or by the succeeding forging equipment.

To conclude, the cold-mold melting technique which began in the laboratories in Germany in the early 1900's has graduated to sizes and applications beyond the imagination of the inventors. It soon will be, like the blast furnace, among the "classic" methods, accepted if not understood.

REFERENCES

1. Adams, R. P., and R. A. Beall. Preparation and Evaluation of Fused Hafnium Carbide. BuMines Rept. of Inv. 6304, 1963, 17 pp.
2. Anable, W. E., and R. A. Beall. Electron-Beam Melting of Yttrium. BuMines Rept. of Inv. 6661, 1965, 14 pp.
3. ———. Electron Beam Purification of Hafnium. Bu Mines Rept. of Inv. 6560, 1964, 30 pp.
4. Ausmus, S. L., and R. A. Beall. Electroslag Melting of Titanium Slabs. Trans. Internat. Vacuum Metallurgy Conf. 1967, ed. by Ellis Foster, Am. Vacuum Soc., Boston, Mass., 1968, pp. 675–694.
5. Buehl, R. C. Means of Preventing Segregation in Vacuum Arc Melting. U.S. Pat. 3,213,495, Oct. 26, 1965.
6. Calvert, E. D., M. M. Kirk, and R. A. Beall. Chemical Reactions in the Electric Arc: Reactive Metal Carbides. BuMines Rept. of Inv. 5951, 1962, 13 pp.
7. Clites, P. G. Vacuum Induction Melting of Reactive Metals in Water-Cooled Crucibles. Trans. Vacuum Metallurgy Conf. 1966, ed. by M. A. Orehoski and

R. F. Bunshah, Am. Vacuum Soc., Boston, Mass., 1967, pp. 183–194.

8. Gurevich, S. M., and Others. The Properties of Technical Grade Titanium and OT4 Alloys Produced by Electroslag Melting. Automatic Welding (U.S.S.R.) (English transl.), v. 16, No. 4, 1963, pp. 20–26. (See original article in Avt. Svarka., No. 4, 1963, pp. 17–23.)

9. Hayashi, C., S. Kashu, M. Kosaki, and H. Hiruta. Casting Titanium by Using an Electron Beam Skull Furnace. Pres. at Internat. Conf. on Electron and Ion Beam Technology, Toronto, Canada, May 6, 1964; Abs. in J. Metals, v. 16, No. 4, April 1964, p. 333.

10. Hopkins, R. K. The Electric Ingot Process. Proc. Electric Furnace Steel Conf., 1948, pub. by AIME, New York, v. 6, 1949, pp. 91–105.

11. Jaffe, L. D., and R. K. Pitler. Production of TiCl$_4$ in an Arc Furnace. Trans. AIME, v. 188, November 1950, p. 1396.

12. Magnusson, P. C., G. L. Schmidt, F. Caputo, and R. A. Beall. A Pilot Model Three Phase A. C. Consumable Electrode Arc Furnace. Paper in Arcs in Inert Atmospheres and Vacuum, ed. by W. E. Kuhn. John Wiley & Sons, Inc., New York, December 1956, 188 pp.

13. Metals Review. Vacuum Melting of Steel, A Report of the Baltimore Chapter Meeting of ASM. V. 39, No. 7, July 1966, p. 39.

14. Mischler, H. W. A Review of Available Information on the Welding of Thick Titanium Plate in the U.S.S.R. Battelle Memorial Inst., Dayton, Ohio, DMIC Memo. 188, Mar. 6, 1964, 21 pp.

15. Morozov, E. I., and Others. Electroslag Melting of Titanium Ingots. Paper in Mono Titan v Promyshlennosti (Titanium in Industry), Oborongiz, Moscow, 1961, pp. 314–316; transl. available from U.S. Dept. Commerce, Office of Technical Services, JPRS; 16,144, Nov. 13, 1962.

16. Wood, F. W., J. L. Hoffman, W. E. Anable, and R. A. Beall. A System for Electron-Beam Melting. BuMines Rept. of Inv. 6341, 1963, 35 pp.